Pharmacognosy of Raw Materials for Black Cohosh Dietary Supplements

BY

AYANO IMAI
B.S. Ochanomizu University, 2001
M.S. Ochanomizu University, 2004

DISSERTATION

Submitted as partial fulfillment of the requirements for the degree of Doctor of Philosophy in Pharmacognosy in the Graduate College of the University of Illinois at Chicago, 2012

Chicago, Illinois

Defense Committee:
Guido F. Pauli, Chair and Advisor
Jimmy Orjala
Richard B. van Breemen
David C. Lankin
Chun-Tao Che
John B. Friesen, Dominican University
David S. Seigler, University of Illinois at Urbana-Champaign

ACKNOWLEDGEMENTS

This dissertation would not have been possible without the generous support and insightful wisdom of many people. First and foremost, I thank my advisor, Dr. Guido F. Pauli for being the rudder that guided me through the treacherous waters of Ph.D. candidacy. His continued dedication and genuine excitement for research kept me focused on the task at hand and striving to improve with every step. Without his help, I never would have completed my research.

Secondly, I would like to thank Dr. Norman R. Farnsworth for being the lighthouse that I could always look to for guidance. I am honored to have worked with someone who is held in such high regard throughout the pharmacognosy community. His big-picture outlook helped shape my ability to approach problems and without his continued dedication to funding, none of my research would have been possible. A special thanks is in order for Dr. Richard B. van Breemen and his group. Dr. van Breemen's active role in the Botanical Center was key to the completion of my research. I also can't say enough about how much I appreciate the work by Project 3 that Drs. Dejan Nikolić, Jinghu Li, and Soyoun Ahn gave me while working on my research. I would never have made it this far without them.

The various bioassays that Dr. Judy L. Bolton and her group Project 2 of the Botanical Center provided throughout my research were invaluable in helping me reach the necessary conclusions to finalize my research. Specifically, Dr. Cassia Overk and Ms. Ping Yao were instrumental in all the estrogenic bioassays presented in my dissertation while Drs. Ghenet Hagos and Birgit Dietz helped tremendously with the chemoprevention assays. Dr. Sharla Powell's assistance with serotonergic assays was also necessary for the completion of my research. Even though I only had the opportunity to work with Dr. Chun-Tao Che for a short time, his comprehensive knowledge of natural product chemistry

and Chinese medicine will be an inspiration to me for a long time to come. My study of pharmacognosy began with a class I took by Dr. Jimmy Orjala. That class sparked my interest in pharmacognosy and taught me the basic techniques that have been invaluable in my research. I thank him for always being supportive and caring about his students. The extensive knowledge held by Dr. David C. Lankin of NMR was a constant reminder that there is always more to learn and ways to enhance my methodology. His encouraging comments and passion for science helped me stay positive when times were tough. I also thank Dr. John B. Friesen for making CCC approachable for me. Whenever I had trouble with the instruments or had trouble figuring out the solvent system, he always had the answer I was looking for. I'm grateful to Dr. David Seigler for sparking my interest in botany and following my progress through my whole stay at UIC, including as a committee member for my preliminary exam and now participating in my dissertation defense. Dr. Jim McAlpine was a pleasure to work with on so many levels. His smile always brightened the room while his advanced knowledge and willingness to share made me look forward to every opportunity to work with him. In addition to this, I also thank him for creating an environment that encouraged both students and professors to foster friendships that will last a lifetime.

I would like to thank the National Institutes of Health (NIH) (grant P50 AT00155), the Office of Dietary Supplements (ODS), the National Center for Complementary and Alternative Medicine (NCCAM) for financially supporting this work. I am forever grateful to the University of Illinois at Chicago, the College of Pharmacy, and particularly the Department of Medicinal Chemistry and Pharmacognosy for providing the infrastructure as well as a tuition waiver and stipend for much of my time here.

To everyone in my lab, starting with Dr. Shao-Nong Chen, I wish to express my deepest gratitude. Regardless of what I needed, you always provided just the right advice to help me see the shore on the horizon. I learned so much from Dr. Tanja Gödecke and appreciate her persistence and dedication. Drs. Andreas Schinkovitz, Brigit Jaki, Florencia Brasco, Jose Napolitano, and Charlotte Simmler were always there when I needed something to help me through. I am also thankful to Elizabeth Krause for being so nice and helpful from the day I started grad school. I am prostrate in my gratitude to be surrounded by so many talented and intellectual individuals who never hesitated to freely share their expertise and wisdom.

Former graduate students, particularly Drs. George Chilipala, Shunyan Mo, Brian Doyle, Tracie D. Locklear, Taichi Inui, Huu T. Nguyen, and Donna Webster for providing the perfect amount of pressure and release at the right times to help me through. My friends and colleagues Bethany Elkington, Matthew Main, Kim Bean, Chang Hwa Hwang, Wei Gao, Feng Qiu, Rene Ramos Alvarenga, Nan Zhang, Tareisha L. Dunlap and Geping Cai were always supportive and inspiring. They have added a level of enjoyment to my experience at UIC that I feel extremely lucky to be a part of. At last, I thank my husband Clayton Morton. He has been the biggest support while I was going through the dissertation writing process. I truly feel lucky to have him in my life.

AI

SUMMARY

This work was conducted within Project 1 in collaboration with Project 2 and 3 of the UIC/NIH Center for Botanical Dietary Supplements Research. The primary concern of Project 1 is the standardization of botanical formulations. Black cohosh (*Cimicifuga racemosa* syn. *Actaea racemosa*) roots/rhizomes is one of the most popular botanicals for women's health. This study sought to explore the potential of the aerial part of *Cimicifuga racemosa*. The three specific aims of this work are summarized as follows. **A**) Phytochemical investigation of the aerial parts revealed new compounds; 24-*epi*-1α-hydroxycimigenol-3-*O*-β-D-xylopyranoside (**1**) and 1α-hydroxydahurinol-3-*O*-α-L-arabinopyranoside (**2**) along with known compounds, 1α-hydroxycimigenol-3-*O*-α–L-arabinopyranoside (**3**) 1α-hydroxycimigenol-3-*O*-β-D-xylopyranoside (**4**) 7β-hydroxycimigenol aglycone (**5**) 25-O-acetyl-7β-hydroxycimigenol-3-*O*-β-D-xylopyranoside (**6**), 25-O-acetylcimigenol-3-*O*-β-D- xylopyranoside (**7**), 24-*O*-acetylhydroshengmanol-3-*O*-β-D-xylopyranoside (**8**) cimigenol aglycone (**9**) and cimiaceroside A (**10**) cimiramoside I (**11**) cimigenol-3-*O*-β-D-xylopyranoside (**12**) quercetin 3-*O*-β-arabinopyranosyl-(1→6)-β-galactopyranoside (**13**) and kaempferol 3-*O*-β-arabinopyranosyl-(1→6)-β-galactopyranoside (**14**). N_{ω}-methylserotonin (**15**) was also identified. **B**) The Metabolomics and standardization aim sought to differentiate *C. racemosa* from other *Cimicifuga* species, using visual observation, quantitative ^{1}H NMR, and statistical methods. **C**) Biological assessment of aerial *C. racemosa* was carried out for four biological activities, namely chemoprevention, estrogenicity, serotonergic activity and inhibition of cytochromes P450 3A4 and 2D6, in comparison to the roots/rhizomes of the same plants. It was shown that aerial *C. racemosa* has similar activity to the root/rhizomes, which suggests potential as an alternative source for a black cohosh dietary supplement. However, as differences

were also seen, further careful examination will be further needed. Finally, serotonergic activity of the aerial parts was attributed to the single entity, compound **15.** Compounds **5**, **6**, and **11** exhibited inhibitory activity for cytochromes P450 3A4.

TABLE OF CONTENTS

TABLE OF CONTENTS (continued)

LIST OF TABLES

LIST OF TABLES (continued)

LIST OF FIGURES

LIST OF FIGURES (continued)

LIST OF FIGURES (continued)

LIST OF FIGURES (continued)

LIST OF FIGURES (continued)

LIST OF ABBREVIATIONS

#	any Latin numeral in bold font represents isolated compound
μg	10^{-6} gram(s) or microgram(s)
μM	10^{-6} mol/liter
^{13}C NMR	carbon-13 nuclear magnetic resonance
^{1}H NMR	proton nuclear magnetic resonance
ACN	acetonitrile
ALP	alkaline phosphatase
APCI	atmospheric-pressure chemical ionization
CA	*Cimicifuga americana*
CCC	counter-current chromatography
CD	concentration doubling activity
CD	*Cimicifuga dahurica*
CE	*Cimicifuga acerina*
$CDCl_3$	deuterated chloroform
CH	*Cimicifuga heracleifolia*
$CHCl_3$	chloroform
ChMWat	chloroform: ethyl acetate: methanol: water mixture for use in CCC
CID	collision-induced dissociation
CJ	*Cimicifuga japonica*
COSY	2D $^{1}H,^{1}H$-correlative NMR spectrum
CPC	centrifugal partition chromatography
CR	*Cimicifuga racemosa*
CRPX	*Cimicifuga racemosa* aerial parts
CRRR	*Cimicifuga racemosa* roots/rhizomes
CS	*Cimicifuga simplex*

CU	*Cimicifuga rubifolia*
CYP	cytochromes P450
δ (ppm)	chemical shift (in parts per million)
DCM	dichloromethane
DMBA	7,12-dimethylbenz[a]anthracene
DMSO	dimethyl sulfoxide
DPPH	1,1-diphenyl-2-picrylhydrazyl
E_2	estradiol
EDTA	ethylenediaminetetraacetic acid
ELSD	evaporative light scattering detector
EM	exponential multiplication
ER	estrogen receptor
ERα	alpha estrogen receptor
ERβ	beta estrogen receptor
EtOAc	ethyl acetate
EtOH	ethanol
FCPC	fast centrifugal partition chromatography
Fr. / fr.	fraction after solvent removal
g	gram(s)
GB	Gaussian broadening factor
GC-MS	gas chromatography – mass spectrometry
GCP	good clinical practice
GF	Gaussian factor for line broadening
GM	Gaussian window multiplication
H_2O	water

H_2SO_4	sulfuric acid
HAPs	hydroxyapatite slurry
HEMWat	hexane: ethyl acetate: methanol: water mixture for use in CCC
HeTeMwat	hexane: tert-butyl methyl ether: methanol: water mixture for use in CCC
Hex	hexanes
HMBC	heteronuclear multiple-bond correlation spectroscopy
HMQC	heteronuclear multiple-bond quantum coherence spectroscopy
HPLC	high-pressure liquid chromatography
HR-ESI-MS	high resolution - electrospray ionization - mass spectrometry
HRT	hormone replacement therapy
HSCCC	high-speed countercurrent chromatography
HSQC	heteronuclear single quantum coherence spectroscopy
Hz	hertz
i.d.	inner diameter
L	liter(s)
LB	line broadening
LC-MS	liquid chromatography-mass spectrometry
m/z	mass-to-charge ratio
marc	plant material remaining after solvent extraction and filtration
MCP	the department of Medicinal Chemistry and Pharmacognosy
MeOH	methanol
μg	10^{-6} gram(s) or microgram(s)
mg	10^{-3} gram(s) or milligram(s)
MHz	10^{6} hertz or megahertz

min	minute
ml	10^{-3} liter(s) or milliliter(s)
μl	10^{-6} liter(s) or microliter(s)
mM	10^{-6} mol/liter
mm	10^{-3} meter(s) or millimeter(s)
MS	mass spectrometry or mass spectrum
MTT	3-(4,5-dimethylthiazo-2-yl)-2,5-diphenyltetrazolium bromide
NADP	nicotinamide adenine dinucleotide phosphate
NIH	National Institute of Health
nm	nanometers or 10^{-9} meters
NMR	Nuclear Magnetic Resonance
NP	normal phase
NQO1	NAD(P)H:quinone oxidoreductase 1
NUTS	NMR simulation and processing tool used in the present work
o.d.	outer diameter
PC	principal component
PCA	principal component analysis
PDA	Photo Diode Array
PE	petroleum ether
ppm	parts per million
pS2	presenelin-2
PX	aerial parts
qHNMR	quantitative ^{1}H NMR
QSINE	sine squared
RF	radio frequency

RMP	rifampin
ROESY	Rotating-Frame Overhauser Effect SpectroscopY
RP	reverse phase
rpm	rotations per minute
RR	roots/rhizomes
RT-PCR	reverse transcriptase-polymerase chain reaction;
s.c.s.	substituent chemical shift
SERT	serotonin transporter
SRB	sulphorhodamine B
SRM	selected reaction monitoring
SINE	sine
SSB	sine bell shift
SSRIs	selective serotonin re-uptake inhibitors
SWH	spectral width
TAM	tamoxifen
tBME	tert-butyl methyl ether
TCA	trichloroacetic acid
TLC	thin-layer chromatography
TMS	tetramethylsilane
TPA	12-O-tetra-decanoylphorbol-13-acetate
TT	triterpene
UIC	University of Illinois at Chicago
UV	ultraviolet
VLC	Vacuum Liquid Chromatography

1. **Hypothesis and Direction of this Study**

Dietary supplements manufactured from the roots and rhizomes of black cohosh (*Cimicifuga racemosa* (L.) Nutt., syn. *Actaea racemosa*) are widely used in the U.S. for the management of menopause. Currently, the plant source of the products primarily relies on wild collections, which increasingly threaten wild populations. However, if the plant collection only involved the use of the aerial parts, the plants would remain alive so that new sprouts could come back in the following season as black cohosh is a perennial plant. A search of the literature, together with our preliminary experiments, showed that the aerial parts in principle contain the same type of chemical constituents as the roots/rhizomes. Also, preliminary bioassay data confirmed serotonergic activity in extracts of the aerial parts. Therefore, this study investigated specifically the aerial parts as a renewable source for black cohosh botanical supplements.

> **The core hypothesis to be addressed is that aerial *C. racemosa* can be developed into a botanical dietary supplement that can substitute for products currently produced from below-ground parts.**

To evaluate the potential of the aerial parts of *C. racemosa* as alternative botanical dietary supplements from several angles of pharmacognostic research, the following three aims were conducted:

AIM1. Phytochemical Investigation

To isolate and identify as many secondary metabolites as possible from the aerial parts of *C. racemosa* and to compare these metabolites with those known from the roots and believed to have therapeutic effects.

AIM 2. Metabolomic Fingerprinting and Standardization

To establish a method for differentiation and identification of *Cimicifuga* species and plant parts in black cohosh dietary supplements.

AIM 3. Biological Assessment

To evaluate the biological potential of extracts of the aerial parts *of C. racemosa* extract and individual compounds in terms of chemoprevention, estrogenicity, serotonergic activity, and drug interactions.

2. **Background**

2.1. *Cimicifuga Species*

The genus *Cimicifuga*, belonging to family Ranunculaceae (Buttercup family), is composed of perennial herbaceous plants found widely in the USA, Europe and Asia. The genus name *Cimicifuga* originated from the Latin *cimex*, the generic name for the bedbug (*Cimex lectularius* L., Cimicidae) and the Latin *fugare*, meaning to drive away. This primarily refers to the fact that some species, including the Asian *C. foetida*, the European *C. europaea*, and the North American *C. elata*, produce insecticidal principles which give off a strong, unpleasant fragrance. Unlike the species mentioned above, *C. racemosa* does not possess a strong odor. The genus *Cimicifuga* contains about 27 species, and 6 species such as *C. dahurica*, *C. foetida*, *C. heracleifolia*, *C. acerina*, *C. simplex*, *C. racemosa* are used medicinally (1). In 1998 Compton (2) proposed that *Cimicifuga* should be included in the genus *Actaea* based on morphology, nrDNA ITS, and cpDNA trnL-F sequence variation. Although very recent publications have used the revised assignment of *C. racemosa* and other related species to the genus *Actaea* for, the previous genus *Cimicifuga* is used in the present study to avoid confusion with previous studies from the UIC/NIH Botanical Center. Table II provides details of botanical species transfers and synonyms (3). Throughout this study, the UIC/NIH Botanical Center plant coding system was used for *Cimicifuga* species and plant parts and is summarized in Table I.

TABLE I. PLANT CODE AND PLANT PARTS CODE IN THIS STUDY

Plant species code		Plant parts code	
CR	*C. racemosa*	RR	roots/rhizomes
CA	*C. americana*	PX	aerial parts
CU	*C. rubifolia*		
CE	*C. acerina*		
CD	*C. dahurica*		
CS	*C. simplex*		
CJ	*C. japonica*		
CH	*C. heracleifolia*		

TABLE II SPECIES TRANSFERS IN THE TAXONOMY OF *CIMICIFUGA*/*ACTAEA* (3)

Accepted name	Synomym	Representative other synonyms	Plant Code
Actaea arizonica (S. Watson) J. Compton	*Cimicifuga arizonica* S. Watson		
Actaea bifida (Nakai) J. Compton	*Cimicifuga heracleifolia* var. bifida Nakai		
Actaea biternata (Siebold & Zucc.) Prantl	*Cimicifuga biternata* (Siebold & Zucc.) Miq.	*Pityrosperma obtusifolium* Siebold & Zucc., *Cimicifuga obtusiloba* (Siebold & Zucc.) Miq., *C. japonica* var. *biternata* (Siebold & Zucc.) Maxim. ex Makino, *C. japonica* var. *obtusiloba* (Siebold & Zucc.) Yatabe, etc.	
Actaea brachycarpa (P. K. Hsiao) J. Compton	*Cimicifuga brachycarpa* P. K. Hsiao	*Cimicifuga lancifoliolata* X. F. Pu & M. R. Jia	
Actaea cimicifuga L.	*Cimicifuga foetida* L.		
Actaea cordifolia DC.	*Cimicifuga rubifolia* Kearney	*Cimicifuga cordifolia* (DC.) Torr. & A. Gray [non Pursh 1814, nom. illeg.], *Thalictrodes cordifolia* (DC.) Kuntze, *Cimicifuga racemosa* var. *cordifolia* (DC.) A. Gray	CU
Actaea dahurica (Turcz. ex Fish. & C. A. Mey.) Franch.	*Cimicifuga dahurica* (Turcz. ex Fish. & C. A. Mey.) Maxim.	*Actinospora dahurica* Turcz. ex Fisch. & C. A. Mey.	CD
Actaea elata (Nutt.) Prantl	*Cimicifuga elata* Nutt.	*Thalictrodes elata* (Nutt.) Kuntze	
Actaea europea (Schipcz.) J. Compton	*Cimicifuga europaea* Schipcz.		
Actaea frigida (Royle) Prantl	*Cimicifuga frigida* Royle	*Cimicifuga foetida* var. *longibracteata* P. K. Hsiao, *Cimicifuga foetida* var. *bifida* W. T. Wang & P. K. Hsiao, etc.	
Actaea heracleifolia (Kom.) J. Compton	*Cimicifuga heracleifolia* Kom.		CH
Actaea japonica Thunb.	*Cimicifuga japonica* (Thunb.) Spreng.	*Actaea acerina* Prantl, *Cimicifuga acerina* Tanaka, *Pityrosperma acerinum* Siebold & Zucc., etc.	CJ
Actaea kashmiriana (J. Compton & Hedd.) J. Compton	*Cimicifuga kashmiriana* J. Compton & Hedd.		
Actaea lacinata (S. Watson) J. Compton	*Cimicifuga lacinata* S. Watson		
Actaea mairei (H. Lév.) J. Compton	*Cimicifuga mairei* H. Lév.	*Cimicifuga foetida* L. var. *foliolosa* P. K. Hsiao, etc.	
Actaea matsumaurae (Nakai) J. Compton & Hedd.	*Cimicifuga foetida* var. *matsumurae* Nakai	*Cimicifuga foetida* f. *femina* Huth, *C. foetida* var *leiogyna* H. Takeda	
Actaea podocarpa DC	*Cimicifuga americana* Michx.	*Cimicifuga cordifolia* Pursh, *Cimicifuga podocarpa* (DC.) Elliot, etc.	CA
Actaea purpurea (P. K. Hsiao) J. Compton	*Cimicifuga acerina* f. *purpurea* Hsiao	*Cimicifuga purpurea* (P. K. Hsiao) C. W. Park & H. W.Lee, *Cimicifuga acerina* f. *strigulosa* P. K. Hsiao, etc.	CE
Actaea racemosa L.	*Cimicifuga racemosa* (L.) Nutt.	*Cimicifuga serpentaria* Pursh; Botrophis *serpentaria* Raf., *Botrophis actaeoides* Fisch. & C. A. Mey; *Thalictrodes racemosa* (Kl. Kuntze	CR
Actaea racemosa var. *dissecta* (A. Gray) J. Compton	*Cimicifuga racemosa* var. *dissecta* A. Gray		
Actaea simplex (DC.) Wormsk. ex Prantl	*Cimicifuga foetida* var. *simplex* (DC.) G. Don.	*Cimicifuga simplex* (DC.) Wormsk. ex Trucz., *C. foetida* var. *intermedia* Regel, *C. dahurica*, var. *tschonoskii* Huth, *C. foetid* f. *hermaphrodita* Huth, *C. dahurica* var. *candollei* Huth, etc.	CS
Actaea taiwanensis J. Compton, Hedd. & T. Y. Yang	(new species), related to the N. American A. laciniata		
Actaea yesoensis (Nakai) J. Compton & Hedd.	*Cimicifuga simplex* var. *yesoensis* Nakai	*C. yesoensis* (Nakai) Kudo, *Cimicifuga simplex* f. villosa Nakai	
Actaea yunnanensis (P. K. Hsiao) J. Compton	*Cimicifuga yunnanensis* Hsiao		

2.2. ***Black Cohosh***

The common name black cohosh refers to *Cimicifuga racemosa* (L.) Nutt. [syn. *Actaea racemosa* L.] (CR), which is the most commonly known of the six North American species and the focus of this project. The Native North Americans used the rhizome of this plant for the treatment of a variety of disorders. In the middle of the 20th century it was introduced into Western Europe and has gained increasing importance for the treatment of menopausal complaints (e.g., hot flashes or depression) and dysmenorrhea (4). In 2009, black cohosh based supplements were listed in the top 10 selling herbal supplements in the Food, Drug, Mass Market channel in the United States, and their sales are over eight million USD (5). One concern is that the material source for black cohosh products relies mostly on wild collection, exclusively from Eastern North American hardwood forests, where *C. racemosa* grows as an understory, shade-tolerant, hardy perennial (6). Although some researchers have tried to establish the propagation and cultivation of black cohosh, the plant is over-harvested and wild populations are threatened due to the expanding popularity of the dietary supplement. Since black cohosh is a perennial plant, it can produce new aerial parts in the growth season of every year if only the aerial part would be harvested and roots/rhizomes preserved. Hence, the significance of investigating the chemical constituents and biological potential of the aerial parts, with the aim of determining if they could be used as a replacement for the root/rhizome to diminish the impacts of wild harvest. Considering that there is insufficient knowledge about the aerial parts (PX) of CR, “safety” and “toxicity” evaluations will also be beneficial.

Figure 1. *Cimicifuga racemosa* (L.) Nutt. (Taken in the Atkins medicinal plants garden at UIC, Chicago, IL)

2.3. *Black Cohosh and Women's Health*

Menopause is the period of passage when a women's reproductive system is shutting down. In particular, the ovaries stop producing estrogen and progesterone and there is an increased production of gonadotropin hormones such as luteinizing hormone and follicle stimulating hormone. These hormonal changes can induce a wide variety of vasomotor, vaginal and psychological symptoms and disorders including hot flashes, tissue atrophy, sexual dysfunction, impaired sleep, and emotional disturbances. Accelerated bone demineralization leading to osteoporosis, acceleration of the rate of development of coronary heart disease and cardiovascular fatality can also occur. Hormone replacement therapy (HRT) is an effective intervention for these complaints. However, HRT is implied to be associated with adverse effects and an increased risk of endometrial or breast cancer. Therefore, many women are switching to alternatives (7,8) such as black cohosh in preference to HRT to alleviate menopausal symptoms (9).

Multiple clinical investigations have suggested that black cohosh extracts are effective in reducing the frequency and intensity of hot flashes among perimenopausal and postmenopausal women (10-12), whereas other randomized controlled trials have reported no vasomotor symptom benefits (13,14). Even within double blind, randomized clinical trials, study designs vary in a large degree in terms of trial duration, test material, and outcome measurements (15).

In 2008, the UIC/NIH Botanical Center conducted a randomized, controlled trial, double-blind, 12-month Phase II clinical trial of black cohosh together with red clover (16). The specifics of this study include three important points (17). First, the study recruited a much higher number of non-Caucasian women than in most other menopausal studies.

This could have led to the study cohorts having women with genomic differences from those women historically included in menopausal studies. Second, the test duration of 12 months was longer than many other symptomatic menopausal studies. Third, and possibly most important, is that the botanical products used in this study were authenticated and chemically and biologically standardized. Earlier studies may not have necessarily used botanical intervention materials that underwent such rigorous production and analysis, potentially allowing for the presence of other phytochemical constituents, or even adulterants, in those studies products that could have altered clinical outcomes (17). As a result, of the clinical study neither of the botanicals reduced the frequency of vasomotor symptoms; however, standardized black cohosh and red clover were shown to be safe.

With mixed clinical trial results of black cohosh root extracts, identification of the active principle of *C. racemosa* has represented a challenge. Hence, a variety of *in vitro* assays have been employed to evaluate the activity of *C. racemosa* root/rhizome extracts. Even though the plant is primarily used to alleviate symptoms of menopause in women and as an alternative treatment to hormone replacement therapy (18), evidence for interaction with the estrogen receptors (ER) is scarce.

Interestingly, selective serotonin re-uptake inhibitors (SSRIs), which operate through the serotonin transporter (SERT), have been shown to alleviate hot flashes (19,20). In addition to the SERT, the 5-HT_7 and 5-HT_{1A} serotonin receptors are also involved in thermoregulation, which suggests that agonists for these receptors might be beneficial for the alleviation of hot flashes (21). Accordingly, the serotonergic system was examined as an alternative pathway through which black cohosh may reduce menopausal hot flashes. In this study, it was shown that black cohosh extracts had an affinity for various serotonin receptors, in particular 5-HT_{1A}, 5-HT_{1D}, and 5-HT_7 (21-23).

2.4. *Chemistry of Cimicifuga*

2.4.1 *Roots/Rhizomes Black Cohosh Compounds*

As of May 2011, a total of 112 compounds have been isolated and reported from CRRR. The main components have been identified as triterpenoids and phenyl propanoic acids. Alkaloids have been identified but in considerably smaller amounts (24). Most of the compounds reported are highly oxidized cycloartane-type triterpenoids, that possess a three-member cyclopropane ring formed by carbons C-9, -10, and -19. Advances in NMR technology have enabled the identification of numerous cimigenol type triterpenoids, mostly as glycosides according to NAPRALERT search. Many of the compounds were reported in the 1990s. A characteristic of the cimigenol type compounds is the presence of internal ketal between position C-16/23 and C-16/24, to form a six-and a five-membered ring, respectively. A large number of acteol type triterpenoids has also been isolated from *C. racemosa*. This type of triterpenoid consists of two subtypes, typified by C23-*R* and –*S* configurations, respectively. One of the acteol (23*S*)-type compounds, 23-*epi*-26-deoxyactein, is often used as a marker compound when standardizing black cohosh dietary supplements for their triterpenoid content. Other types of triterpenes, such as the cimiaceroside, dahurinol, shengmanol types are also reported. At present, 23 phenolic compounds have been isolated. Although the isoflavone formononetin was reported in 1985 (25,26), later studies failed to confirm formononetin in CRRR extract (27,28). Most of the phenolic compounds include a cinnamic acid moiety. In terms of alkaloids, 6 compounds, including cimipronidine-type alkaloids, dopargine and N_{ω}-methylserotonin have been reported (24,29). Representative compounds are shown in Figure 2.

Triterpene

Cimigenol type

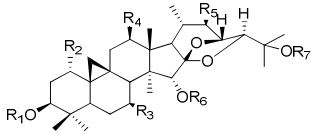

	R1	R2	R3	R4	R5	R6	R7
Cimigenol	H	H	H	H	H	H	H
Cimigenoside=Cimigenol xyloside	xyl	H	H	H	H	H	H
Cimiracemoside C	ara	H	H	H	H	H	H
25-*O*- Methylcimigenoside	xyl	H	H	H	H	H	Me
25-*O* -Methylcimigenosid-3-*O* -α-L-arabinopyranoside	ara	H	H	H	H	H	Me
25-*O* -Acetylcimigenoside	xyl	H	H	H	H	H	Ac
25-*O* -Acetylcimigenol-3-*O*- α-L-arabinopyranoside	ara	H	H	H	H	H	Ac
12β-hydroxycimigenol-3-*O*- α-L-arabinos							
12β-Acetoxycimigenol-3-*O*-β-D-xyloside							

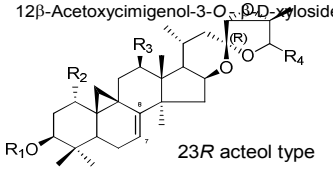

23*R* acteol type

	R1	R2	R3	R4	7,8
26-Desoxyactylacteol	H	H	OAc	H	2H
27-Deoxyacetin=26-Deoxyacetin	xyl	H	OAc	H	2H
Acetylacteol	H	H	H	OH	2H
Acetin (26*S* =α-OH, 26*R* =β-OH)	xyl	H	OAc	α&β-C	2H

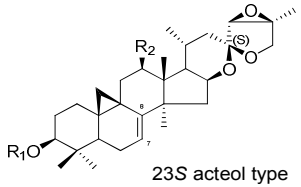

23*S* acteol type

	R1	R2	7,8
23-*epi* -26-Deoxyactein	xyl	OAc	2H
Cimiracemoside N	ara	OAc	2H
Cimiracemoside I	xyl	H	$\Delta^{7,8}$

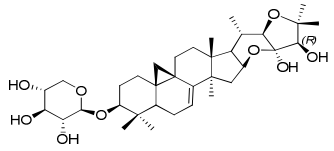

Cimiaceroside A

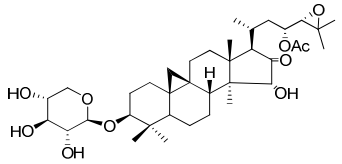

23-*O*-Acetylshengmanol xyloside

Phenolics

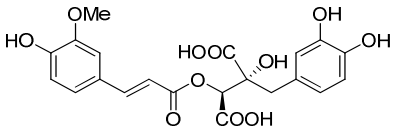

Cimicifugic acid A

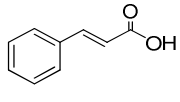

Cinnamic acid

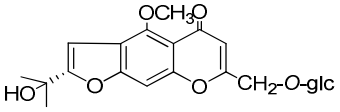

Cimicifugin glucoside

Alkaloids

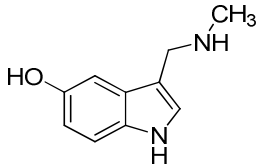

N_{ω}-methylserotonin

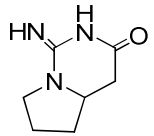

Cyclo-cimipronidine

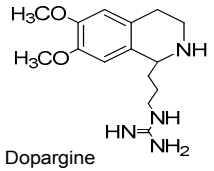

Dopargine

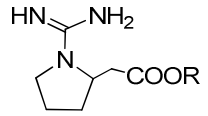

Cimipronidine R=H
Cimipronidine methyl ester R= CH_3

Figure 2. Representative known constituents of *C. racemosa*

2.4.2 *Aerial parts-compound Studies*

Although the NAPRALERT database contains a large number of studies of *C. racemosa* (54 citations and 112 compounds), none of the studies focus on the aerial parts. In 1965, Crum *et al*. (30) screened some native Ohio plants, including *C. racemosa*, in terms of their alkaloid content using alkaloid reagents (Dragendorff, Mayer, Sonnenschein etc.). In that study, plants were separated into three parts: leaves/stems, roots and seeds. Of these 3 parts, alkaloids were detected only in the seeds of CR. However, to date the chemical content of the seed alkaloids has not been determined. The first alkaloid cimipronidine was reported from the roots/rhizome of *C. racemosa* in 2005 by Fabricant *et al*. (24,31). Recently, Gödecke *et al*. (29) reported several new guanidine alkaloids from CRRR. These reports suggest that it will be useful to identify alkaloids and determine their contents in the aerial parts of the plants.

Extensive literature searches for other medicinally used *Cimicifuga* species such as *C. simplex* (listed in the Japanese pharmacopoeia) and *C. dahurica* (listed in both the Japanese and Chinese pharmacopoeia) revealed that several research groups are working on these species. The research of Kusano *et al*., Liu *et al*. and Akihisa *et al*., discovered 40 compounds from the aerial parts (32,33). There are unique compounds in the aerial parts, although many compounds are found in both the aerial parts and the roots/rhizomes. Significantly, a new alkaloid, 2-hydroxy-7-methyl-9H-carbazole, was isolated from the aerial parts of *C. simplex*, although no nitrogen-containing compounds have been reported from the roots/rhizomes of this plant (34). In 2001, Kusano *et al*. reported differences in phytoconstituents between the roots/rhizome and the aerial parts of *C. simplex* by analyzing a total of 66 cycloartane triterpene glycosides and their malonic

esters (35). While 1α/7β/12β-OH derivatives of triterpenes, such as 1α-hydroxycimigenol glycosides, were isolated both from the aerial parts and the roots/rhizomes. A 7β-OH derivative has not been isolated from the roots/rhizomes, but a 7,8-dehydro derivative was found instead (36,37). Based on previous studies of *C. racemosa,* and other medicinally-used *Cimicifuga* species, it is significant to explore the chemical diversity of the aerial parts of *C. racemosa*.

TABLE III. REPORTS ON COMPOUNDS FROM *CIMICIFUGA* SPECIES

Species	Parts	Literature	Compounds	Note
C. racemosa	**Aerial**	**0**	**0**	
	All	54	112	
C. simplex	**Aerial**	**8**	**31 (aerial unique 28)**	Triterpene, Indole alkaloid
	All	33	138	
C. dahurica	**Aerial**	**3**	**9 (all aerial unique)**	Triterpene
	All	31	86	

2.5. *Cimicifuga Adulteration and Standardization Method*

Ensuring the authenticity of a botanical is an essential step for the safe use of botanical dietary supplements. Toxicity resulting from the misidentification of plant material used in the production of botanical dietary supplements has been reported (38). In black cohosh-based dietary supplements, adulterations have been observed in which *C. racemosa* is mixed with other species of the same genus, most commonly *C. americana* (syn.: *Actaea podocarpa* DC. yellow cohosh) (36). *C. americana* is easily confused with black cohosh since both species share the same habitat in the eastern United States; furthermore, the dry, dark rhizomes alone are difficult to distinguish outside the laboratory. Two other plants, red cohosh (*C. rubra* (Aiton) Willd., syn.: *A. neglecta* Gillman) and white

cohosh *(A. pachypoda* Elliott), also occupy the same habitat, but adulteration with black cohosh occurs rarely because the smaller roots of these species are generally not harvested by wildcrafters. As a consequence of the growing popularity of CR dietary supplements in North America, adulteration with the more abundant and less-expensive Asian *Cimicifug*a species is increasing. In the United States and Europe, Asian *C. foetida* L. (syn.: *A. cimicifuga* L.), *C. heracleifolia* Kom., and *C. dahurica* (Turcz.) Maxim are regarded as adulterants. The genus *Actaea* also has temperate species with numerous common names, that can contribute to the misidentification of plant material (39). Adulteration and/or plant misidentification of black cohosh can potentially lead to serious health concerns. Several species of *Actaea* that are listed as potential adulterants of black cohosh are even described as poisonous. For example, *Actaea rubra* is reported to include a poisonous essential oil or glycoside in all parts of the plant but mostly concentrated in the berries, sap, and roots (40,41). Symptoms of poisoning include gastroenteritis, stomach cramps, headache, dizziness, vomiting, diarrhea and circulatory failure.

As described above, the adulteration of the black cohosh dietary supplements involves numerous related species. It is, therefore, difficult to develop standardization methods that recognize all potential adulterants. Current mainstream methods in the United States Pharmacopeia for *C. racemosa* standardization rely on triterpene glycoside determination by HPLC using evaporative light-scattering detection (ELSD). Although the quantity of triterpene glycosides is calculated based on 23-*epi*-26-deoxyactein according to the US pharmacopeia, this compound is present in many American species (*A. racemosa* [syn. *C. racemosa*] *A. podocarpa* [syn. *C. americana*], *A. pachypoda*, and *A. rubra*) examined and all Asian species in commerce (42,43). Currently, cimiracemoside C

appears to be a better exclusive marker for *A racemosa*, whereas cimicifugin and its glycoside might best serve as indicators for the Asian species (44,45).

Of several *Cimicifuga* and *Actaea* species studied for standardization purpose, *C. americana* (syn.: *A. podocarpa*) exhibited a clearly distinctive profile. He *et al*. identified cimicifugic acid A, ferulic acid, 2-feruloyl piscidic acid in the 75% methanol extract of *C. americana* by an HPLC method (46). *C. americana* has thus far been shown to contain distinctive compounds, the podocarpasides (47) (Figure 3 represents an example), which have been isolated from the roots (48). The important common features in all the podocarpasides are six tertiary methyls (Me-18, 28, 26, 27, 29 and 30) a secondary methyl (Me-21), a hydroxyl at C-25, α-L-arabinose attached to C-3, ketones at C-16 and C-23, and a C-9-C-11 olefinic bond. The most notable is that podocarpasides do not possess a cyclopropane ring at C9 and 10, which is present in the major triterpene type of *Cimicifuga* species. *C. americana* did not show the presence of cimiracemoside A, 23-*epi*-26-deoxyactein, or actein.

Studies that investigate the adulteration of black cohosh by other plant parts of CR have not been reported.

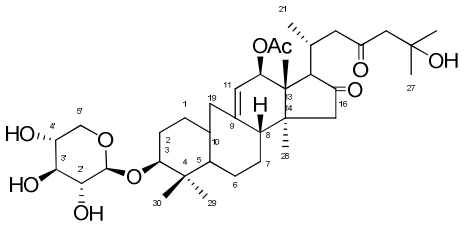

Figure 3. Podocarpaside A

3. **Aim 1 Phytochemical Proofing of CR Aerial Parts**

3.1. *Materials and Methods*

3.1.1 *Plant Material*

The sources of materials for the present study are summarized in Table IV. The aerial parts of *Cimicifuga racemosa* (L.) Nutt. (CRPX) was cultivated in the Dorothy Bradley Atkins Medicinal Plant Garden at UIC by Mike Totura. Wild collections of CR were also performed by the UIC/ NIH Botanical Center by Dr. Daniel Fabricant with support by Dr. Gwynn Ramsey from several different locations in Pennsylvania, Illinois and Tennessee (48). Voucher specimens are housed at the Searle Herbarium of the Field Museum of Natural History (Chicago, IL) and the Ramsey-Freer Herbarium of Lynchburg College (Lynchburg, VA).

In the present study, two separate extraction/isolation processes were carried out. The first experiment was conducted with 200g of BC 026. A second extraction involved a combination of BC 401, 032, 043, and 018 for a total of 4.7kg of CRPX.

TABLE IV. LIST OF PLANT MATERIAL OF CR FOR THE PRESENT STUDY + ISOLATION OF COMPOUNDS

Genus	Species	Parts	BC number	Collection date	Collection Site
Cimicifuga	*racemosa*	PX	BC018	8/26/1999	Sevier County, TN. Elevation 3300 ft.
Cimicifuga	*racemosa*	PX	BC026	6/29/1999	Sevier County, TN. Elevation 3500 ft.
Cimicifuga	*racemosa*	PX	BC032	6/22/1999	Butler County, PA.
Cimicifuga	*racemosa*	PX	BC043	5/30/1999	Somerset County,.PA.
Cimicifuga	*racemosa*	PX	BC401	10/1/2007	Cook County, IL.
Cimicifuga	*racemosa*	PX	BC017	8/26/1999	Sevier County, TN. Elevation 3300 ft.
Cimicifuga	*racemosa*	PX	BC582	10/6/2009	Atkins Garden, Cook County, IL
Cimicifuga	*racemosa*	RR	BC581	10/6/2009	Atkins Garden, Cook County, IL

3.1.2 *Thin-Layer Chromatography (TLC)*

Preparative chromatography was monitored by TLC analysis. Analytical TLC was performed on pre-coated Alugram® SIL G/UV silica gel 60 aluminum plates (0.20 mm) with UV_{254} fluorescent indicator (10 x 20 cm; Macherey-Nagel, Düren, Germany). Plates were carefully spotted with samples in evenly spaced 4 mm wide dashes. All TLC plates were monitored under UV light at wavelengths of 254 and 365 nm, then sprayed with general purpose reagent (1:4:94 vanillin: H_2SO_4: EtOH) followed by heating with a heat gun. The developing solvent systems varied based on sample polarity.

3.1.3 *Countercurrent Chromatography (CCC)*

High Speed Countercurrent Chromatography (HSCCC) separations were conducted on a CCC-1000 J-type three-coiled planetary motion instrument (Pharma-Tech Research Corp., Baltimore, MD, USA), which has a rotation radius of 7.5 cm and was equipped with a Lab-Alliance Series III digital single-piston solvent pump, and a Pharmacia Biotech RediFrac 95-tube fraction collector. Two different coil sets were used in accord and with the size of the sample for the separation, as follows:

- 850 ml set, using 3 x 283 ml PTFE Teflon coils with 2.6 mm i.d., 4.1 mm o.d., and beta values from 0.47 to 0.73.
- 320 ml set, using 3 x 107 ml PTFE Teflon tubing coils with 1.6 mm i.d., 2.6 mm o.d., and beta values from 0.47 to 0.73.

FCPC separations were performed on a Kromaton FCPC instrument with 1 L (true volume 943 ml) and 200 ml (true volume 195 ml) rotors, using 1/16” connections.

The choice of solvent system was based on the polarity of the sample and the conditions of the previous separation step. Solvent system nomenclature is in accord with the GUESS system (49).

3.1.4 *Vacuum Liquid Chromatography (VLC)*

Appropriately-sized “Quick Separation Funnels” (Chemglass Inc., Vineland, NJ) were prepared by first cutting three pieces of filter paper into disks with the same diameter as the inner diameter of the column. The first paper disk was then nested on top of the frits at the bottom of the column. Next, while applying a vacuum, the indicated amount of dry silica gel (Merck 60Å, 70-230 mesh) was poured evenly and slowly while still maintaining a constant flow of the powder into the column. The vacuum was continuously applied after all the silica gel had been loaded, and the column tapped and tamped until a uniform cylinder of silica gel was obtained. The second filter paper disk was then placed on top of the silica gel as the bottom half of the sample sandwich, and the third was the top half. The sample, in an appropriate solvent, was mixed with silica gel to homogenize the sample and placed between the second and the third disks. The eluting solvent was introduced onto the top of the column above the third disk and reduced pressure was applied to the bottom of the column. Fractions were then collected into appropriate sized round bottom flasks, which were then evaporated to dryness. The residues were transferred to small vials using a minimum volume of the appropriate solvent.

3.1.5 *High Pressure Liquid Chromatography (HPLC)*

HPLC was carried out with a Waters Delta 600 system equipped with a Waters 996 photodiode array (PDA) detector, Waters 717 plus autosampler, and Millennium 32,

Empower, Chromatography Manager (Waters Corp.), using a YMC ODS-AQ (10x250mm) column. An inline Sedex 75 Evaporative Light Scattering Detector (ELSD) (Sedere, France) was also used for some triterpene isolation at variable nitrogen pressure and variable nebulizing temperature, with the output signal (mV) connected to the Millennium 32™ Empower software through a SAT/IN analogue box. The following solvent system was used unless noted: a gradient from 30%−40% A in 30 min, and then 40%-60% A between 30 to 70 min, all at a flow rate of 4 mL/min, where A is ACN and B is H_2O.

3.1.6 *Mass Spectrometry (MS)*

Accurate mass was obtained by HR-LC-ESI-MS using a Waters SYNAPT Quadrupole/ Time-of-Flight spectrometer. A Hypersil GOLD 2.1 × 150-mm 5-µm column was used with a gradient solvent system from 30%−70% B in 20 min and then 70%-100% B in 25 min at a flow rate of 0.2 mL/min, where A is 0.1% aqueous formic acid and B is 95% ACN/0.1% formic acid. Unless explicitly stated, the mass spectrometer was operated in positive ionization mode.

3.1.7 *Nuclear Magnetic Resonance (NMR)*

NMR spectra were recorded on a Bruker AVANCE 400 MHz spectrometer equipped with a 5 mm BBO probe, a Bruker AVANCE 600 MHz or a 900 MHz NMR spectrometer equipped with 5 mm TCI cryoprobes at 25 °C. Routine NMR experiments were carried out with assistance of or by Dr. David C. Lankin. For select samples, data were also collected on a Bruker AVANCE III 700 MHz instrument with a 1.7 mm TXI cryoprobe at NRC-IMB (The National Research Council Institute for Marine Biosciences, Halifax, N.S., Canada) by Mr. Ian Burton, Drs. John Walter and Tobias Karakach. Offline

data processing and analysis was conducted using the following software packages: TopSpin version 3.0 (Bruker, Billerica, Massachusetts, USA), NUTS 2D Professional Version - 20070706 (AcornNMR, Livermore, CA, USA), MestReNova version 6.2.1 (MESTRELAB RESEARCH SL, Santiago de Compostela, SPAIN), PERCH version 2008.1 SA (PERCH solutions, Kuopio, Finland), and the HNMR and CNMR databases of ACD Labs NMR Suite version 12.01 (Advanced Chemistry Development, Inc.). The line resolution of routine ^{1}H NMR experimental data was enhanced by Gaussian Multiplication (GM) transformation of the FID using the following function (Equation 1 (50)), which represents the Gaussian Resolution Enhancement envelope ($Y_{GRE}(t)$). Bruker's Topspin software permits indirect control of the parameter ρ by means of the parameter GB, where GB = t_{max}/AQ, with AQ being the acquisition time of the FID. Equation 1 can be rewritten by using Bruker parameters as shown in Equation 2. Exponential Multiplication (EM), Sine Multiplication, Sine squared Multiplication were also used as required, along with appropriate parameters, such as SSB (Sine bell shift). The list of dependent parameters for each window function is Table V. Standard pulse programs used were: zg30 for ^{1}H NMR, cosygpqf for ^{1}H-^{1}H COSY, hsqcetgpsi2 for ^{1}H-^{13}C HSQC, and hmbcetgpnd for HMBC. Other pulse programs were used as required.

Gaussian multiplication (GM)

$$Y_{GRE}(t) = \mathbf{exp}\left[(\pi W_0 t) - \frac{(\boldsymbol{\pi \rho W_0 t})}{(\boldsymbol{4ln2})}\right] \quad \textbf{Equation 1}$$

where the shown parameters are defined by:

$t_{max} = \frac{2ln2}{\pi W_0 \rho^2}$, W_0: the final line width

$$\boldsymbol{Y_{GRE}(t)} = \mathbf{exp}\left((-\boldsymbol{at}) - \left(-\boldsymbol{bt^2}\right)\right) \qquad \textbf{Equation 2}$$

where t is the acquisition time in seconds and a and b are defined by:

$$a = \pi \cdot LB \text{ and } b = -\frac{a}{2GB \cdot AQ}$$

GB: Gaussian broadening factor, LB: Line broadening factor (in Bruker's Topspin)

TABLE V. NMR PROCESSING WINDOW FUNCTION AND PARAMETERS

	Function	Dependent Parameters
EM	Exponential	LB
GM	Gaussian	GB, LB
SINE	Sine	SSB (Sine bell shift)
QSINE	Sine squared	SSB

3.2. *Phytochemical Results and Discussion*

3.2.1 *Dry Mass and Extract Yields of Aerial Parts and Roots/rhizomes*

Whole CR plants of were collected on 10/06/2009 from the Dorothy Bradley Atkins Medicinal Plant Garden at UIC. The roots/rhizomes (CRRR) and the aerial parts (CRPX) were carefully separated and the dry mass was obtained after drying at room temperature. As an example, one plant yielded 49 g of roots/rhizomes and 24 g of aerial parts. Dried material (1 g) yielded 207.3 mg (CRPX) and 255.4 mg (CRRR) of total extracts by sequential extraction with PE, DCM and 75% EtOH. The composition of the extractables in the three extracts varied in PX vs. RR. More lipophilic extractables were obtained from CRPX than from CRRR. The combined lipophilic (PE and DCM) extracts of CRPX consisted of a total of ca. 3 % of dry plants. By comparison, the lipophilic extracts of CRRR dried plant material comprised only 0.1 % (PE extract) and 0.7 % (DCM extract).

TABLE VI. EXTRACT YIELDS IN mg / 1g OF DRY MATERIAL (CRPX: AERIAL PARTS BC582, CRRR: ROOTS BC581)

	PX		RR	
Column1	**yield (mg)**	**yield % of dry plant**	**yield (mg)**	**yield % of dry plant**
PE	10.3	1.1%	0.8	0.1 %
DCM	19.0	1.9 %	6.5	0.7 %
75%EtOH	178.0	17.8 %	248.1	24.8 %
Total	207.3	20.7 %	255.4	25.5 %

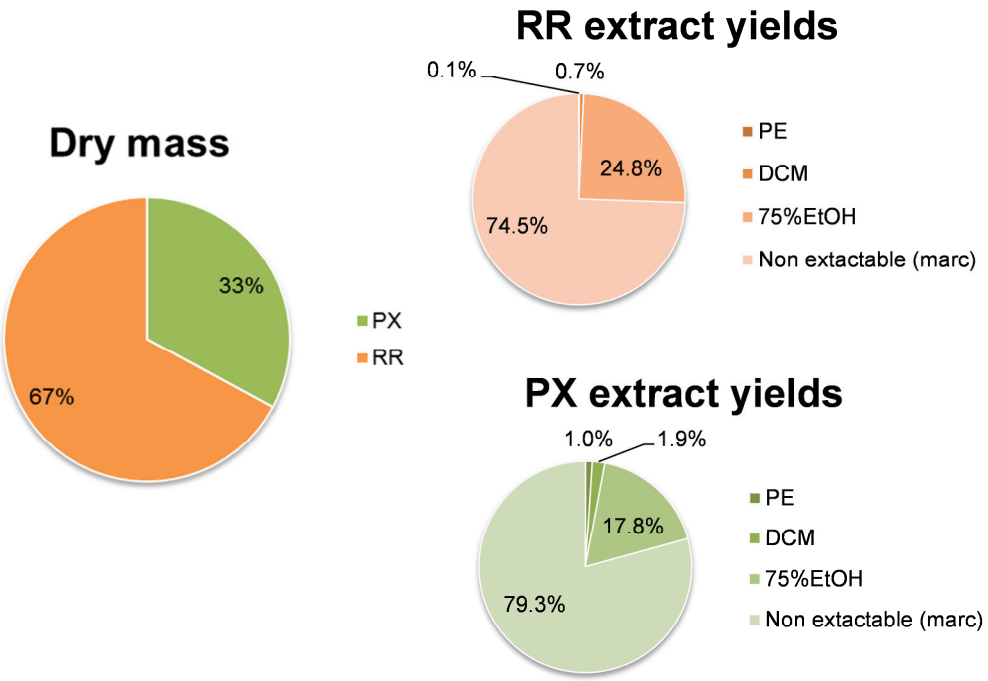

Figure 4. Dry mass of CRRR and CRPX, and ratio of extract yields extraction of plant material and first level partition

Two batches of plant material were dried, ground and sequentially extracted with PE, DCM and 75% EtOH by percolation to cover a wide polarity range. The first batch was 298 g of BC026 and the second batch was 4688 g of combined plant material (BC401 2959 g, BC032 650 g, BC043 766 g, BC 018 313 g). The extracts were concentrated *in vacuo* and the yields are shown in Table VII. The efficiency of this large scale extraction was lower than that of the small scale extraction.

TABLE VII. WEIGHT AND YIELD OF EXTRACTS OBTAINED

Plant material	Solvent	Sample code	Extract weight (g)	Percentage yield
200 g	PE	CR02-43-11	1.55	1%
(BC026)	DCM	CR02-43-18	4.89	2%
	75%EtOH	CR02-43-34	101.35	34%

Plant material	Solvent	Sample code	Extract weight (g)	Percentage yield
4.7 kg	PE	CR10-56-25	128.61	3%
(BC401 2959 g, BC032 650 g, BC043 766 g, BC 018 313g)	DCM	CR10-56-27	68.4	1%
	75%EtOH	CR10-56-29	551.81	12%

The dried extracts (CR02-43-11, 18, 34) from BC 026 were combined in proportion to the yield of each of the extracts to produce 20 g of a total extract. This combined extract was partitioned in a separatory funnel in 400 ml of a solvent system consisting of *n*-Hexane, EtOAc, MeOH, Water 1:9:1:9 (HEMWat +7) for five times to provide 3.2 g of upper phase-soluble partition (CR10-77-01) and 16.0 g of lower phase-soluble partition (CR10-77-03). Insoluble material (0.3 g) was obtained from the boundary area between upper phase and lower phase.

The extracts from 4.688 kg of combined plant material, CR10-56-25, 27, 29, were not partitioned prior to the fractionation.

3.2.2 *Isolation of Compounds*

Isolation of New Compounds 1 and 2 Together with Known compounds 3-8

The lower-phase of partition, CR10-77-03 (16 g), was chromatographed on a normal phase silica gel VLC (240 g) and eluted with Hex to EtOAc, then EtOAc to MeOH, and finally MeOH to H_2O each in a 5% step gradient to yield 62 fractions. Fractions 19-27, which eluted from a mixture of 10% Hex and 90% EtOAc to a mixture of 70% EtOAc and

30% MeOH were combined based on their TLC profiles and further fractionated by CPC with the ChMWat 0 solvent system ($CHCl_3$: MeOH: Water, 10:3:7) using upper-phase as a mobile phase into 6 subfractions. Preparative HPLC of subfraction 4 with was carried out as a next step. An ACN-water gradient solvent system was employed with gradient from 30 % ACN to 40% ACN within 30 min and 40% to 60 % in the following 40 min at a flow rate of 4 ml/min. The new compounds 24-*epi*-1α-hydroxycimigenol-3-*O*-β-D-xylopyranoside (**1**) eluted at a retention time of 41 to 44 min and 1α-hydroxydahurinol-3-*O*-α-L-arabinopyranoside at a retention time of 62 min (**2**) together with known compounds, 1α-hydroxycimigenol-3-*O*-α-L-arabinopyranoside (**3**) at a retention time of 54 to 58 min 1α-hydroxycimigenol-3-*O*-β-D-xylopyranoside (**4**) at a retention time of 66 min.

VLC fractions 11-16, which eluted with a mixture of 50% Hex and 50% EtOAc to a mixture of 25% Hex and 75% EtOAc, were further chromatographed in a NP VLC using a solvent system gradient of PE: $CHCl_3$: MeOH (5: 9: 1) to $CHCl_3$: MeOH (9:1) to MeOH to yield 44 subfractions. Subtractions 6-10, which eluted with PE: $CHCl_3$: MeOH (5: 9: 1) after ca. one column volume, were combined according to TLC profile. Preparative HPLC of combined fraction, with previously described condition, yielded 7β-hydroxycimigenol aglycone (**5**) at a retention time of 43 min and of subfractions of 11-13 yielded 25-*O*-acetyl-7β-hydroxycimigenol-3-*O*-β-D-xylopyranoside (**6**) at a retention time of 26 min, 25-*O*-acetylcimigenol-3-*O*-β-D-xylopyranoside (**7**) at a retention time of 43 min, and 24-*O*-acetylhydroshengmanol-3-*O*-β-D-xylopyranoside (**8**) at a retention time of 54 min.

Isolation of Known Compounds 9 and 10

The upper-phase partition, CR10-77-01 (3.2 g), was subjected to FCPC using the ChMWat 0 solvent system ($CHCl_3$: MeOH: Water, 10: 3: 3mixture) using upper phase as a

mobile phase to yield 4 combined fractions. FCPC fraction 2 was further fractionated by HSCCC with an orthogonal solvent system, HETeMWat (Hex: *tert*-Butyl methyl ether: MeOH, Water mixture), a derivative of the HEMWat solvent system family that uses tBME instead of EtOAc. Nine combined fractions were obtained from this fractionation, and subfractions 1-5 were combined on the basis of the TLC profile. The combined subfraction (1-5) was then subjected to another HSCCC with HEMWat -4 (Hex: EtOAc: MeOH: Water 7: 3: 6: 4) to yield cimigenol aglycone (**9**) and cimiaceroside A (**10**).

Isolation of Known Compounds 11 and 12

The DCM extract (CR10-56-27, 68 g) of the combined plant material was defatted by partitioning between PE (CR10-87-03) and 10% MeOH in H_2O (CR10-87-04) in a separatory funnel. The methanolic aqueous solubles, CR10-87-04 were chromatographed by RP VLC using a 50% MeOH/H_2O-100% MeOH-DCM gradient to yield 11 fractions (CR10-90-x series). Fraction 4 was further fractionated by NP VLC using a 95% $CHCl_3$ 5% MeOH to 35% $CHCl_3$ 65% MeOH gradient to yield 31 fractions. The 31 subfractions were combined to 11 (CR10-91-x series) according to their TLC profile. During evaporation, fraction 5 separated into a white powder, cimiramoside I (**11**), and a greenish yellow residue. Two more steps of chromatography on CR10-91-06 yielded cimigenol-3-*O*-β-D-xylopyranoside (**12**), as follows: The first step was an HSCCC using a HEMWat +3 (Hex: EtOAc: MeOH: Water 4: 6: 4: 6) to yield 6 fractions (CR10-96-x series). Then, fraction 2 (CR10-96-02) was subjected to RP HPLC using an ACN and H_2O gradient solvent system to yield **12**.

Isolation of Known Compounds 13 and 14

The 75% EtOH extract (CR10-56-29 551.8 g) of the combined plant material was reconstituted in deionized water (2000 mL) and partitioned with PE (1000ml ×3; 23.9 g).

The aqueous fraction was then partitioned with EtOAc (1000ml ×11; 204.6 g), and the aqueous phase was directly subjected to column chromatography on Amberlite XAD-2 (Sigma, St. Louis, MO; 350g, 8.5 x 20 cm, 1 L) and then washed with MeOH (2 L), yielding two fractions (H_2O; CR10-80-09 287.2 g and MeOH; CR10-90-11 54.1 g). The MeOH fraction (CR10-90-11) was further fractionated by RP VLC (Polygoprep 100, Macherey-Nagel, 350g, 8.5 x 20 cm, 1L) using a 20% MeOH- 100% MeOH step gradient to yield 13 fractions (CR10-88-x series). Fraction 5 (CR10-88-05), was subjected to Sephadex LH-20 (Amersham Biosciences, Piscataway, NJ; 100 g, 20 cm × 2 m , 200 mL). Elution was carried out with the isocratic solvent system of 75% MeOH, yielding quercetin-3-*O*-β-arabinopyranosyl-(1→6)-β-galactopyranoside (**13**) and kaempferol-3-*O*-β-arabinopyranosyl-(1→6)-β-galactopyranoside (**14**).

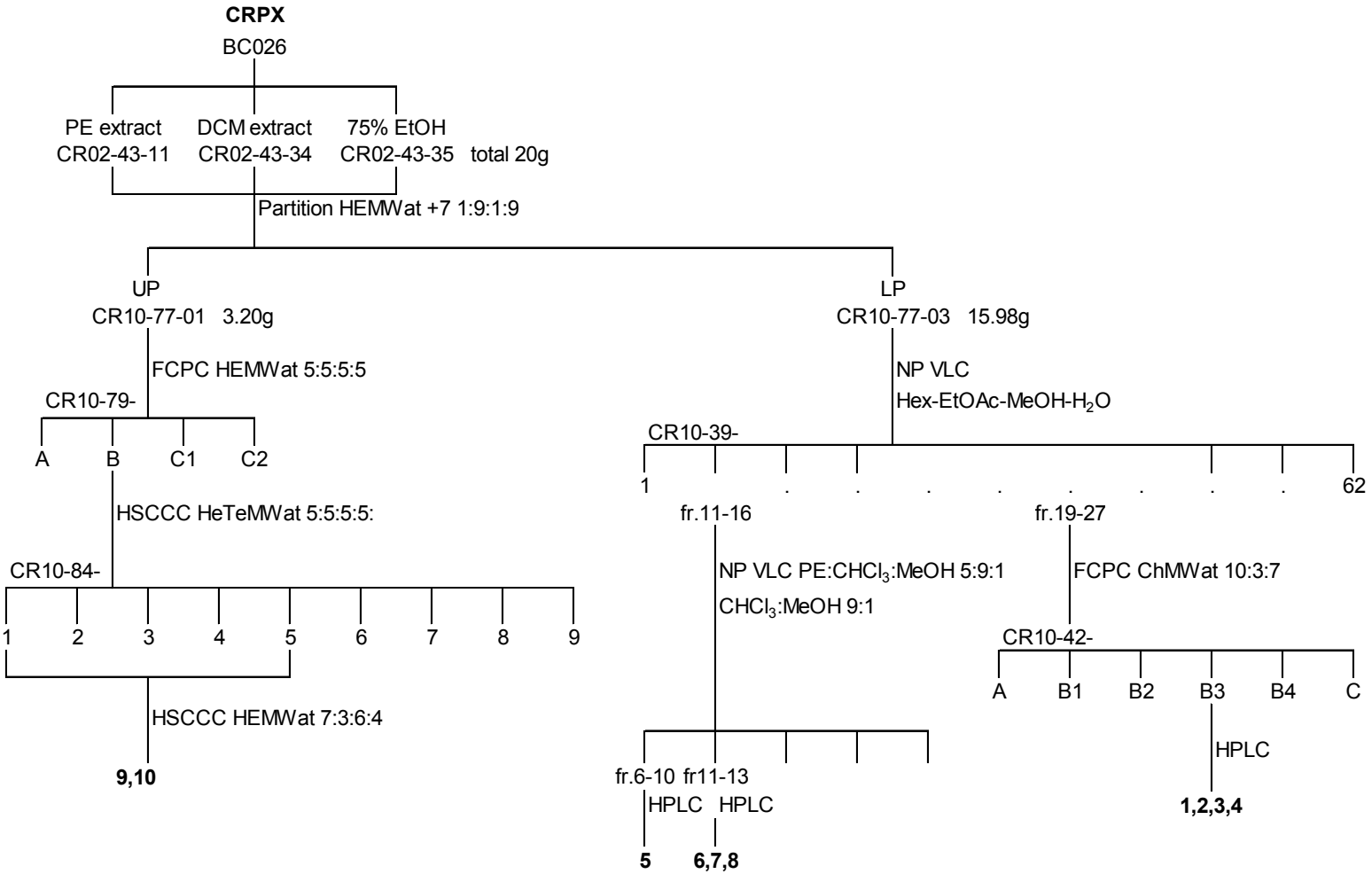

Figure 5. Fractionation/isolation scheme for compounds 1-10

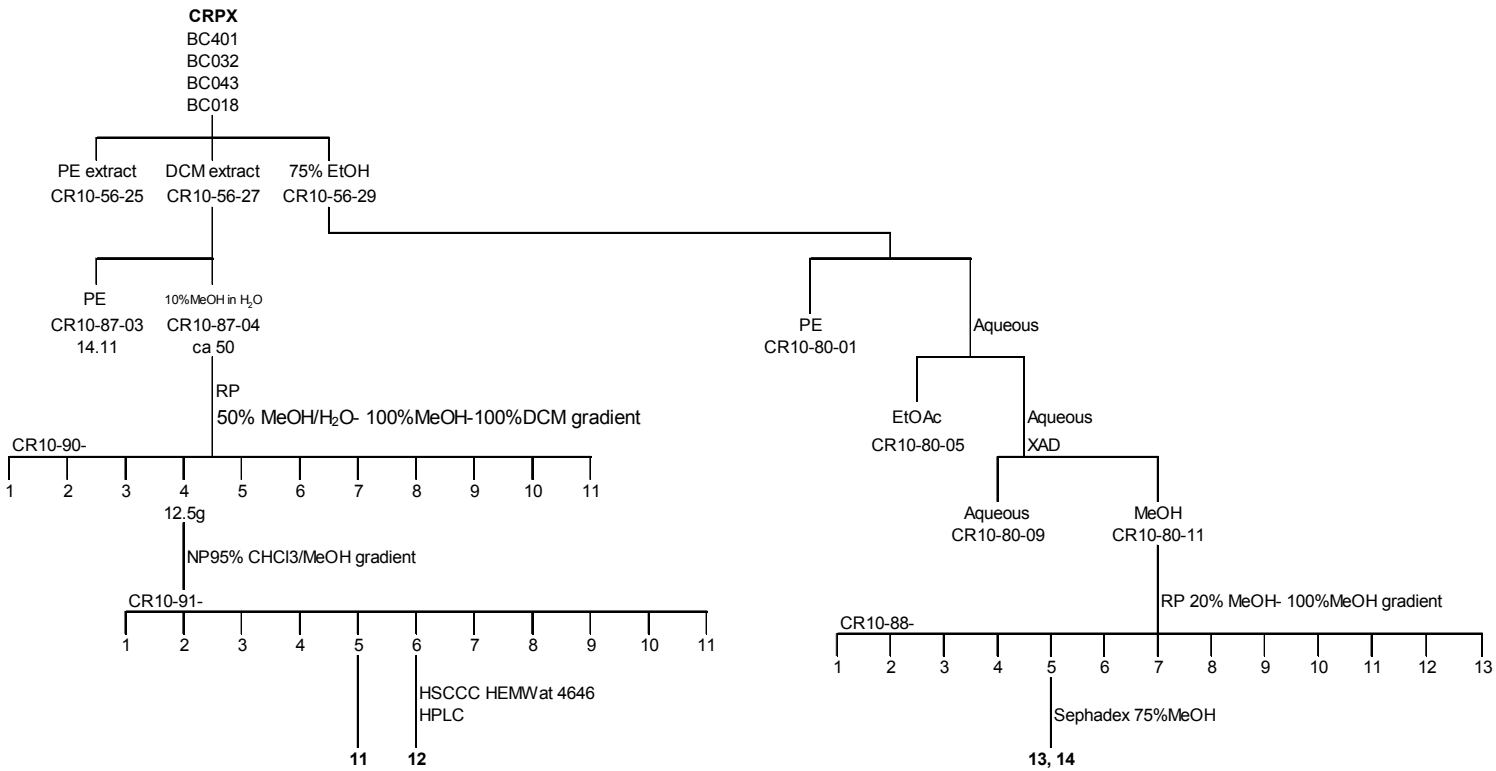

Figure 6. Fractionation/isolation scheme for compounds 11-14

3.2.3 *Characterization of Compounds: Triterpenes*

Dereplication of Cimicifuga Cycloartane Triterpenes

To date, over 150 triterpene glycosides and aglycones have been reported from *Cimicifuga* species. The majority of them belong to the class of cycloartanols and possess a cyclopropane ring fused to C-9, C-10 and C-19, i.e., they have the cycloartane skeleton, which gives rise to a pair of unique signals in the high field region of the ^{1}H NMR spectrum.

In this study, 12 cycloartane triterpenes were isolated and their structures elucidated by extensive combination of NMR techniques together with HR-LC-MS. The isolates included both glycosides and aglycones of several analogs of cycloartane triterpenes including cimigenol, acteol, dahurinol, and the shengmanol type compounds. Out of all the isolates, there were two new compounds. Five have previously been reported but from other *Cimicifuga* species or as semisynthetic derivatives and were isolated from the aerial parts of *C. racemosa* for the first time. For the new compounds, extensive analysis of ^{1}H NMR spectra was performed using high magnetic field NMR (700 MHz / 900 MHz), post-acquisition processing of the acquired NMR data, 2D NMR experiments (e.g., gradient COSY, phase sensitive HSQC, HMBC, and ROESY) together with full spin analysis using PERCH. Through this intensive analysis, all of the signals (both ^{1}H and ^{13}C) could be unambiguously assigned, as could the relative configurations of the compounds. By accumulating a thorough knowledge about ^{1}H NMR spectra of cycloartane triterpenes including the chemical shifts and coupling patterns, dereplication of known compounds and partial dereplication of new compounds can be facilitated. As a partial result of this study, two approaches for Structure Elucidation of TriTerpenes (SETT) are proposed.

SETT 1. The Building Block Method

Several substructural components within the cycloartane triterpene ring system vary and hence these define the specific compound within this class. They are: 1) the nature of the side chain, 2) the carbohydrate component, 3) the presence and positions of hydroxyl and acetyl substitutions, and 4) presence and position of double bonds (unsaturation). Determination of the nature of each of these components is indicated by the appropriate diagnostic peaks in the NMR spectrum and then by assembling the pieces permits elucidation of the whole structure. This methodology is useful for the dereplication of known compounds, as well as partial structure elucidation of new compounds.

SETT 2. The Survey Method Using Chemical Shift Information of Methyls + 19 Methylenes

Even in a complex ^{1}H NMR spectrum such as that of the cycloartane triterpene, methyl signals are easily identified because they are usually intense, sharp singlets or doublets. In the case of CR triterpenes, the C-21 methyl is a doublet and the triterpene skeletal methyls and side chain methyls are typically singlets. In addition to the methyl signals, in the cycloartanes, the cyclopropane methylene protons at C-19 are readily identified because of their unique high-field chemical shifts. Thus, the combination of chemical shift and multiplicity information of the methyl signals and the C-19 methylene protons usually provides 8 or 9 characteristic pieces of information that can be easily recognized, even in low resolution spectra, impure samples, or in mixtures. The

chemical shift of every signal in the ^{1}H NMR spectrum will be affected by its chemical environment, and some typical examples of the resulting substituent chemical shifts (s.c.s.) are presented in the following section. It is reasonable to consider that each methyl/methylene signal acts as a "reporter nucleus" for its surrounding environment, and that every compound gives rise to a unique signal pattern of these 8-9 representative "reporter" signals. In other words, pattern recognition of the methyls and C-19 methylene "reporter" protons can assist in the dereplication of known compounds and in the identification of partial structures.

SETT1 The Building Block Method: A typical flow of the structure determination process using this method is described below. In each step, one portion of the partial structure is identified.

Steps

Step A. Is there a sugar? If yes, which sugar?

e.g. arabinopyranoside? xylopyranoside? Or other sugar?

Step B. What type of triterpene is it? What type of side chain does it contain?

e.g. cimigenol

Step C. Is there 7-8 unsaturation in the triterpene?

e.g. 7,8-dehydrocimigenol-3-*O*-β–D-xylopyranoside

Step D. Are there any ring substitutions? In particular, hydroxylation and acetylation?

e.g. 1α-OH 1α –hydroxyl- 7,8-dehydrocimigenol-3-O-β D-xylopyranoside

SETT 1A. The Presence and Nature of the Sugar

Xylose and arabinose in their pyranoside form represent the predominant sugar moieties in cycloartane triterpene glycosides isolated from *Cimicifuga* species. A full spin system analysis was carried out for those sugars using the ^{1}H spectra of isolates from CRPX, **4** and **2**, to analyze fully their spin-spin coupling patterns (Figure 7) and the glycoside numbering system (1'-5') was employed in this section for both aldopentoses. This xyl-*p* and ara-*p* pair of stereoisomers is epimeric at the chiral center C-4', which affects the signal pattern of protons 3,' 4' and the methylene 5'. Based on all the changes observed, protons H-5'α, β are the most suitable marker signals for the purpose of dereplication, due to their clear multiplicity and appearance in a relatively uncrowded spectral region. In arabinose, H-5'β appears at higher field compared to H-5'α as a pseudo-doublet with a splitting of about ~12 Hz (Figure 8). Upon close inspection using PERCH simulation, the H-5'β signal of is a dd because H-5'β has a small ^{3}J coupling to H-4'. H-5'α is observed as a dd with coupling constants of 9.8 and 5.4 Hz. In contrast, the H-5'α signal of D-xylopyranoside appears as in the higher field as a pseudo-triplet with a 9.5 Hz splitting (Figure 7). A precise measurement of this coupling was obtained by a spectral iteration method which resulted in actual coupling constants of 9.8 and -11.4 Hz. In this study, compounds from the CR aerial parts give rise to H-5' signals appearing in the range of 3.55 -3.80 ppm.

The chemical shift of H-5' is highly affected by substitution in the aglycone. A substitution at C-1 is commonly seen in *Cimicifuga* triterpenes, and the effect of a C-1 hydroxylation group can be as large as $\Delta\delta$ 0.163 ppm for H-5'β when comparing **4** and **3**. In this study, the only arabinosides were the 1-hydroxycimigenols isolated and the H-5'β signals were around 3.65 ppm. It is not unusual for arabinosyl H-5'β signals to be as low

field as 3.81 ppm or lower. The multiplicity of the signal is a more reliable criterion than the chemical shift when identifying a key signal, because the chemical shift is strongly influenced by other factors such as solvent, through space shielding effects and even conformational changes. Once the sugar is identified, assignment of the other five signals can be achieved from their coupling patterns. Another interesting difference between xylopyranosides and arabinopyranosides was observed. In xylopyranosides, *J* couplings between H and OH were observed, which were not observed in arabinopyranoside samples. The H-2' absorption shows this difference most clearly. In arabinopyranosides, the H-2' is observed as a pseudo-triplet (iteration yields: dd, *J* = 8.4, 7.1 Hz.) that is coupled with H-1' and H-3' (Figure 8). In contrast, the H-2' of xylopyranosides is observed as a complex multiplet and its iteration revealed a ddd with *J* = 7.6, 8.8, 4.5 Hz, which is coupled with OH-2' at 4.5 Hz in addition to the couplings with H-1' and H-3'. Such ^{3}J H-O-CH couplings were observed in all 7 xylopyranosides isolated in this study. In contrast, no ^{3}J HO-CH couplings were detected in the arabinopyranosides (Figure 7). This suggests that different hydrogen bonding networks may be present in the pentose rings of these two series of epimeric glycosides.

Key signal for SETT 1A:

Check ^{1}H spectral region from 3.0 to 4.0 ppm;

- **If H-5' is a pseudo-triplet, the sugar is xylopyranose**
- **If H-5' is a pseudo-doublet, the sugar is arabinopyranose**

Key signals of the isolates were marked with dotted squares. (Figure 10)

	H1'	H2'	H3'	H4'	H5'α	H5'β	OH2'	OH3'	OH4'
	d	Ddd	ddd	dddd	dd	dd			
H1'	-	7.55	0	0	0	0	0	0	0
H2'	7.55	-	8.82	0	0	0	4.49	0	0
H3'	0	8.82	-	-8.55	0	0	0	1.20	0
H4'	0	0	-8.55	-	9.82	5.37	0	0	-2.74
H5'α	0	0	0	9.82	-	-11.38	0	0	0
H5'β	0	0	0	5.37	-11.38	-	0	0	0
OH2'	0	4.49	0	0	0	0	-	0	0
OH3'	0	0	1.20	0	0	0	0	-	0
OH4'	0	0	0	-2.74	0	0	0	0	-

TABLE VIII. ITERATED *J* COUPLING CONSTANTS OF THE XYLOPYRANOSE SPIN SYSTEM IN 4

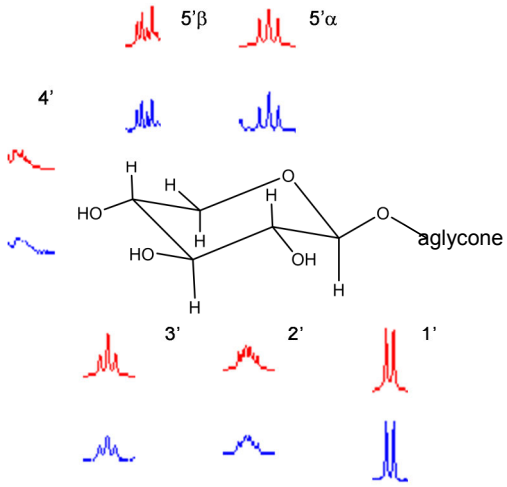

Figure 7. Spin-spin analysis of *O*-xylopyranosyl moiety

Top signals (in red) represent iterated signals, bottom signals (in blue) are observed in **4**

	H1'	H2'	H3'	H4'	H5'α	H5'β
	d	Dd	dd	ddd	dd	dd
H1'	-	7.11	0	0	0	0
H2'	7.11	-	8.38	0	0	0
H3'	0	8.38	-	3.52	0	0
H4'	0	0	3.52	-	2.91	1.61
H5'α	0	0	0	2.91	-	-12.40
H5'β	0	0	0	1.61	-12.40	-

TABLE IX. ITERATED *J* COUPLING CONSTANTS OF THE ARABINOPYRANOSE SPIN SYSTEM 2

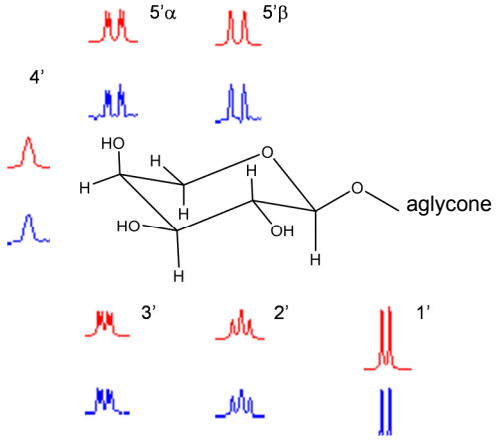

Figure 8. Spin-spin analysis of *O*-arabinopyranosyl moiety

Top signals (in red) represent iterated signals, bottom signals (in blue) are observed in **2**

SETT 1B. Nature of the side chain (type of triterpene)

The region between 3.5 and 5.5 ppm in the ^{1}H spectra of *Cimicifuga* triterpenes is rich in information about key portions of the compounds. In particular, the side chains of the *Cimicifuga* triterpenes are highly oxygenated, and some of the key protons with their unique splitting patterns appear in this region. Once the structure of the sugar has been identified, the six sugar resonances can be eliminated from consideration in this chemical shift region and concentration on the key signals of the side chain is next. The key proton signals of the isolates are shown in the Table X. Analogous to the sugar signals, these chemical shifts are largely affected by the neighboring chemical environment. On the other hand, the coupling constants are very similar and exhibit little variation, as long as the compound conformation is the same. Hence, the signal multiplicity and their observed *J* values are valuable indicators.

TABLE X. SETT1B KEY SIGNALS FOR TRITERPENE SIDE CHAINS

Structure	Key signal	Multiplicity	*J* value (Hz)	Approximate chemical shift
23*R*,24*S* cimigenol	H-24	s	NA	3.8-4.2
	H-23	d	4.2	4.6-4.8
23*R*,24*R* cimigenol	H-24	d	4.1	3.7
	H-23	ddd	9.8, 2.4, 3.8	4.6
Dahurinol	H-16	d	10.1	3.9
	H-23	ddd	2.5, 6.0, 11.4	4.0
	H-24	d	11.4	3.9

Key signal for SETT1B:

Check ^{1}H spectral region 3.5-5.0 ppm, and identify H-23, 24 and 16 by the multiplicity and the *J* values with support of chemical shift date.

The key signals of the isolates were marked with a solid line in Figure 10.

SETT 1C. The presence of 7-8 unsaturation

Of all *Cimicifuga* cycloartane triterpenes, the only double bond location that has been reported is between C-7 and C-8 (Ring B), with the exception of one compound, cimicifugenol, which has a $\Delta_{16, 17}$ double bond as well as a $\Delta_{24, 25}$ double bond in the side chain (51). Thus, when the presence of an olefinic proton is observed in the range 4.5 - 6.5 ppm, it is most likely that the compound contains a $\Delta_{7,8}$ unsaturation. The H-7 signal of a $\Delta_{7,8}$ triterpene is typically observed around 5.1 ppm as a doublet with a 7.2 Hz splitting. Although this is a marker signal for the presence of the $\Delta_{7,8}$ unsaturation, it can be confusing because of possible overlap with OH resonances which also appear as doublets in the same spectral region.

In support of these criteria, the cyclopropane methylenes, H-19 exo/endo, can also serve as markers for the presence of $\Delta_{7,8}$ unsaturation. The characteristic methylene signals of saturated cycloartane triterpenes appear as a pair of doublets in the range 0.25-0.90 ppm in ^{1}H spectra. In the C-7/C-8 unsaturated triterpenes, the methylene protons at C-19 experience a deshielding effect from the double bond and are observed at a lower field, one in the range 0.45-0.55 ppm and the other between 0.75 and 0.9 ppm. From analysis of the present isolates, the triterpenes without $\Delta_{7,8}$ unsaturation give rise to one doublet in the range of 0.25-0.55 ppm for the 19-exo proton and another doublet in the range of 0.5-0.6 ppm for the 19 endo proton.

TABLE XI. KEY SIGNALS FOR UNSATURATED CYCLOARTANE TRITERPENES

	d at 5.1ppm	H19 chemical shift
$\Delta_{7,8}$ unsaturated	Y	0.45-0.55 (H19 exo), 0.75-0.90 (H19 endo)
Saturated	N	0.25- 0.55, 0.50-0.60

Key signals for SETT 1C:

If there is a doublet at 5.1 ppm, it suggests a $\Delta_{7,8}$ unsaturated triterpene. The key signals of the isolates were marked with a solid line in Figure 9.

SETT 1D. Substitutions on the ABCD rings

Other than the side chain, ring substitutions are frequently known to occur at locations C-1, C-7, and C-12. Hydroxylation at C-11 has also been reported for some *Cimicifuga* cycloartane triterpenes found in Asian species such as C. *foetida*, C. *simplex*, and C. *dahurica* (34,52,53), but it has not yet been reported from an American *Cimicifuga* species.. At positions C-1 and C-7, hydroxylation represents a typical substitution pattern. At C-12, both hydroxylation and acetylation have been reported. When an isolated triterpene compound is shown to have an extra hydroxyl group, the methine proton on this same site appears in the region 3.5-4.0 ppm. Proton H-1β of 1α-hydroxy triterpenes is typically observed as a broad singlet around 3.8-3.9 ppm. Proton H-7α of 7β-hydroxy triterpenes is typically observed as a broad pseudo-triplet centered around 3.7 ppm. Acetyl groups are easily identified by their sharp singlet peaks of OAc in the range 1.9-2.1 ppm.

Key signal for SETT 1D:

The presence of broad singlets around 3.8-3.9 ppm indicates 1α-hydroxylation

The presence of broad pseudo-triplets around 3.7 ppm indicates 7β-hydroxylation

Sharp singlets in 1.9-2.1 ppm are indicative of acetylation

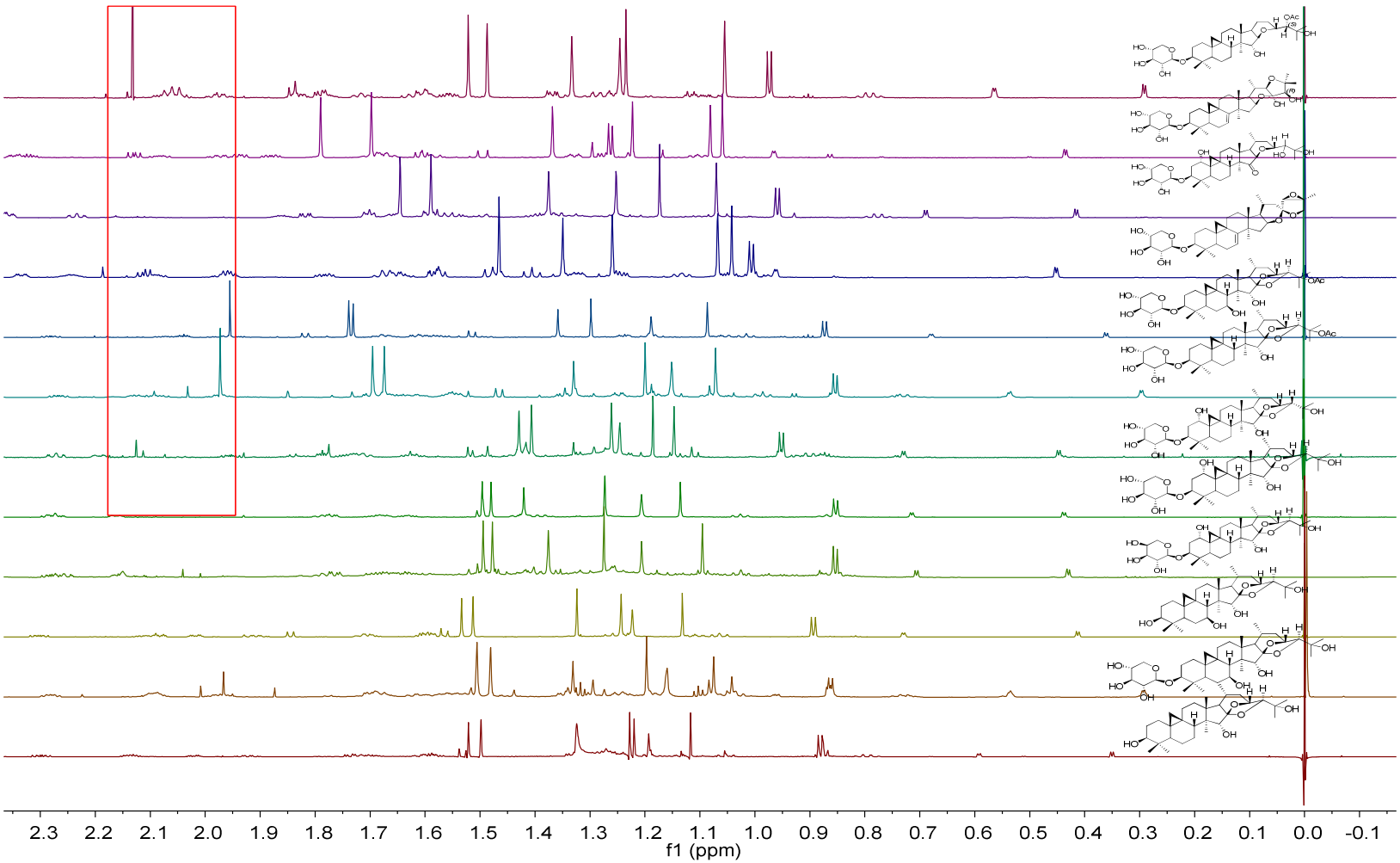

Figure 9. All of CR aerial triterpenes at 900 MHz ^{1}H NMR in pyridine-d_5 0-2.55 ppm

Chemical shifts were calibrated to 7.217 ppm for the residual protonated species of pyridine. Digitization was as follows: GM (LB -1.0 Hz, GB 0.1). Rectangular region includes characteristic OAc group signals

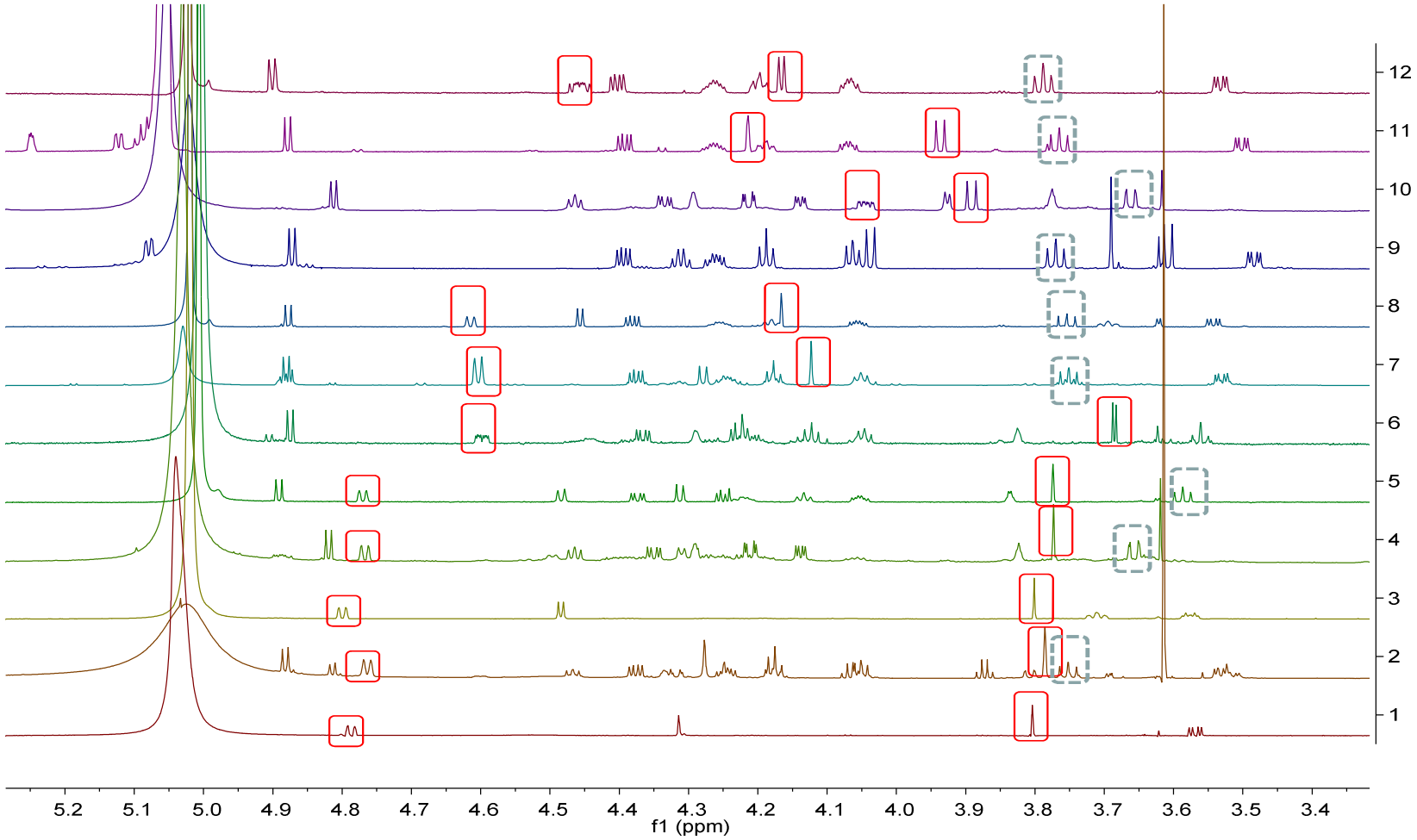

Figure 10. All of CR aerial triterpenes at 900 MHz ^{1}H NMR in pyridine-d_5 3.3- 5.3 ppm

Chemical shifts were calibrated to 7.217 ppm for the residual protonated species of pyridine. Digitization was as follows: GM (LB -1.0 Hz, GB 0.1). Sugar finger print peak is shown in a dotted square; side chain finger print peaks are shown in a solid square or rectangular.

SETT 2. The Survey Method Using Chemical Shift Information of Methyls + C-19 Methylenes

Cimigenol triterpenes have 7 or 8 methyl groups that are positioned throughout the entire structure. Each methyl group can play a role as a reporter signal that reflects its local chemical environment. The C-19 cyclopropane methylene signals can also operate as reporter signals because they are unique to cimigenol triterpenes and also they are easy to distinguish in the complex spectrum due to their very high field positions. A summary of chemical shifts of C-19 methylene protons together with all methyl signals appears in Table XII. The $\Delta\delta$ of methyls in a pair of compounds differing in one functional group, one can evaluate the functional group substituent chemical shift (s.c.s). When the knowledge of the s.c.s. behavior is accumulated, the methyl signal patterns only in the complex ^{1}H NMR spectrum can represent the whole structure. For example, $\Delta\delta$ value for compound **3**, (1α-hydroxydahurinol-3-*O*-α-L-arabinopyranoside), and compound **4**, (1α-hydroxydahurinol-3-*O*-α-D-xylopyranoside), in which the only difference is a chirality in pentose, are obtained and explained in the following. It is shown that the methyl ^{1}H chemical shifts at C-21, C-18, C-28, C-26, and C-27 are virtually identical to each other and their $\Delta\delta$ values are < 0.01 ppm. The ^{1}H chemical shifts of the geminal methyl C-29 and C-30 are the only resonances that are affected by the change in the sugar moiety at C-3^1 with $\Delta\delta$ of 0.039 ppm and 0.049 ppm, respectively. In other words, a change in the ^{1}H chemical shift of C-29 and C-30 is associated with and represents the difference in the two C-3^1 epimeric structures. Another example is the (comparison) of compound **1** (24-*epi*-1α-hydroxycimigenol-3-*O*-β-D-xylopyranoside) with **4** (1α-hydroxycimigenol-3-O-β-D-xylopyranoside), where the only observed difference between the two is the

stereochemistry at C-24 in the side chain. As expected, the $\Delta\delta$ values of methyls that are close to C-24 are larger, and the $\Delta\delta$ value gets smaller as the location gets farther from the change. The most prominent s.c.s of 0.218 ppm is observed for Me-27. The signals in the A and B rings (H-19 exo, endo, Me-29, Me-30), which are the groups farthest from C-24 are unaffected. The s.c.s effects associated with 7-hydroxylation and 1-hydroxylation have also been evaluated and shown in Table XII.

In conclusion, the ^{1}H chemical shifts of the methyl signals and the C-19 methylene proton signals are sensitive reporters of their surrounding structural environments. This includes sites of hydroxylation, stereochemical differences in the side chain, and the nature of the sugar. Even though the ^{1}H NMR spectrum of a triterpene is very complex, the chemical shifts of the essential methyl and cyclopropane signals usually stand out and can provide essential structural information. The accumulation of knowledge about these reporter signals is genrerally useful for identification and dereplication of cycloartane triterpenes.

TABLE XII. ^{1}H CHEMICAL SHIFTS OF THE METHYL AND 19 METHYLENE SIGNALS OF TRITERPENE AT 900 MHZ (PYRIDINE-d_5)

Compound number	1	3	4	6	7	12	Δδ (ppm) 3,4 (sugar)	Δδ (ppm) 1,4 (24*S*/*R*)	Δδ (ppm) 6,7(7-OH)	Δδ (ppm) 4,12 (1-OH)
19 exo	0.447	0.431	0.437	0.299	0.361	0.293	0.007	0.010	0.062	0.144
19 endo	0.729	0.707	0.714	0.537	0.679	0.536	0.007	0.015	0.141	0.178
21	0.952	0.854	0.853	0.853	0.874	0.863	0.002	0.099	0.021	0.011
30	1.147	1.096	1.135	1.071	1.087	1.075	0.039	0.012	0.016	0.061
18	1.246	1.207	1.206	1.153	1.189	1.160	0.001	0.040	0.036	0.046
28	1.186	1.275	1.273	1.202	1.299	1.198	0.002	0.087	0.097	0.074
29	1.430	1.377	1.426	1.331	1.360	1.329	0.049	0.004	0.029	0.096
27	1.262	1.477	1.480	1.674	1.731	1.480	0.002	0.218	0.056	0.001
26	1.406	1.495	1.501	1.695	1.739	1.507	0.006	0.095	0.044	0.007

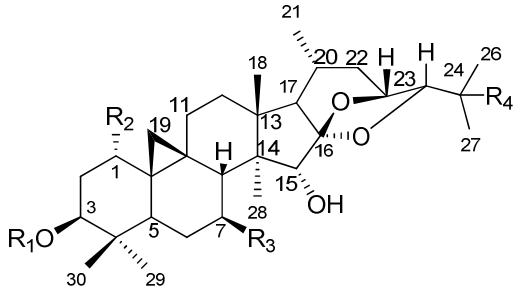

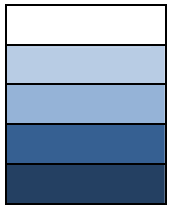

less than 0.03
0.03 - 0.05
0.05 - 0.1
0.1 0 - 0.20
greater than 0.2

Compound number		R1	R2	R3	R4	24
1	1α-24-*epi*-Cimigenol-3-*O*-β-D-xylopyranoside	xyl	OH	H	H	*R*
3	1α-Hydroxycimigenol-3-*O*-α-L-arabinopyranoside	ara	OH	H	H	*S*
4	1α-Hydroxycimigenol 3-*O*-β-D-xylopyranoside	xyl	OH	H	H	*S*
6	25-*O*-Acetyl-cimigenol-3-*O*-β-D-xylopyranoside	xyl	H	H	Ac	*S*
7	25-*O*-Acetyl-7β-cimigenol-3-*O*-β-D-xylopyranoside	xyl	H	OH	Ac	*S*
12	Cimigenol-3-O-β-D-xylopyranoside	xyl	H	H	H	*S*

Calibration of Chemical Shifts in Pyridine-d_5

Major fluctuations in the chemical shifts of the residual solvent signals in pyridine-d_5 were observed in relation to TMS peaks in the range of -4.2 ppb to 4.6 ppb, for various reasons including sample concentration and temperature. In this study, all of the ^{1}H NMR spectra were calibrated in reference to one of the residual solvent peaks, to allow the alignment of different spectra including samples that do not contain TMS. The precise chemical shifts of residual solvents were obtained as an average of six cycloartane triterpene samples that contain both traces of TMS and residual pyridine-d_5 (TABLE XIII). Based on the carefully considered calibration of spectra, ^{1}H chemical shifts were calibrated to 7.217 ppm and described to three decimal points in this study.

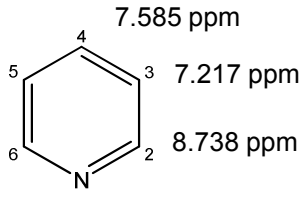

TABLE XIII. CHEMICAL SHIFTS OF RESIDUAL PYRIDINE SIGNALS IN ^{1}H NMR (900 MHz) IN REFERENCE TO TMS (0.000 PPM)

Pyridine ^{1}H	DCL208	DCL183	DCL171	DCL156	DCL172	DCL62	average
H3,5	7.217	7.222	7.217	7.217	7.216	7.216	7.217
H4	7.587	7.589	7.586	7.582	7.584	7.584	7.585
H2,6	8.739	8.740	8.739	8.734	8.740	8.738	8.738

Since ^{13}C NMR spectra are more dispersed than ^{1}H spectra, the significance of obtaining detailed chemical shift data is low. For carbon calibration, 123.5 ppm for H-3,5 of pyridine-d_5 was employed according to CIL database.

3.2.3.1. **Compound 1. 24-*epi*-1α-Hydroxycimigenol-3-*O*-β-D-xylopyranoside**

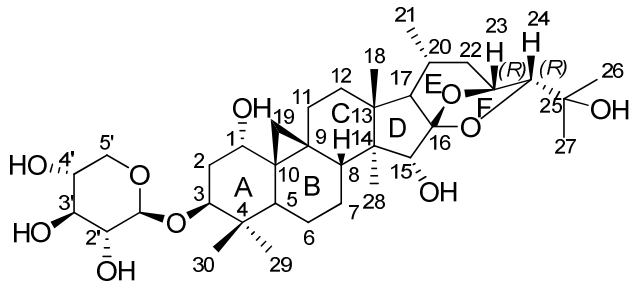

24-*epi*-1α-Hydroxycimigenol-3-*O*-β-D-xylopyranoside (**1**) was obtained as a white powder. The HR-ESI-MS revealed a sodium molecule adduct at *m/z* 659.3743 $[M+Na]^+$ (calculated for $C_{35}H_{56}O_{10}Na$, 659.3771) indicating a molecular formula of the sample as $C_{35}H_{56}O_{10}$, which is identical to the molecular formula of previously isolated 1α-hydroxycimigenol-3-*O*-β-D-xylopyranoside. The ^1H NMR spectrum revealed a pair of cyclopropane methylene protons at 0.447 and 0.729 ppm, six tertiary methyls at 1.147, 1.186, 1.246, 1.262, 1.406 and 1.429 ppm, and a secondary methyl at 0.952 ppm.

A deshielded 1-proton signal 1-eq at 3.825 ppm appearing as a broad singlet revealed the presence of hydroxyl group at C-1. The OH at C-1 imparts a deshielding effect on H-11α and the methylene protons at C-2 (2.811, 2.738 and 2.269 ppm, respectively). The sugar region of the ^1H NMR spectrum indicated the presence of one sugar moiety, which was identified as a xylose with a diagnostic triplet for H-5'α that was observed at 3.561 ppm. The COSY spectrum confirmed the correlations between sugar protons. The ROESY spectrum (Figure 20) showed linkage cross-peaks to H-3/Me-29, H-1'/H-3 and H-1'/H-29 which suggested that the sugar moiety is attached to C-3-OH.

The chemical shifts of protonated carbon were assigned unambiguously from a phase sensitive HSQC experiment. Quaternary carbon chemical shifts were assigned from an HMBC spectrum, except for C-9 and C-10. Chemical shifts of C-9 and C-10 could not be observed due to the limited sample size (140 μg). However, when compared with a known compound, 1-OH cimigenol, the ^{1}H and ^{13}C chemical shifts of the A/B/C/D rings were found to be identical. This leaves the side chain as the remaining problem for the structure elucidation of this compound.

The HMBC experiment exhibited correlations between a carbon signal at 112.4 ppm and the signals of H-17 and H-15. Hence the 112.4 ppm signal was attributed to the characteristic spiroketal carbon at C-16 and indicates that compound **1** possesses a spiroketal partial structure at C-16. However, ^{1}H NMR spectral pattern of compound **1** does not match that of a possible spiroketal compound, 1α-hydroxycimigenol-3-*O*-β-D-xylopyranoside (23*R*,24*S*) (54), which suggested that **1** is a stereoisomer of 1α-hydroxycimigenol-3-*O*-β-D-xylopyranoside.

24-*epi*-1α-Hydroxycimigenol-3-*O*-β-D-xylopyranoside (1): White powder; HR-ESI-MS [M+Na]+ at m/z 659.3743 calcd 659.3771 for C35H56O10Na (-4.2 ppm); NMR (900 MHz, C5D5N) see Table XVI.

Stereochemistry of the Side Chain Chiral Centers, 23 and 24

First, the relative configuration of the side chain in compound **1** was determined by comparison of a ^{1}H signal splitting pattern of the side chain spin system with that of a 23*R,*24*S* cimigenol type isolate 7–β-hydroxycimigenol (**5**). The signal multiplicities of H-17, Me-21, H-22α, H-22β couplings were identical with those of 23*R,*24*S* cimigenol, even though their chemical shifts are different. The signal of H-20 was not analyzed due to the nature of the complex multiplicity confounded by spectral overlap with signals from other

protons. A noteworthy observation was that H-23 in **1** appeared as a ddd (9.8, 2.3, 4.2 Hz), while H-23 of **5** is only a dd (9.8, 2.3 Hz). Moreover, H-24 of **1** possessed an additional coupling of 4.2 Hz compared to H-24 in **5**. The additional couplings arising between H-23 and H-24 suggest that the dihedral angle between H-23 and H-24 in compound **1** is different from 23*R,*24*S.* Even though both 23*R,*24*R* and 23*S,*24*S* configurations were considered as possibilities, the configuration had to be 23*R*,24*R* because of the coupling pattern as follows: When considering the couplings between the methylene protons H-22α and H-22β with H-23, both **5** and **1** exhibit identical coupling constants of 9.8 Hz and 2.3 Hz, respectively. This means that the configuration of ring E in compound **1** is identical to that in compound **5**. Hence, the relative configuration of the chiral center at C-23 was determined as 23*R*. As a consequence, the side chain was determined as 23*R,*24*R.*

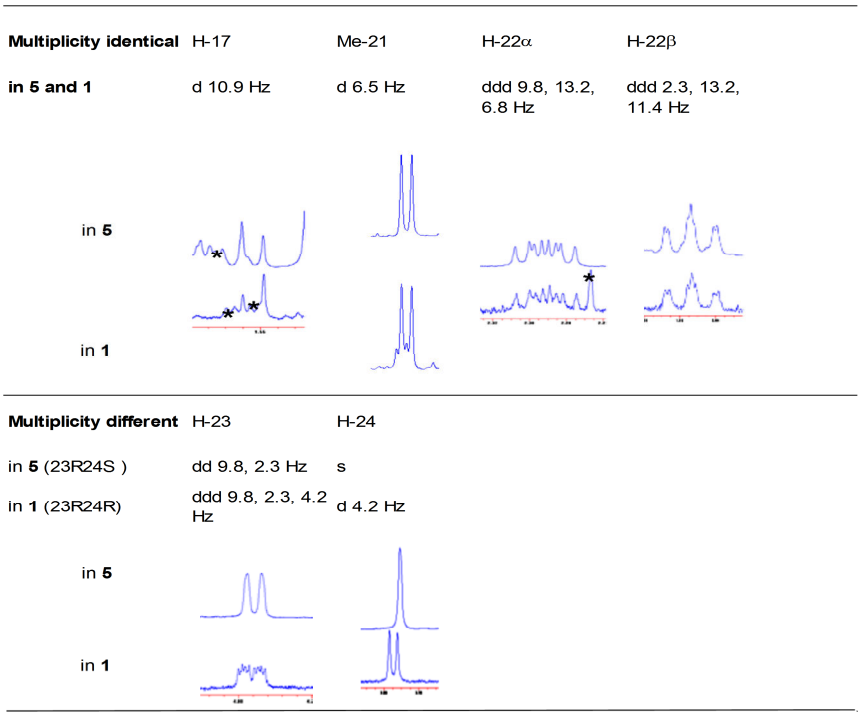

Figure 11. Comparison of the ^{1}H NMR signals of 1 (top) and 5 (bottom) in rings E and F.

Signal of H-20 is was not analyzed and not displayed due to a complex multiplicity and overlapping by other signals. * Signals marked with asterisks belong to peaks of other spin systems. Digitizations were done on Nuts. The parameters were: zfzfzf LB-1.0 GB 0.1

To confirm the stereochemistry of the side chain, 3D models of the two epimers were created using Chem3D software and a theoretical *J* value for H-23;H-24 was calculated. The energy was minimized with the MM2 Dynamics Force Field. According to the model, the dihedral angle between H-23 and H-24 in 23*R*,24*S* cimigenol is calculated to be 38°, whereas the same angle in the 23*R*,24*R* analog was 107°. Since the correlation between a dihedral angle and its ^{3}J coupling constant is theoretically explained by Karplus theory (55-57), the approximate coupling constants were calculated using Equation 3: $^{3}J_{ab} = J^{0}\cos^{2}f\text{-}0.28$ ($0^{o} < f < 90$) and $^{3}J_{ab} = J^{180}\cos^{2}f\text{-}0.28$ ($90^{o} < f < 180^{o}$), where $J^{0} = 8.5$ and $J^{180} = 9.5$ are constants which depend upon the substituents on the carbon atoms and f is the dihedral angle. Calculated values were 0.45 Hz for the 23*R*,24*S* and 4.99 Hz for the 23*R*,24*R* analogs, respectively. The latter is close to the actual measured value of 4.2 Hz.

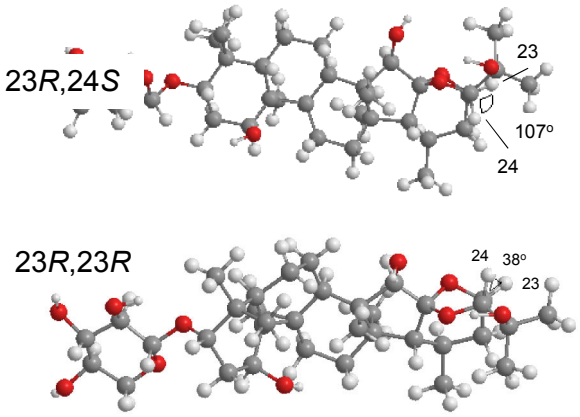

	Theoretical *J* value	Observed *J* value
23*R*,24*S*	0.42 Hz	0 Hz
23*R*,24*R*	4.99 Hz	4.2 Hz

Figure 12. Energy-minimized in silico models of the two epimers Considered for the Structure of 1

Full Spin Simulation

The spin-spin coupling of **1** was analyzed by iterative full-spin analysis using the PERCH software tool. There are four largely independent spin systems in **1**. The spin system of the xylose moiety was demonstrated separately. The simulation allowed the identification of small couplings that would otherwise be ignored. In particular, this software revealed that Me-18 is coupled to H-12β through 4 bonds with a small ^{4}J coupling constant of 0.72 Hz. In all previous reports, the Me-18 signal was assigned as a singlet. Interestingly, none of the other methyls showed such long-range couplings. Thus makes it easy to distinguish the Me-18 signal from other methyl resonances. To accurately assign methyl ^{1}H signals, ^{1}H NMR and COSY experiments are otherwise insufficient, and HMBC experiments are required. However the identification of the small coupling to Me-18 assists in the assignment of the methyl signals. This likely applies to any other cycloartanes that are un-substituted at C-12. Although the Me-18 signal appears to be a singlet, it is the lowest intensity and broadest of all the methyl signals in the spectrum.

Another long range coupling of 0.80 Hz was observed between H-19 exo and H-5. This is a typical ^{4}J coupling seen across from a W arrangement. It is important to note that H-19 endo does not have a long range coupling, which makes this pair of signals look slightly different from each other as shown in Figure 13. H-19 exo and H-19 endo are geminally coupled to each other by 4.2 Hz, and H-19 exo has an additional coupling of 0.80 Hz with H-5. Although the additional coupling of ^{4}J=0.80 Hz was iterated for the H-19 exo signal, it is about 10% taller than H-19 endo signal. The same signal characteristics are observed in other cycloartane isolates Figure14. It suggests that although only one long-range coupling (H-19 exo/H-5) was iterated, a number of small un-iterated couplings (< 0.8 Hz) contribute to the signal shape. This was confirmed by high quality COSY

spectra of similar compounds (**5**, **8**) (Figure 15). Unfortunately, the cross-peaks of the long-range couplings were not observed in the COSY of **1** because of an insufficient signal to noise ratio derived from low sample concentration. In **5** and **8**, the observed cross-peak pattern was similar. Mutually observed cross-peaks were H-19 endo/ H-1a, 8,11a and H-19 exo/H-5, 8. The cross-peak between H-19 endo and H5 was observed in **5**, but not in **8**.

H-1β is observed in lower field at 3.822 ppm is observed as a broad singlet due to OH-1α. Spectral iteration revealed that it actually is a ddd and that H-1β is coupled to H-2α, H-2β and OH-1 by 3.65, 2.70, and 3.67 Hz, respectively.

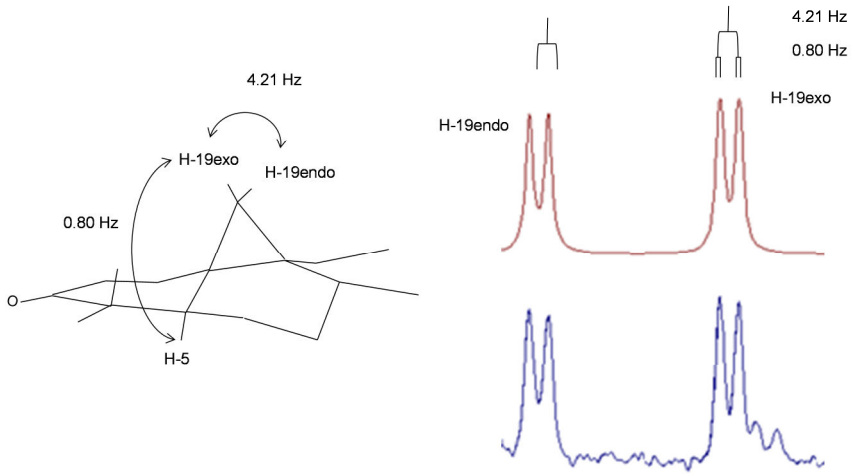

Figure 13. Partial structure of compound 1 and ^{1}H NMR signals of the methylene protons H-19.

The iterated spectrum shown on the top (red), the observed spectrum on the bottom (blue). ^{3}J coupling between H-19 exo and H-19 endo, ^{4}J coupling between H-19 exo and H-5 were iterated.

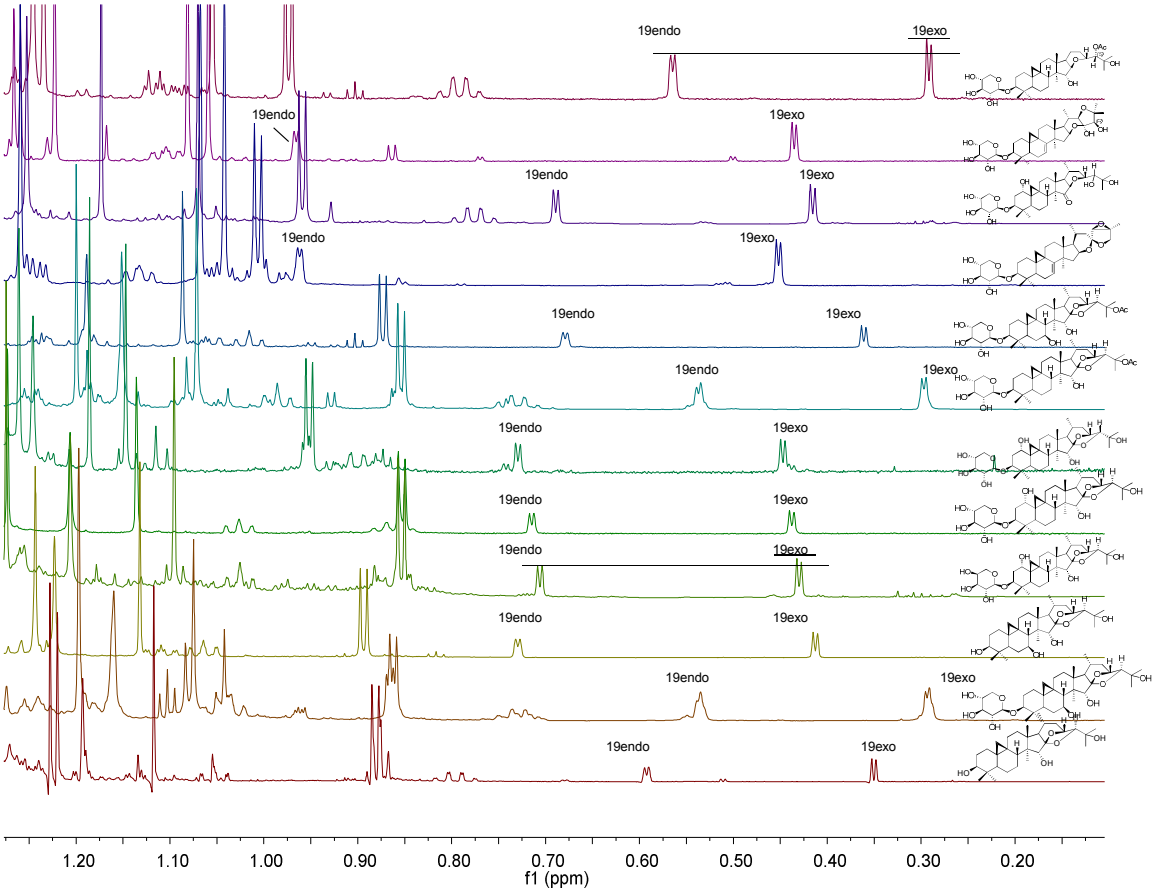

Figure 14. Region of the cyclopropane methylene resonances of the ^{1}H NMR spectra of the isolated triterpenes

A difference of height is observed within each signal pair. In any case, the signal of H-19 exo is taller than H-19 endo. This results from accumulation of long-range couplings. See text for details.

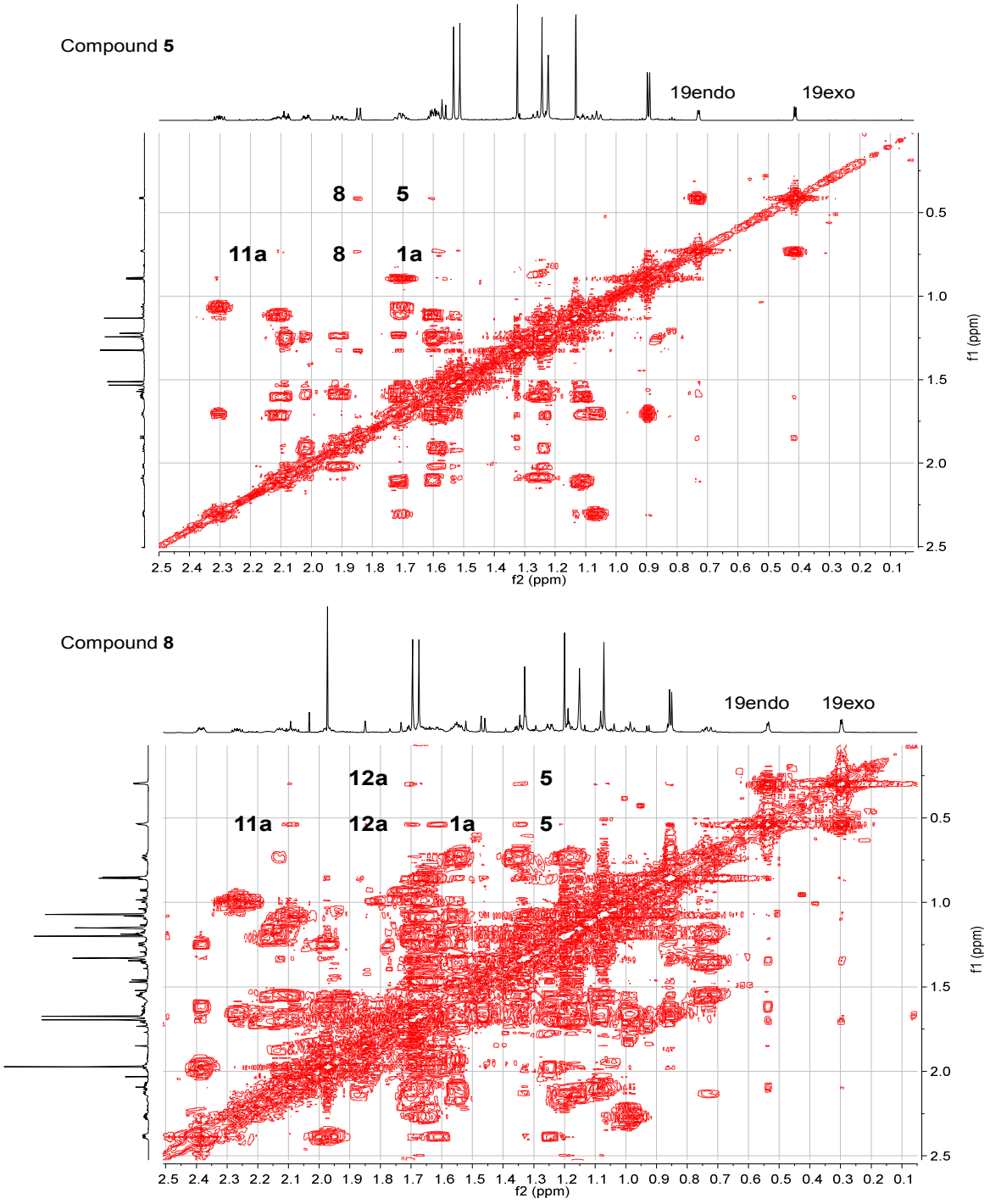

Figure 15. Region of the cyclopropane methylene cross-peaks in the COSY spectra of 5 and 8

Intensity was increased to show small long-range coupling cross-peaks. Cross-peaks for ^{4}J couplings; H-19 endo/H-5,1a,11a and H-19 exo/H-5 and ^{5}J couplings H-19 endo/H-12a and H-19 exo/H12a were observed.

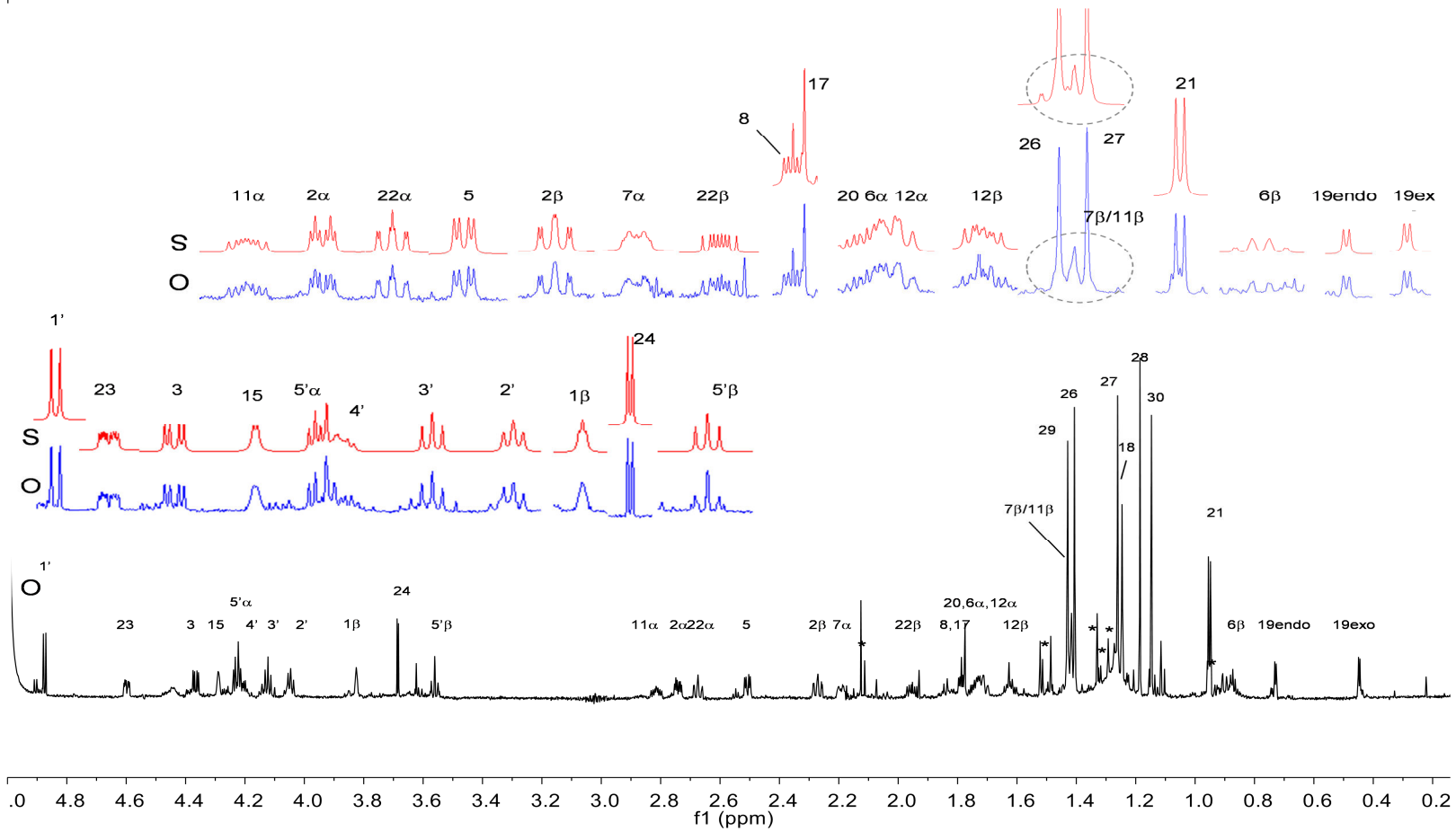

Figure 16. Compound 1; 900 MHz ^{1}H NMR in pyridine-d_5 (marked with "O") and Iterated Signals (marked with "S")

Chemical shifts were calibrated to 7.217 ppm for the residual protonated species of pyridine. The sample includes 22-28% of another triterpene impurity (calculated using 1' peaks (29%: 71%) and 19 endo (22%:78%)) Digitization was as follows: GM (LB -1.0 Hz, GB 0.1). Impurity peaks are marked with *.

TABLE XIV. THE COUPLING CONSTANTS OF COMPOUND 1 AS DETERMINED FROM FULL SPIN ANALYSIS

Spin system 1	H23	H24	H22β	H22α	H17	H20	Me21
H23	-	4.16	2.26	9.80	0	0	0
H24	4.16	-	0	0	0	0	0
H22β	2.26	0	-	-13.16	0	11.44	0
H22α	9.80	0	-13.16	-	0	6.84	0
H17	0	0	0	0	-	10.91	0
H20	0	0	11.44	6.84	10.91	-	6.48
Me21	0	0	0	0	0	6.48	-

Spin system 2	H18	H12α	H12β	H11α	H11β
H18	-	0	0.76	0	0
H12α	0	-	13.30	12.00	2.70
H12β	0.76	13.30	-	2.30	2.30
H11α	0	12.00	2.30	-	14.70
H11β	0	2.70	2.30	14.70	-

Spin system 3	H8	H19 endo	H19 exo	H7α	H7β	H6α	H6β	H5
H8	-	0	0	12.85	3.14	0	0	0
H19 endo	0	-	-4.31	0	0	0	0	0
H19 exo	0	-4.31	-	0	0	0	0	0.80
H7α	-12.85	0	0	-	-12.75	14.34	2.61	0
H7β	3.14	0	0	-12.75	-	2.65	3.73	0
H6α	0	0	0	14.34	2.65	-	-12.64	12.59
H6β	0	0	0	2.61	3.73	-12.64	-	4.60
H5	0	0	0.80	0	0	12.59	4.60	-

Spin system 4	H3	H2α	H2β	H1	OH1
H3	-	4.45	12.00	0	0
H2α	4.45	-	-13.10	3.65	0
H2β	12.00	-13.10	-	2.70	0
H1	0	3.65	2.70	-	3.67
OH1	0	0	0	3.67	-

Substituent Chemical Shift (s.c.s) Effect

Epimerization at C-24 causes the tertiary alcohol moiety to be folded behind the E ring instead of being pointed out away from the E, F rings as shown in Figure 17. Significant dislocation of OH-25 causes deshielding/shielding s.c.s. effects on neighboring protons from 0.06 ppm to as much as 1.63 ppm. In general, protons behind the E-ring were deshielded. For example H-22α, H-17, Me-21 and H-20 are deshielded by 1.63, 0.23, 0.07 and 0.06 ppm, respectively. Protons H-22β, H-23, H-24 are shielded by 0.37, 0.20 and 0.12 ppm, respectively. The methylene protons at 22 receive a significant effect from the epimerization and the signal for H-22α appears downfield of that of H-22β, whereas their relative positions are reversed in 23*R*,24*S* cimigenol (Figure 18, Table XV).

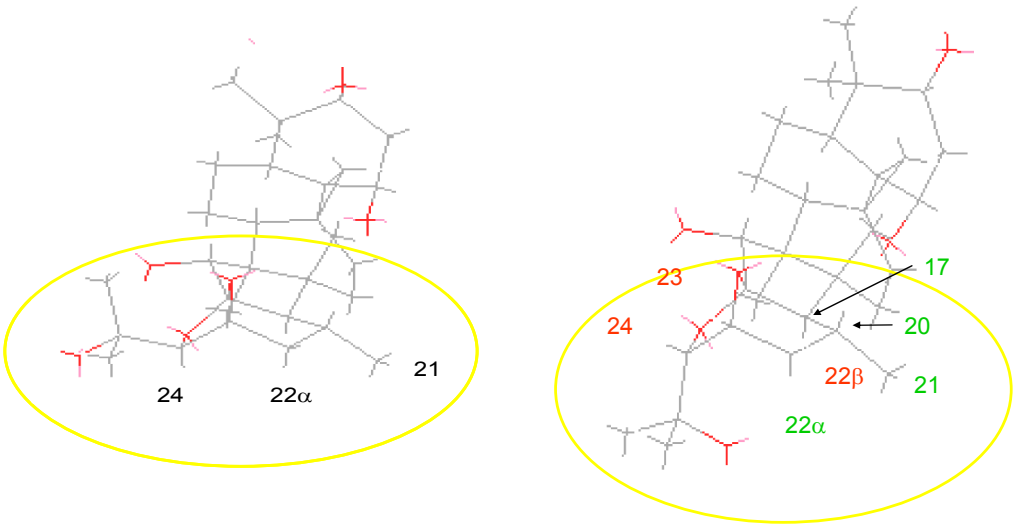

Figure 17. Compound 5; 3D model (left) and compound 1; 3D model without sugar moiety

3D models were made using Chem3D and the MM2 energy minimization calculation was performed. Protons in red were shielded, those in green were deshielded by OH-25.

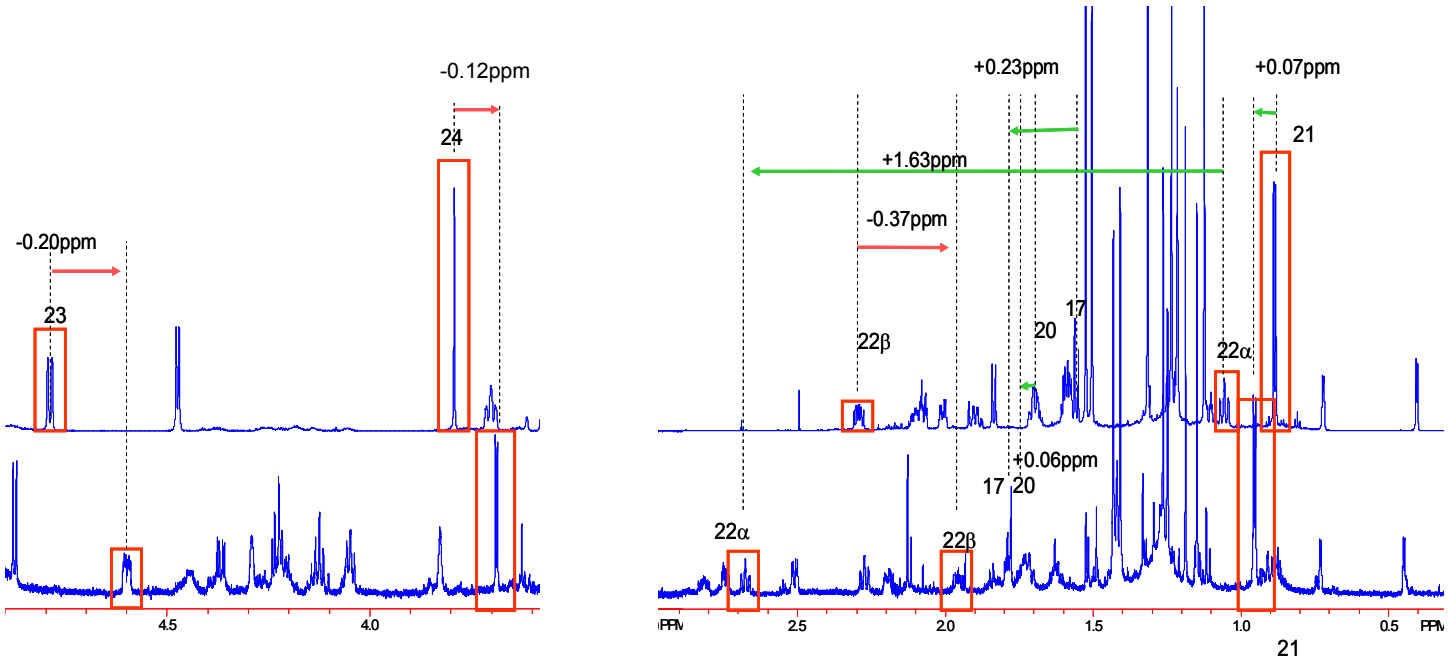

Figure 18. Shielding/deshielding effects (900 MHz); top spectrum compound 5; bottom spectrum compound 1

Shielding effect of 23*R*,24*R* cimigenol type and 23*R*,24*S* cimigenol type were directly compared. H-22α is affected the most (+1.63 ppm) from the change. Details are discussed in the text.

TABLE XV. DEGREE OF SHIELDING/DESHIELDING

Deshielded		Shielded	
22 α	1.63 ppm	22 β	0.37 ppm
17	0.23 ppm	23	0.20 ppm
21	0.07 ppm	24	0.12 ppm
20	0.06 ppm		

TABLE XVI. NMR DATA OF COMPOUND 1

Compound **1** 900 MHz/ 700 MHz								
24-*epi*-1α-hydroxycimigenol-3-*O*-β-xylopyranoside								
position		δ_C	δH, (*J* in Hz)			HMBC(H→C)	COSY	ROESY
1	β	72.7	3.825	Brs			2α/β	2α,19 exo
2	β	37.8	2.272	Dt	2.3, 12.7		2α, 1β, 3	19 exo, 30
2	α	37.8	2.741	Dt	12.7, 3.7		2β, 1β, 3	3
3		84.6	4.366	Dd	4.2, 11.7		2α/β	29, 5, 2α
4		41.6	na					
5		40.1	2.508	Dd	2.5, 12.6		6α	6α, 7β,3
6	β	20.9	0.901	overlapped			6β, 5,7β	19 endo
6	α	20.9	1.721	overlapped			7α,5	5,
7	β	26.4	1.423	overlapped			7α, 8	5, 7α
7	α	26.4	2.193	overlapped			6α,7β, 8	7b, 6α, 8
8		49.1	1.787	Dd	4.2, 12.5		7α	19 endo, 6β, 2β, 15
9		*	na					
10		*	na					
11	β	26.3	1.429	overlapped	6.0, 11.3		11α, 12α/β	19 exo, 11α
11	α	26.3	2.814	Ddd	14.7		11β, 12α/β	28,11b, 12α
12	β	34.1	1.620	overlapped			11α, 12α	21, 18,
12	α	34.1	1.707	overlapped			11α, 12β	11α
13		41.8	na					
14		47.8	na					
15		81.0	4.291	D	6.8			18,8
16		112.4	na					
17		60.8	1.781	D	10.8			22α
18	Me	19.5	1.246	S		12,13,14, 17		15
19	exo	30.6	0.447	d	4.2		19 endo	11β, 2β, 1β
19	endo	30.6	0.729	d	4.2		19 exo	6β, 30, 8
20		23.3	1.743	M			22α	22β
21	Me	19.4	0.952	D	6.5	20,22,17	20	12β,22α, 22β
22	β	29.6	1.954	M			22α, 23	21, 17
22	α	29.6	2.675	Dt	12.1, 1.6		22β,20,23	20, 21,27
23		73.8	4.598	Dt	12.1, 1.6	3	22α/β, 24	
24		84.1	3.685	D	6.8			
26	Me	30.7	1.406	S		27, 25, 24		24
27	Me	25.9	1.262	S		26, 25, 24		22α, 22β, 23, 24
28	Me	11.6	1.186	S		13,8,14,15		11α
29	Me	25.7	1.430	S		30,3,4,5		3
30	Me	14.7	1.147	S		29,3,4,5		19 endo, 6β, 2β
1'		107.7	4.874	D	7.3	3	2'	
2'		75.0	4.046	t	8.7		3'	
3'		78.7	4.123	t	8.7		4'	
4'		71.4	4.206	M				
5'	α	67.1	3.561	t	9.5		5'β	
5'	β	67.1	4.228	dd	5.3, 14.0			

* δ_C could not be obtained due to insufficient signal intensity

Nuclear Overhauser Effect

The 2D ROESY (Rotating-frame Overhauser Effect SpectroscopY) (58) spectrum was obtained with high sensitivity on a 700 MHz using a 1.7 mm NMR tube and is shown in Figure 20. The key ROE cross-peaks were observed and serve to confirm the stereochemistry in Compound **1**, specifically the C-19 cyclopropane ring methylene endo/exo protons, the side chain configuration, and the presence of hydroxyl groups at C-1 and C-15.

For the side chain, the three signals for H-24, Me-26, and Me-27 were used as a focal point. The H-24 exhibited an ROE to H-23, Me-26 and Me-27. The ROE cross-peaks between H-23 and neighboring protons at 22α, 22β, 17, 20, and 15 were not observed, which is consistent considering the distances would be > 3.9 Å according to the 3D model (Table XVII and Figure 19, 20). Me-27 exhibits an ROE to three protons; H-24, H-22α and H-22β. To represent 23*R,*24*S* cimigenol, a ROESY spectrum of **4** was also analyzed and compared in terms of the side chain system (full analysis is described in Figure 21). Compound **4** shows an ROE between H-24 and H-22α. Although another cross-peak was observed, it was not clearly assigned due to cross peak overlap. However, this cross-peak should represent either H-24-17 and/or H-24-26 and/or H-24-27. The important discriminating ROE correlations for establishing the configuration of the side chain are as follows: Me-27 to H-22α and H-22β only present in 23*R*,24S and H-24 to H-22α only present in 23*R*,24*R*.

TABLE XVII. INTERNUCLEAR DISTANCE OF KEY PROTONS IN COMPOUND 1 (23*R*,24*S* CIMIGENOL TYPE) AND 4 (23*R*,24*R* CIMIGENOL TYPE)

The values were obtained from 3D model created using chem 3D software. Correlations, of which ROE cross-peaks were observed in ROESY spectrum, shown in bold.

Internuclear distance of key protons in compound **1** (Å)		Internuclear distance of key protons in **4** (Å)	
24-23	**2.115**	**24-23**	**2.916**
24-22α	3.943	**24-22α**	**2.232**
24-22β	4.287	24-22β	3.709
24-17	4.190	**24-17***	**2.622**
24-20	4.861	24-20	4.361
24-26	**2.581, 3.151, 3.819**	**24-26***	**2.380, 3.001, 3.620**
24-27	**2.765, 2.777, 3.881**	**24-27***	**3.936, 3.100, 4.493**
24-15	4.428	24-15	5.027
22α-27	**2.434, 3.115, 3.806**	22α-27	3.540, 3.672, 4.712
22β-27	**3.201, 4.119, 4.942**	22β-27	3.934, 4.883, 5.626

*Due to overlapping, ROE cross-peaks were unclear

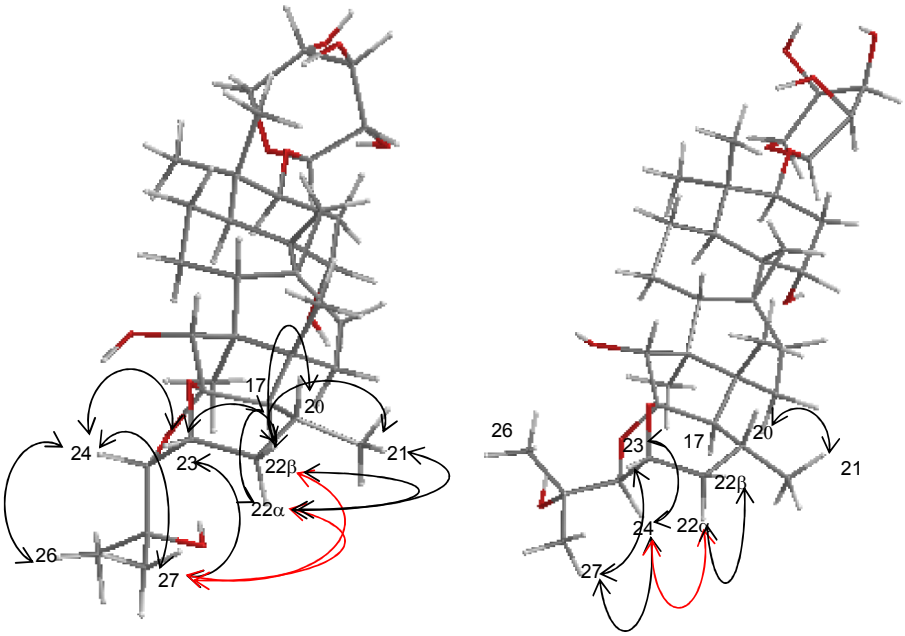

Figure 19. 3D model of compounds 1 (left) and 4 (right)

Key ROE correlations were shown in the figure; especially discriminating correlations for stereochemistry of C24 are shown in red.

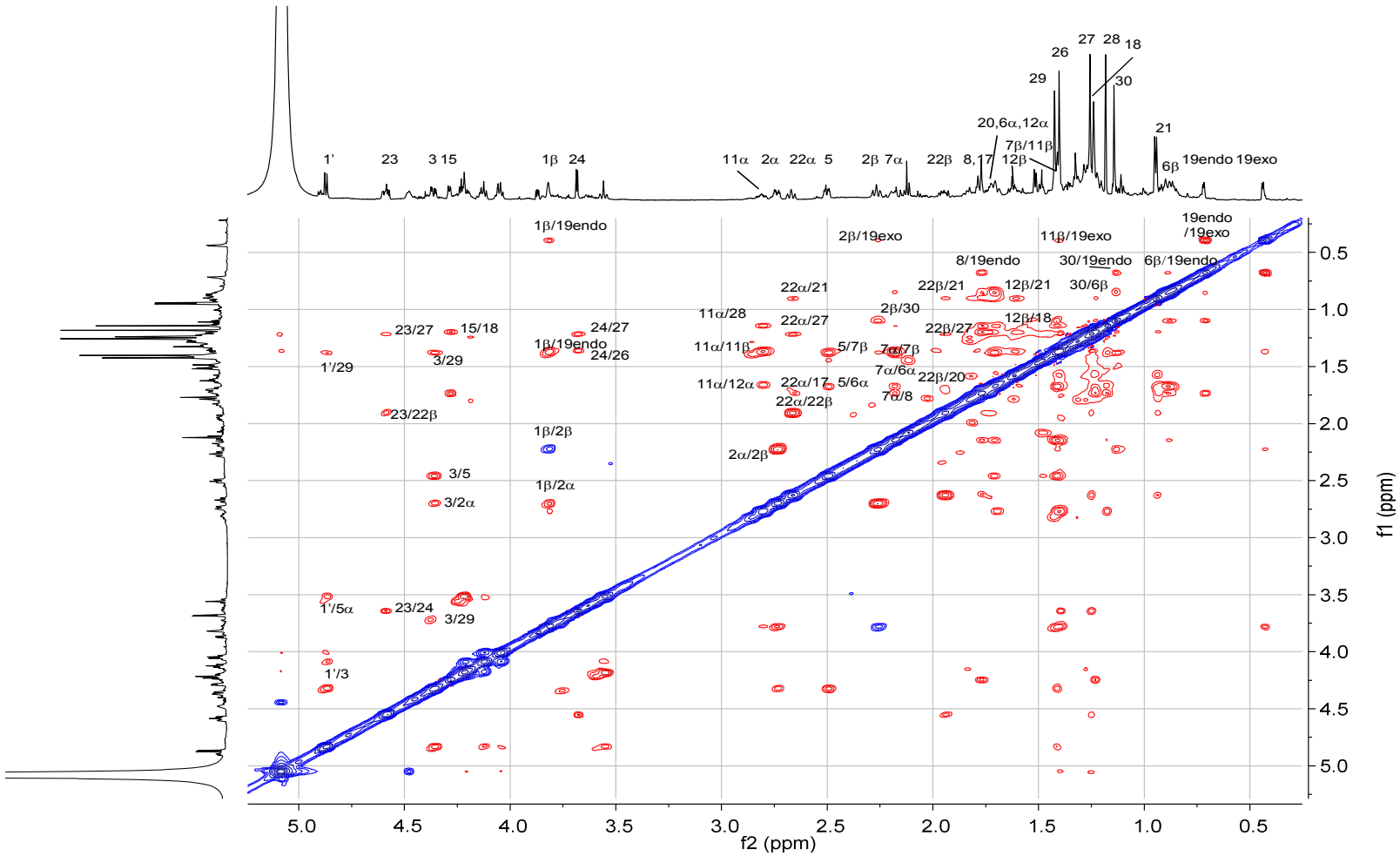

Figure 20. Compound 1; 700 MHz ROESY spectrum in pyridine-d_5

Chemical shifts were calibrated to 7.217 ppm for the residual protonated species of pyridine. Digitization was follows: F1 QSINE (SSB2), F2 QSINE (SSB 2).

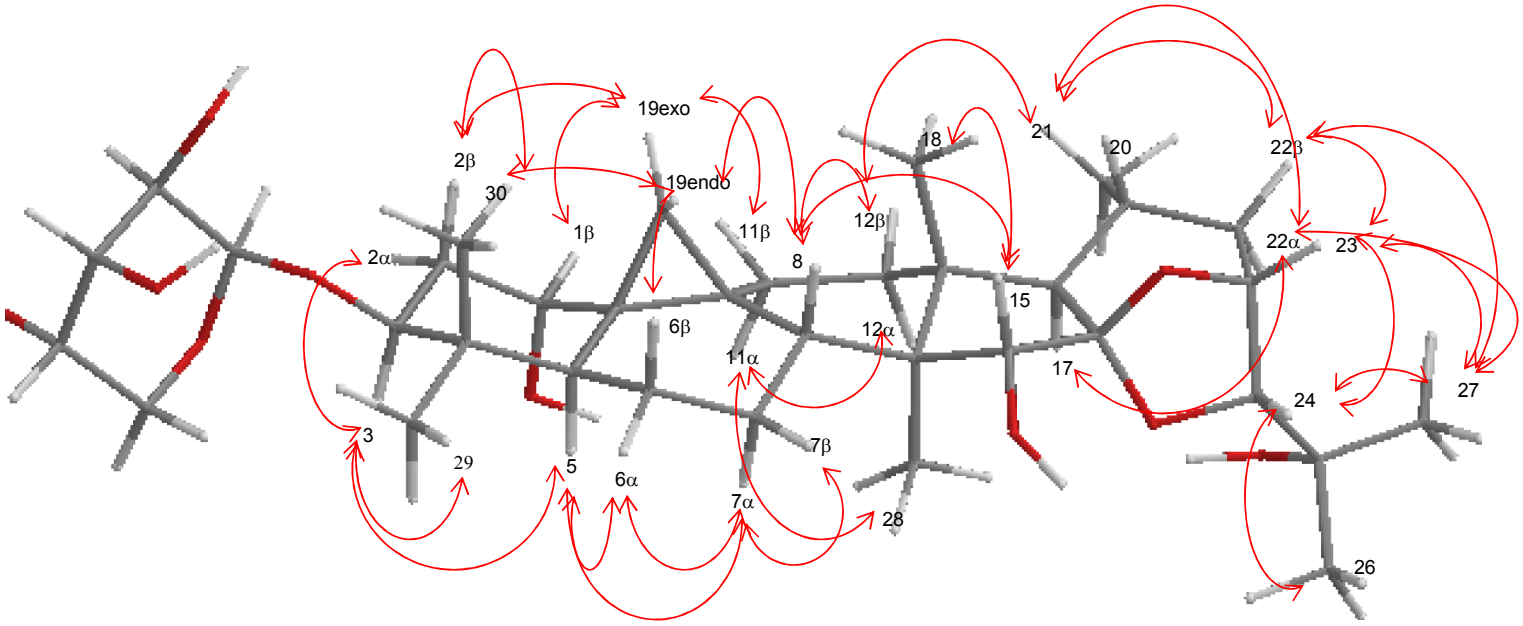

Figure 21. Key ROESY interactions in compound 1

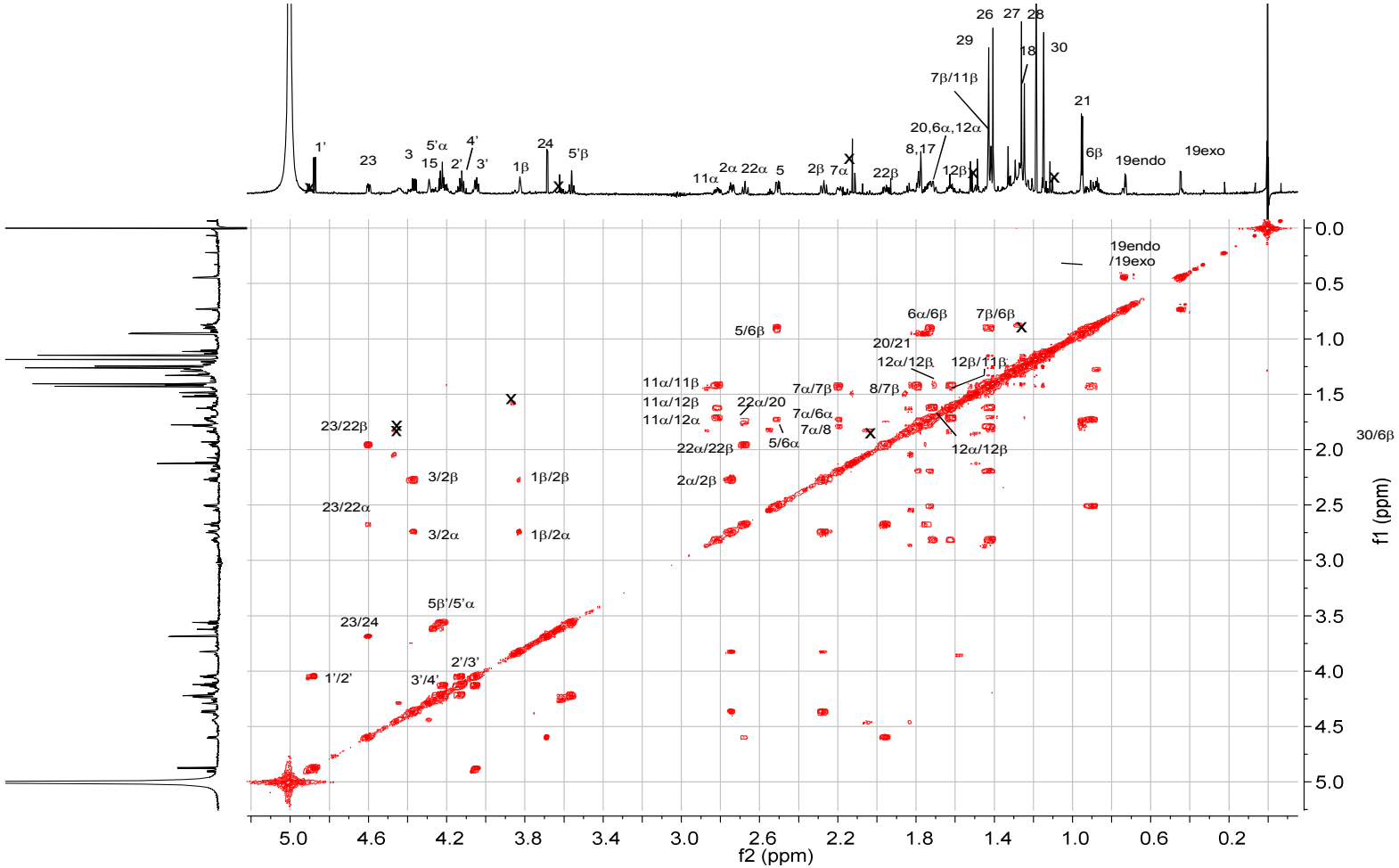

Figure 22. Compound 1; 900 MHz gCOSY spectrum in pyridine-d_5

Chemical shifts were calibrated to 7.217 ppm for the residual protonated species of pyridine. Digitization was as follows: F1 SINE (SSB0) F2 SINE (SSB0)

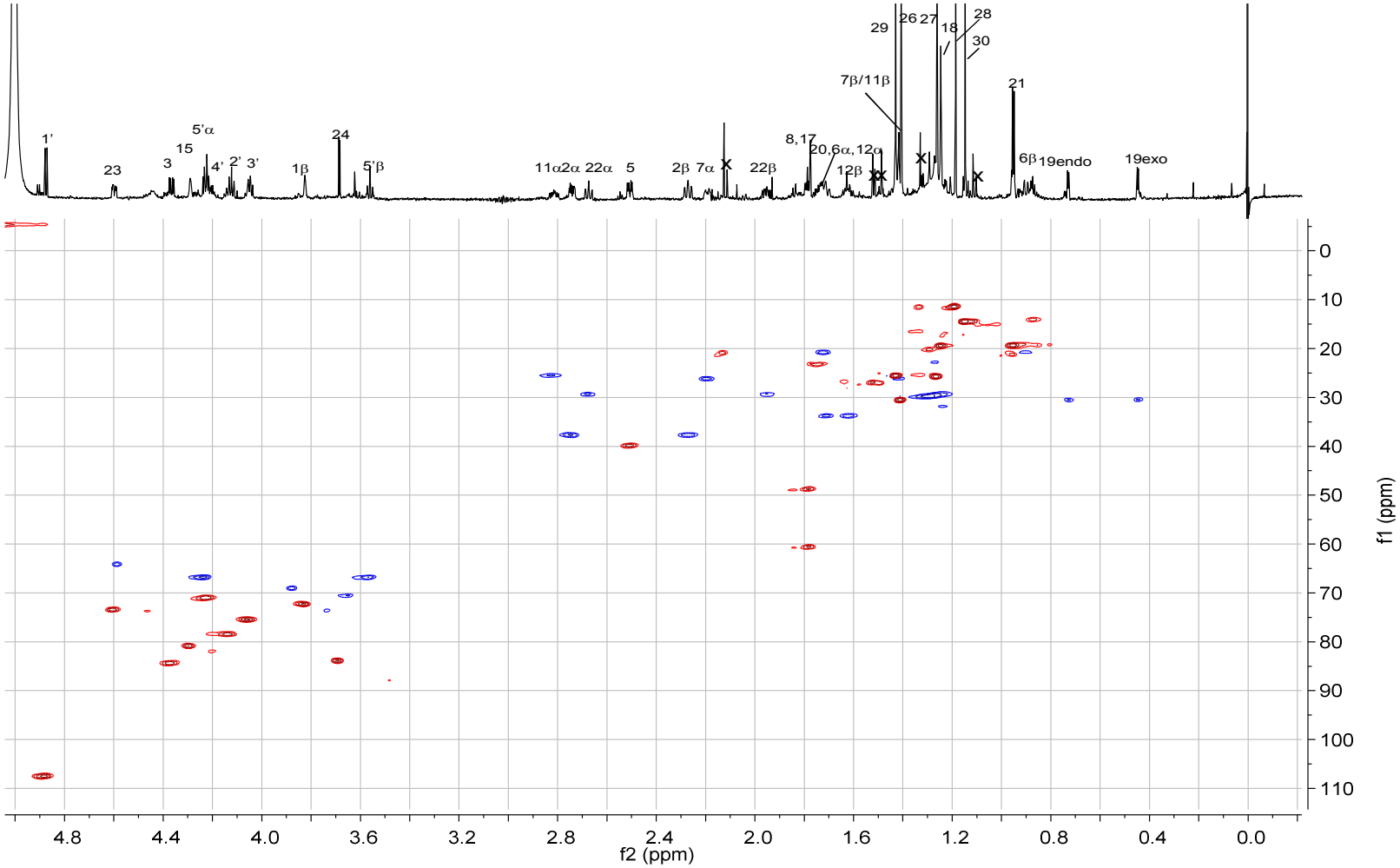

Figure 23. Compound 1; 700 MHz gHSQC spectrum in pyridine-*d*$_5$

Chemical shifts were calibrated to 7.217 ppm for the residual protonated species of pyridine on F1 and to 123.5 ppm on F2. Digitization was as follows: F1 QSINE (SSB 2), F2 SINE (SSB 2). Pulse sequence hsqxedetgpsisp2.4 was used.

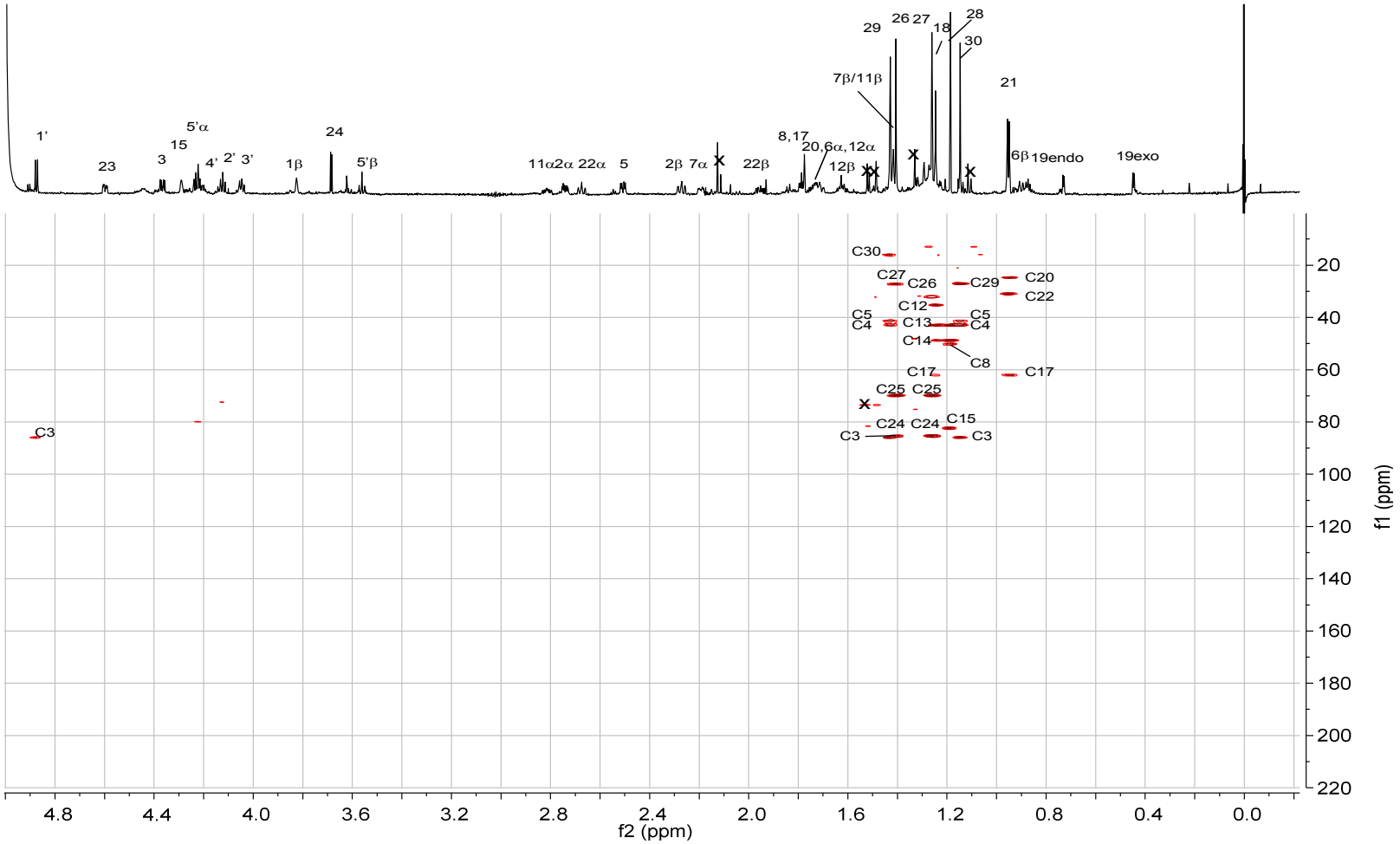

Figure 24. Compound 1; 700 MHz gHMBC spectrum in pyridine-d_5

Chemical shifts were calibrated to 7.217 ppm for the residual protonated species of pyridine on F1 and to 123.5 ppm on F2. Digitization was as follows: F1 SI 1k SINE (SSB0), F2 SI 1k SINE (SSB0) pulse sequence hsqxedetgpsisp2.4 was used.

3.2.3.2. **Compound 2. 1α-Hydroxydahurinol-3-*O*-α-L-arabinopyranoside**

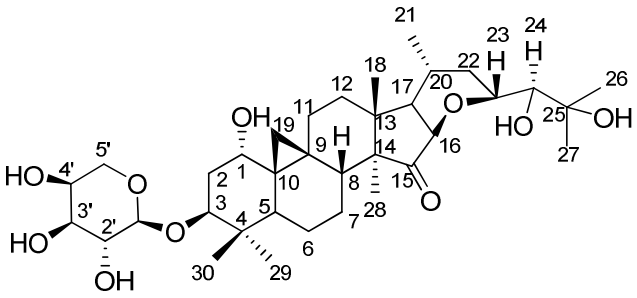

1-α-Hydroxydahurinol-3-*O*-α-L-arabinopyranoside (**2**) was isolated as a white powder. The HR-ESI-MS revealed protonated molecule $[M+H]^+$ at *m/z* 637.3939 (calculated for $C_{35}H_{57}O_{10}$, 637.3952) indicating a molecular formula for the analyte of $C_{35}H_{56}O_{10}$. The ^1H NMR spectrum displayed a cyclopropane methylene at 0.424 and 0.697 ppm, six tertiary methyls at 1.078, 1.181, 1.260, 1.383, 1.587 and 1.654 ppm, a secondary methyl at 0.967 ppm and an anomeric proton at 4.821 ppm (d, *J* = 7.2 Hz). Carbon chemical shifts were assigned from an HSQC experiment. The saccharide was assigned to be α-arabinopyranose, since the ^{13}C and ^1H signal pattern for the sugar spin-spin coupling system were identical to a previously isolated compound (compound **3**). The saccharide spin-spin coupling was also compared with a PERCH spin simulation and the result is shown in Figure 8. The spin iteration method revealed indistinct couplings, which were otherwise overlooked. For example, the signal of H-4' looks like a broad singlet on the spectrum and it is difficult to resolve its multiplicity and coupling constants by observation. However, the PERCH iteration method presented the multiplicity as ddd and the *J*-values as 1.61, 2.91 and 3.52 Hz. In the same manner as the case of compound **1**, the H-1 signal at 3.777 ppm indicated the presence of a hydroxyl group at position 1.

Two HMBC cross-peaks (d 3.899 ppm/214.5ppm and 1.181ppm/214.5ppm) indicate an underivatized carbonyl group at C15. The gCOSY spectrum showed spin-spin coupling systems and confirmed the proposed carbon-carbon connectivity. Therefore, the structure of Compound **2** was deduced to be 1-α-hydroxydahurinol-3-*O*-L-arabinopyranoside.

1-α-Hydroxydahurinol-3-*O*-α-L-arabinopyranoside (2): White powder; HR-ESI-MS [M+H]+ at m/z 637.3939 calcd 637.3952 for C35H57O10 (-2.0 ppm); NMR (900 MHz, C5D5N) see Table XVIII.

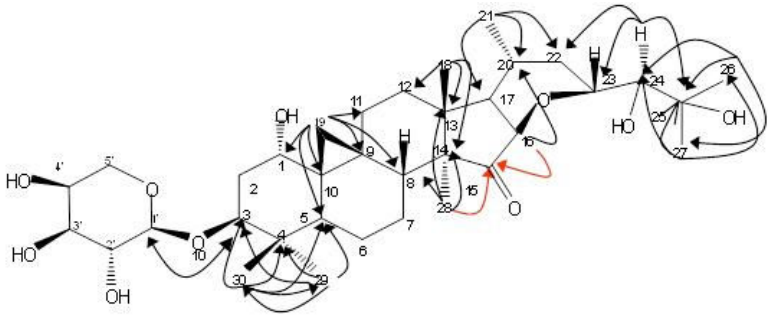

Figure 25. Key HMBC correlations of compound 2

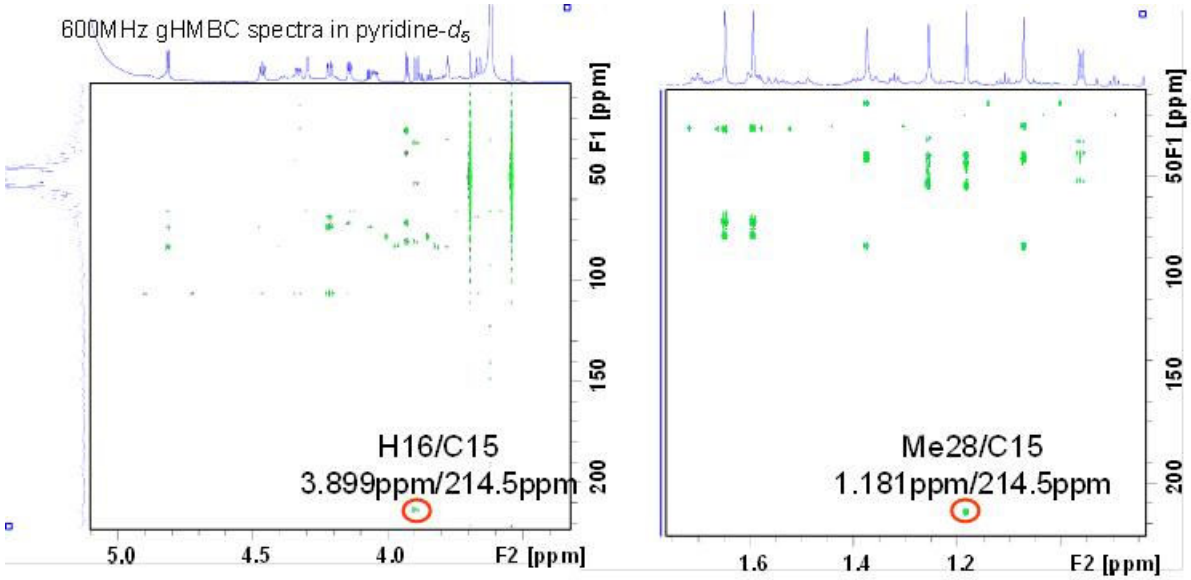

Figure 26. Key HMBC cross-peaks of compound 2; 600 MHz in pyridine-d_5

TABLE XVIII. NMR DATA OF COMPOUND 2

Compound **2** 900 MHz/600 MHz

1α-Hydroxydahurinol-3-*O*-α-arabinopyranoside							
position	proton	δC	δH, (*J* in Hz)			HMBC (H→C)	COSY
1		71.9	3.777	brs		10	2α/β
2	α	37.3	2.738	dt	13.3, 4.1	10,4,3	2β, 1, 3
2	β		2.233	dt	2.7, 12.7		2α, 3
3		83.8	4.335	dd	4.5, 11.9		2α/β
4		41.1	NA				
5		39.3	2.445	dd	12.3, 2.8	7,10,4,	6α/β,
6	α	20.3	1.653	m	overlapped		6β,5
6	β		0.775	dt	12.4,12.4		6β, 5,7β
7	α	25.3	2.372	m	overlapped		7β
7	β		1.352	m	overlapped		7α, 8
8		43.1	1.817	dd	4.3, 12.8		7α/β
9		20.8	NA				
10		31.0	NA				
11	α	25.0	2.784	m			11β, 12
11	β		1.380	m			11α, 12α/β
12	α/β	30.9	1.700	m			11α/β
13		39.6	NA				
14		54.7	NA				
15		214.5	NA				
16		83.4	3.891	d	10.1	20,17,23,15	17
17		52.6	1.574		overlapped		16
18	Me	20.1	1.252	s		12,13,8,14	
19	endo	30.68	0.689	d	4.5	9,11,10,8,1	19β
19	exo	30.7	0.416	d	4.5	9,11,10,8,1	19α
20		32.5	1.860	ddt	3.9, 6.1, 10.5		21Me, 22α
21	Me	20.1	0.959	d	6.7	20,22,17	20
22	α	38.0	2.356	m	overlapped		22β,20
22	β		1.551	m	overlapped		22α, 23
23		81.5	4.044	ddd	2.5, 6.0, 11.4		24, 22α/β
24		78.9	3.928	d	11.4	27,22,25,23	23
26	Me	20.2	1.646	s		27,25,14	
27	Me	26.8	1.589	s		26,25,14	
28	Me	17.7	1.173	s		13,8,14,15	
29	Me	14.6	1.070	s		30,5,4,3	
30	Me	25.5	1.375	s		29,5,4,3	
1'		107.0	4.813	d	7.2	5',3',3	2'
2'		72.5	4.465	t	8.0	3',1'	1',3'
3'		74.0	4.142	dd	3.6, 9.0	1	2', 4'
4'		68.9	4.291	brs			5'α/β, 3'
5'	α	66.4	4.213	dd	2.9, 12.3	4', 3', 1'	5'β, 4'
5'	β	66.4	3.661	dd	1.7,12.3		5'α, 4'

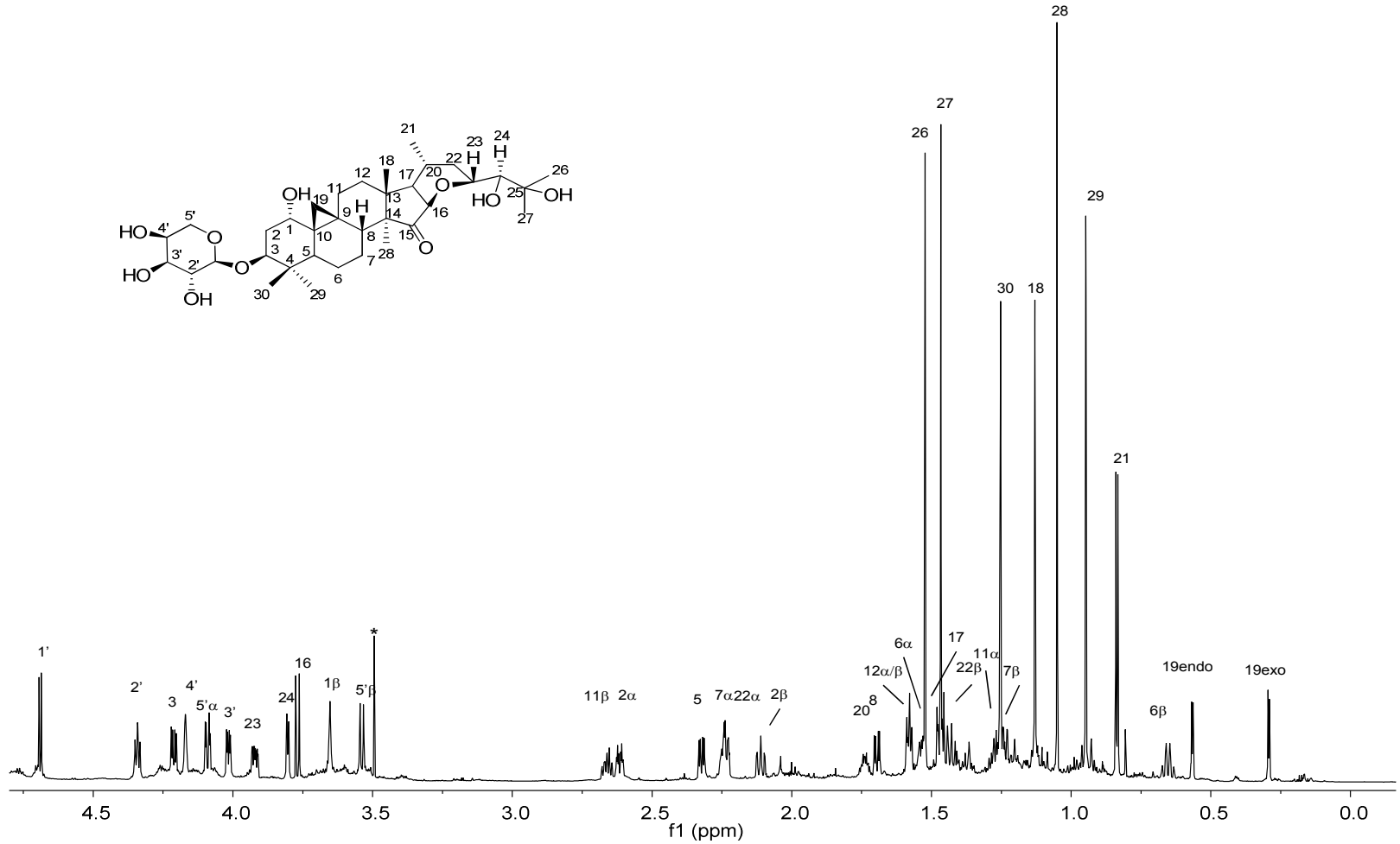

Figure 27. Compound 2; 900 MHz ^{1}H NMR in pyridine-d_5.

Chemical shifts were calibrated to 7.217 ppm for the residual protonated species of pyridine. Digitization was as follows: GM (LB -1.0 Hz, GB 0.1).* is residual MeOH.

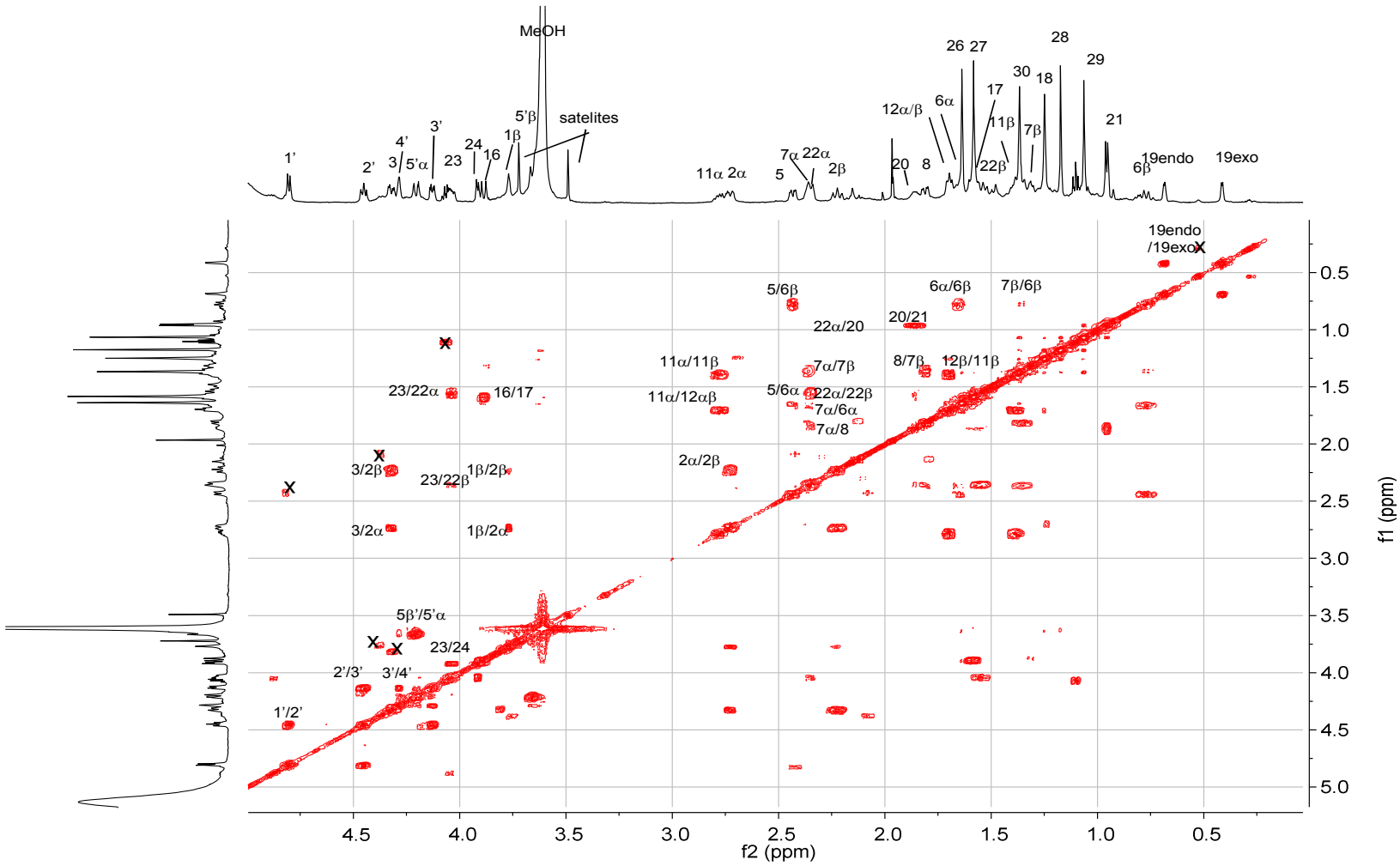

Figure 28. Compound 2; 600 MHz gCOSY spectrum in pyridine-d_5

Chemical shifts were calibrated to 7.217 ppm for the residual protonated species of pyridine. Digitization was as follows: F2 SINE (SSB 0), F1 SINE (SSB0). x indicates peaks from impurity.

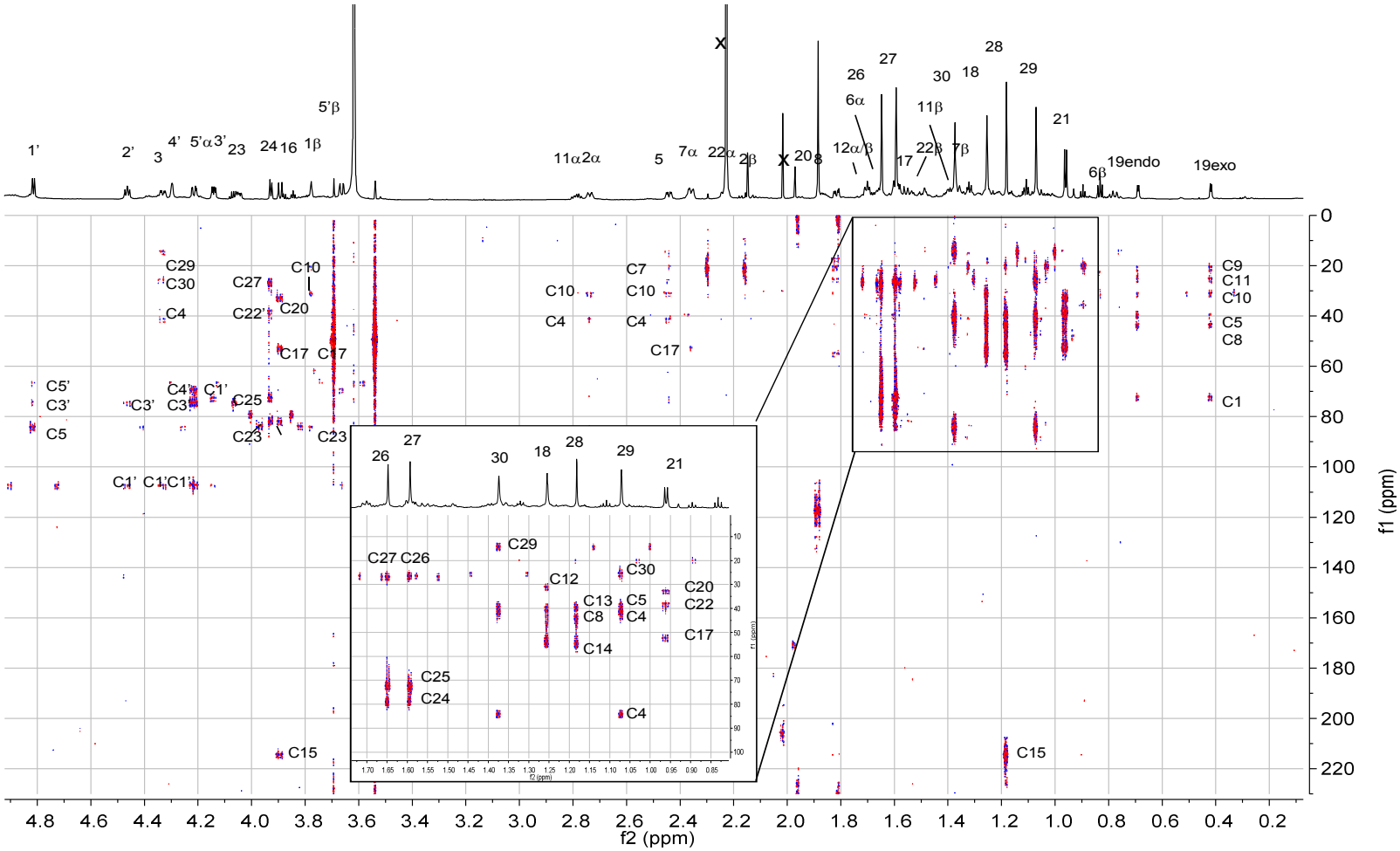

Figure 29. Compound 2; 600 MHz gHMBC spectrum in pyridine-d_5

Chemical shifts were calibrated to 7.217 ppm for the residual protonated species of pyridine on F1 and to 123.5 ppm on F2. Original Data TD F1 256 F2 8k. Digitization was as follows: F1 SI 8k SINE (SSB0) F2 SI 4k SINE(SSB 0)

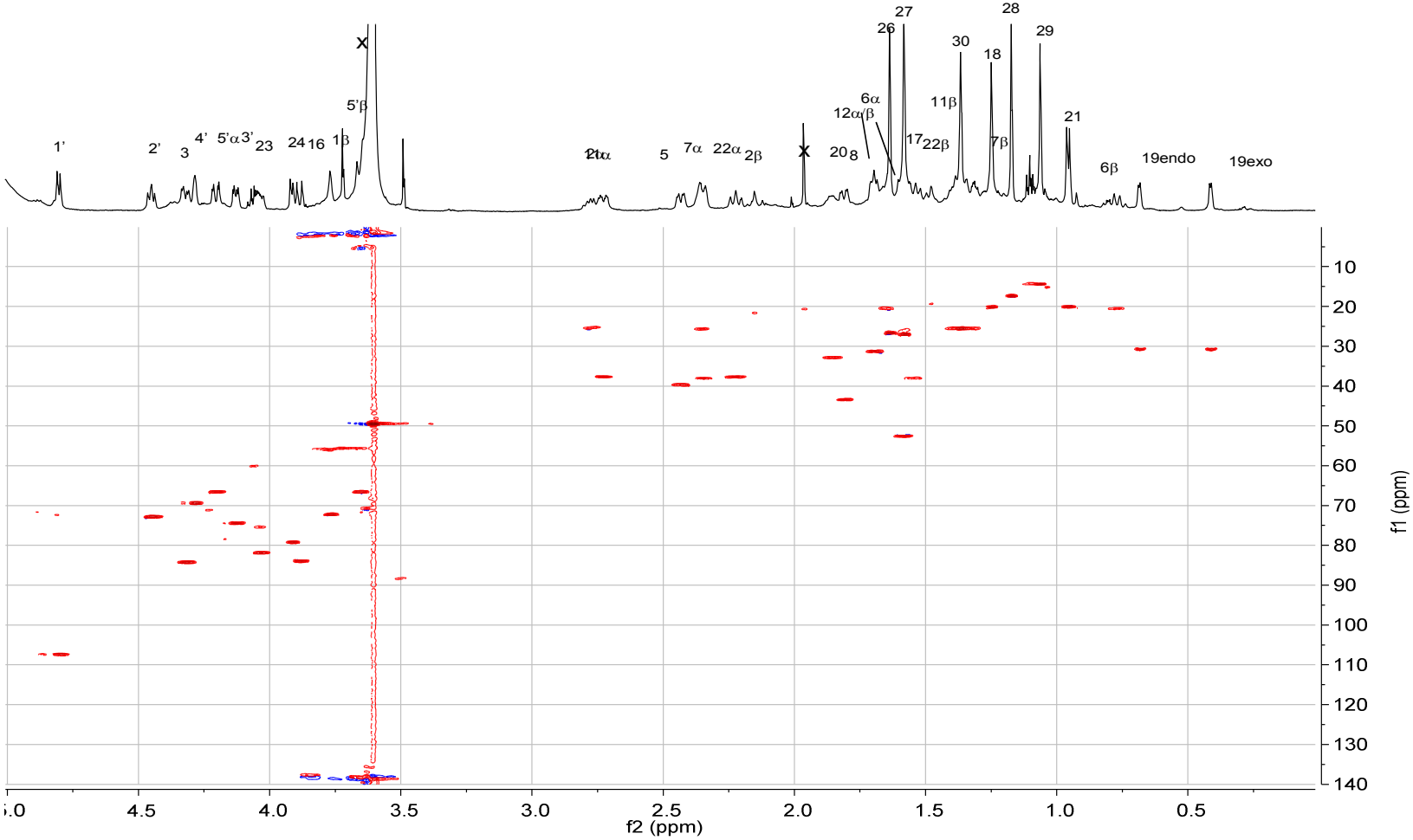

Figure 30. Compound 2; 600 MHz gHSQC spectrum in pyridine-d_5

Chemical shifts were calibrated to 0.416 ppm for H-19 exo on F1 and to the 30.7 ppm on F2. The number was obtained from a qHMBC experiment. Original Data TD F1 256 F2 660. Digitization was as follows: F1 SI 4k QSINE (SSB 0), F2 SI 4k QSINE (SSB 2).

3.2.3.3. **Compound 3.**

1α-Hydroxycimigenol-3-*O*-α-L-arabinopyranoside

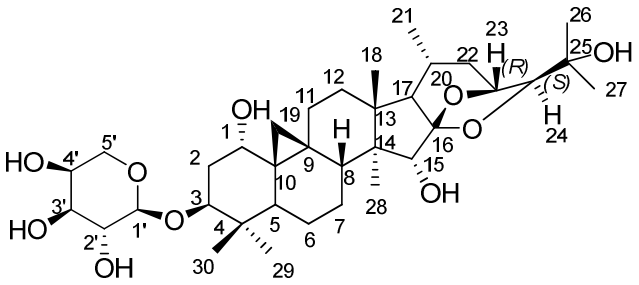

1-α-Hydroxycimigenol-3-*O*-α-L-arabinopyranoside (**3**) was obtained as a white powder. The HR-ESI-MS revealed a sodiated ion $[M+Na]^+$ at *m/z* 659.3777 (calculated for $C_{35}H_{56}O_{10}Na$, 559.3771) indicating a molecular formula for the analyte of $C_{35}H_{56}O_{10}$. The ^1H NMR spectrum revealed one cyclopropane methylene at 0.431 and 0.707 ppm, six tertiary methyls at 1.096, 1.207, 1.275, 1.377, 1.477 and 1.495 ppm, a secondary methyl at 0.854 ppm. A broad singlet for proton 1 was observed at 3.823 ppm, suggested a hydroxyl group at position 1 of this triterpene. At lower field, H-23 (4.767 ppm, broad d, *J* = 9.2 Hz) and H-24 (3.774 ppm, s) indicates that the side chain is a 23*R,*24*S* cimigenol type. The sugar proton splitting pattern was identical to that of **2**. Hence the structure was identified as 1-α-hydroxycimigenol-3-*O*-α-L-arabinopyranoside.

Kusano *et al*. previously isolated and characterized this compound from *Cimicifuga simplex* (34). The NMR assignment of the aglycone was done with the aid of COSY and HMBC spectra, as well as comparison with reported data (32,54,59,60).

1-α-Hydroxycimigenol-3-*O*-α-L-arabinopyranoside (**3**): ^1H NMR (900 MHz, C_5D_5N) Aglycone moiety δ 4.767 (1H, brd, *J* = 9.2 Hz, H-23), 4.353 (1H, dd, *J* = 4.5, 12.0 Hz, H-3), 4.312 (1H, d, *J* = 7.6 Hz, H-15), 3.824 (1H, brs, H-1), 3.774 (1H, s, H-24), 2.879 (1H, m, H-

11α), 2.754 (1H, ddd, *J* = 13.3, 4.1, 4.1 Hz, H-2α), 2.475 (1H, dd, *J* = 4.7, 12.6 Hz, H-5, 2.281 (1H, overlapped, H-22β), 2.258 (1H, overlapped, H-2β), 2.159 (1H, m, H-7α), 1.788 (1H, overlapped, H-12β), 1.766 (1H, dd, *J* = 3.8, 12.5 Hz, H-8), 1.686 (1H, m, H-20), 1.667 (1H, overlapped, H-6α), 1.627 (1H, overlapped, H-12β), 1.513 (1H, d, *J* = 14.8, H-17), 1.495 (3H, s, H-27), 1.477 (3H, s, H-26), 1.414 (1H, m, 11β), 1.384 (1H, overlapped, H-7β), 1.377 (3H, s, H-29), 1.275 (3H, s, H-28), 1.207 (3H, s, H-18), 1.096 (3H, s, H-30), 1.026 (1H, dt, *J* = 1.8, 11.9 Hz, H-22α), 0.854 (3H, d, *J* = 6.5 Hz, H- 21), 0.852 (1H, m, H-6β), 0.707 (1H , d, *J* = 4.2 Hz, H-19 endo), 0.431 (1H, d, *J* = 4.2 Hz, H-19 exo); sugar moiety δ 4.820 (1H, d, *J* = 7.1 Hz, H-1'), 4.465 (1H, dd, *J* = 7.1, 8.1 Hz, H-2', 4.139 (1H, dd, *J* = 3.5, 8.8 Hz, H-3'), 4.291 (1H, m, H-4'), 3.658 (1H, dd, *J* = 12.2, 1.1 Hz, H-5'β), 4.212 (1H, dd, *J* = 12.2, 2.9 Hz, H-5'α)

,

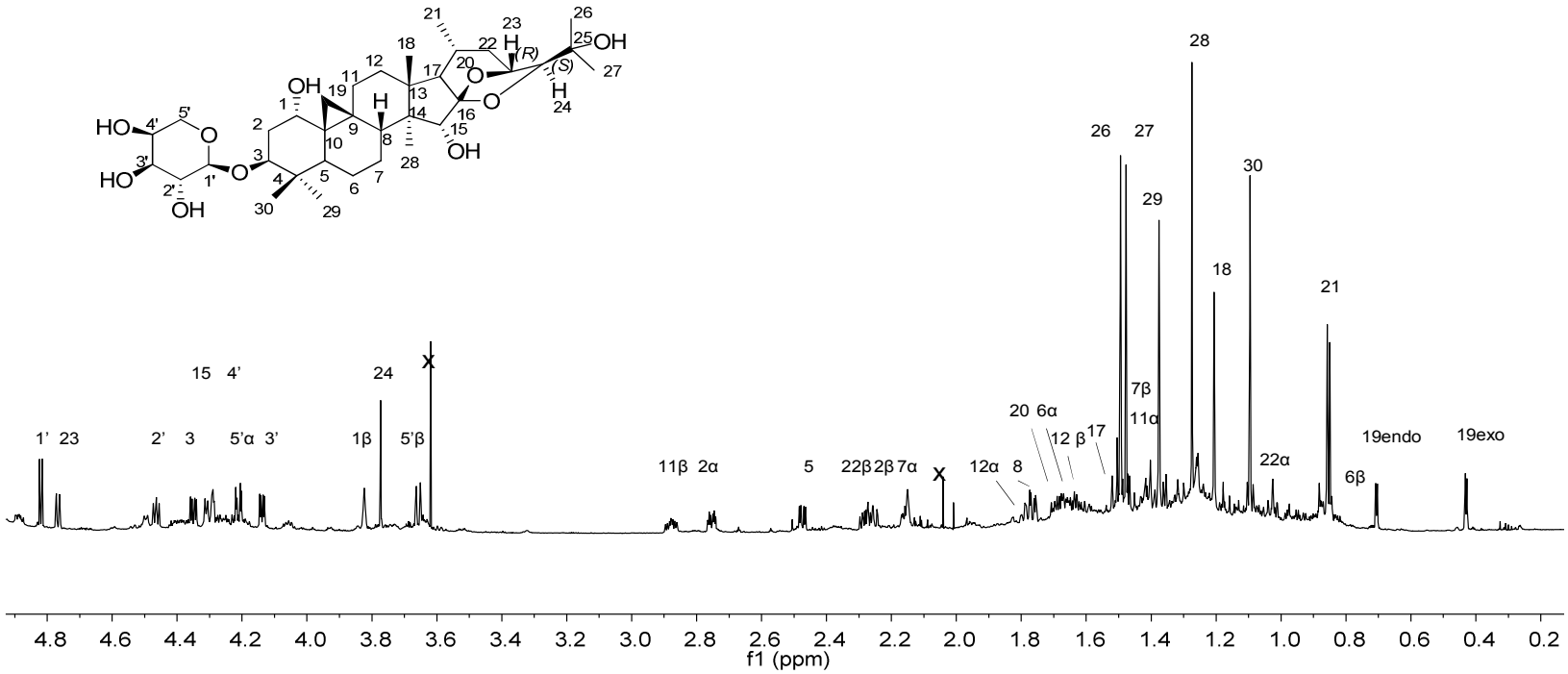

Figure 31. Compound 3; 900 MHz ^{1}H NMR in pyridine-d_5

Chemical shifts were calibrated to 7.217 ppm for the residual protonated species of pyridine. Digitization was as follows: GM (LB -1.0 Hz, GB 0.1).

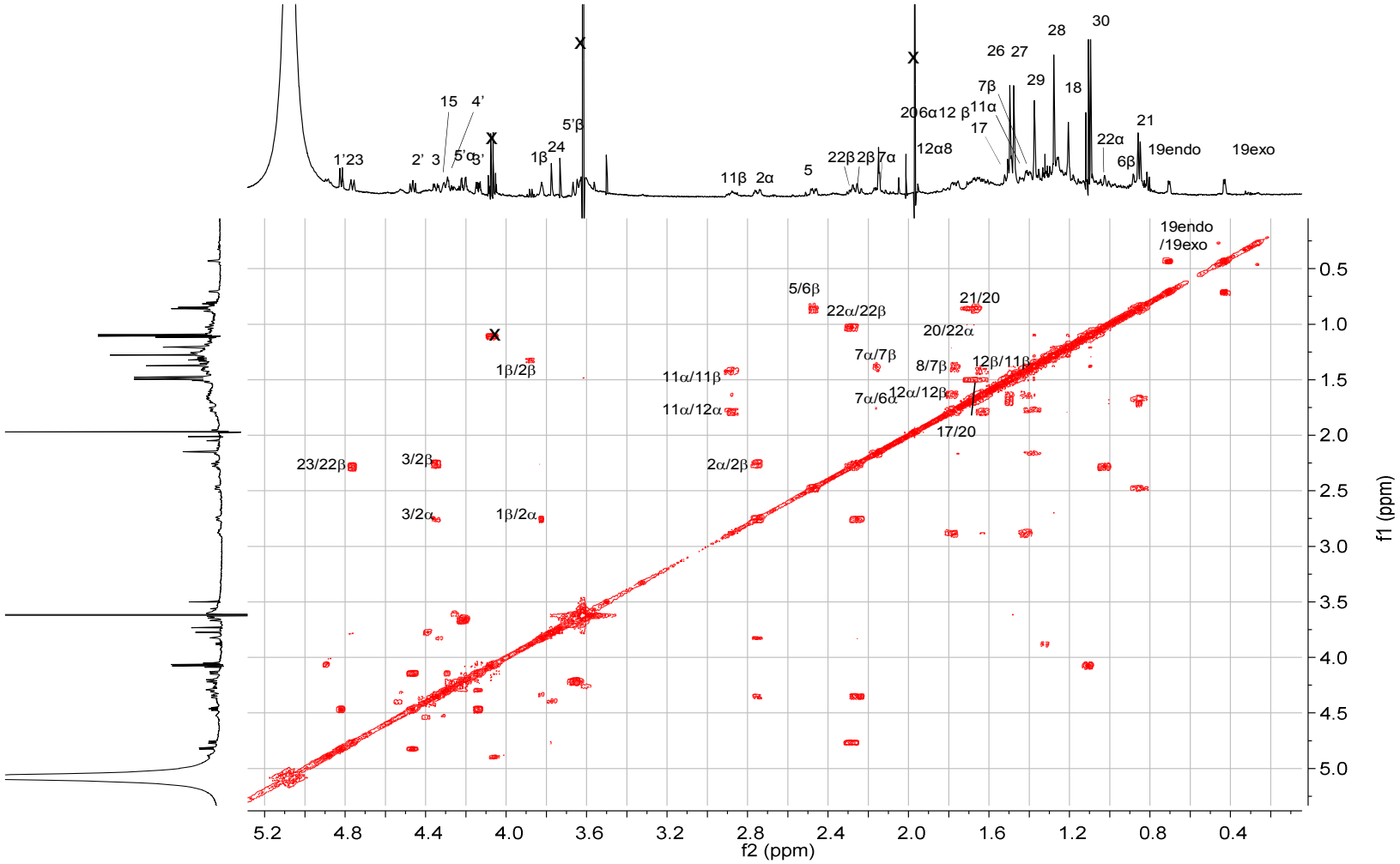

Figure 32. Compound 3; 600 MHz gCOSY spectrum in pyridine-d_5

Chemical shifts were calibrated to 7.217 ppm for the residual protonated species of pyridine. Digitization was as follows: F2 SI 4k SINE (SSB0), F1 SI 4k SINE (SSB 0).

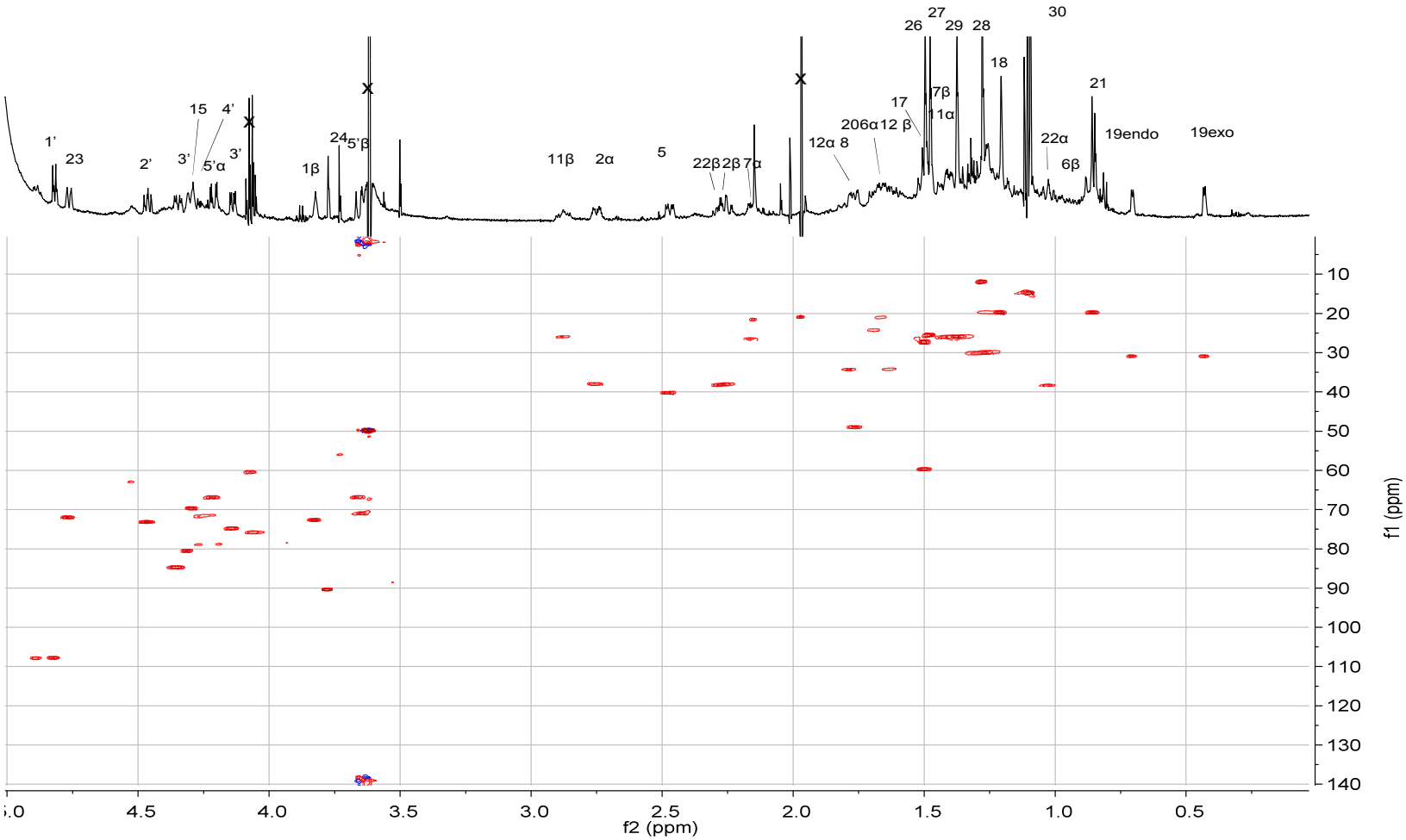

Figure 33. Compound 3; 600 MHz gHMBC spectrum in pyridine-d_5

Chemical shifts were calibrated to 7.217 ppm for the residual protonated species of pyridine on F1 and to 123.5 ppm on F2. Original Data TD F1 256 F2 4k. Digitization was as follows: F1 SI 4k SINE (SSB 0) F2 SI 8k SINE (SSB0)

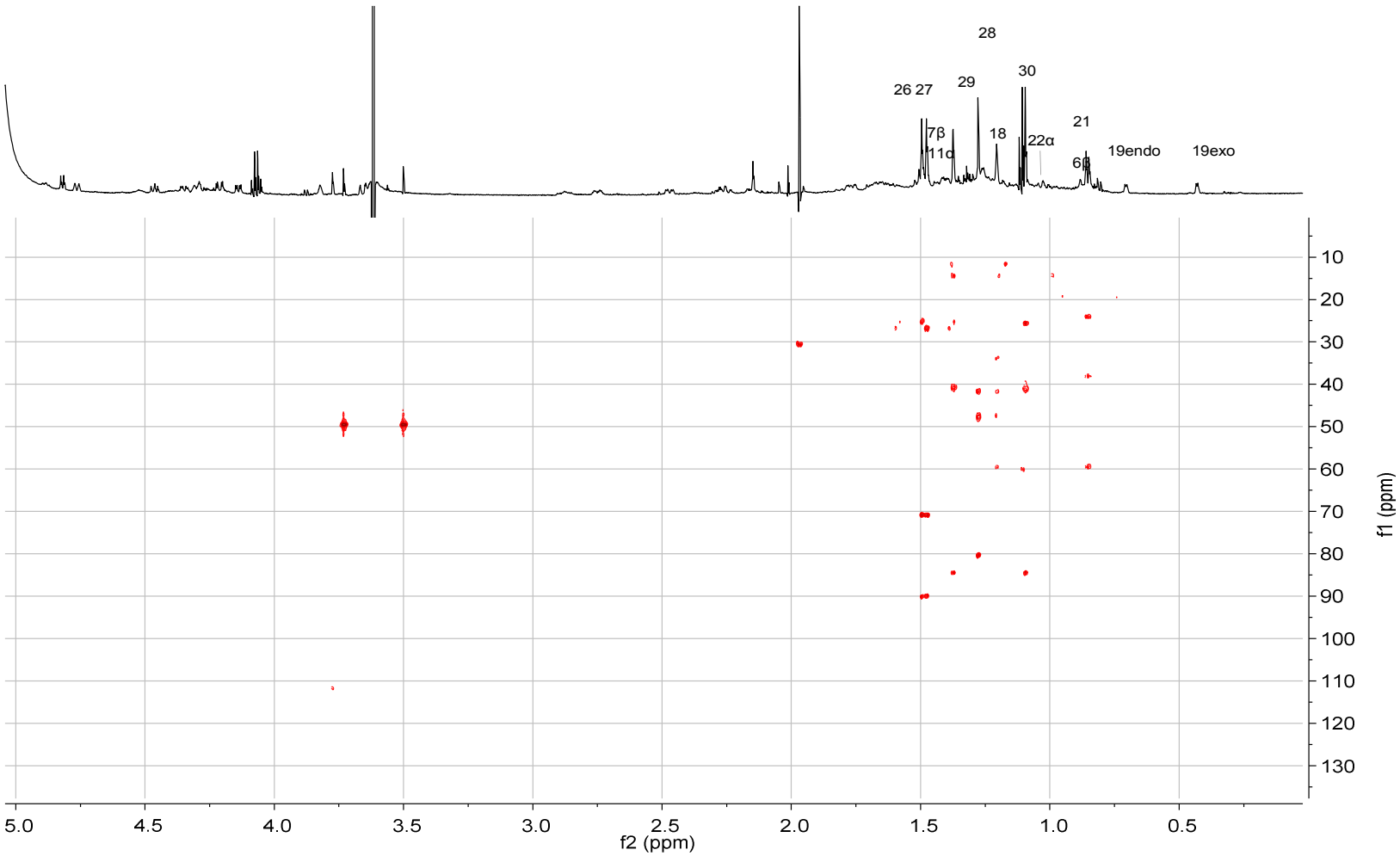

Figure 34. Compound 3; 600 MHz gHSQC spectrum in pyridine-d_5

Chemical shifts were calibrated to 0.416 ppm for H-19 exo on F1 and to 30.7 ppm on F2. The number was obtained from a qHMBC experiment. Original Data TD F1 256 F2 660. Digitization was as follows: F1 SI 2k QSINE (SSB 2), F2 SI 4k QSINE (SSB 2).

3.2.3.4. **Compound 4. 1α-Hydroxycimigenol-3-*O*-β-D-xylopyranoside**

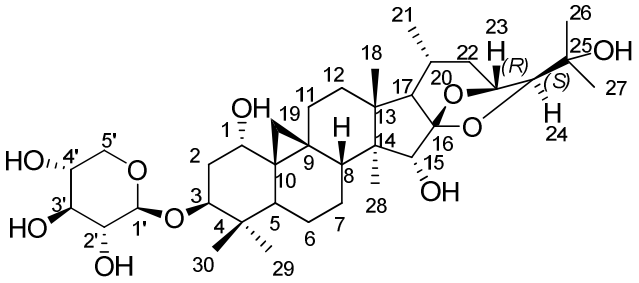

1α-Hydroxycimigenol-3-*O*-β--D-xylopyranoside (**4**) was obtained as a white powder. The HR-ESI-MS revealed a sodiated molecule $[M+Na]^+$ at *m/z* 659.3743 (calculated for $C_{35}H_{56}O_{10}Na$, 659.3771) indicating a molecular formula for the analyte of $C_{35}H_{56}O_{10}$, which is identical to the molecular formula of previously isolated compound **3**. The ^1H NMR spectrum revealed one cyclopropane methylene at 0.437 and 0.714 ppm, six tertiary methyls at 1.135, 1.206, 1.273, 1.420, 1.480 and 1.632 ppm, and a secondary methyl at 0.853 ppm. The sugar was determined to be an L-arabinopyranoside from the signal pattern especially the characteristic triplet peak of H5'β at 3.586 ppm. A detailed spin simulation of the saccharide was carried out by PERCH iteration software and shown in the previous section (Figure 7). A broad singlet of proton 1 was observed at 3.836 ppm, suggesting a hydroxyl group at position 1 of this triterpene. For the side chain determination, the characteristic singlet at 3.774 ppm and a doublet at 4.769 ppm (9.2 Hz) were used to show that this compound is a 23*R*,24*S* cimigenol type unlike the 23*R*,24*R* compound **1**.

NMR experiments at 700 MHz gave abundant information on **4** with high sensitivity. The phase sensitive HSQC spectrum showed methylene carbons as positive peaks. This helped confirm assignments of otherwise ambiguous peaks especially in regions of signal

overlap. Methine and methyl carbon cross peaks were shown in negative peaks. The HMBC spectrum was also obtained.

1α-Hydroxycimigenol-3-*O*-β-D-xylopyranoside (**4**): ^{1}H NMR (900 MHz, C_5D_5N) Aglycone moiety δ 4.769 (1H, d, *J* = 9.2 Hz, H-23), 4.483 (1H, d, *J* = 8.7 Hz, OH-15), 4.374 (1H, dd, *J* = 4.5, 12.1 Hz, H-3), 4.312 (1H, d, *J* = 8.7 Hz, H-15), 3.836 (1H, brs, H-1), 3.774 (1H, s, H-24), 2.884 (1H, m, H-11α), 2.749 (1H, ddd, *J* = 13.3, 4.1, 4.1 Hz, H-2a), 2.489 (1H, dd, *J* = 4.7, 12.7, H-5), 2.281 (1H, overlapped, H-22α), 2.272 (1H, overlapped, H-2β), 2.162(1H, m, H-7α), 1.787 (1H, overlapped, H-12α), 1.769 (1H, dd, *J* = 4.2, 12.4 Hz, H-8), 1.687 (1H, overlapped, H-6α), 1.678 (1H, overlapped, H-20), 1.632 (1H, m, H-12β), 1.501 (3H, s, H-27), 1.495 (1H, overlapped, H-17), 1.480 (3H, s, H-26), 1.426 (1H, overlapped,H-11β), 1.420 (3H, s, H-29), 1.388 (1H, m, H-7β), 1.273 (3H, s, H-28), 1.206 (3H, s, H-18), 1.135 (3H, s, H-30), 1.026 (1H, dt, *J* = 1.8, 11.9 Hz, H-22β), 0.861 (1H, overlapped, H-6β), 0.853 (3H, d, *J* = 6.2 Hz, H-21), 0.714 (1H, d, *J* = 4.2 Hz, H-19 endo), 0.437 (1H, d, *J* = 4.2 Hz, H-19 exo); sugar moiety δ 4.890 (1H, d, *J* = 7.6 Hz, H-1'), 4.249 (1H, dd, *J* = 5.0, 11.0 Hz, H-5'β), 4.223 (1H, m, H-4'), 4.133 (1H, t, *J* = 8.8 Hz, H-3'), 4.052 (1H, m, H-2'), 3.586 (1H, t, *J* = 10.5 Hz, 5'α)

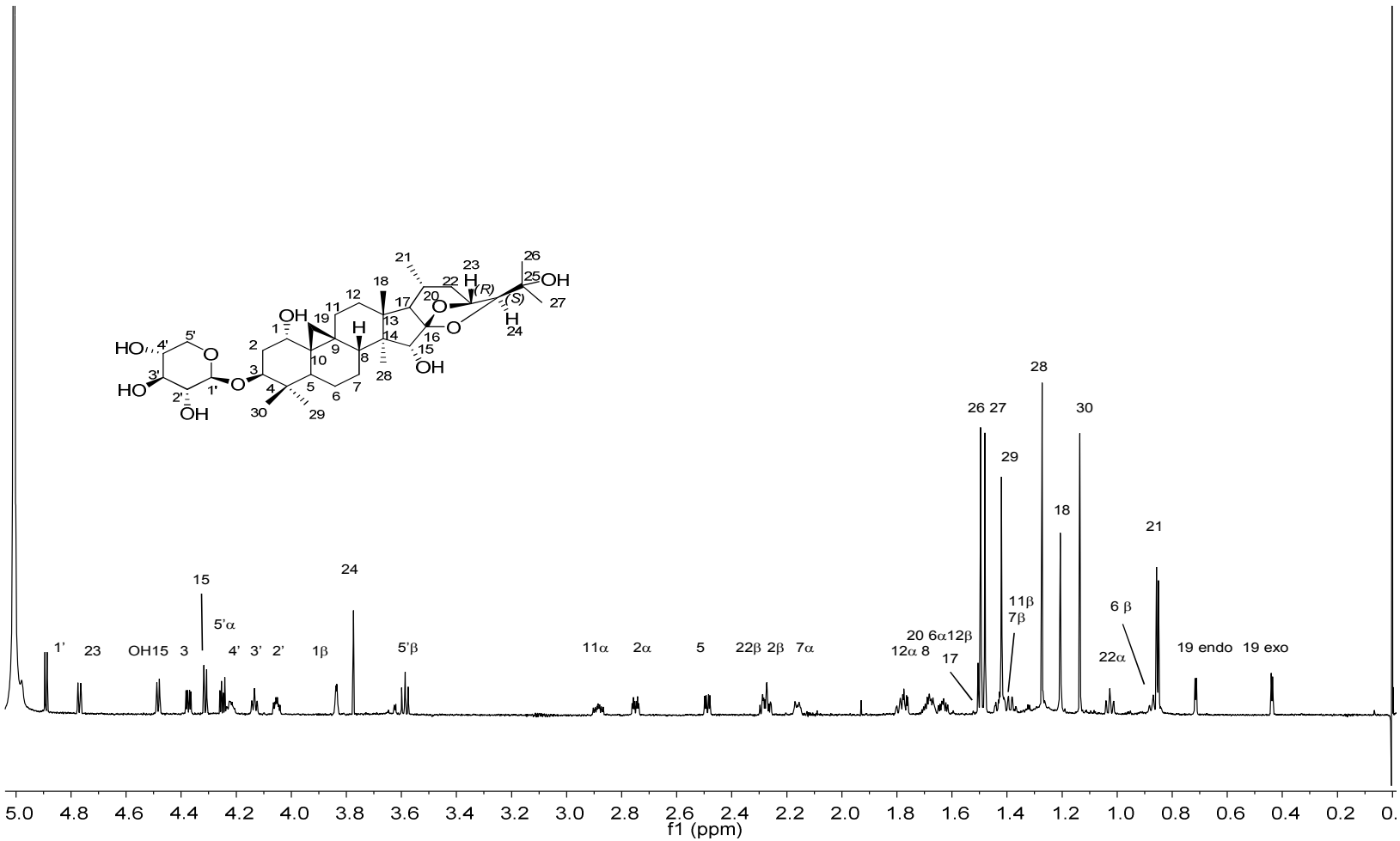

Figure 35. Compound 4; 900 MHz ^{1}H NMR in pyridine-d_5

Chemical shifts were calibrated to 7.217 ppm for the residual protonated species of pyridine. Digitization was as follows: GM (LB -1.0 Hz, GB 0.1).

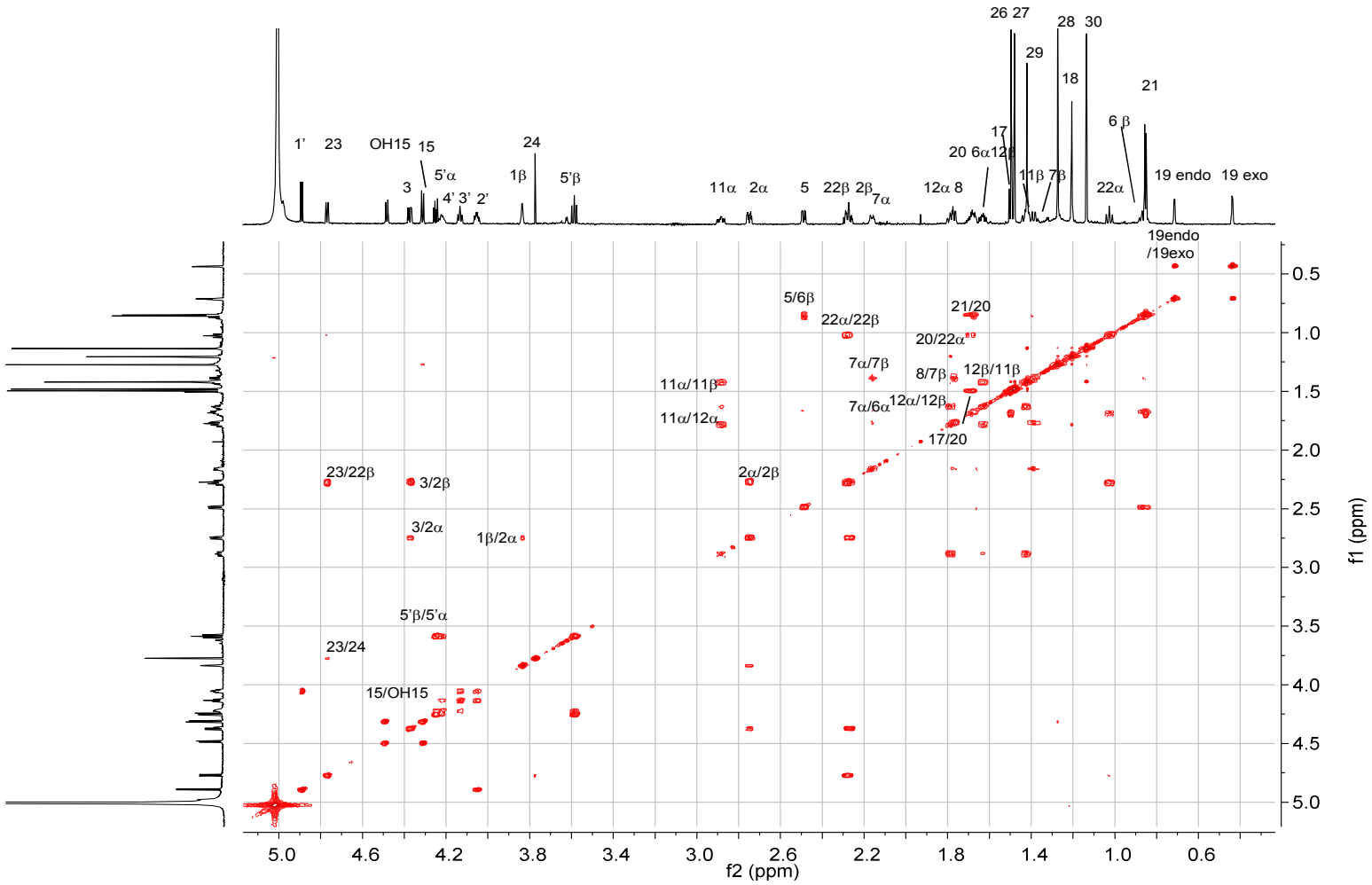

Figure 36. Compound 4; 600 MHz gCOSY spectrum in pyridine-d_5

Chemical shifts were calibrated to 5.00 ppm for the residual HOD. Original data F1 256 F2 4k. Digitization was as follows: F1 SI 4k SINE (SSB 0), F2 SI 4k SINE (SSB 0).

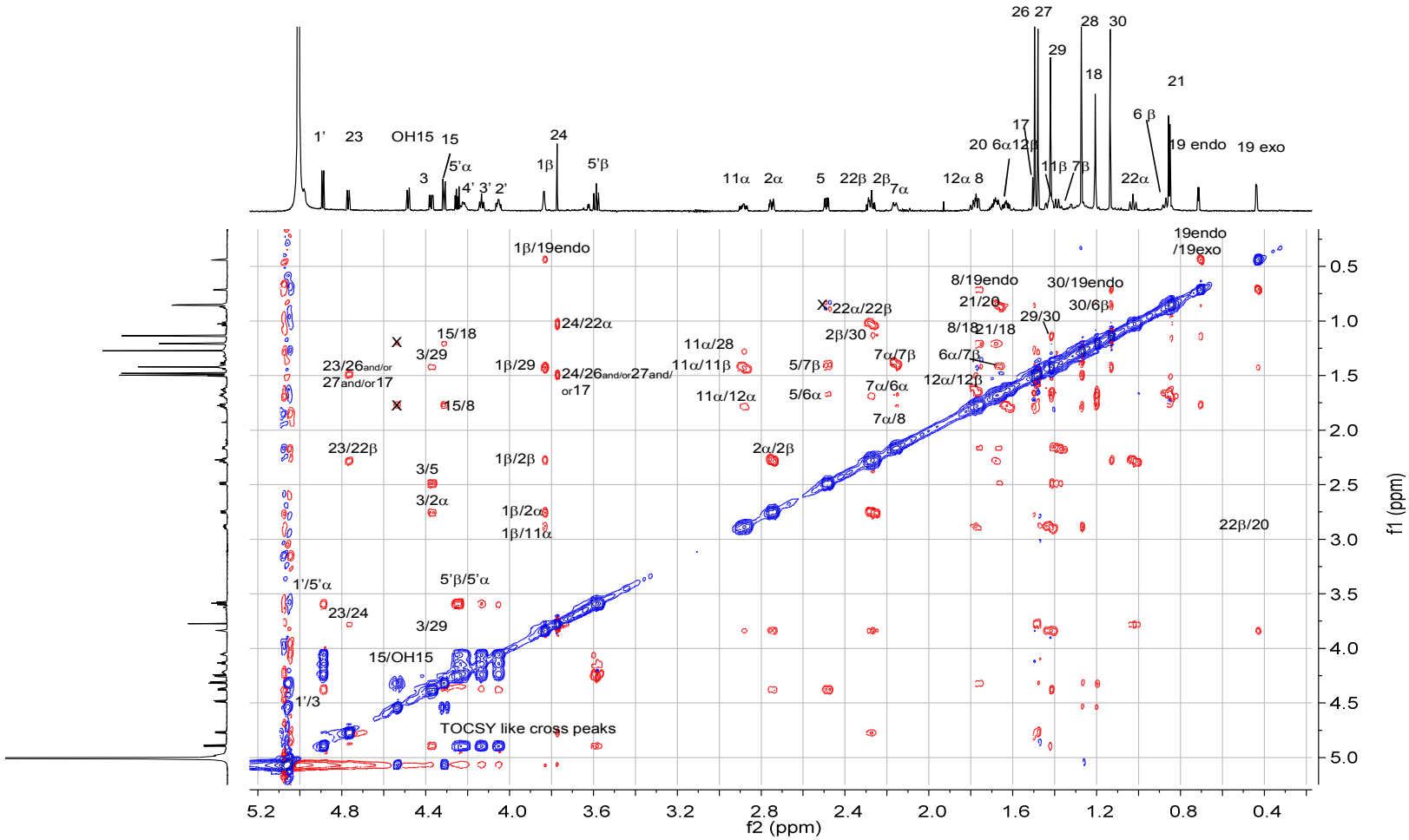

Figure 37. Compound 4; 700 MHz ROESY spectrum in pyridine-d_5

Chemical shifts were calibrated to 7.217 ppm for the residual protonated species of pyridine. Original data F1 256 F2 2k. Digitization was as follows: F1 SI 4k QSINE (SSB 2), F2 SI 4k QSINE (SSB 2).

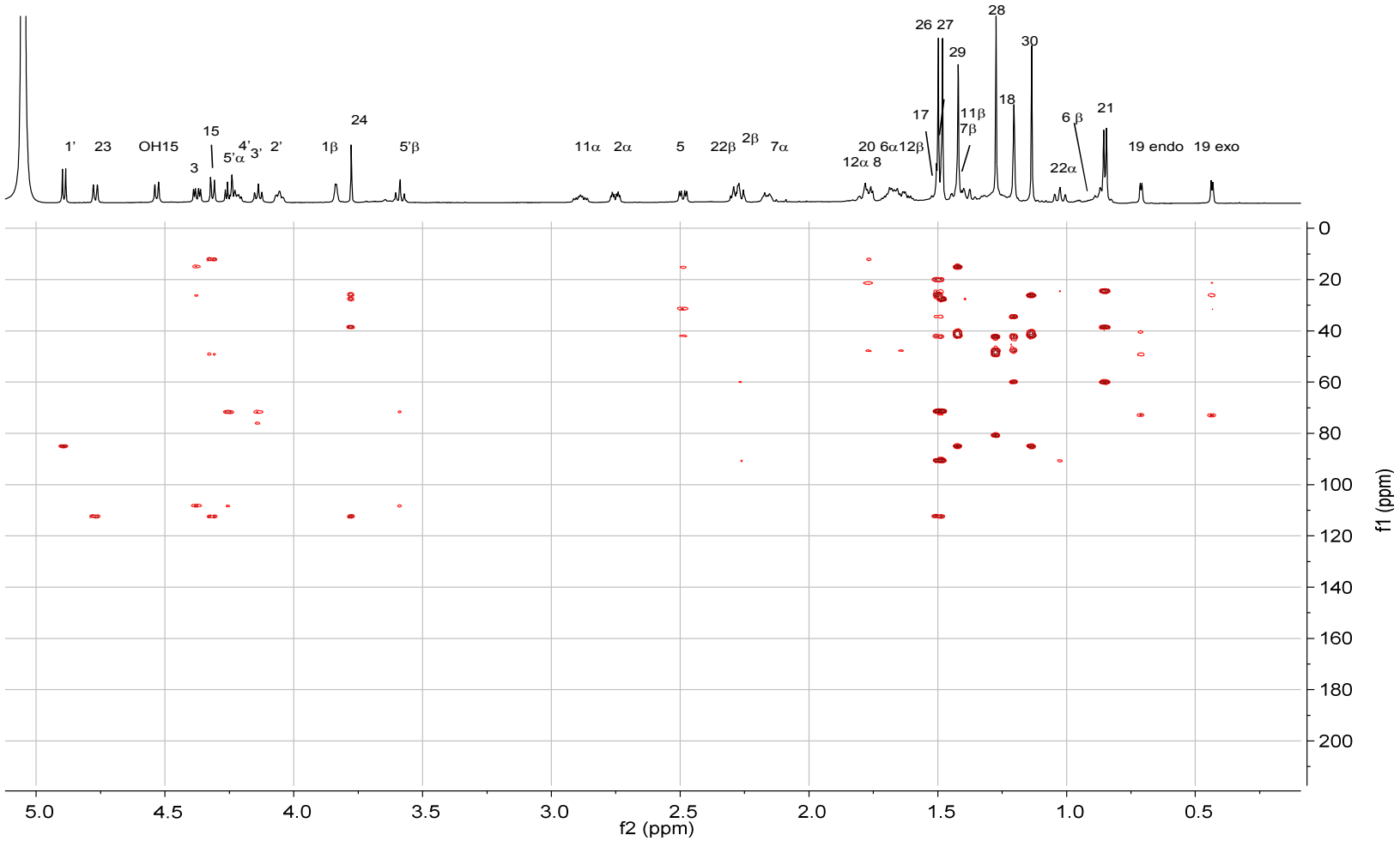

Figure 38. Compound 4; 600 MHz gHMBC spectrum in pyridine-d_5

Chemical shifts were calibrated to 7.217 ppm for the residual protonated species of pyridine on F1 and to 123.5 ppm on F2. Original data F1 256 F2 2k. Digitization was as follows: F1 SI 1k SINE (SSB0) F2 SI 2k SINE (SSB0)

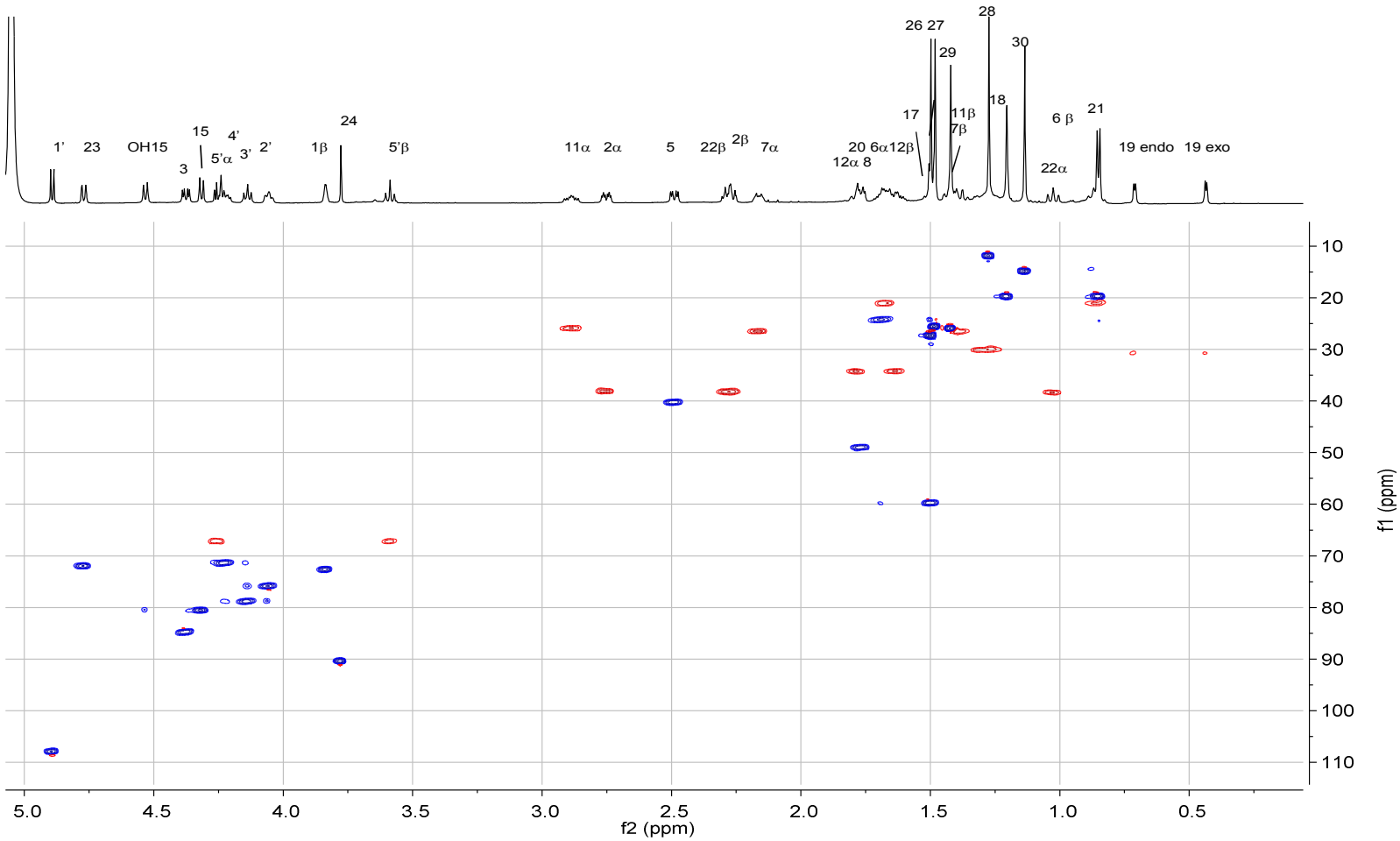

Figure 39. Compound 4; 600 MHz gHSQC spectrum in pyridine-d_5

Chemical shifts were calibrated to 7.217 ppm for the residual protonated species of pyridine on F1 and to 123.5 ppm on F2. Original data F1 256 F2 660. Digitization was as follows: F1 SI 2k QSINE (SSB 2), F2 SI 4k QSINE (SSB 2).

3.2.3.5. **Compound 5. 7β-Hydroxycimigenol aglycone**

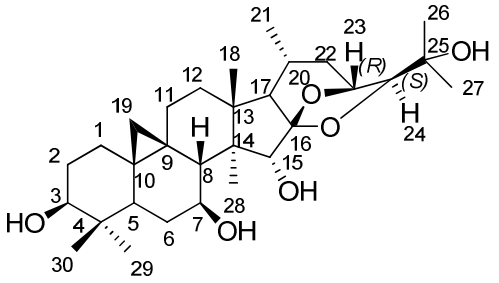

7β-Hydroxycimigenol aglycone (**5**) was obtained as a white powder. The high-resolution exact mass measurement of **5** gave a protonated molecule $[M+H]^+$ at *m/z* 505.3512 (calculated for $C_{30}H_{49}O_6$, 505.3526) indicating a molecular formula for the analyte of $C_{30}H_{48}O_6$. The ^{1}H-NMR spectrum revealed one cyclopropane methylene at 0.414 and 0.731 ppm, six tertiary methyls at 1.132, 1.223, 1.246, 1.324, 1.513 and 1.534 ppm, and a secondary methyl at 0.894 ppm. No signals associated with a saccharide moiety were observed. A singlet at 3.801 ppm and a doublet at 4.800 ppm (*J* = 9.2 Hz) are assigned as H-24 and H-23, respectively, as indicated from both the COSY connectivity and the magnitude of the coupling constants. This demonstrates that the side chain of this compound is of the 23*R*,24*S* cimigenol type. The presence of a ^{1}H pseudo-triplet at 3.711 ppm of H-7 suggests the presence of an OH at C-7, which clearly shows coupling correlations with H-6α, β and H-8 in the COSY spectrum.

Compound **5** was previously obtained by enzymatic hydrolysis of a glycoside mixture from *C. simplex* by Kusano *et al.*, but was isolated in the present study from *Cimicifuga* species for the first time (61,62). Assignments in the previously reported ^{1}H NMR data were not supported by our 2D NMR. Two neighboring methyl signals Me-29 and Me-28 were incorrectly assigned as a singlet at 1.23 ppm as Me-29 and a singlet at 1.33

ppm as Me-28. In this study, seven methyls were unambiguously assigned with a gHMBC spectrum. The methyl signal at lower field (1.324 ppm) is assigned as Me-29 and the higher field methyl signal (1.246 ppm) as Me-28. The assignment of methyl signals was performed starting with the Me-18 signal because its appearance is unique due to a long range coupling between H-12β in cimigenol type of compound as shown by the PERCH simulation in (Figure 16) for compound **1**. In the ^{1}H spectrum, the Me18 signal appears at 1.223 ppm as the shortest of all tertiary methyl singlets (Figure 40).

7β-Hydroxycimigenol (**5**) ^{1}H NMR (900 MHz, C_5D_5N) Aglycone moiety δ 4.800 (1H, d, *J* = 9.2 Hz, H-23), 4.485 (1H, d, *J* = 6.5 Hz, H-15), 3.802 (1H, s, H-24), 3.711 (1H, brt, *J* = 10.7 Hz, H-7 (3.577, 1H, ddd, *J* = 11.2, 4.5, 4.5 Hz, H-3), 2.301 (1H, m, H-22α), 2.110 (1H, m, H-11), 2.085 (1H, ddd, *J* = 12.6, 3.7, 3.7 Hz, H-6a), 2.017 (1H, m, H-2α), 1.909 (1H, m, H-2β), 1.846 (1H, d, *J* = 10.7 Hz, H-8), 1.711 (1H, overlapped, H-12a), 1.695 (1H, overlapped, H-20), 1.605 (1H, overlapped, H-12b), 1.600 (1H, overlapped, H-5), 1.586 (1H, overlapped, H-1a), 1.566 (1H, d, *J* = 11.0 Hz, H-17), 1.534 (3H, s, H-26), 1.513 (3H, s, H-27), 1.324 (3H, s, H-28), 1.253 (1H, overlapped, H-6b), 1.246 (3H, s, H-29), 1.237 (1H, overlapped, H-1b), 1.223 (3H, s, H-18), 1.132 (3H, s, H-30), 1.110 (1H, m, H-11), 1.065 (1H, dt, *J* = 1.8, 11.9 Hz, H-22β), 0.894 (3H, s, H-21), 0.731 (1H, d, *J* = 4.3 Hz, H-19 endo), 0.414 (1H, d, *J* = 4.3 Hz, H-19 exo)

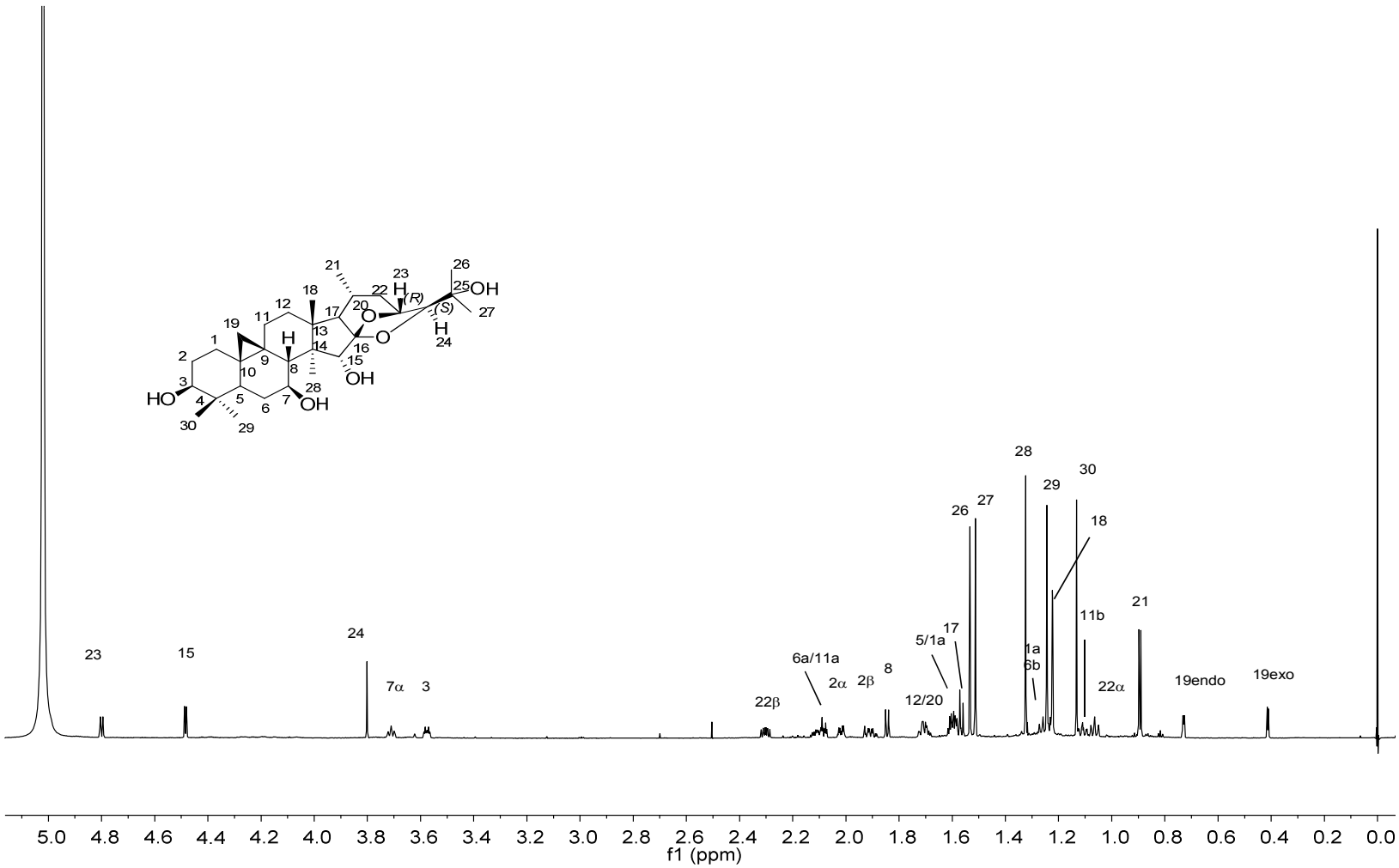

Figure 40. Compound 5; 900 MHz ^{1}H NMR in pyridine-d_5

Chemical shifts were calibrated to 7.217 ppm for the residual protonated species of pyridine. Digitization was as follows: GM (LB -1.0 Hz, GB 0.1).

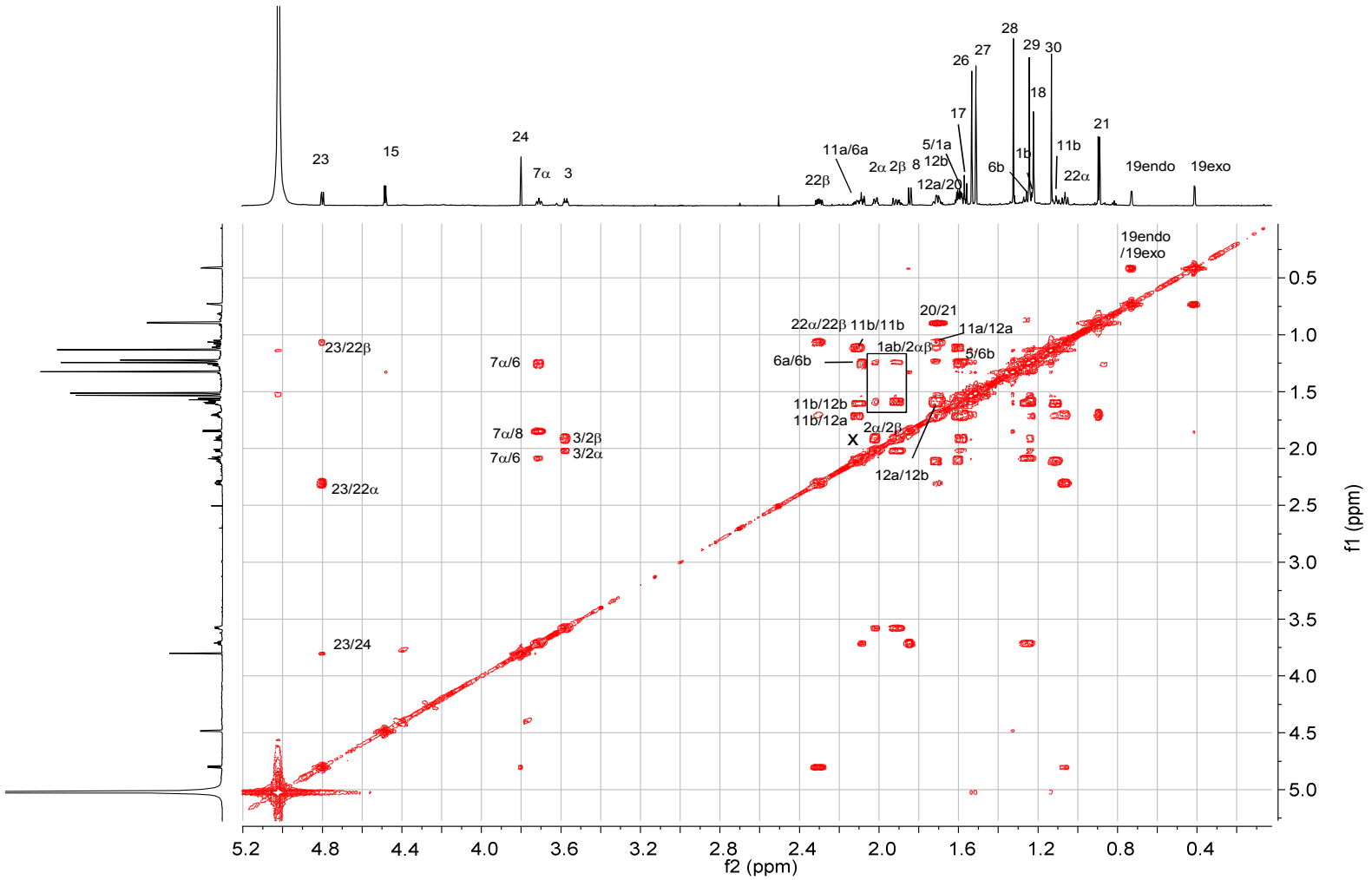

Figure 41. Compound 5; 900 MHz gCOSY spectrum in pyridine-d_5

Chemical shifts were calibrated to 7.217 ppm for the residual protonated species of pyridine. Original data F1 256 F2 2k. Digitization was as follows: F1 SI 4k SINE (SSB 0), F2 SI 4k SINE (SSB 0).

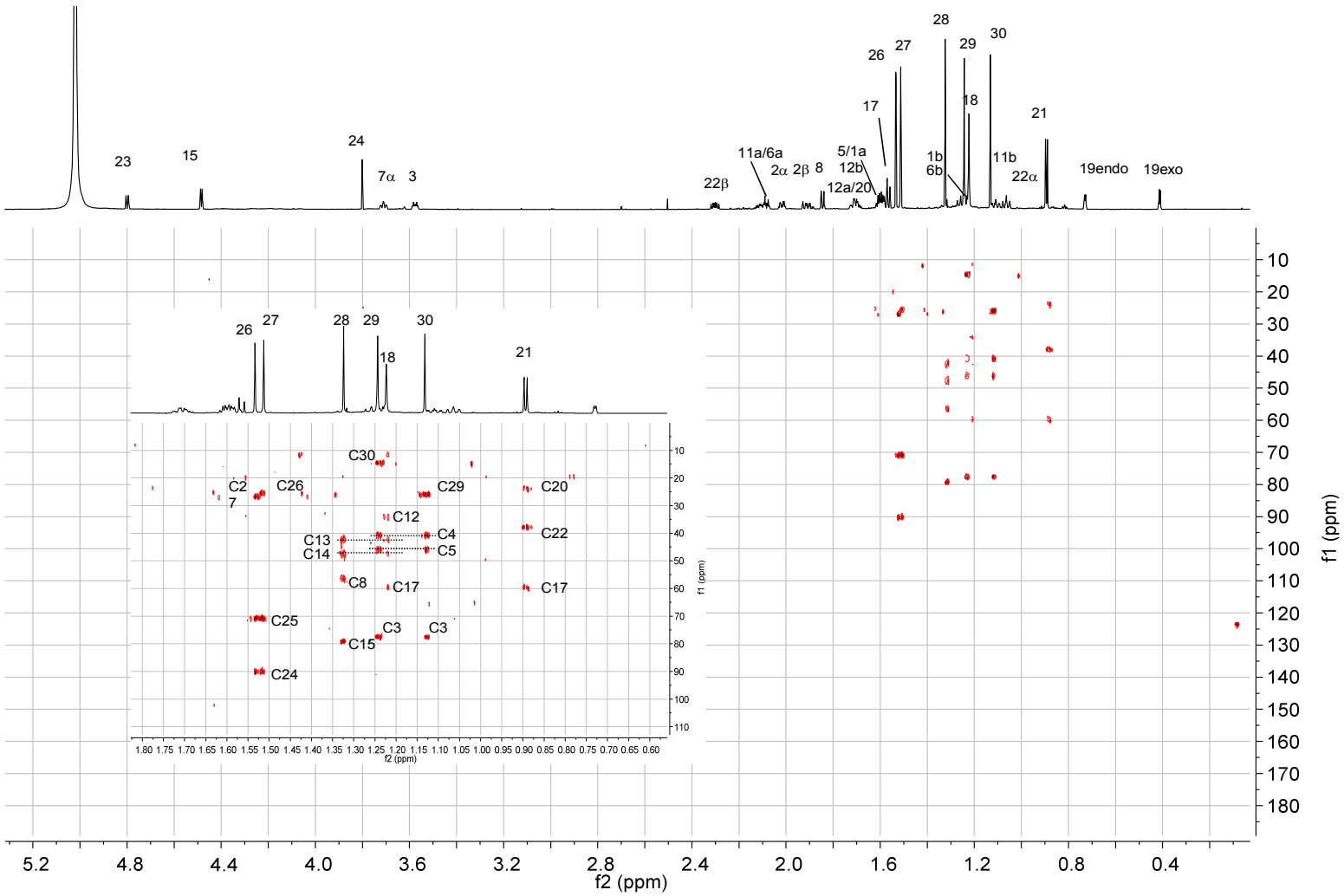

Figure 42. Compound 5; 600 MHz gHMBC spectrum in pyridine-d_5

Chemical shifts were calibrated to 7.217 ppm for the residual protonated species of pyridine. Original data F1 256 F2 4k. Digitization was as follows: F1 SI4k SINE (SSB0) F2 SI 8k SINE (SSB0)

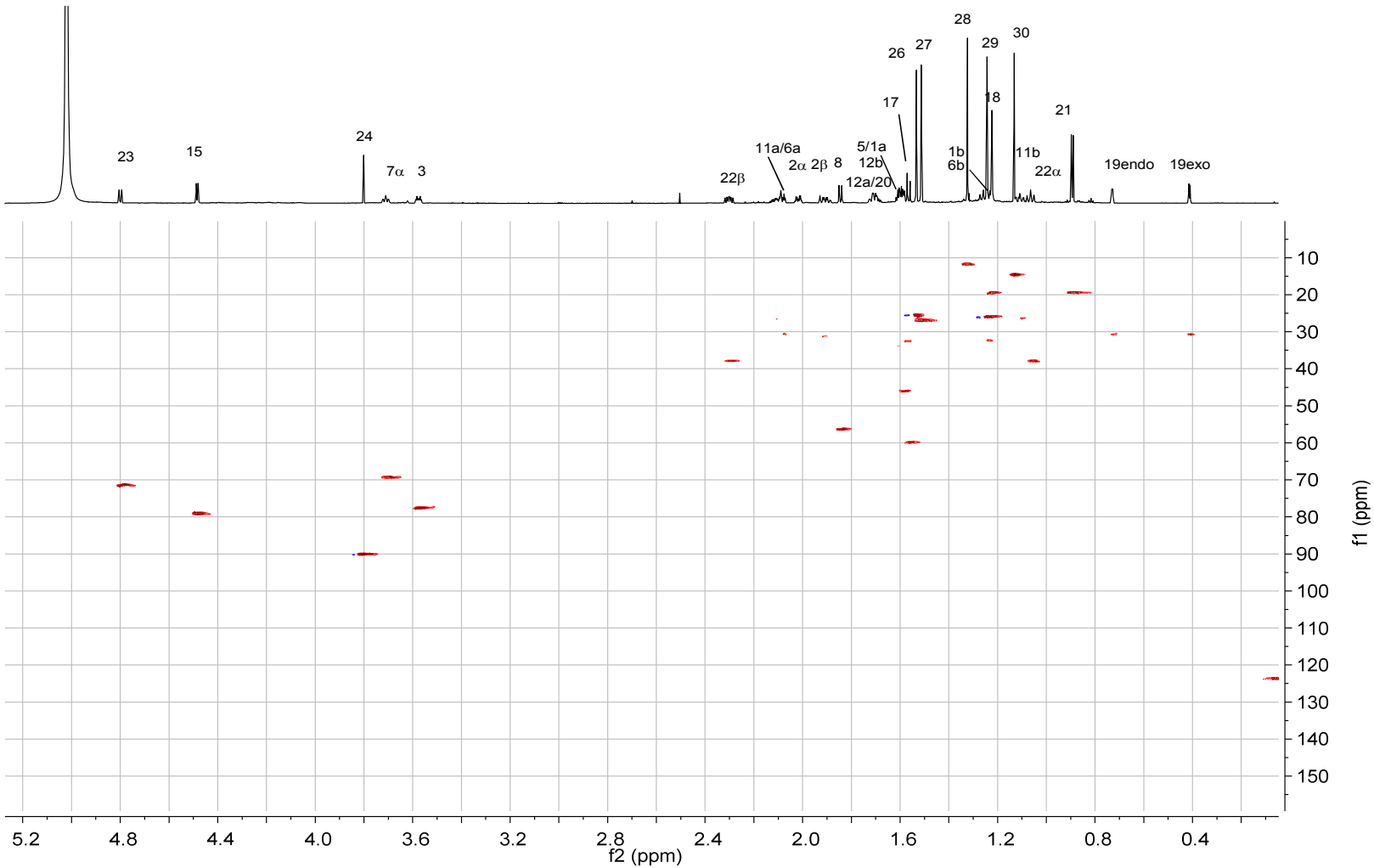

Figure 43. Compound 5; 600 MHz gHSQC spectrum in pyridine-d_5

Chemical shifts were calibrated to 7.217 ppm for the residual protonated species of pyridine. Original Data F1 256 F2 660. Digitization was as follows: F1 SI 2k QSINE (SSB 2), F2 SI 4k QSINE (SSB 0).

3.2.3.6. **Compound 6.**

25-*O*-Acetyl-7β-hydroxycimigenol-3-*O*-β-D-xylopyranoside

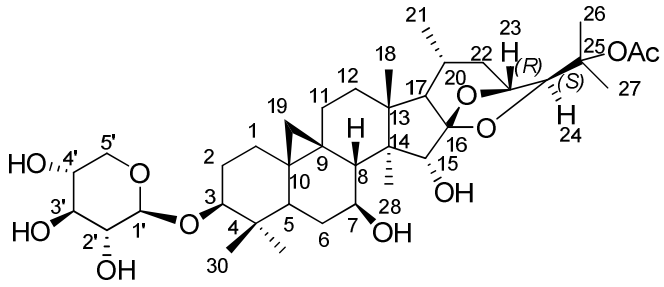

25-*O*-Acetyl-7β-hydroxycimigenol-3-*O*-β-D-xylopyranoside (**6**) was obtained as a white powder. The HR-ESI-MS revealed a protonated molecule $[M+H]^+$ at 679.4030 *m/z* (calculated for $C_{37}H_{59}O_{11}$, 679.4057) indicating the molecular formula of $C_{37}H_{58}O_{11}$. One acetate methyl peak was observed at 1.956 ppm in ^{1}H NMR spectrum. The ^{1}H NMR spectrum also revealed one cyclopropane methylene at 0.361 and 0.679 ppm, six tertiary methyls at 1.087, 1.189, 1.299, 1.360, 1.731, and 1.739 and ppm, a secondary methyl at 0.874 ppm. The monosaccharide is assigned as a D-xylopyranoside at C-3 due to the presence of the H-5'α triplet signal at 3.753 ppm. Other saccharide signals showed the same pattern as demonstrated for the xylopyranose of **4** (Figure 7), and the correlation was supported by a COSY spectrum. The presence of a pseudo-triplet of H-7 at 3.698 ppm suggests an OH at C-7, and the carbon chemical shift of C-7 at 69.2 ppm supports this. Methyl signals of C26 and C27 appeared relatively downfield compared to their positions in the spectrum of compound **5**, at 1.731 and 1.739 ppm respectively. This indicates that the OAc is attached to C-25.

Compound **6** has been isolated from *C. simplex* and reported in 1995 along with Compound **5** by Kusano *et al*. (62). The assignments of signals for Me-29 and Me-28 were corrected with the support of HMBC correlations.

25-*O*-Acetyl-7β-hydroxycimigenol-3-*O*-β-D-xylopyranoside (**6**) ^{1}H NMR (900 MHz, C_5D_5N) Aglycone moiety δ 4.616 (1H, d, *J* = 9.2 Hz, H-23), 4.458 (1H, d, *J* = 6.8 Hz, H-15), 4.167 (1H, s, H-24), 3.698 (1H, brt, *J* = 10.7 Hz, H-7), 3.542 (1H, dd, *J* = 11.2, 4.3 Hz, H-3), 2.390 (1H, m, H-2β), 2.281 (1H, m, H-22b), 2.072 (1H, m, H-11a), 2.039 (1H, m, H-6a), 1.964 (1H, overlapped, H-2α), 1.956 (3H, s, 25-OAc), 1.817 (1H, d, *J* = 10.2, H-8), 1.739 (3H, s, H-27), 1.731 (3H, s, H-26), 1.677 (1H, overlapped, H-12a), 1.667 (1H, overlapped, H-20), 1.618 (1H, overlapped, H-5), 1.605 (1H, overlapped, H-1a), 1.581 (1H, overlapped, H-12b), 1.516 (1H, d, *J* = 10.9 Hz, H-17), 1.360 (3H, s, H-29), 1.299 (3H, s, H-28), 1.241 (1H, m, H-1b), 1.189 (3H, s, H-18), 1.187 (1H, overlapped, H-6a), 1.087 (3H, s, H-30), 1.063 (1H, overlapped, H-11b), 1.016 (1H, overlapped, H-22α), 0.874 (3H, d, *J* = 6.6 Hz, H-21), 0.679 (1H, d, *J* = 4.3 Hz, H-19 endo), 0.361 (1H, d, *J* = 4.3 Hz, H-19 exo); Sugar moiety δ 4.879 (1H, d, *J* = 7.5 Hz, H-1'), 4.382 (1H, brt, *J* = 10.8, 10.8 Hz, H-5'β), 4.257 (1H, m, H-4'), 4.181 (1H, overlapped, H-3'), 4.056 (1H, m, H-2'), 3.753 (1H, dd, *J* = 5.2, 11.4 Hz, H-5'α)

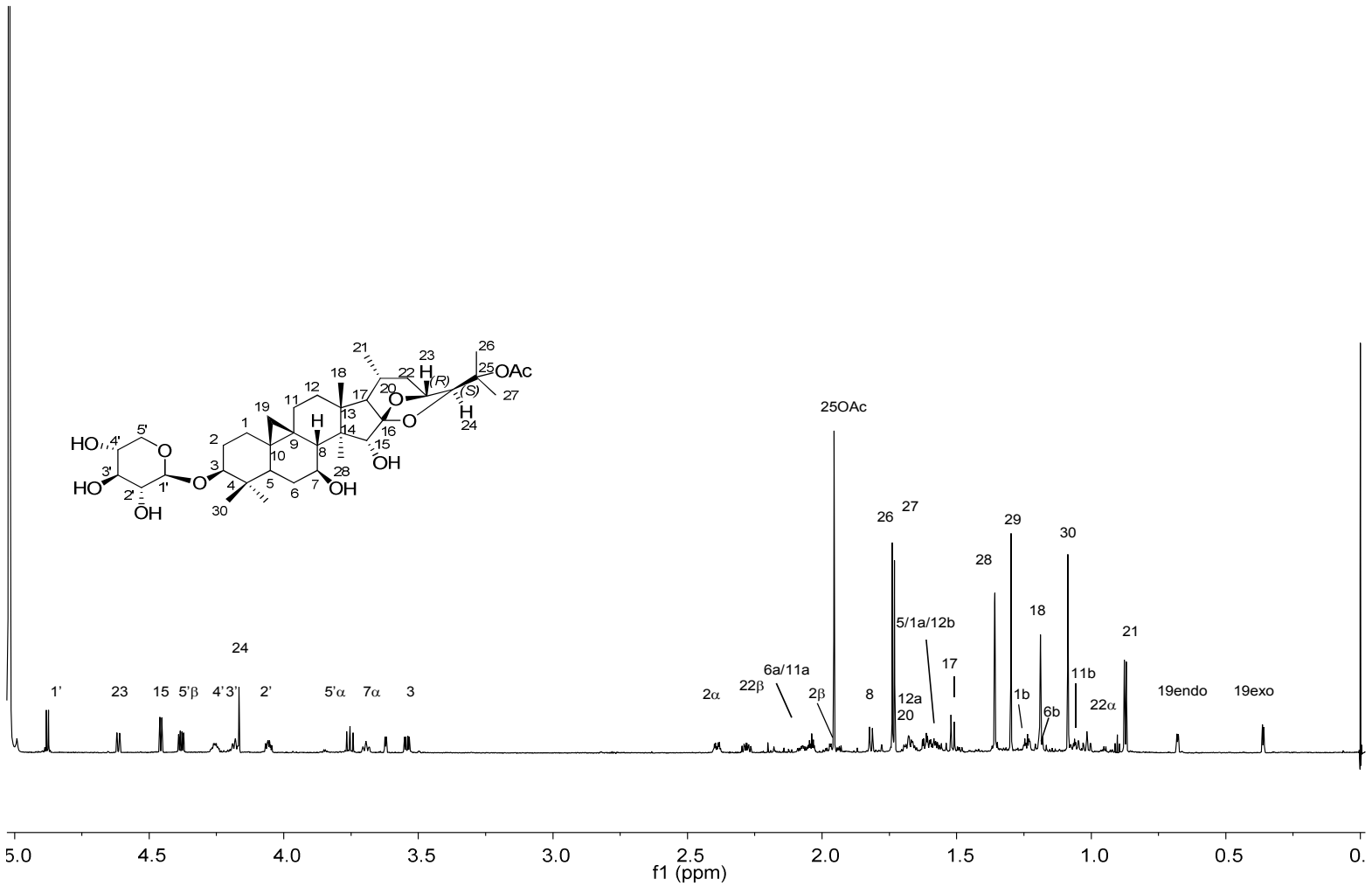

Figure 44. Compound 6; 900 MHz ^{1}H NMR in pyridine-*d*$_5$

Chemical shifts were calibrated to 7.217 ppm for the residual protonated species of pyridine. Digitization was as follows: GM (LB -1.0 Hz, GB 0.1).

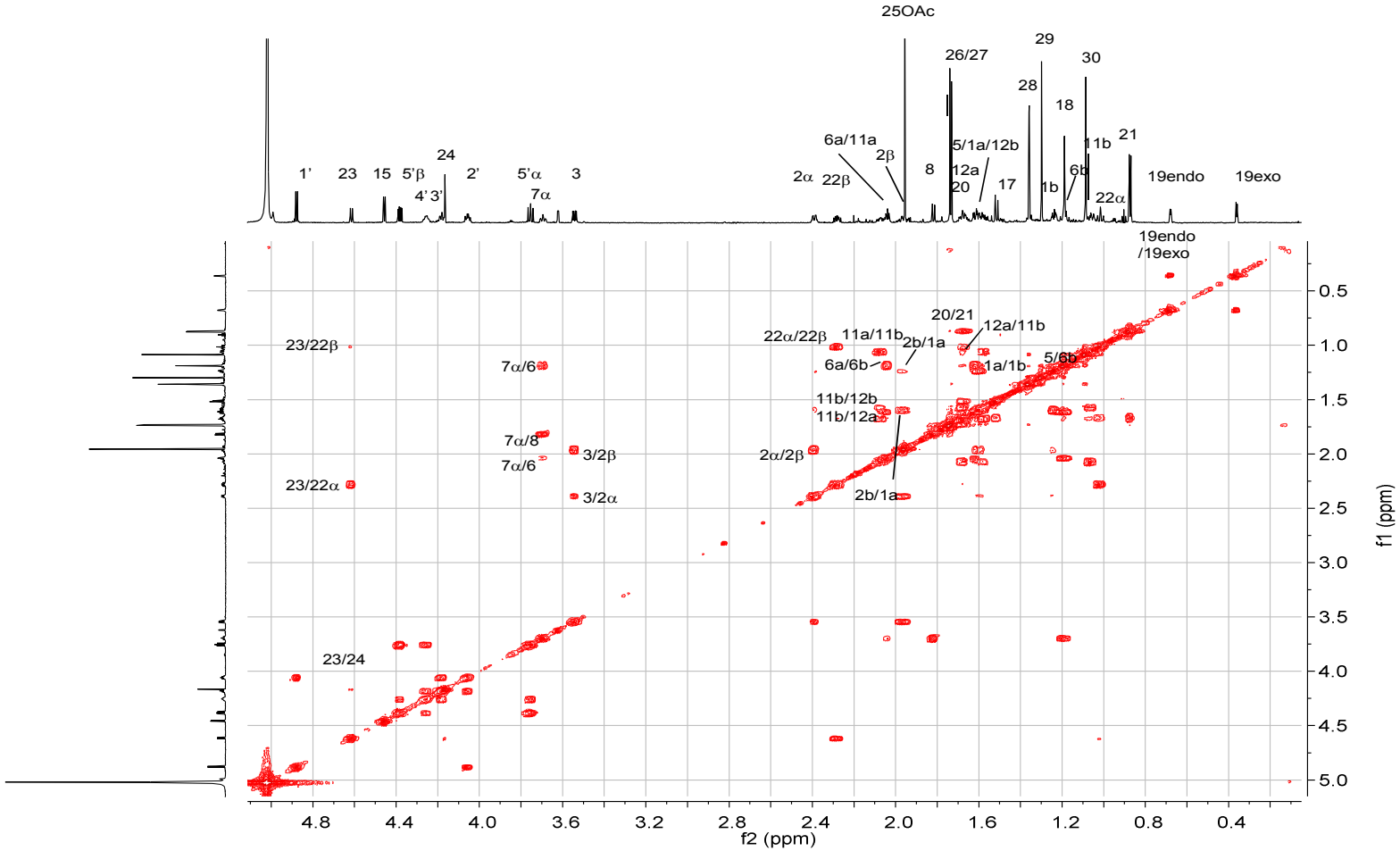

Figure 45. Compound 6; 900 MHz gCOSY spectrum in pyridine-*d*$_5$

Chemical shifts were calibrated to 7.217 ppm for the residual protonated species of pyridine. Original data F1 256 F2 2k. Digitization was as follows: F1 SI 4k SINE (SSB 0), F2 SI 4k SINE (SSB 0).

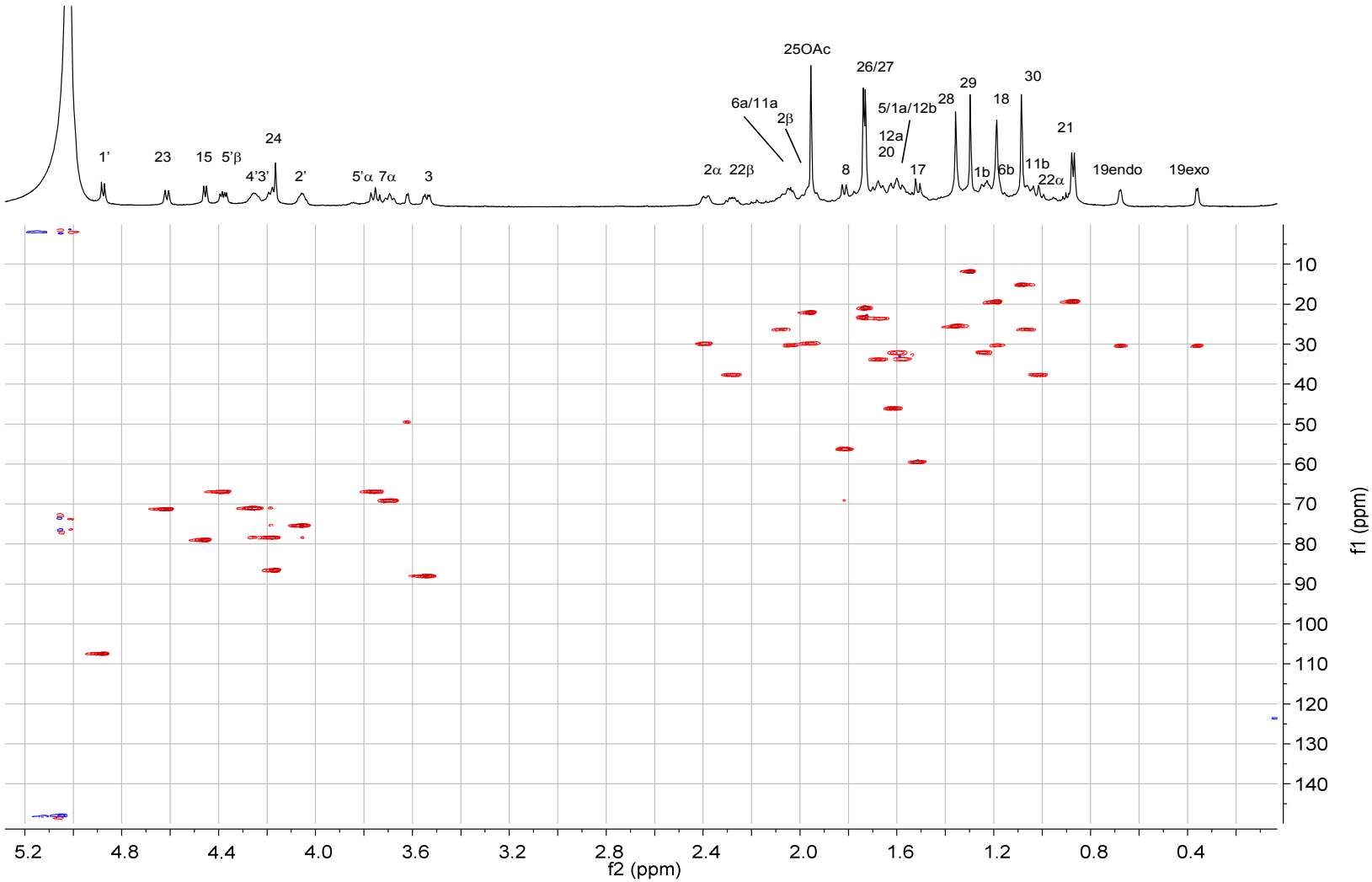

Figure 46. Compound 6; 600 MHz gHMBC spectrum in pyridine-d_5

Chemical shifts were calibrated to 7.217 ppm for the residual protonated species of pyridine on F1 and to 123.5 ppm on F2. Original data F1 256 F2 4k. Digitization was as follows: F1 SI 4k SINE (SSB 0) F2 SI 8k SINE (SSB0)

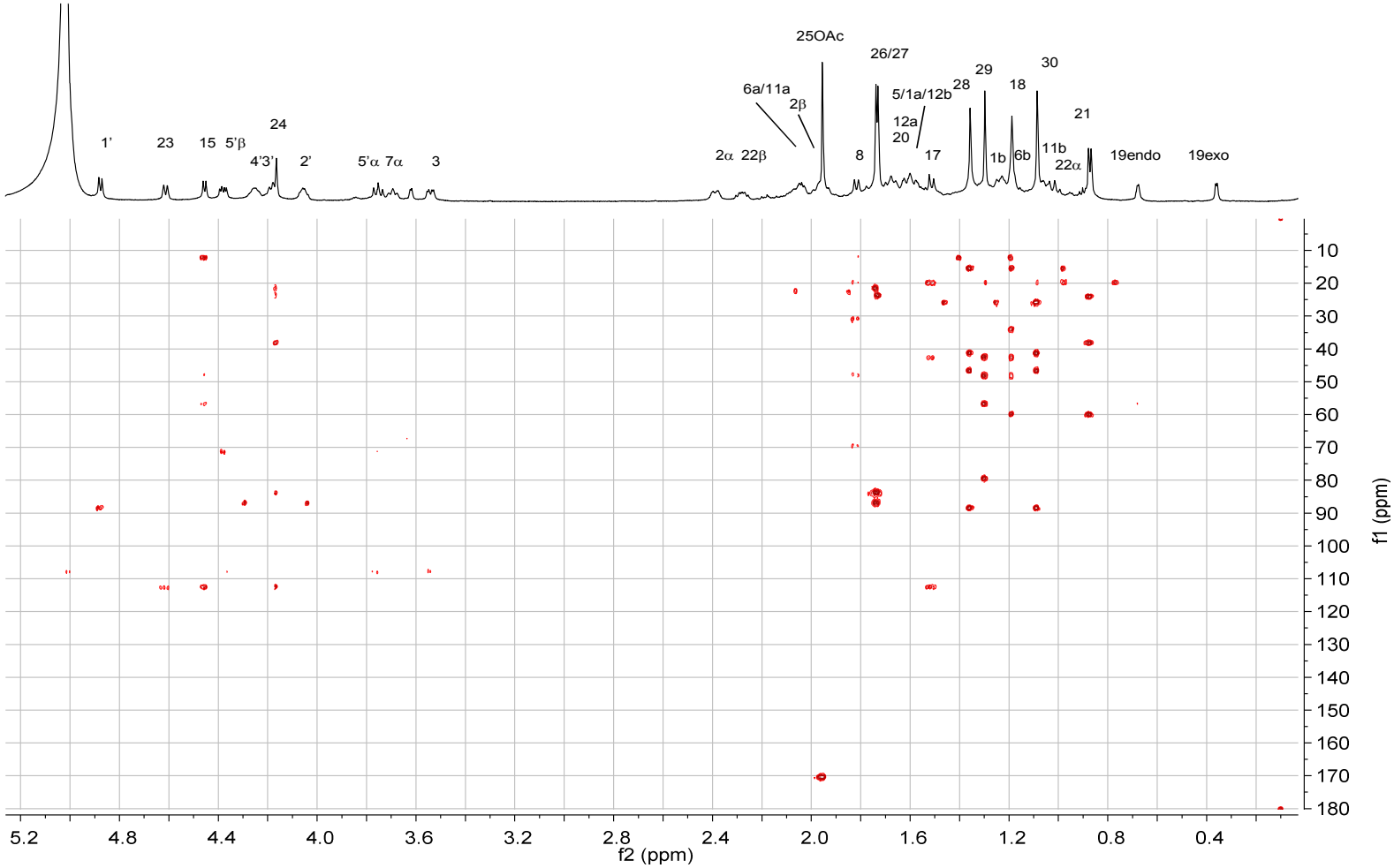

Figure 47. Compound 6; 600 MHz gHSQC spectrum in pyridine-d_5

Chemical shifts were calibrated to 7.217 ppm for the residual protonated species of pyridine on F1 and to 123.5 ppm on F2. Original Data F1 256 F2 960. Digitization was as follows: F1 SI 2k QSINE (SSB 2), F2 SI 4k QSINE (SSB 2).

3.2.3.7. **Compound 7.**

25-*O*-Acetylcimigenol-3-*O*-β-D-xylopyranoside

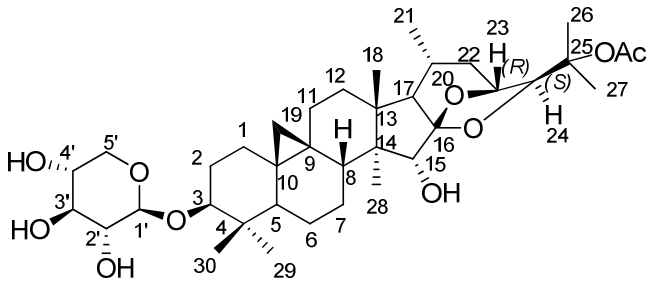

25-*O*-Acetyl cimigenol-3-*O*-β-D-xylopyranoside (**7**) was obtained as a white powder. The HR-ESI-MS revealed a protonated molecule $[M+H]^+$ at 663.4092 *m/z* (calculated for $C_{37}H_{59}O_{10}$, 663.4108) indicating a molecular formula of $C_{37}H_{58}O_{10}$. One acetate methyl peak was observed at 1.745 ppm in the ^{1}H NMR spectrum. The ^{1}H-NMR spectrum also revealed one cyclopropane methylene at 0.299 and 0.537 ppm, six tertiary methyls at 1.071, 1.153, 1.202, 1.331, 1.674, and 1.685 ppm, a secondary methyl at 0.853 ppm. The monosaccharide is assigned as a D-xylopyranoside at C-3 due to the presence of the H-5'α triplet signal at 3.755 ppm. Additional monosaccharide signals showed the same pattern as demonstrated for the D-xylopyranoside of **4**, and the correlation was supported by a gCOSY spectrum. The ^{13}C assignment was accomplished from gHSQC and gHMBC experiments. The signals of both C-26 and C-27 methyls, are more deshielded by 0.194 ppm compared to their positions in the spectrum of compound **4** (1α-hydroxycimigenol-3-*O*-β-D-xylopyranoside), which suggests that the substitution occurs at C-25. The compound was deduced to be 25-*O*-acetyl cimigenol-3-*O*-β-D-xylopyranoside, since ^{1}H NMR assignment was consistent with that of reported NMR data (32,63). This compound has been previously isolated from the roots/rhizomes of *C. racemosa* (64), C.

acerina (65) and also from the aerial parts of *C. simplex* (66) and *C. dahurica* (67). This compound was originally reported as 25-*O*-acetylcimigenoside (65) .

25-*O*-Acetyl cimigenol-3-*O*-β-D-xylopyranoside (**7**) ^{1}H NMR (900 MHz, C_5D_5N) Aglycone moiety δ 4.603 (1H, d, *J* = 9.2 Hz, H-23), 4.280 (1H, d, *J* = 9.2 Hz, H-15), 4.123 (1H, s, H-24), 3.532 (1H, dd, *J* = 4.3, 11.8 Hz, H-3), 2.386 (1H, m, H-2α), 2.267 (1H, m, H-22β), 2.128 (1H, m, H-7b), 2.086 (1H, m, H-11a), 1.975 (1H, overlapped, H-2β), 1.975 (3H, s, 25-OAc), 1.706 (1H, overlapped, H-8), 1.695 (3H, s, H-26), 1.680 (1H, overlapped, H-12a), 1.674 (3H, s, H-27), 1.660 (1H, overlapped, H-20), 1.615 (1H, m, 1α), 1.553 (1H, overlapped, H-12b), 1.542 (1H, overlapped, H-6α), 1.465 (1H, d, *J* = 11.1Hz, H-17), 1.353 (1H, overlapped, H-5), 1.331 (3H, s, H-29), 1.250 (1H, m, 1β), 1.202 (3H, s, H-28), 1.190 (1H, overlapped, H-7b), 1.153 (3H, s, H-18), 1.078 (1H, overlapped, H-11), 1.071 (3H, s, H-30), 0.987 (1H, dt, *J* = 1.8, 11.8 Hz, H-22α), 0.853 (3H, d, *J* = 6.5 Hz, H-21), 0.730 (1H, m, H-6α), 0.537 (1H, d, *J* = 4.2 Hz, H-19 endo), 0.299 (1H d, *J* = 4.2 Hz, H-19 exo); Sugar moiety δ 4.879 (1H, d, *J* = 7.5 Hz, H-1'), 4.376 (1H, dd, *J* = 5.3, 11.4 Hz, H-5'β), 4.245 (1H, m, H-4'), 4.179 (1H, t, *J* = 8.8 Hz, H-3'), 4.055 (1H, m, H-2'), 3.755 (1H, t, *J* = 11.0 Hz, H-5'α)

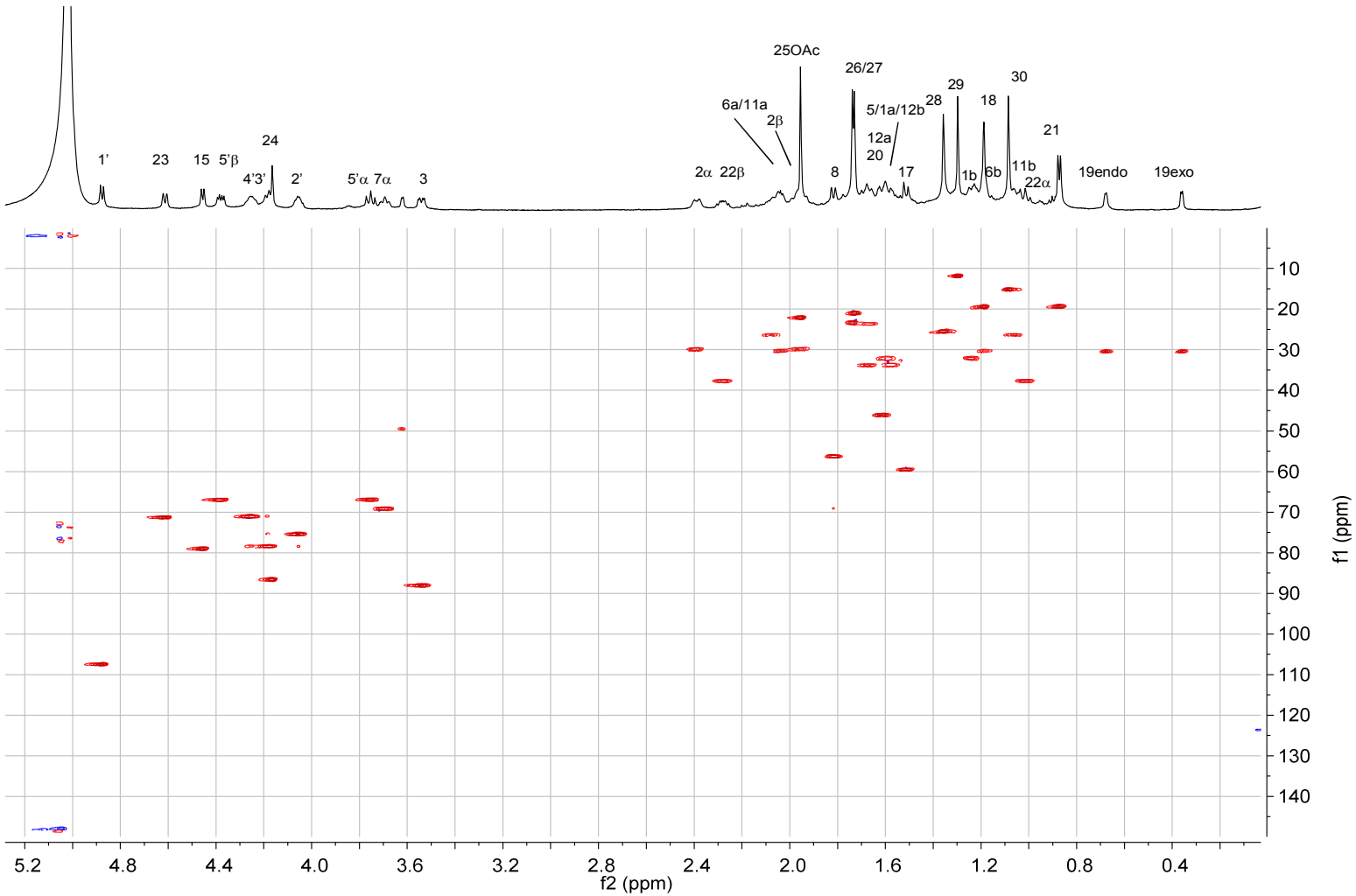

Figure 48. Compound 7; 900 MHz HSQC in pyridine-d_5

Chemical shifts were calibrated to 7.217 ppm for the residual protonated species of pyridine. Digitization was as follows: GM (LB -1.0 Hz, GB 0.1).

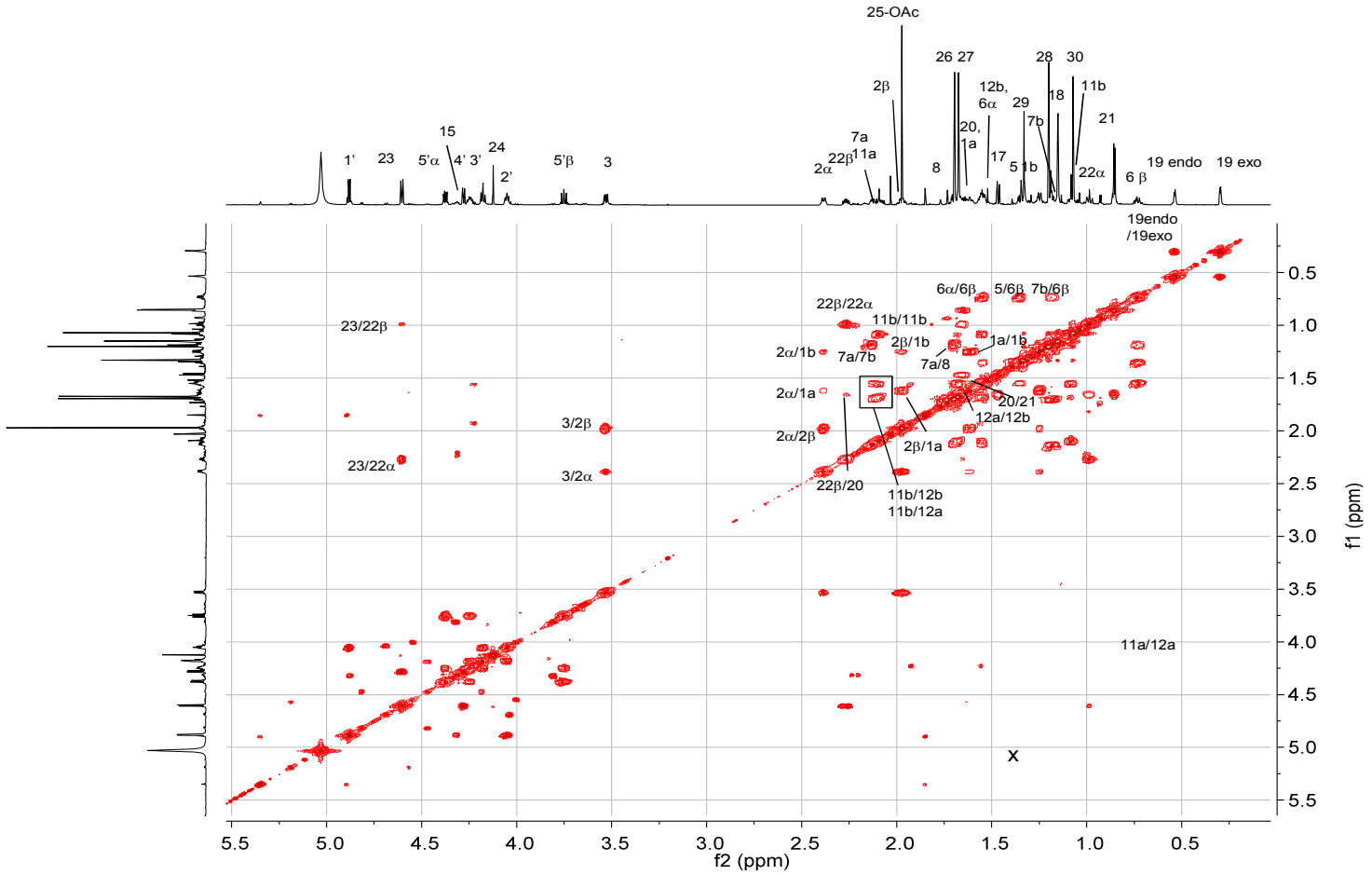

Figure 49. Compound 7; 900 MHz gCOSY spectrum in pyridine-d_5

Chemical shifts were calibrated to 7.217 ppm for the residual protonated species of pyridine. Original data F1 256 F2 4k. Digitization was as follows: F1 SI 4k SINE (SSB 0), F2 SI 4k SINE (SSB 0).

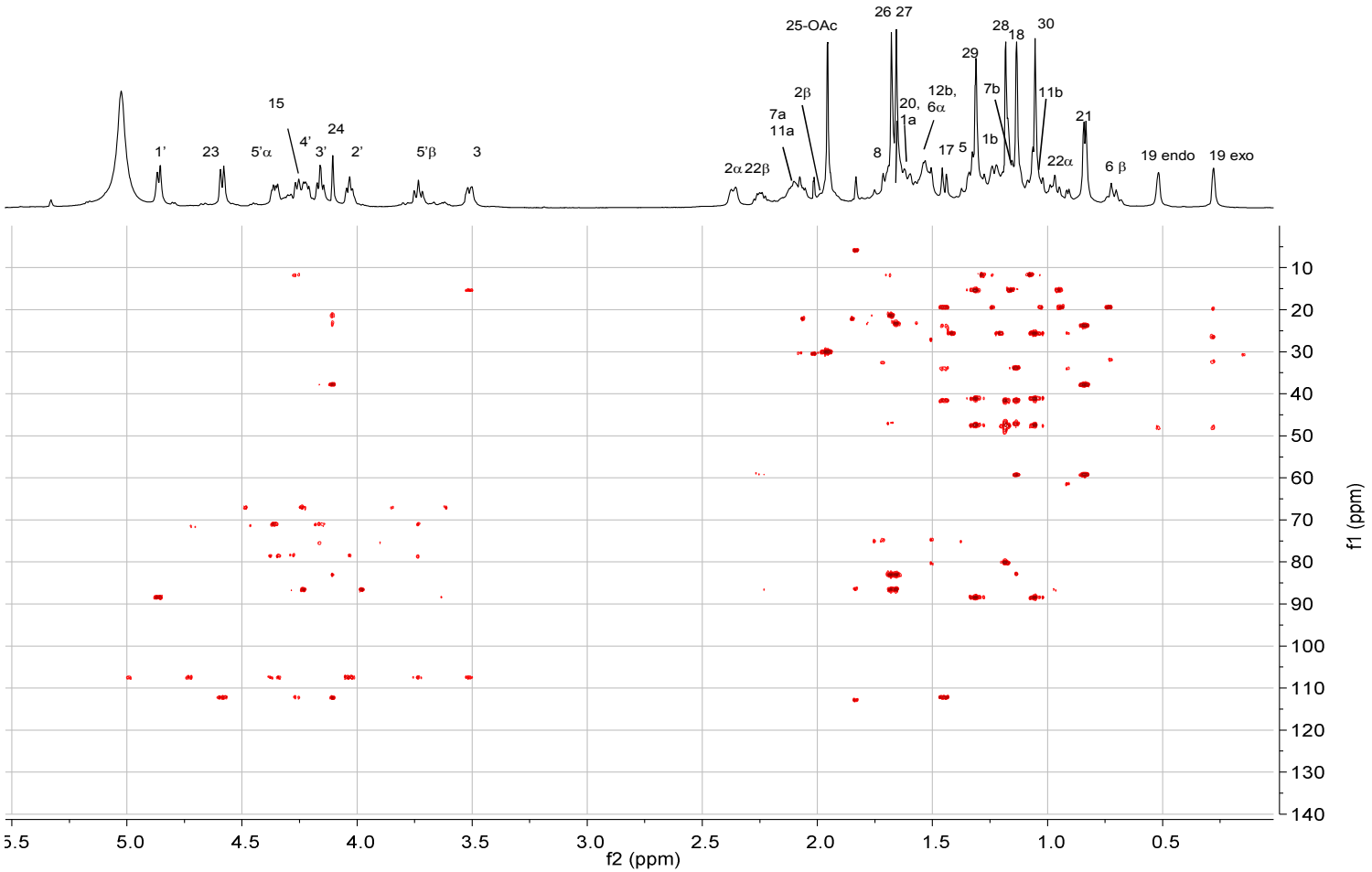

Figure 50. Compound 7; 600 MHz gHMBC spectrum in pyridine-d_5

Chemical shifts were calibrated to 7.217 ppm for the residual protonated species of pyridine on F1 and to 123.5 ppm on F2. Original data F1 256 F2 4k. Digitization was as follows: F1 SI4k SINE (SSB 0) F2 SI 8k SINE (SSB 0)

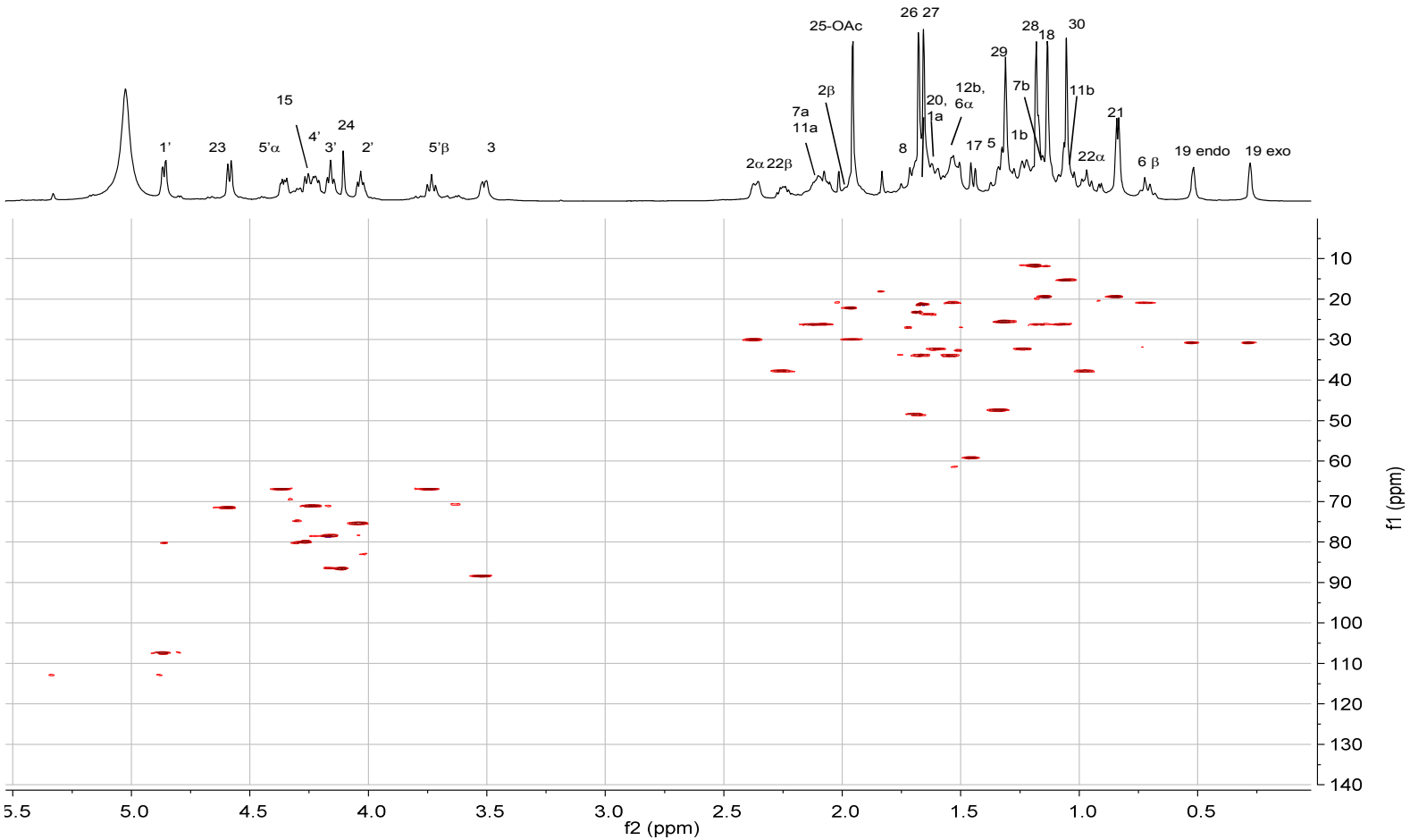

Figure 51. Compound 7; 600 MHz gHSQC spectrum in pyridine-d_5

Chemical shifts were calibrated to 0.416 ppm for H-19 exo on F1 and to 30.7 ppm on F2. The number was obtained from a qHMBC experiment. Original Data F1 256 F2 660. Digitization as follows: F1 SI 1k QSINE (SSB 2), F2 SI 2k QSINE (SSB 2).

3.2.3.8. **Compound 8.**

24-*O*-Acetylhydroxyshengmanol-3-*O*-β-D-xylopyranoside

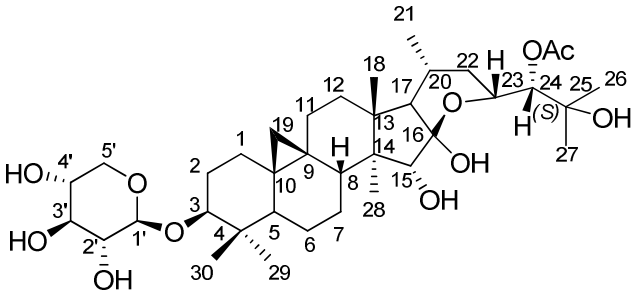

24-*O*-Acetylhydroxyshengmanol-3-*O*-β-D-xylopyranoside (**8**) was obtained as a white powder. The HR-ESI-MS revealed a sodiated molecule $[M+Na]^+$ at 703.4036 *m/z* (calculated for $C_{37}H_{60}O_{11}Na$, 703.4033) indicating a molecular formula of $C_{37}H_{60}O_{11}$. One acetyl methyl peak was observed at 2.133 ppm in ^1H NMR spectrum. The ^1H NMR spectrum also revealed two cyclopropane methylene protons, each centered at 0.292 and 0.565 ppm, six tertiary methyls at 1.055, 1.235, 1.246, 1.333, 1.488, and 1.522 ppm, and a secondary methyl at 0.974 ppm. The ^1H NMR signals associated with the monosaccharide are assigned as a xylopyranoside at C-3 due to the presence of the H-5'α triplet signal at 3.789 ppm.

Compound **8** was isolated from *C. japonica* in 1981 by Sakurai *et al*. for the first time (64,68). Subsequently this compound has been isolated from *C. dahurica* and *A. rubra* (69,70).

24-*O*-Acetylhydroshengmanol-3-*O*-β-D-xylopyranoside (**8**) ^1H NMR (900 MHz, C_5D_5N) Aglycone moiety δ 5.785 (1H, d, *J* = 8.5 Hz, H-24), 4.457 (1H, m, H-23), 4.166 (1H, d, *J* = 6.7 Hz, H-15), 3.533 (1H, dd, *J* = 11.8, 4.4 Hz, H-3), 2.389 (1H, m, H-2α), 2.133 (3H, s, 24-OAc), 2.079 (1H, overlapped, H-11a), 2.061 (1H, overlapped, H-7a), 2.054 (1H,

overlapped, H-22a), 1.974 (1H, m, H-2β), 1.843 (1H, d, *J* = 10.0 Hz, H-17), 1.830 (1H, overlapped, H-22b), 1.791 (1H, dd, *J* = 12.4, 5.0 Hz, H-8), 1.778 (1H, m, H-20), 1.716 (1H, m, H-12a), 1.619 (1H, overlapped, H-1a), 1.600 (1H, overlapped, H-6a), 1.557 (1H, m, H-12b), 1.522 (3H, s, H-26), 1.488 (3H, s, H-27), 1.369 (1H, dd, *J* = 4.1, 12.4 Hz, H-5), 1.333 (3H, s, H-29), 1.288 (1H, m, H-7b), 1.257 (1H, m, H-1b), 1.246 (3H, s, H-18), 1.235 (3H, s, H-28), 1.111 (1H, m, H-11b), 1.055 (3H, s, H-30), 0.974 (3H,d, *J* = 6.5 Hz, H-21), 0.791 (1H, m, 6b), 0.565 (1H, d, *J* = 3.9 Hz, H-19 endo), 0.292 (1H, d, *J* = 3.9 Hz, H-19 exo); Sugar moiety δ 4.901 (1H, d, *J* = 7.6 Hz, H-1'), 4.403 (1H, dd, 5.0, 11.2 Hz, H-5'β), 4.264 (1H, m, H-4'), 4.198 (1H, t, *J* = 8.9 Hz, H-3'), 4.068 (1H, m, H-2'), 3.789 (1H, d, *J* = 10.8 Hz, H-5'α)

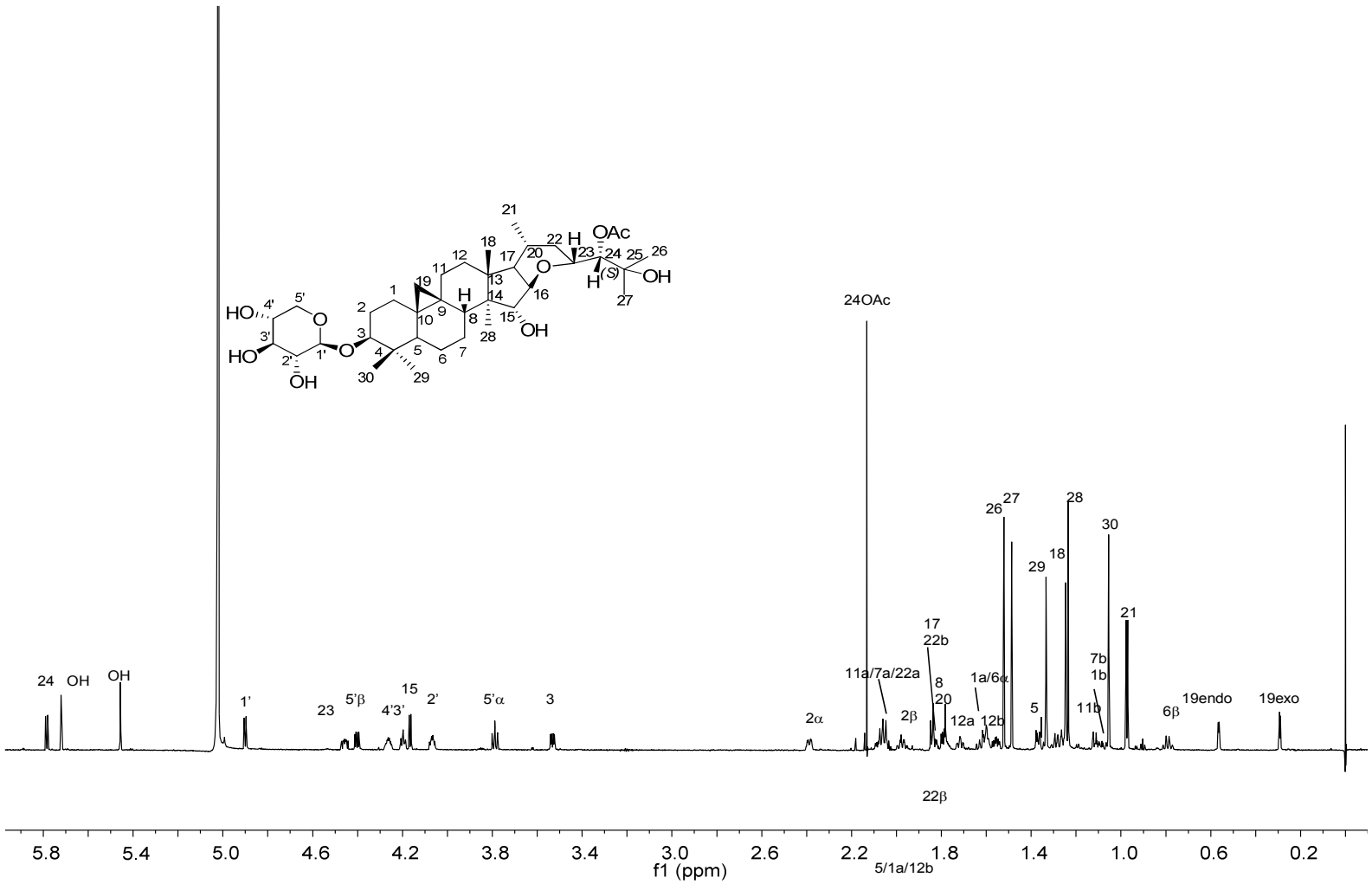

Figure 52. Compound 8; 900 MHz ^{1}H NMR in pyridine-d_5

Chemical shifts were calibrated to 7.217 ppm for the residual protonated species of pyridine. Digitization was as follows: GM (LB -1.0 Hz, GB 0.1).

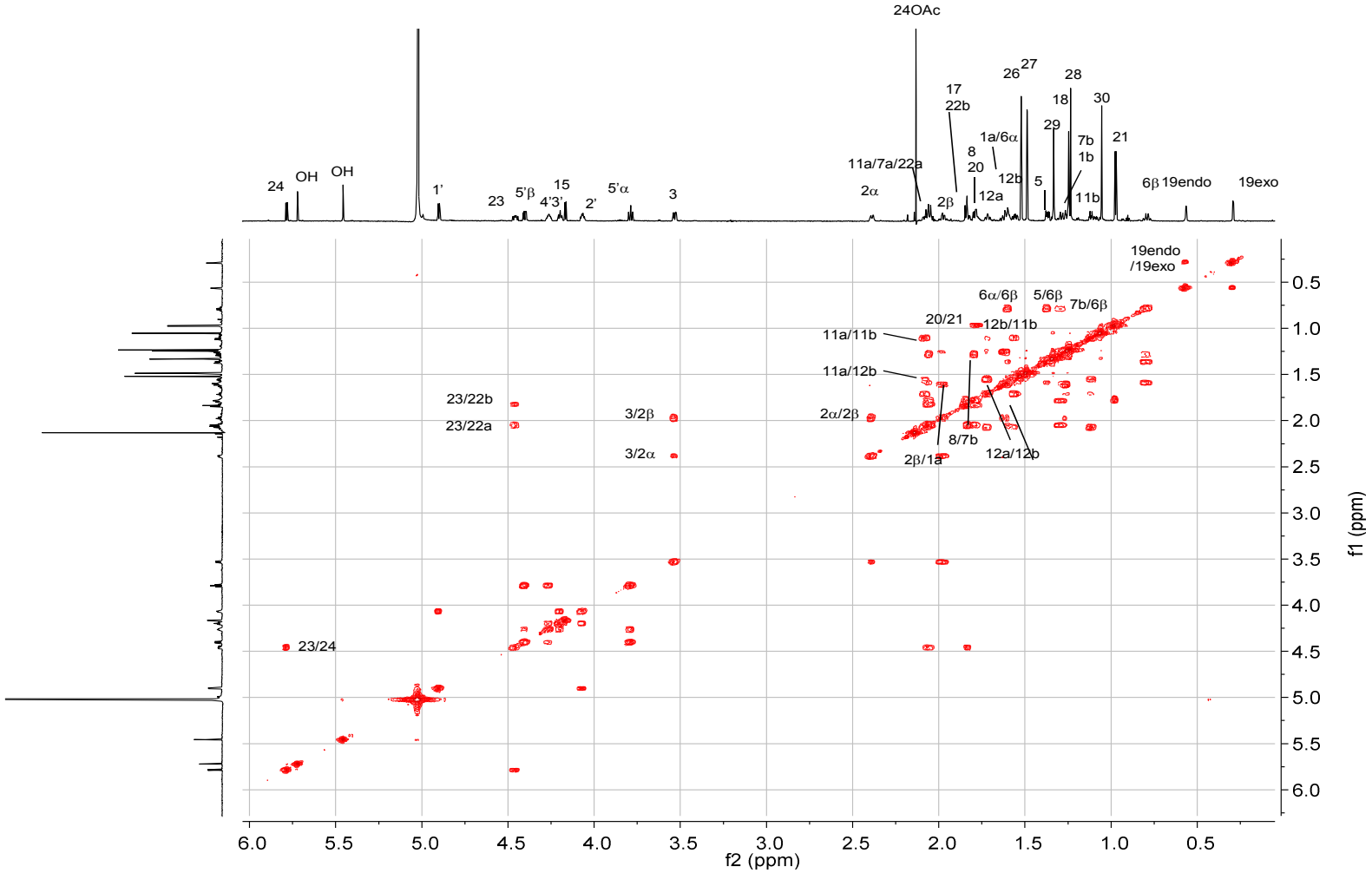

Figure 53. Compound 8; 900 MHz gCOSY spectrum in pyridine-d_5

Chemical shifts were calibrated to 7.217 ppm for the residual protonated species of pyridine. Original data F1 256 F2 2k. Digitization was as follows. F1 SI 4k SINE (SSB 0), F2 SI 4k SINE (SSB 0).

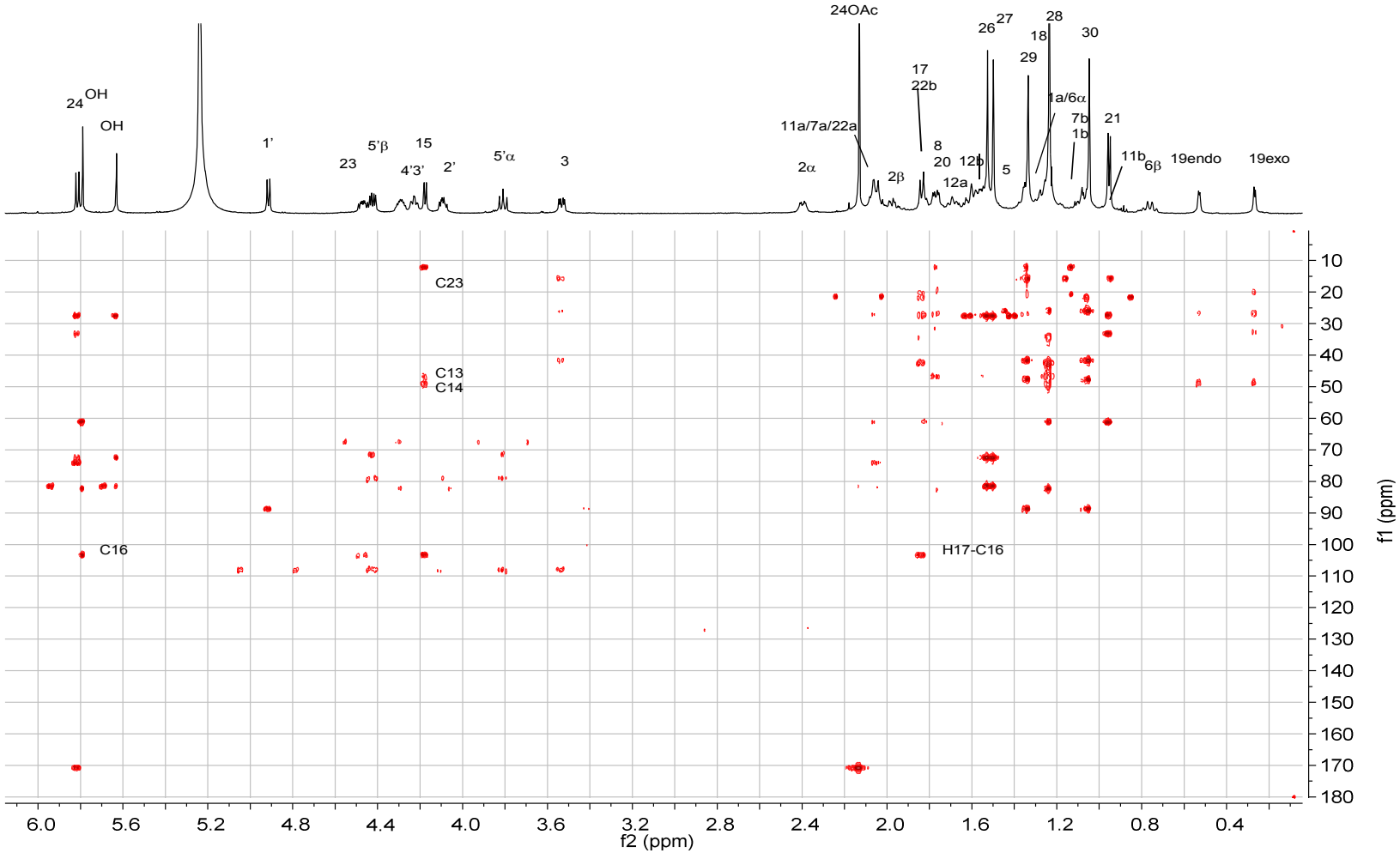

Figure 54. Compound 8; 600 MHz gHMBC spectrum in pyridine-d_5

Chemical shifts were calibrated to 7.217 ppm for the residual protonated species of pyridine on F1 and to 123.5 ppm on F2. Original data F1 256 F2 4k. Digitization was as follows: F1 SI4k SINE (SSB 0) F2 SI 8k SINE (SSB 0).

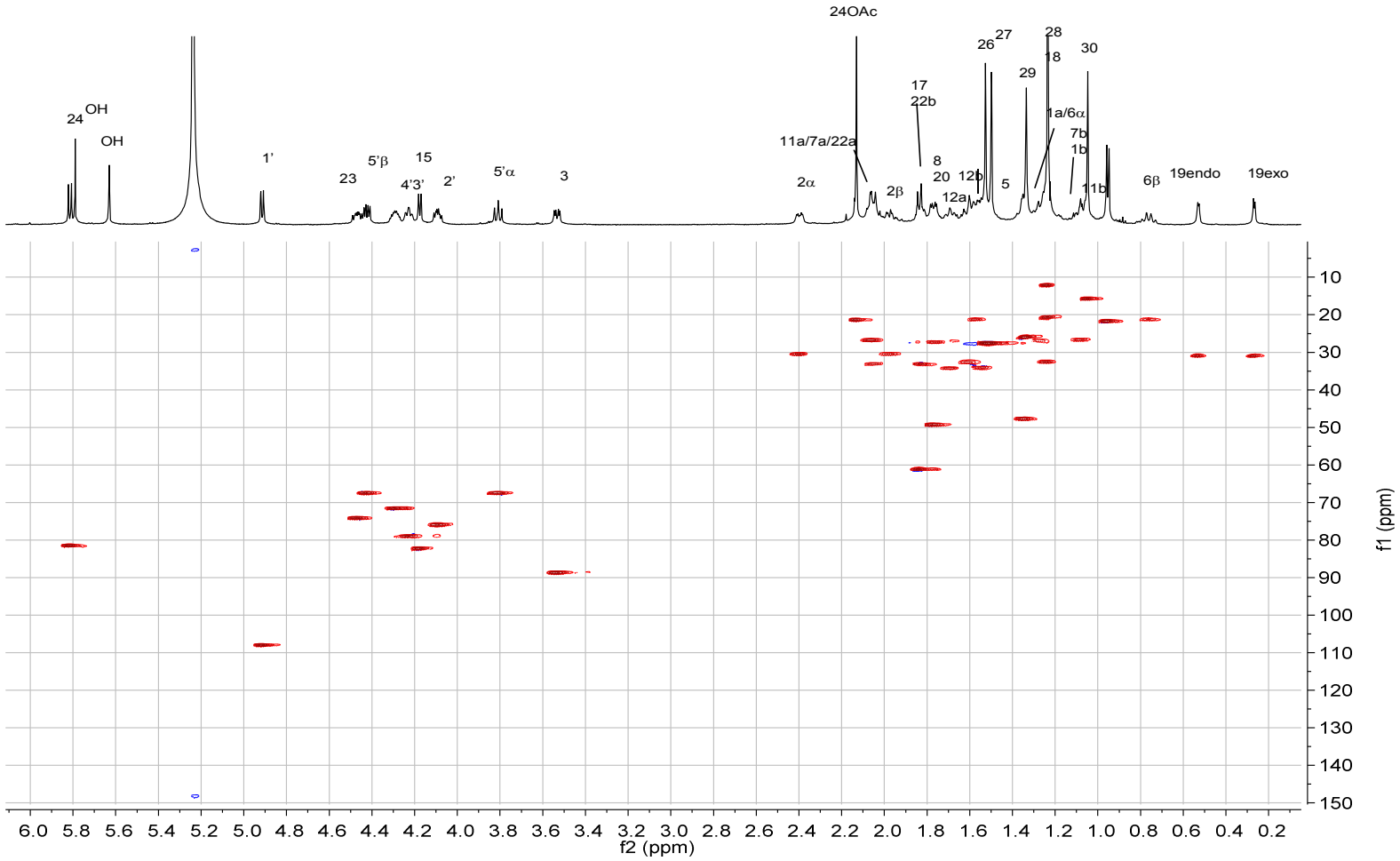

Figure 55. Compound 8; 600 MHz gHSQC spectrum in pyridine-d_5

Chemical shifts were calibrated to 7.217 ppm for the residual protonated species of pyridine on F1 and to 123.5 ppm on F2. Original Data F1 256 F2 660. Digitization was as follows: F1 SI 2k QSINE (SSB 2), F2 SI 4k QSINE (SSB 2).

3.2.3.9. **Compound 9. Cimigenol Aglycone**

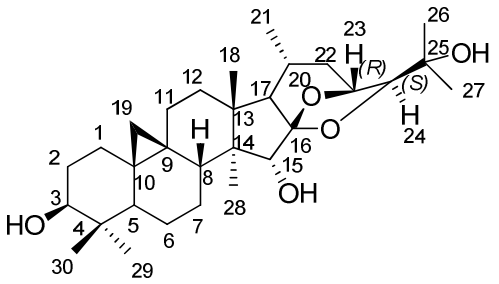

Cimigenol aglycone (**9**) was obtained as a white powder. The HR-ESI-MS revealed a sodiated molecule $[M+Na]^+$ at 511.3381 *m/z* (calculated for $C_{30}H_{48}O_5Na$, 511.3399) suggesting the molecular formula of $C_{30}H_{48}O_5$. The ^1H NMR spectrum revealed one cyclopropane methylene at 0.351 and 0.593 ppm, six tertiary methyls at 1.119, 1.195, 1.228, 1.324, 1.500 and 1.522 ppm, and a secondary methyl at 0.881 ppm. Typical saccharide signals were not observed in the ^1H NMR spectrum, and it clearly shows other downfield proton signals of H-3, H-24, H-15 and H-23 between 3.5 ppm and 5.0 ppm. A sharp singlet at 3.804 ppm and a doublet at 4.789 ppm suggest the side chain is the normal cimigenol type. H-3 was observed as a dd (*J* = 4.6, 11.6 Hz) at 3.569. Other significant changes in the aglycone structure were not observed, and the structure was deduced to be cimigenol aglycone.

The compound has been previously isolated from the rhizome of *C. simplex*. In 1994 (66), the rhizome of *C. dahurica* in 1972 (71), and the underground part of *C. japonica* in 1981 (68). The earlier reports did not include full assignment of the ^1H NMR spectrum.

Cimigenol (**9**) ^1H NMR (900 MHz, C_5D_5N) δ 4.789 (1H, brd, *J* = 8.9 Hz, H-23), 3.804 (1H, s, H-24), 3.569 (1H, dd, *J* = 4.6, 11.6 Hz, H-3), 2.299 (1H, m, H-22α) 2.136 (2H,

overlapped, H-11, 7), 2.020 (1H, m, H-2α), 1.923 (1H, m, H-2β), 1.737 (1H, dd, *J* = 4.5, 12.6 Hz, H-8), 1.698 (1H, m, overlapped, H-20), 1.610 (1H, overlapped, H-1a), 1.585 (1H, overlapped, H-7a), 1.5312 (1H, d, *J* = 11.0, H-17), 1.522 (3H, s, H-26), 1.500 (3H, s, H-27), 1.335 (1H, overlapped, H-6α), 1.324 (3H, s, H-27), 1.240 (1H, overlapped, H-1b), 1.228 (3H, s, H-29), 1.219 (3H, s, H-28), 1.195 (3H, s, H-18), 1.134 (1H, overlapped, H-7b), 1.117 (1H, s, H-30), 1.055 (1H, m, H-22α), 0.881 (1H, d, *J* = 6.6 Hz, H-21), 0.796 (1H, m, H-6β), 0.593 (1H, d, *J* = 4.2 Hz, H-19 endo), 0.351 (1H, d, *J* = 4.2 Hz, 19 exo)

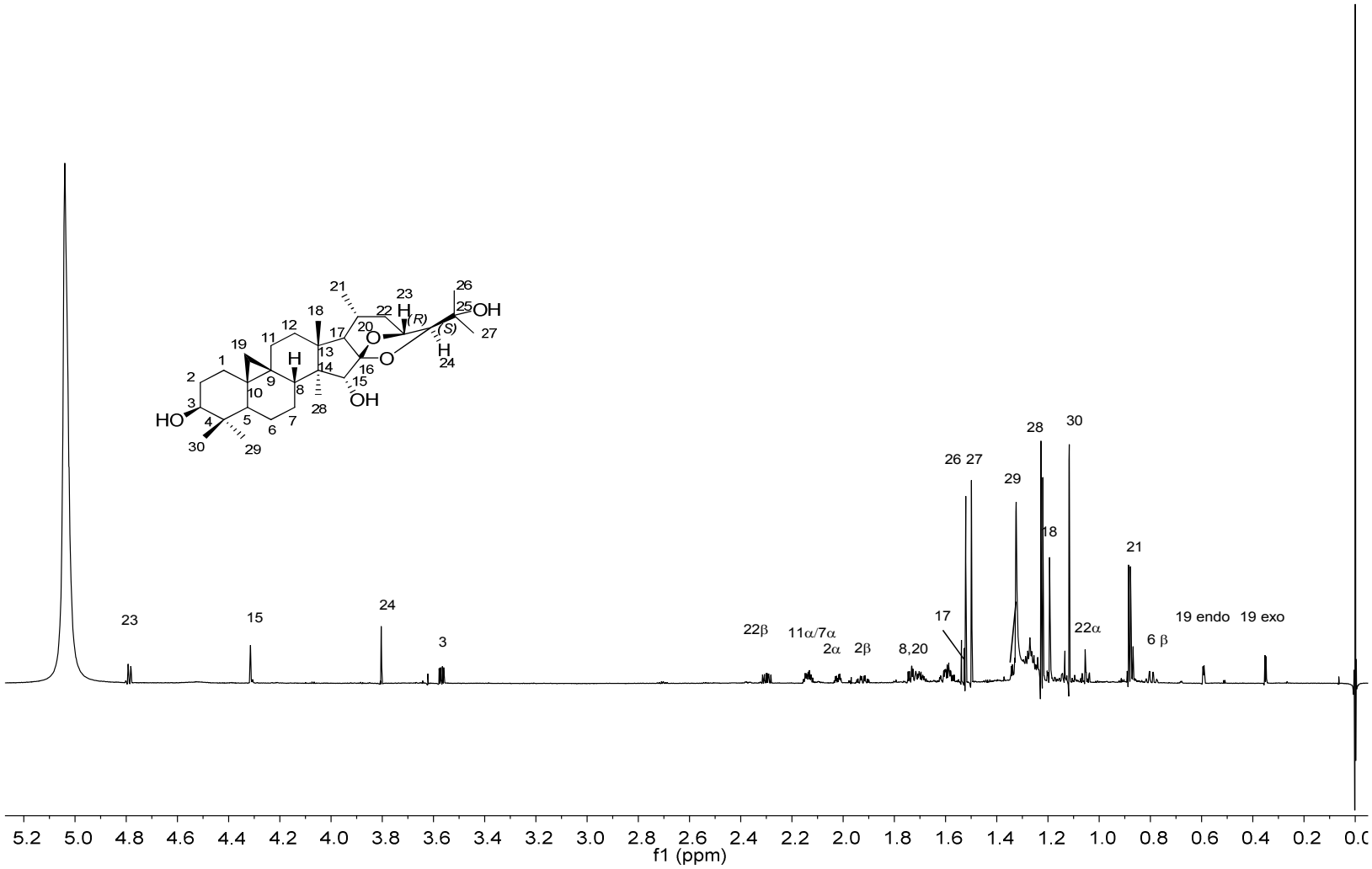

Figure 56. Compound 9; 900 MHz ^{1}H NMR in pyridine-d_5

Chemical shifts were calibrated to 7.217 ppm for the residual protonated species of pyridine. Digitization was as follows: GM (LB -1.0 Hz, GB 0.1).

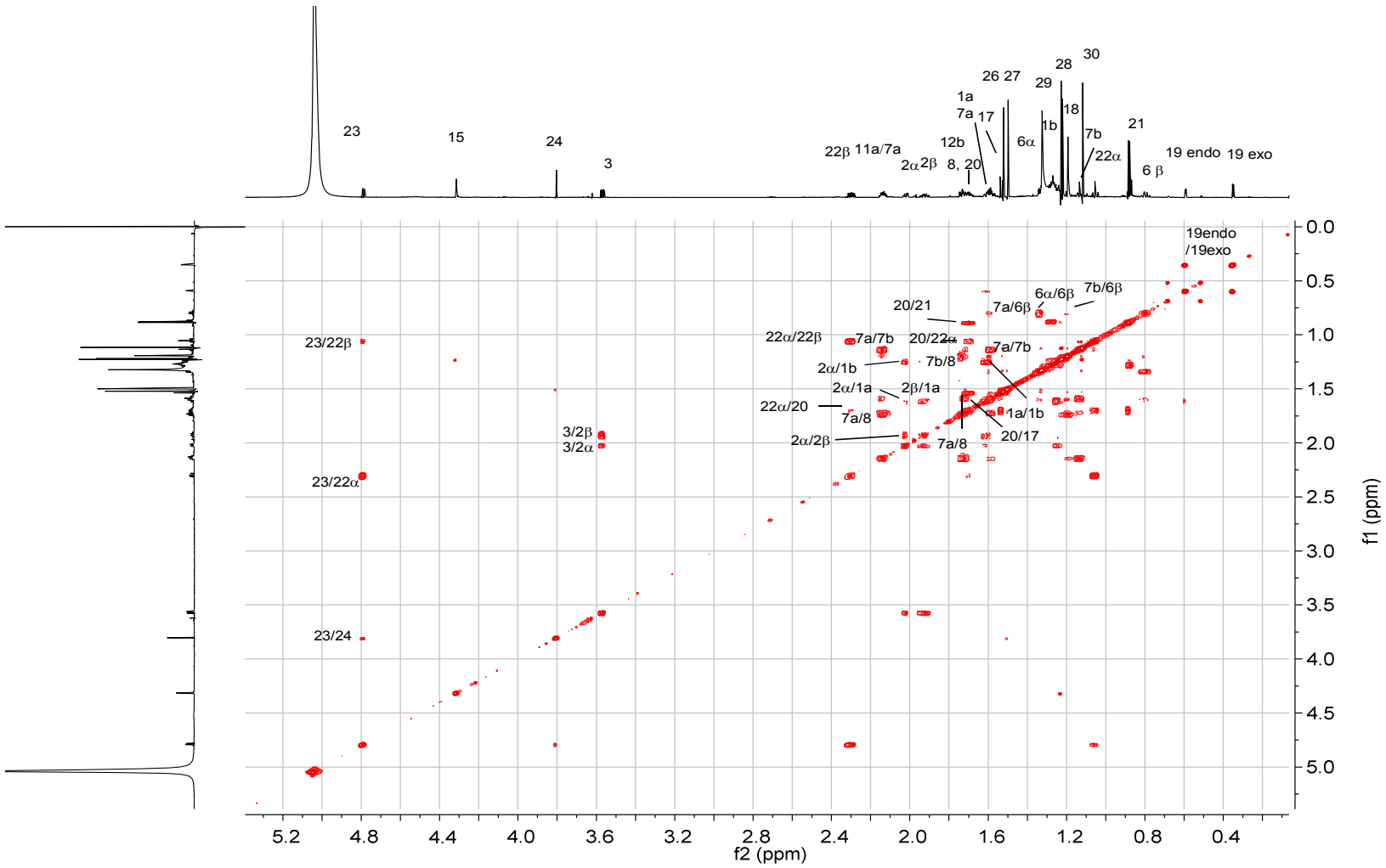

Figure 57. Compound 9; 900 MHz gCOSY spectrum in pyridine-d_5

Chemical shifts were calibrated to 7.217 ppm for the residual protonated species of pyridine. Original data F1 256 F2 4k. Digitization was as follows: F1 SI 4k SINE (SSB 0), F2 SI 4k SINE (SSB 0).

3.2.3.10. **Compound 10. Cimiaceroside A**

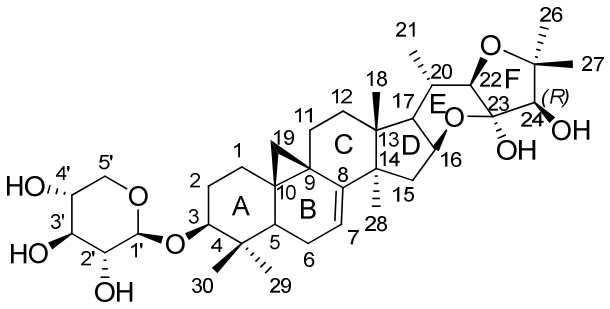

Cimiaceroside A (**10**) was obtained as a white powder. The ^{1}H-NMR spectrum revealed two cyclopropane methylene protons centered at 0.435 and 0.966 ppm, six tertiary methyls at 1.059 1.082, 1.223, 1.368, 1.697, and 1.790 ppm, a secondary methyl at 1.263 ppm. The monosaccharide is again consistent with a D-xylopyranoside present at C-3. The assignment is based on the observation of the H-5'α triplet signal at 3.753 ppm. Other sugar signals exhibited the same pattern as demonstrated for the D-xylopyranoside of **4** (Figure 7), and the assignment was supported by correlations in the gCOSY spectrum. The chemical shift of the Me-21 signal was observed relatively downfield at 1.267 ppm. Starting from the C-21 methyl protons, the spin system of the side chain was identified from the gCOSY spectrum as H-20 at 2.321 ppm (m), H-22 at 3.936 ppm (d, J = 11.0 Hz), H-17 at 1.588 ppm (overlapped), H-15a,b at 1.936 (dd, *J* = 7.8, 12.2 Hz) and 2.130 ppm (overlapped), and H-16 at 5.085 (q, *J* = 7.5 Hz). This side chain pattern was identical to a previously reported compound cimiaceroside A (72). All of the δ ^{1}H values and coupling constants provided a reasonable match to the previous report.

Cimiaceroside A (**10**) ^{1}H NMR (900 MHz, C_5D_5N) aglycone moiety δ 5.123 (1H, dd, *J* = 7.3, 1.6 Hz, H-7), 5.085 (1H, q, *J* = 7.5, H-16), 4.215 (1H, s, H-24), 3.936 (1H, d, *J* = 10.8 Hz, H-22), 3.502 (1H, dd, *J* = 4.2, 11.7 Hz, H-3), 2.347 (1H, m, H-2b), 2.321 (1H, m,

H-20), 2.130 (1H, overlapped, H-15), 2.083 (1H, m, H-11), 1.973 (1H, dq, *J* = 4.2, 12.9 Hz, H-2a), 1.936 (1H, dd, *J* = 7.8, 12.2 Hz, H-15), 1.880 (1H, m, H-6b), 1.790 (3H, s, H-26), 1.697 (3H, s, H-27), 1.678 (1H, overlapped, H-1a), 1.678 (2H, overlapped, H-12ab), 1.609 (1H, m, H-6a), 1.588 (1H, overlapped, H-17), 1.368 (3H, s, H-29), 1.328 (1H, dt, *J* = 13.6, 3.6 Hz, H-1a), 1.275 (1H, overlapped, H-5), 1.263 (3H, d, *J* = 6.5 Hz, H-21), 1.223 (3H, s, H-18), 1.104 (1H, overlapped, H-11a), 1.082 (3H, s, H-28), 1.059 (3H, s, H-30), 0.966 (1H, d, *J* = 4.2 Hz, H-19b), 0.435 (1H, d, H-19a); Sugar moiety δ 4.878 (1H, d, *J* = 7.5 Hz, H-1'), 4.392 (1H, dd, *J* = 5.2, 11.4 Hz, H-5'β), 4.264 (1H, m, H-4'), 4.188 (1H, dt, *J* = 2.8, 8.9 Hz, H-3'), 4.071 (1H, m, H-2'), 3.765 (1H, t, *J* = 10.8 Hz, H-5'α)

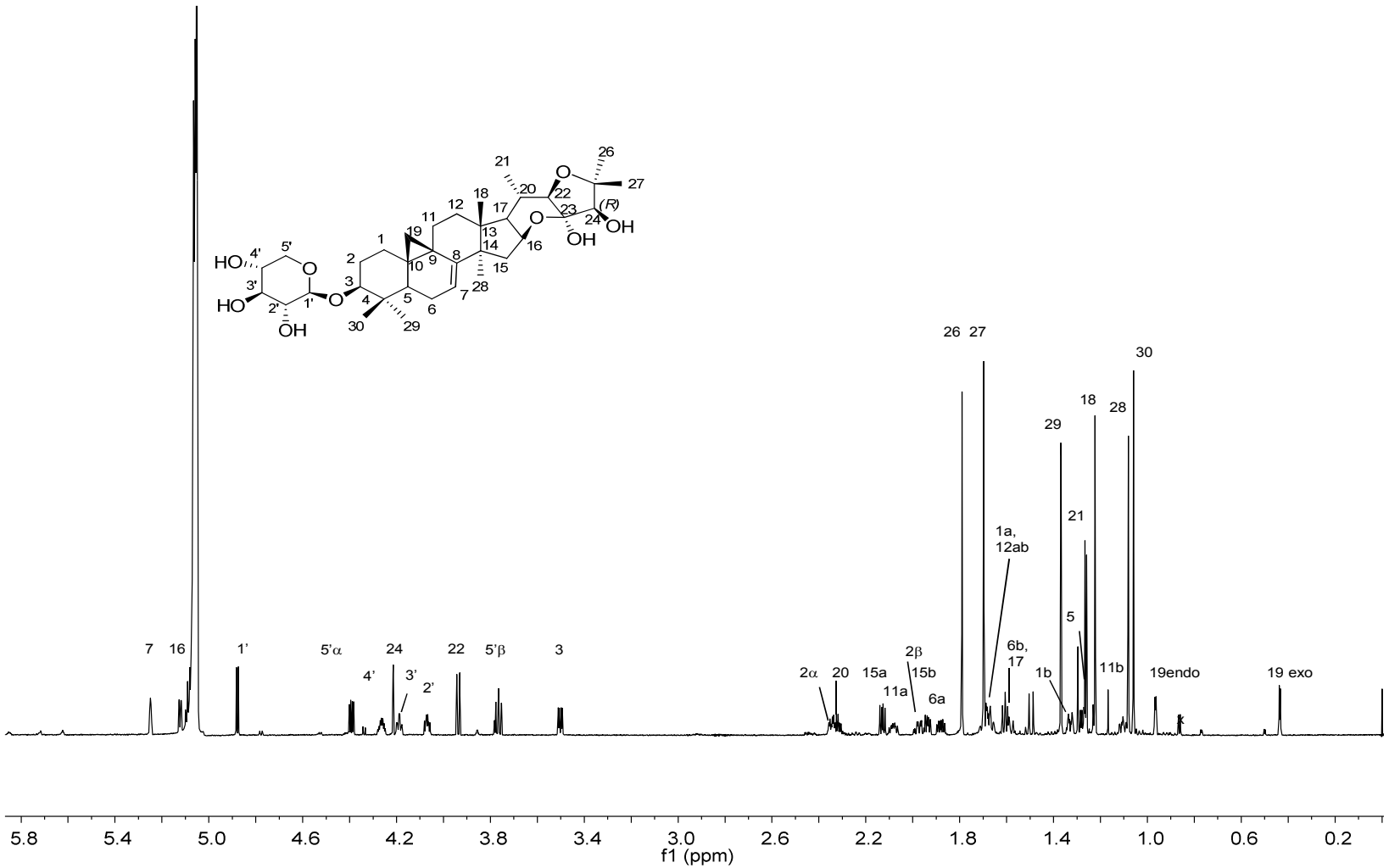

Figure 58. Compound 10; 900 MHz ^{1}H NMR in pyridine-d_5

Chemical shift were calibrated to 7.217 ppm for the residual protonated species of pyridine. Digitization was as follows: GM (LB -1.0 Hz, GB 0.1).

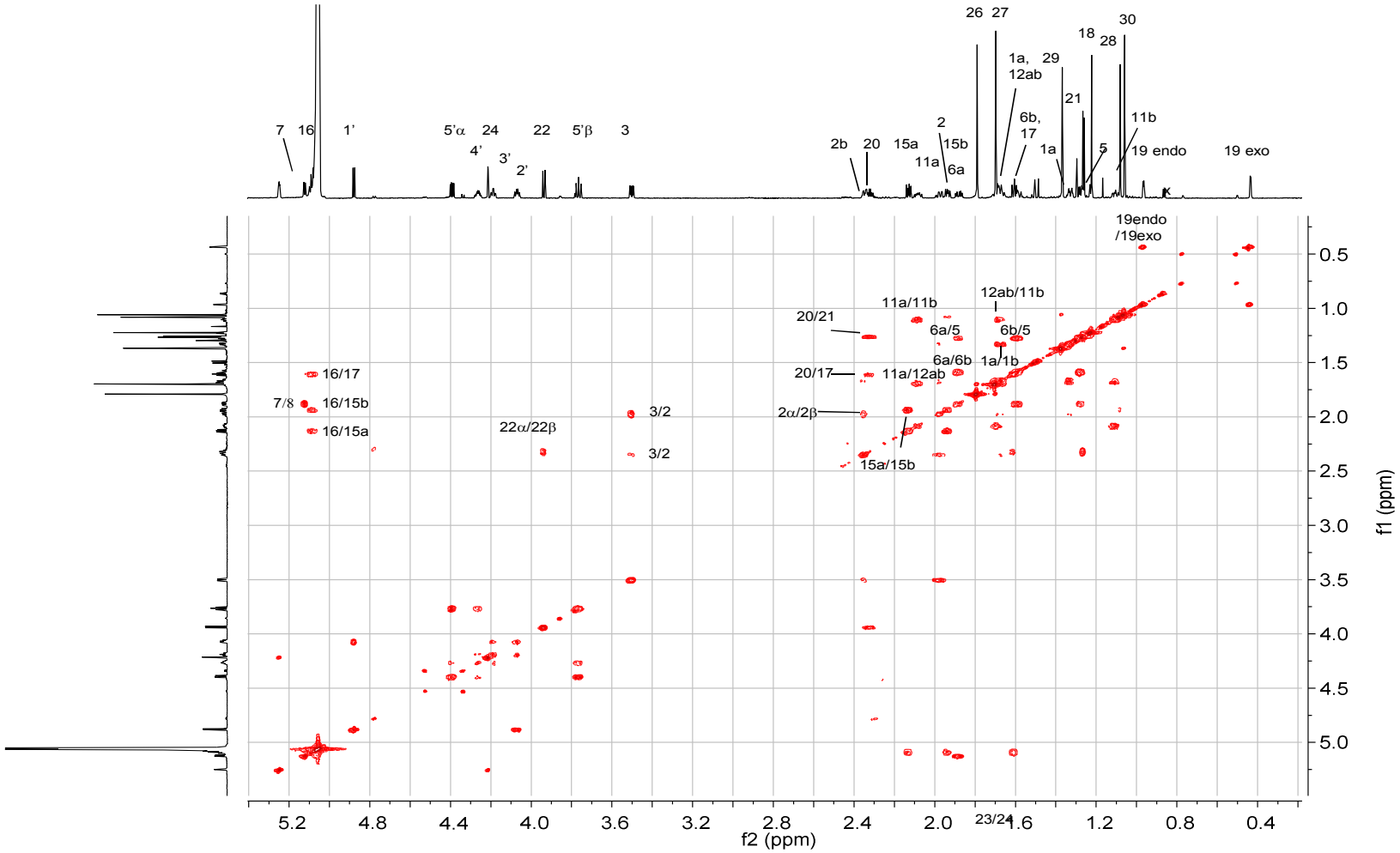

Figure 59. Compound 10; 900 MHz gCOSY spectrum in pyridine-d_5

Chemical shifts were calibrated to 5.00 ppm for the residual HDO. Original data F1 256 F2 2k. Digitization was as follows: F1 SI 4k SINE (SSB 0), F2 SI 4k SINE (SSB 0).

3.2.3.11. **Compound 11. Cimiracemoside I**

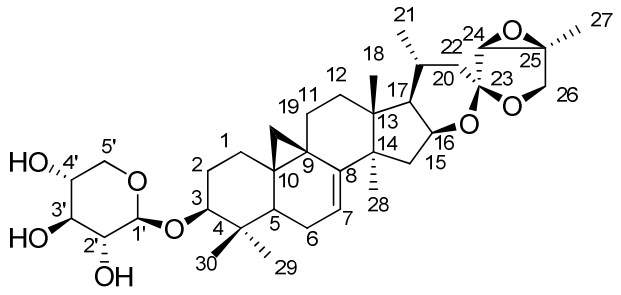

Cimiracemoside I (**11**) was obtained as a white powder. The HR-ESI-MS revealed sodiated molecule $[M+Na]^+$ at 623.3635 *m/z* (Calculated for $C_{35}H_{52}O_8Na$, 623.3560) suggesting the molecular formula of $C_{35}H_{52}O_8$. The ^{1}H-NMR spectrum revealed two cyclopropane methylene protons centered at 0.452 and 0.963 ppm, five tertiary methyls at 1.044, 1.069, 1.262, 1.351, and 1.468 ppm, and a secondary methyl at 1.008 ppm. ^{1}H NMR chemical shifts reasonably match with the reported data for cimiracemoside I (64).

Cimiracemoside I (**11**) ^{1}H NMR (900 MHz, C_5D_5N) aglycone moiety δ 5.079 (1H, brd, *J* = 7.4 Hz, H-7), 4.312 (1H, m, H-16), 4.038 (1H, d, *J* = 10.4 Hz, H-26a), 3.691 (1H, s, H-24), 3.609 (1H, d, *J* = 10.4 Hz, H-26b), 3.485 (1H, dd, *J* = 4.2, 11.7 Hz, H-3), 2.336 (1H, m, H-2a), 2.244 (1H, m, H-20), 2.113 (1H, dd, *J* = 7.8, 12.5 H, H-15a), 2.092 (1H, m, H-11a), 1.975 (1H, overlapped, H-2b), 1.956 (1H, overlapped, H-15b), 1.783 (1H, m, H-6b), 1.672 (2H, m, overlapped, H-12ab), 1.647 (1H, m, overlapped, H-1a), 1.588 (1H, overlapped, H-17), 1.574 (1H, overlapped , H-22a), 1.478 (1H, overlapped, H-6b), 1.468 (3H, s, H-27), 1.407 (1H, t, *J* = 13.0 Hz, H-22b), 1.351 (3H, s, H-29), 1.323 (1H, m, H-1b), 1.262 (3H, s, H-18), 1.244 (1H, dd, *J* = 5.6, 12.6 Hz, H-5), 1.133 (1H, m, H-11b), 1.069 (3H, s, H-28), 1.044 (3H, s, H-30), 1.008 (3H, s, H-21), 0.963 (1H, d, *J* = 3.9 Hz, H-19a), 0.453 (1H, d, *J* = 3.9 Hz, H-19b); sugar moiety δ 4.873 (1H, d, *J* = 7.6 Hz, H-1'), 4.395 (1H,

dd, *J* = 5.3, 11.4 Hz, H-5'β), 4.263 (1H, m, H-4'), 4.190 (1H, t, *J* = 8.9 Hz, H-3'), 4.064 (1H, t, *J* = 8.3 Hz, H-2'), 3.771 (1H, t, *J* = 10.8 Hz, H-5'α)

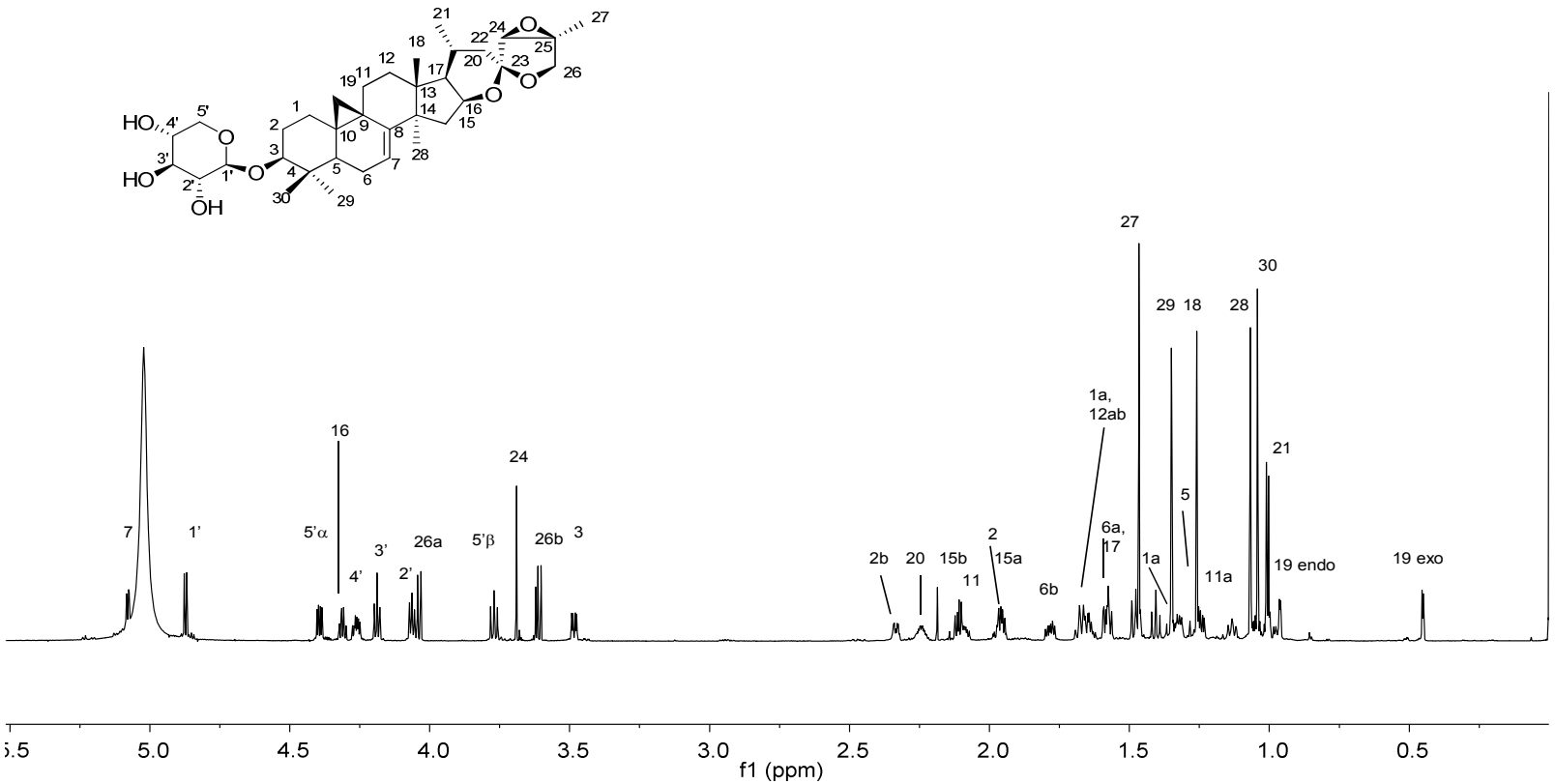

Figure 60. Compound 11; 900 MHz ^{1}H NMR in pyridine-d_5

Chemical shifts were calibrated to 7.217 ppm for the residual protonated species of pyridine. Digitization was as follows: GM (LB -1.0 Hz, GB 0.1).

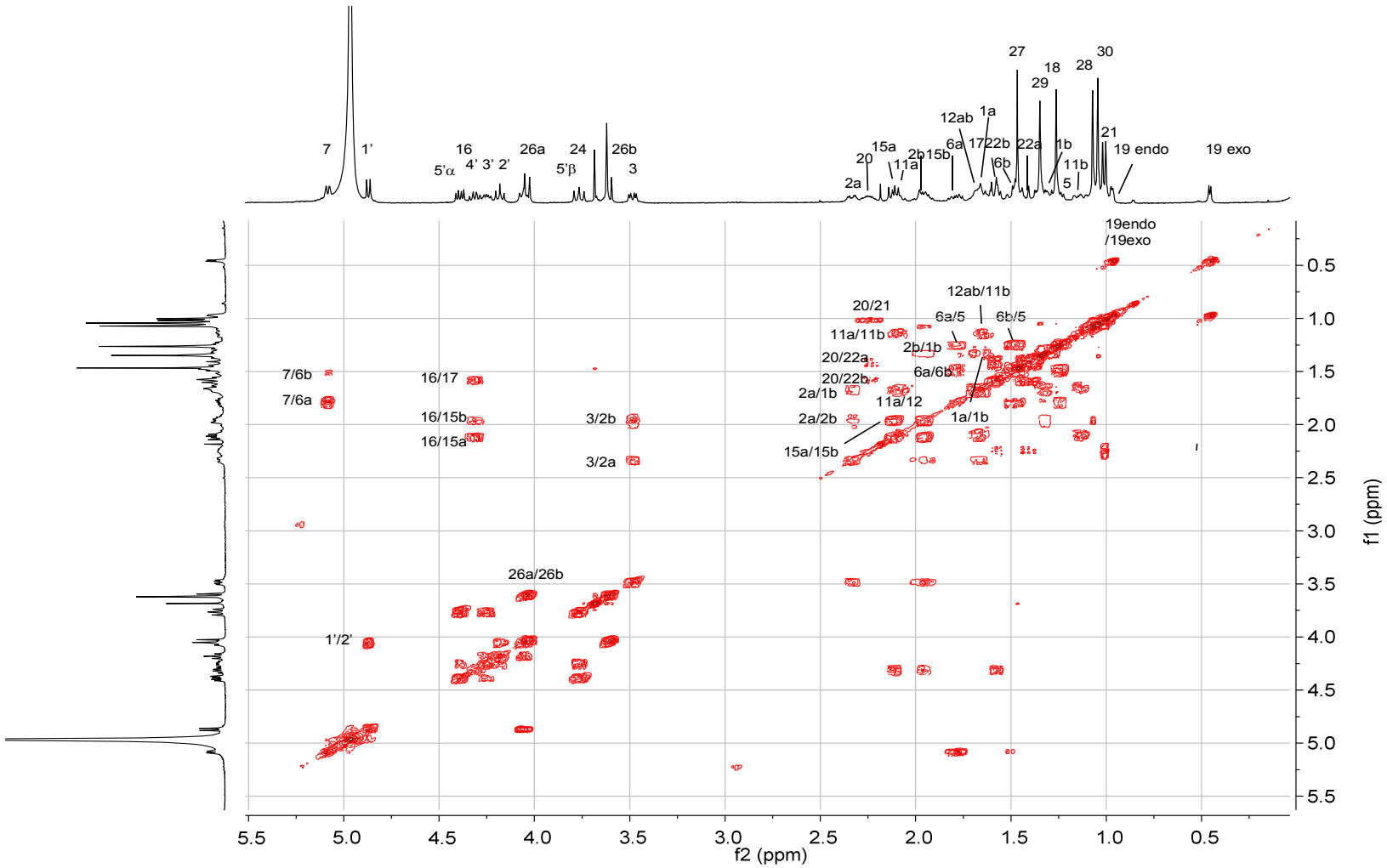

Figure 61. Compound 11; 600 MHz gCOSY spectrum in pyridine-d_5

Chemical shifts were calibrated to 7.217 ppm for the residual protonated species of pyridine. Original data F1 256 F2 2k. Digitization was as follows: F1 SI 4k SINE (SSB 0), F2 SI 4k SINE (SSB 0).

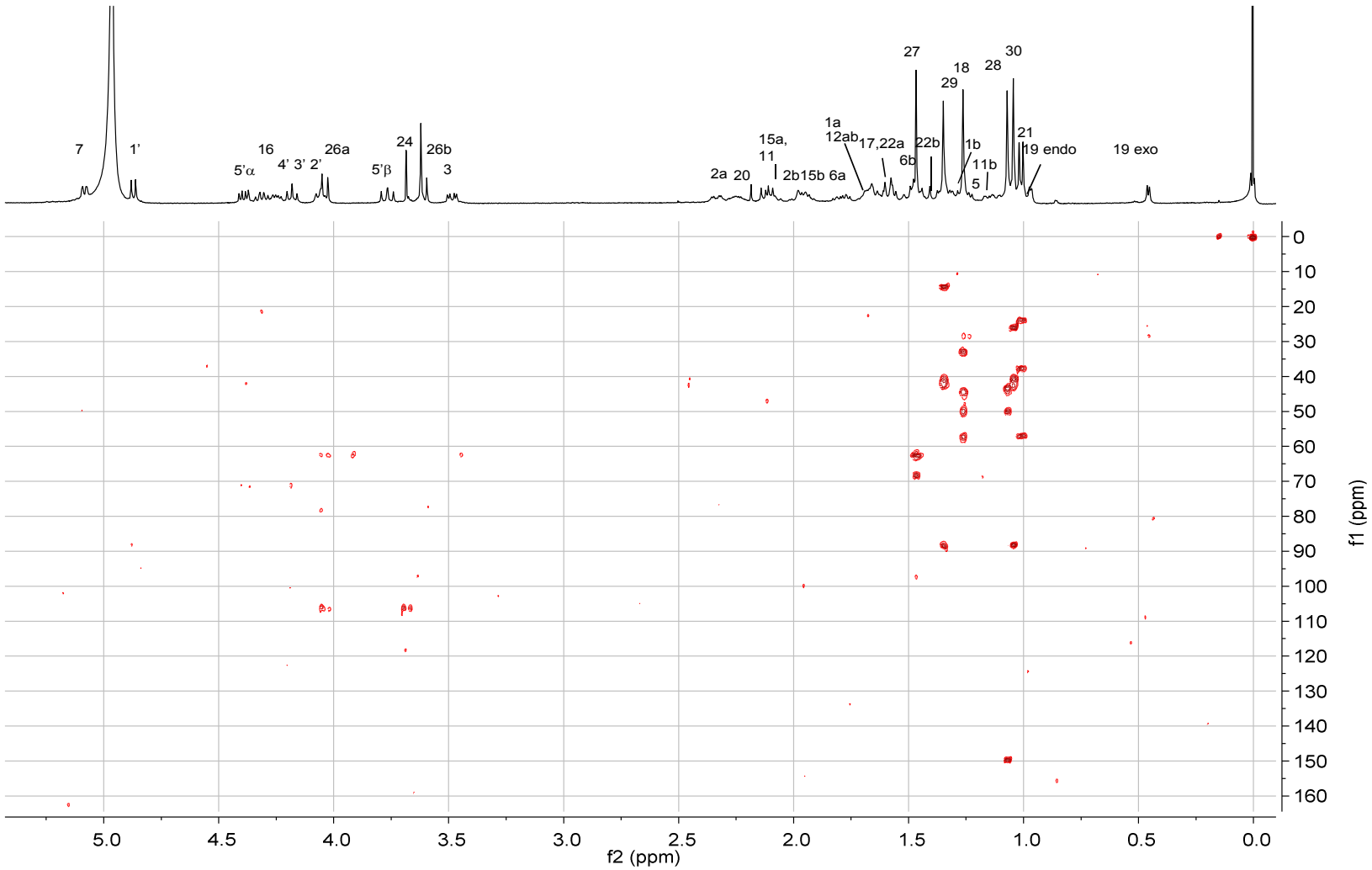

Figure 62. Compound 11; 600 MHz gHMBC spectrum in pyridine-d_5

Chemical shifts were calibrated to 7.217 ppm for the residual protonated species of pyridine on F1 and to 123.5 ppm on F2. Original data F1 128 F2 2k. Digitization was as follows: F1 SI 4k SINE (SSB 0) F2 SI 8k SINE (SSB 0)

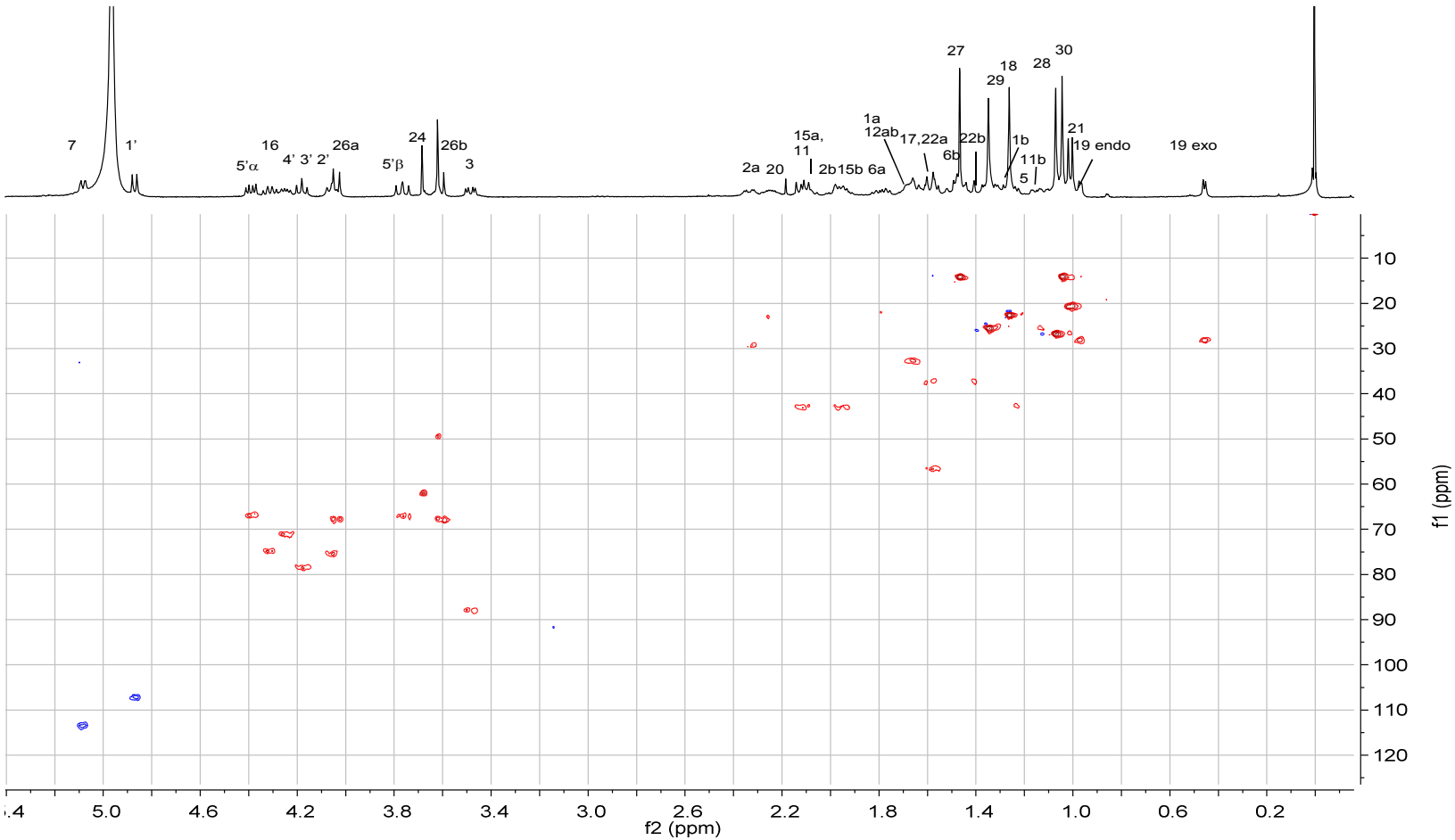

Figure 63. Compound 11; 600 MHz gHSQC spectrum in pyridine-d_5

Chemical shifts were calibrated to 7.217 ppm for the residual protonated species of pyridine on F1 and to 123.5 ppm on F2. Original Data F1 128 F2 2k. Digitization was as follows: F1 SI 1k QSINE (SSB 2), F2 SI 2k QSINE (SSB 2).

3.2.3.12. **Compound 12. Cimigenol-3-*O*-β-D-xylopyranoside**

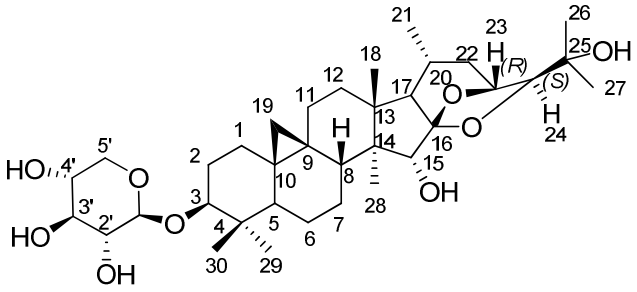

Cimigenol-3-*O*-β-D-xylopyranoside (**12**) was obtained as a white powder. The HR-ESI-MS revealed protonated molecule $[M+H]^+$ at 621.4034 *m/z* (Calculated for $C_{35}H_{57}O_9$, 621.4003) suggesting the molecular formula of $C_{35}H_{56}O_9$. The ^{1}H NMR spectrum revealed two cyclopropane methylene protons centered at 0.293 and 0.536 ppm, six tertiary methyls at 1.075, 1.160, 1.198, 1.329, 1.480 and 1.507 ppm, a secondary methyl at 0.863 ppm. The sugar was determined to be a 3-*O*-β D-xylopyranoside by a signal of H-5β at 3.752 ppm. A combination of H-24 as a singlet at 3.786 and H-23 as a doublet at 4.762 ppm, suggests the side chain/ EF ring system is that of cimigenol 23*R,*24*S* type. No acetyl signals or OH marker signals were observed. Hence, the compound was tentatively assigned to be cimigenol-3-*O*-β-D-xylopyranoside. The ^{1}H NMR chemical shifts of well isolated peaks provided a reasonable match with data for this compound, isolated from the roots/rhizomes of *C. racemosa* (4). The qCOSY spectrum is consistent with the proposed structure.

Cimigenol-3-*O*-β-D-xylopyranoside (**12**) ^{1}H NMR (900 MHz, C_5D_5N) aglycone moiety δ 4.762 (1H, brd, *J* = 9.2 Hz, H-23), 4.277 (1H, brs, H-15), 3.786 (1H, s, H-24), 3.752 (1H, t, *J* = 10.9 Hz, H-5'α), 3.5326 (1H, dd, *J* = 4.4, 11.6 Hz, H-3), 2.389 (1H, m, H-2a), 2.280 (1H, m, H-22β), 2.091 (2H, m, H-7a/11a), 1.972 (1H, m, H-2b), 1.701 (2H,

overlapped, H-8,12a), 1.690 (1H, m, H-20), 1.513 (1H, overlapped, H-17), 1.507 (3H, s, H-26), 1.480 (3H, s, H27), 1.349 (1H, dd, *J* = 12.6, 4.4 Hz, H-5), 1.331 (3H, s, H-29), 1.249 (1H, m, H-1b), 1.198 (3H, s, H-28), 1.160 (3H, s, H-18), 1.103 (1H, t, *J* = 7.1 Hz, H-7b), 1.075 (3H, s, H-30), 1.042 (1H, m, H-22α), 0.863 (3H, d, *J* = 6.5 Hz, H-21), 0.728 (1H, m, H-6β), 0.536 (1H, d, *J* = 3.8 Hz, H-19 endo), 0.293 (1H, d, *J* = 3.8 Hz, H-19 exo); Sugar moiety δ 4.884 (1H, d, *J* = 7.6 Hz, H-1'), 4.377 (1H, m, H-4'), 4.244 (1H, m, H-5'β), 4.175 (1H, t, *J* = 8.5 Hz, H-3'), 4.059 (1H, m, H-2'), 3.752 (1H, t, *J* = 10.9 Hz, H-5'α),

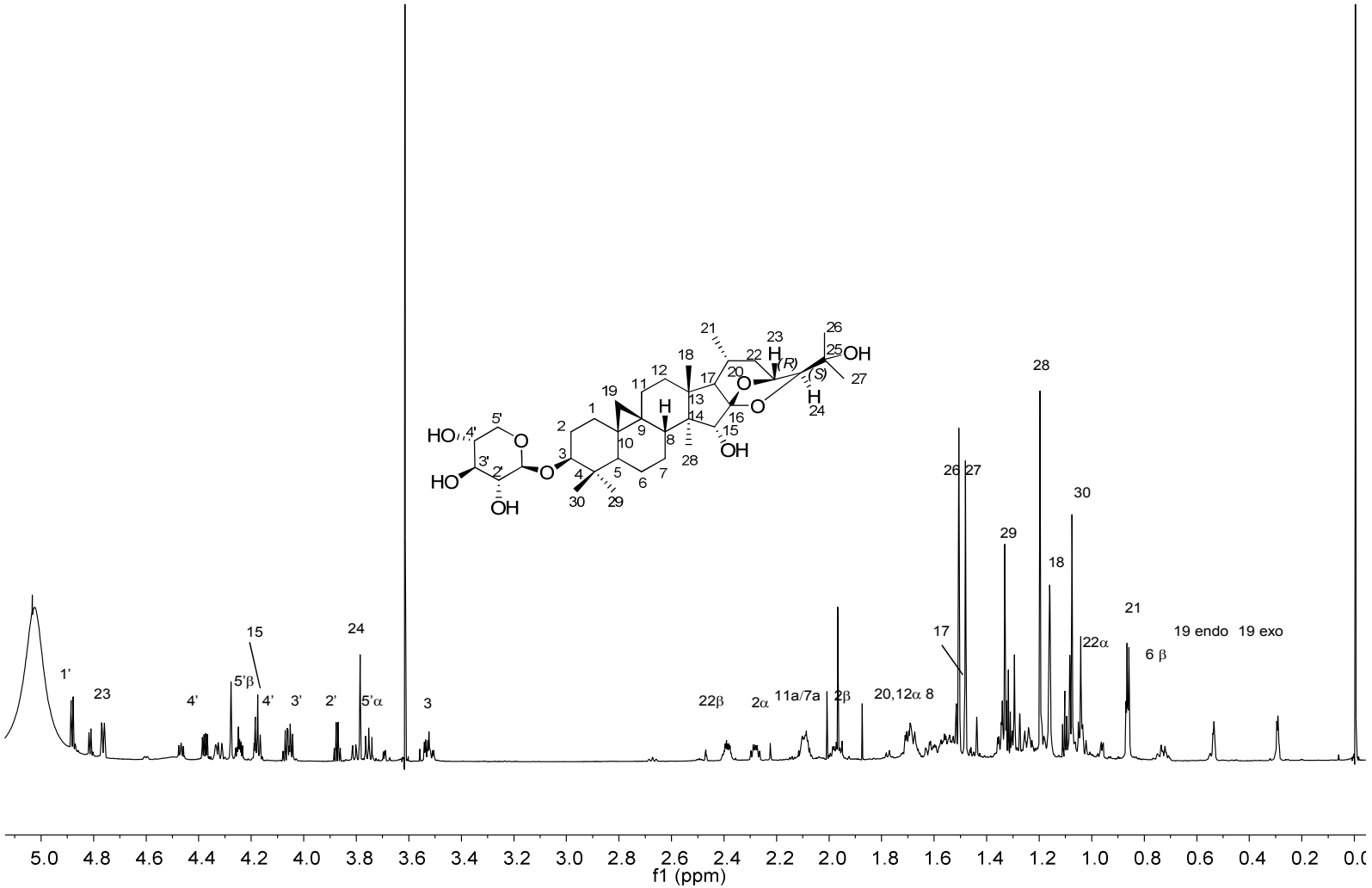

Figure 64. Compound 12; 900 MHz ^{1}H NMR in pyridine-d_5

Chemical shifts were calibrated to 7.217 ppm for the residual protonated species of pyridine. Digitization was as follows: GM (LB -1.0 Hz, GB 0.1).

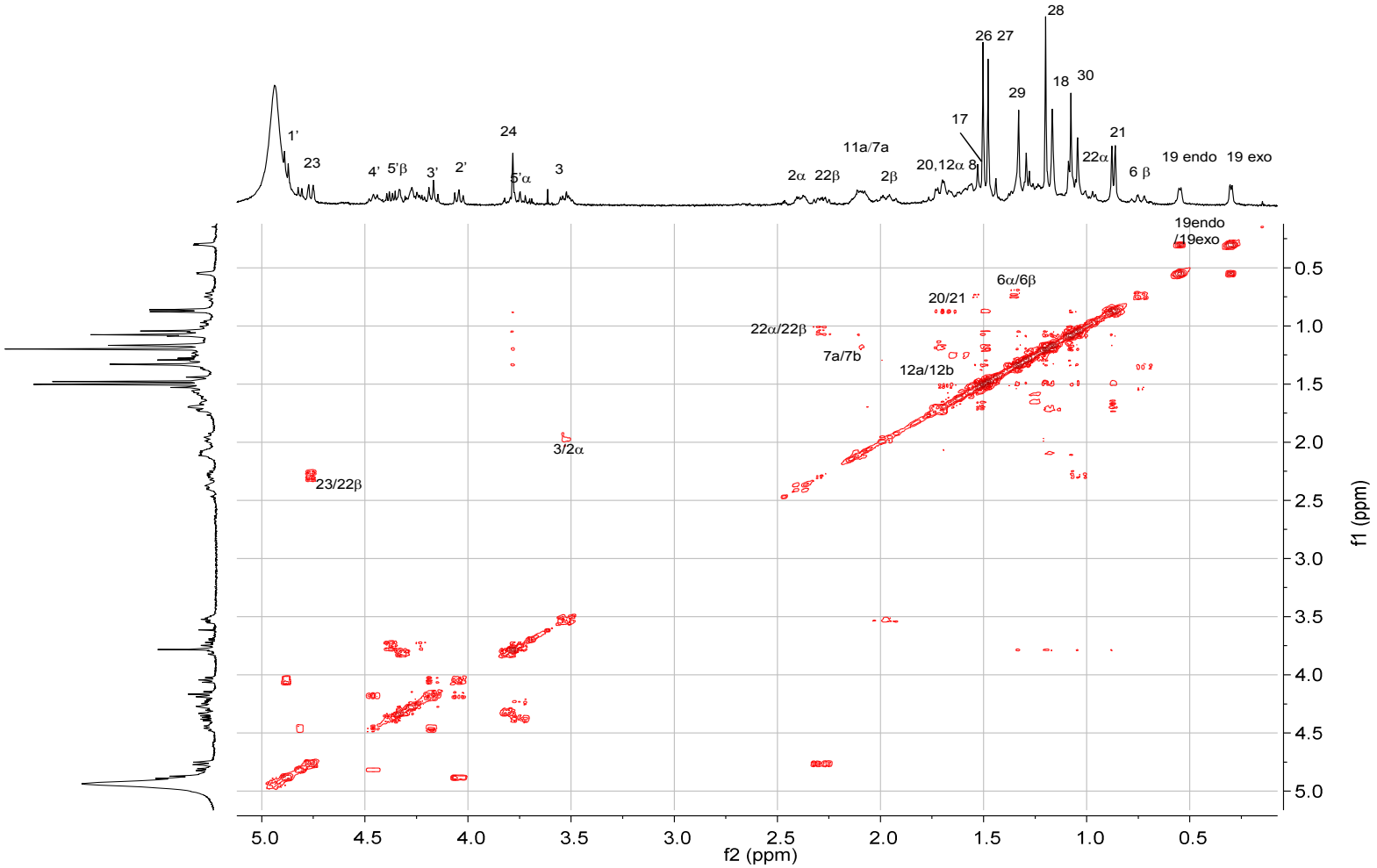

Figure 65. Compound 12; 400 MHz gCOSY spectrum in pyridine-d_5

Chemical shifts were calibrated to 7.217 ppm for the residual protonated species of pyridine. Original data F1 256 F2 2k. Digitization was as follows: F1 SI 2k SINE (SSB 0), F2 SI 4k SINE (SSB 0).

3.2.4 *Characterization of Compounds: Phenolics*

3.2.4.1. **Compounds 13 and 14**

Quercetin 3-*O*-β-arabinopyranosyl-(1→6)-β-galactopyranoside (13)

Kaempferol 3-*O*-β-arabinopyranosyl-(1→6)-β-galactopyranoside (14)

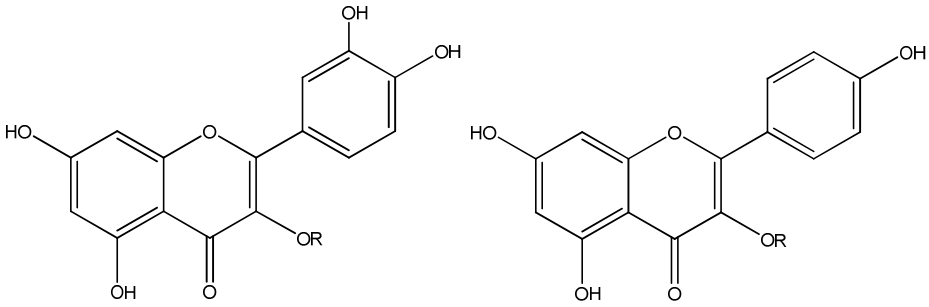

13 R=Gal(6-1)Ara **14** R=Gal(6-1)Ara

Characterization of a mixture of two flavonoids was performed with a 1D ^{1}H NMR spectrum obtained at 900 MHz and ^{1}H, COSY, HMBC and HSQC spectra obtained at 400 MHz, along with exact mass obtained by the HR-ESI-MS. For the major compound, protonated molecule $[M+H]^{+}$ at *m/z* 597.1455 indicated a molecular formula of a species $C_{26}H_{28}O_{16}$. An additional high resolution fragment at *m/z* 465.0921 corresponds to the loss of anhydropentose. The fragment ion at *m/z* 303.05 corresponds to the aglycone of this compound with the molecular formula of $C_{15}H_{11}O_{7}$, which corresponds to the loss of an anhyropentose and an anhydrohexose (a loss of 132 and 162). The minor compound showed $[M+H]^{+}$ at *m/z* 581.1489 and its aglycone fragment peak appeared at *m/z* 287.0534, which correspond to the molecular formulae of $C_{26}H_{28}O_{15}$ and $C_{15}H_{11}O_{6}$ respectively. The minor compound showed the same fragmentation pattern as the major compound. The ^{1}H NMR revealed a typical AMX pattern (2', 7.905 ppm, 6', 7.700 ppm, 5', 6.916 ppm, d, 8.4Hz) for the compound and a AA'XX" (2', 6' 8.181 ppm, 3', 5', 6.936 ppm)

pattern for the minor compound, hence the identification of the aglycones were consistent with kaempferol and quercetin. Because the aromatic ring and the saccharide residue spatially interact with each other in kaempferol (45,73), two pairs of protons AA' and XX' are actually nonisochronous. Hence higher order effects were observed in the ^{1}H NMR spectrum and the AA'XX' signals were observed as pseudo-doublets.

The sugar residue was identified as 3-*O*-β-arabinopyranosyl-(1→6)-β-galactopyranoside by intensive analysis of coupling constants from the ^{1}H spectrum, their connectivity from gCOSY along with the HR-LC-MS. As described above, the compound was shown to possess two sugars including one hexose and one pentose as reflected by the fragmentation pattern of HR-LC-MS spectrum. In fact, two anomeric protons (5.168, 3.960 ppm) observed in the ^{1}H NMR also suggest that the compound has two sugars. Beginning with the anomeric proton, the connectivity of the protons of the sugar spin system could be established from the COSY spectrum as shown in Figure 68. From the COSY analysis, the two separate spin systems, associated with the two different sugar residues, could be identified. For each spin system, the stereochemistry was identified by analyzing the magnitude of the spin-spin coupling constants. Considering the typical *J* values of axial-axial and axial-equatorial couplings in cyclohexane, arabinopyranose and galactopyranose were proposed. Resolution of the ^{1}H NMR spectrum was enhanced by post acquisition processing using NUTS with the following parameters; zfzfzf GM (LB -1.5, GB 0.1). The connection between the sugars and the flavonol were determined by the HMBC signals. The anomeric proton of the β-galactopyranose is correlated with C-3 in the C ring at 135.54 ppm-and the anomeric proton of the β-arabinopyranose is correlated with C-6'' at 68.37 ppm.

The percentage of quercetin and kaempferol was determined by qHNMR to be 64% and 36%, respectively, by taking an average integral value for the B-ring protons. (an average of 2', 5', 6' signal integrals for quercetin and the equivalent 1 proton integral calculated for 2',6', 3',5' of kaempferol.)

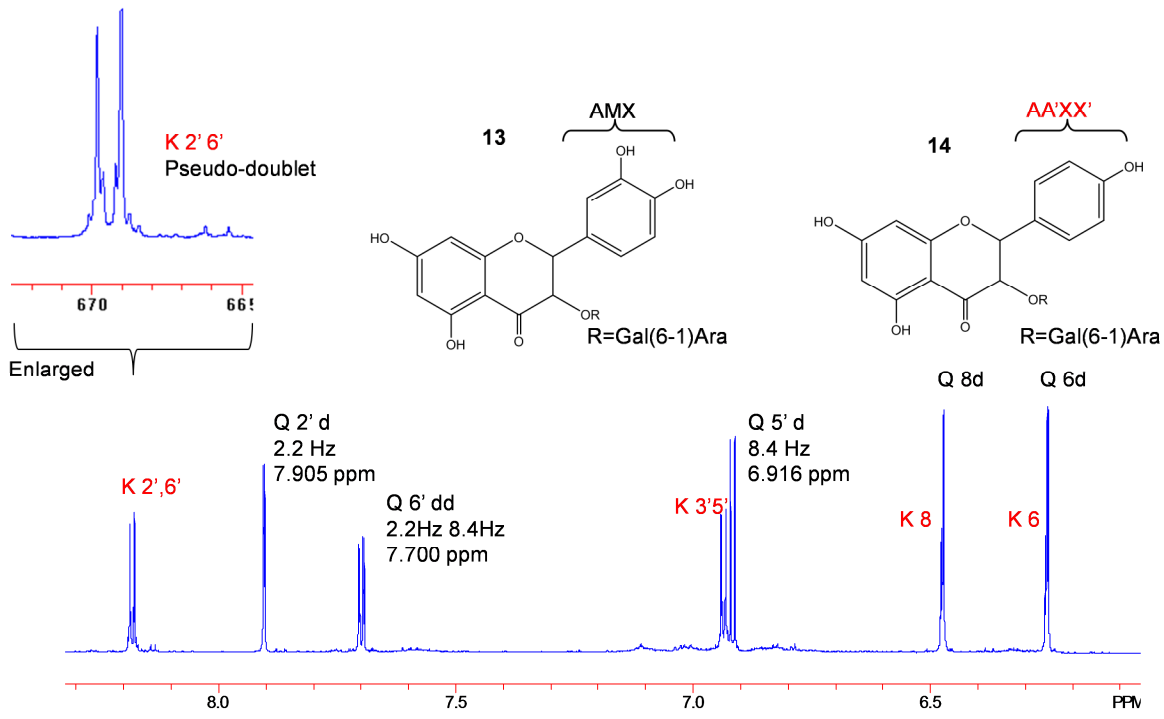

Figure 66. Flavanol region of compounds 13 and 14. 400 MHz ^{1}H NMR in MeOH-d_4

Chemical shifts were calibrated to 3.31 ppm for the residual proton signal in MeOH-d_4. Digitization as follows: GM (LB -1.5 Hz, GB 0.15) zfzfzf. Signals are marked with K for kaempferol and Q for quercetin

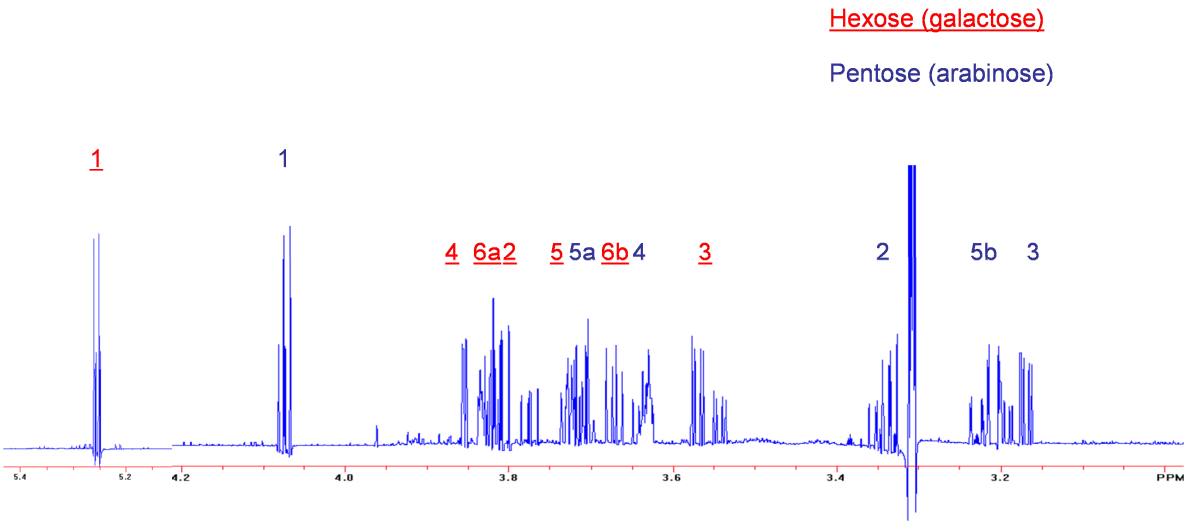

Figure 67. Compounds 13 & 14.
Carbohydrate region of the flavonol glycosides 400 MHz ^{1}H NMR in MeOH-d_4

Chemical shifts were calibrated to 3.31 ppm for the residual proton signal in MeOH-d_4.
Digitization as follows: GM (LB -1.4 Hz, GB 0.15) zfzfzf

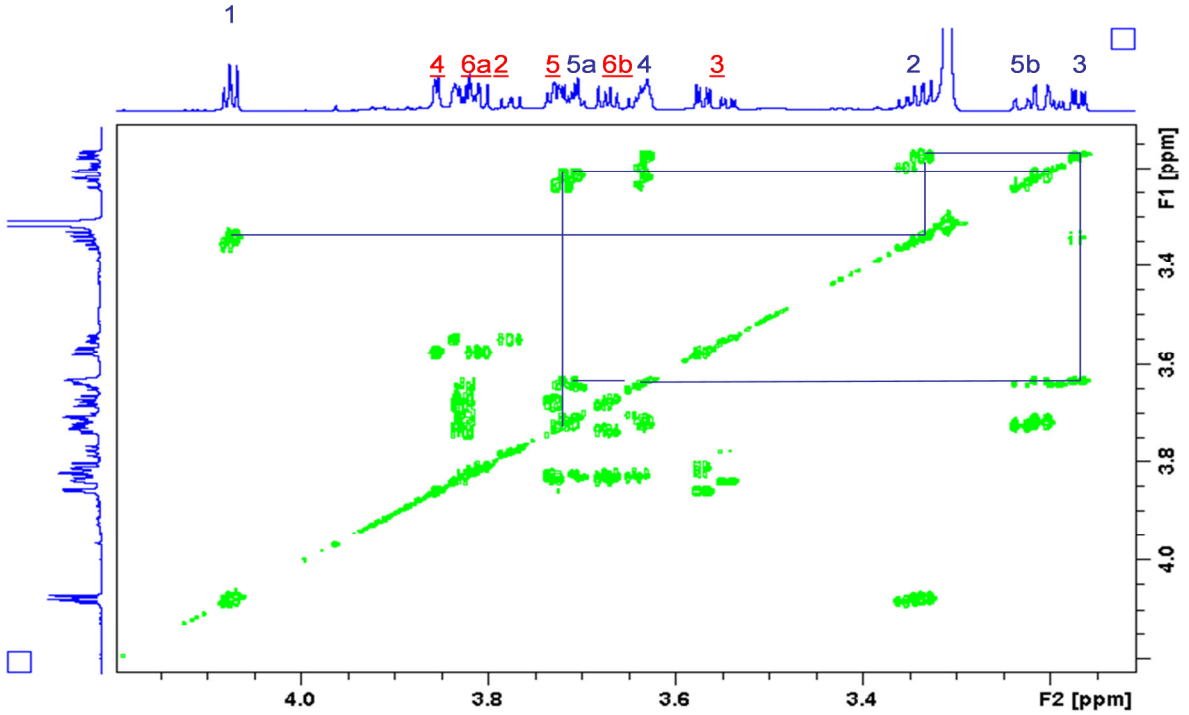

Figure 68. Compounds 13 & 14. 400 MHz gCOSY spectrum in MeOH-d_4

Chemical shifts were calibrated to 3.31 ppm for the residual proton signal in MeOH-d_4.
Arabinopyranoside assignment is shown in solid number and correlation was indicated with lines. Galactopyranoside is shown by numbers with underbars.

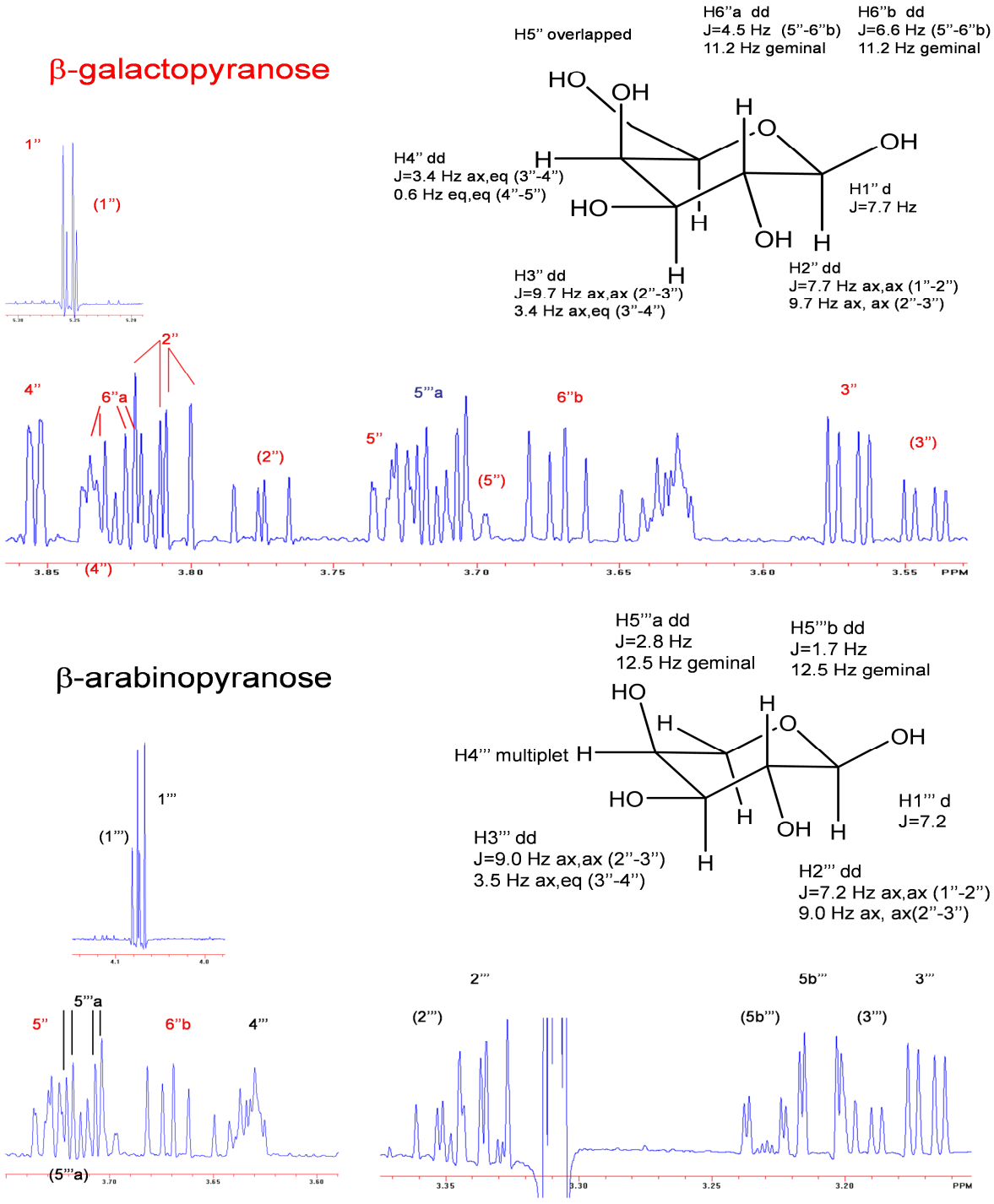

Figure 69. Spin analysis of β-galactose (top) and β-arabinose (bottom) 400 MHz ^{1}H NMR in MeOH-*d*$_4$

Chemical shifts were calibrated to 3.31 ppm for the residual proton signal in MeOH-*d*$_4$.Digitization as follows: GM (LB -1.4 Hz, GB 0.15) zfzfzf

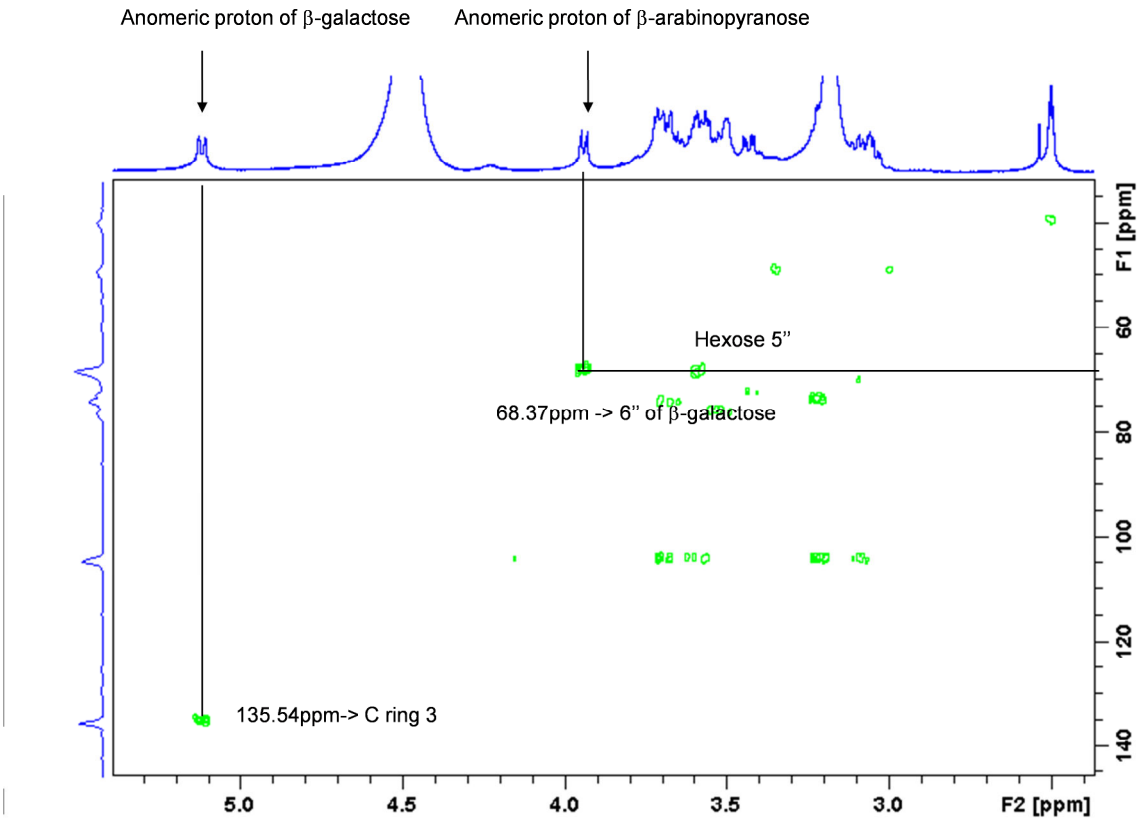

Figure 70. Key HMBC signals of compound 13 and 14. 400 MHz gHMBC in MeOH-d_4

3.2.5 *Characterization of Compounds: Alkaloids*

3.2.5.1. Compound (15) N_ω-Methylserotonin

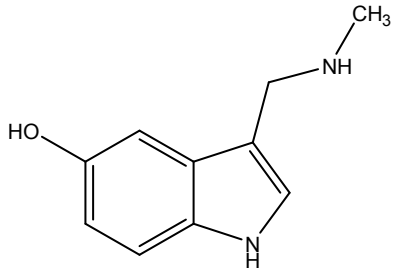

N_ω-Methylserotonin (syn. *N*-methyl-5-hydroxytryptamine) was has been identified from the roots/rhizome of *C. racemosa* and serotonergic activity has been shown with this

compound (23). Since the extract of the aerial parts also showed serotonergic activity, it was suggested that the aerial parts also possesses the active compound, N_{ω}-methylserotonin. The content of N_{ω}-methylserotonin was quantified by LC-MS method by Dr. Soyoun Ahn (Project 3 of the UIC/NIH botanical center). The detail is in section 5.3.

3.3. *Summary of Aim 1*

In this study, two new cycloartane triterpene glycosides, 24-*epi*-1α-hydroxycimigenol-3-*O*-β-D-xylopyranoside and 1α-hydroxydahurinol-3-*O*-α-L-arabinopyranoside were isolated and structures elucidated by a combination of NMR techniques on high field strength instruments (900 MHz, 700 MHz) along with HR-LC-MS. To analyze the stereochemistry of the compounds, full spin simulation was successfully carried out using the PERCH program and revealed several key long range couplings, which otherwise would be ignored such as couplings between H19 exo and H-5 and Me-18 and H-12β.

TABLE XIX. LIST OF ISOLATES FROM *CIMICIFUGA RACEMOSA* AERIAL PARTS AND THEIR PREVIOUS REPORTS

Code includes, CA=*C. acerina*; CD=*C. dahurica*; CS=*C. simplex*; CJ=*C japonica*
RR=rhizome or underground part, PX=aerial parts
[1]obtained by enzymatic hydrolysis of a glycoside

No.	Isolates	Isolated before?	From CR roots?
1	1α-24-*epi*-cimigenol-3-*O*-β-D-xylopyranoside	No	No
2	1α-hydroxydahurinol-3-*O*-α-L-arabinopyranoside	No	No
3	1α-hydroxycimigenol 3-*O*-α-L-arabinopyranoside	Yes (CSRR (43))	No
4	1α-hydroxycimigenol 3-*O*-β-D-xylopyranoside	Yes (CSPX (44))	No
5	7β-hydroxycimigenol aglycone	yes (Not inp[1](34))	No
6	25-O-acetyl-7β- hydroxycimigenol-3-*O*-β-D-xylopyranoside	Yes (CSPX (45))	No
7	25-O-acetyl-cimigenol-3-*O*-β-D-xylopyranoside	Yes (CDRR (63))	Yes (64,74)
8	24-O-acetylhydroshengmanol-3-*O*-β-D-xylopyranoside	Yes (CJRR (68))	Yes (64)
9	cimigenol aglycone	Yes (CARR (31), CDRR, CSRR (42))	No
10	Cimiaceroside A	Yes (CERR(72))	Yes
11	Cimiracemoside I	Yes	Yes ((64))
12	Cimigenol-3-*O*-β-D-xylopyranoside	Yes (several reports)	Yes ((64))
13	Quercetin 3-O-β-arabinopyranosyl-(1→6)-β-galactopyranoside	Yes	No
14	Kaempferol 3-O-β-arabinopyranosyl-(1→6)-β-galactopyranoside	Yes	No
15	N_{ω}-Methylserotonin	Yes	Yes ((23))

Along with the two new compounds, five compounds were isolated for the first time from the *C. racemosa.* In particular, 7β-hydroxycimigenol aglycone previously has only been obtained by enzymatic hydrolysis and it has not been isolated in a form of an aglycone. As seen in the Table XIX, 1α/7β-OH derivatives were isolated from the aerial parts, but they have not been isolated from the roots. This result matches the previously reported case of *C. simplex*, where 1α/7β/12β-OH derivatives were isolated from the aerial parts, but 7β derivatives were not detected in the roots/rhizome (35). Fingerprint signals

were shown for dereplication of cycloartane triterpenes. Key signals that represent partial structures were suggested.

Quercetin 3-*O*-β-arabinopyranosyl-(1→6)-β-galactopyranoside and kaempferol 3-*O*-β-arabinopyranosyl-(1→6)-β-galactopyranoside were identified in a mixture. However, their structures were completely elucidated. Both quercetin and kaempferol are commonly found in plants used in traditional medicine and in plant-derived foods, and various biological activities have been reported, including estrogenicity and anticancer activity (75).

The serotonergic compound N_{ω}-methylserotonin was identified by an LC-MS method from CRPX extracts. The comparison between CRRR is described in 5.3. Other alkaloids were not isolated.

4. Aim 2 Metabolomics and Standardization of CR Aerial Parts

Plant authentication is vital for quality control of widely used dietary supplements such as black cohosh (*Cimicifuga racemosa*, CR). Contamination of CR dietary supplements with other *Cimicifuga* species occurs for two reasons. First, plant species may be misidentified because of morphological and habitat similarities. Second, due to economic considerations, high demand and expense, CR has been substituted with less expensive *Cimicifuga* species (73). In fact, Asian species, including *C. foetida*, *C. dahurica*, and *C. heracleifolia,* were implicated as contaminants in black cohosh products by analysis using HPLC with Selected Ion Monitoring LC-MS methods (73).

Recently, ^{1}H NMR-based metabolic fingerprinting using statistical methods has received considerable attention as an approach to authenticate botanicals (76-79). This method allows for the classification of plants, recognition of adulteration, identification of adulterants and product quality control of botanicals (80). Metabolomics analysis can be applied in two different ways (80,81):

- The microscopic view (targeted approach) examines a specific set of phytoconstituents (e.g. phenolics or terpenoids) that serve as marker compounds for a plant species. This approach is also called metabolic fingerprinting or metabolic profiling.
- The macroscopic view (untargeted approach) which aims at identifying and quantifying all or, in practice, as many as possible of the metabolites produced by a specific species.

In either case, the major advantage of metabolomics is that it can include detection and analysis of previously unknown and unidentified metabolites.

In the previous chapter, 12 triterpenes and 2 flavones were described for the first time from the aerial parts of CR (CRPX). However, these are far from all of the secondary metabolites in CRPX. Presently, over 200 compounds have been identified from the roots/rhizomes of CR (CRRR). Less information is available about the metabolomic constituent profile of the non-medicinal *Cimicifuga* species such as *C. americana* (CA) and *C. rubifolia* (CU). For standardization purposes, however, it is necessary to consider such species as possible adulterants or contaminants. NMR metabolomics is a useful method that encompasses both known and unknown constituents that could potentially be marker compounds for particular species. Moreover, NMR possesses at least two unique advantages over MS-based methods. First, it can provide a detailed analysis of the biomolecule composition very rapidly and with relatively simple sample preparation. Secondly, it is a universal and quantitative detector for all molecules containing NMR-active nuclei (e.g. ^{1}H), unlike MS where the detection of analytes is influenced by selective ionization.

4.1. *Methods*

4.1.1 *Plant Material*

A total of 34 samples taken from different *Cimicifuga* species were used for this study, including three American species: *C. racemosa* (CR), *C. americana* (CA), and *C. rubifolia* (CU). These three American species were in part selected due to the high probability of finding them intermixed during a wild collection, because of their shared

habitat and morphological similarity. For each of the American species, we acquired more than 5 samples. Asian species were also included, but for reference purposes only, since the number of authenticated plant samples we were able to obtain was limited, which also limited the statistical analysis. As shown in Table XXI, samples denoted BC624, BC404, BC582, BC626, BC581, and BC627 were cultivated and collected from the Dorothy Bradley Atkins Medicinal Plant Garden at UIC by Mike Totura. Sample BC629 was cultivated by Katharine Parks, a horticulturist and farmer, in Chillicothe, Ohio, and the specimen was authenticated and deposited in the Herbarium of the Field Museum of Natural History (Chicago, Illinois) by Dr. Doel Soejarto. Other American species were acquired through wild collections in Virginia, North Carolina, and Tennessee by Drs. Daniel Fabricant and Gwynn Ramsey. Voucher specimens are housed at the Searle Herbarium, Field Museum of Natural History and the Ramsey-Freer Herbarium, Lynchburg College (Lynchburg, Virginia). Cultivated Asian species were acquired through Dr. Takahisa Nakane from Showa Pharmaceutical University, Medicinal plant garden (BC587, BC588) and Tokyo Medicinal plant garden (Tokyo, Japan, BC583-586). BC396, BC395, BC397, and BC393 were obtained from Pure World, Inc. The plant part codes used for this study were PX for aerial parts and RR for roots/rhizomes, according to the established UIC/NIH Botanical Center Plant code system.

TABLE XX. SUMMARY OF SPECIES USED FOR THE METABOLOMICS PROJECT

		Aerial Parts (PX)	Roots/Rhizomes (RR)	Total number of samples
American species	*C. americana*	3	3	6
	C. racemosa	6	6	12
	C. rubifolia	2	3	5
Other species	*C. simplex*	1	2	3
	C. acerina	1	2	3
	C. japonica	1	2	3
	C. dahurica	0	1	1
	C. heracleifolia	0	1	1
	Total	14	20	34

TABLE XXI. LIST OF PLANT MATERIAL USED FOR METABOLOMICS STUDY

*NMR number is used in statistical analysis

Genus	Species	Parts	BC number	NMR* number	Collection date	Collection Site
Cimicifuga	*racemosa*	PX	BC026	46	6/29/1999	Sevier County, TN. Elevation 3500 ft.
Cimicifuga	*racemosa*	PX	BC027	38	6/29/1999	Sevier County, TN. Elevation 3300
Cimicifuga	*racemosa*	PX	BC624	14	6/16/2009	Atkins Garden, Cook County, IL
Cimicifuga	*racemosa*	PX	BC404	12	10/1/2008	Atkins Garden, Cook County, IL
Cimicifuga	*racemosa*	PX	BC582	10	10/7/2009	Atkins Garden, Cook County, IL
Cimicifuga	*racemosa*	PX	BC025	3	6/29/1999	Rockbridge County, VA. Elevation 2481 ft.
Cimicifuga	*racemosa*	RR	BC036	44	10/16/1999	Elk township, Chester County, PA
Cimicifuga	*racemosa*	RR	BC007	42	6/30/1999	Sevier County, TN. Elevation 3300 ft.
Cimicifuga	*racemosa*	RR	BC094	40	11/7/2000	Forbes State Forest, Somerset County. PA
Cimicifuga	*racemosa*	RR	BC629	36	6/3/2010	Chillicothe, Ross County, OH
Cimicifuga	*racemosa*	RR	BC626	177	6/16/2009	Atkins Garden, Cook County, IL
Cimicifuga	*racemosa*	RR	BC581	18	10/6/2009	Atkins Garden, Cook County, IL
Cimicifuga	*racemosa*	RR	BC627	16	7/23/2009	Atkins Garden, Cook County, IL
Cimicifuga	*americana*	PX	BC029	48	6/30/1999	Sevier County, TN. Elevation 3300 ft.
Cimicifuga	*americana*	PX	BC020	22	8/26/1999	Swain County, NC. Elevation 2875 ft.
Cimicifuga	*americana*	PX	BC028	32	6/28/1999	Rockbridge County, VA. Elevation 3150 ft.
Cimicifuga	*americana*	RR	BC006	26	6/30/1999	Sevier County, TN. Elevation 3300 ft.
Cimicifuga	*americana*	RR	BC008	1	6/30/1999	Swain County, NC. Elevation 2875 ft.
Cimicifuga	*americana*	RR	BC011	30	8/26/1999	Sevier County, TN. Elevation 3300 ft.
Cimicifuga	*rubifolia*	PX	BC022	56	8/27/1999	Scott County, VA, Elevation 1800 ft.
Cimicifuga	*rubifolia*	PX	BC023	58	6/29/1999	Scott County, VA. Elevation 1800 ft.
Cimicifuga	*rubifolia*	RR	BC015	52	8/27/1999	Scott County, VA, Elevation 1800 ft.
Cimicifuga	*rubifolia*	RR	BC003	50	6/29/1999	Scott County, VA. Elevation 1800 ft.
Cimicifuga	*rubifolia*	RR	BC016	54	8/27/1999	Scott County, VA, Elevation 1800 ft.
Cimicifuga	*heracleifolia*	RR	BC396	78	n/a	Pure World
Cimicifuga	*japonica*	PX	BC586	70	6/2008	Tokyo Medicinal Plant Garden, Japan
Cimicifuga	*japonica*	RR	BC585	68	6/2008	Tokyo Medicinal Plant Garden, Japan
Cimicifuga	*japonica*	RR	BC395	66	n/a	Pure World
Cimicifuga	*acerina*	PX	BC584	76	6/2008	Tokyo Medicinal Plant Garden, Japan
Cimicifuga	*acerina*	RR	BC583	74	6/2008	Tokyo Medicinal Plant Garden, Japan
Cimicifuga	*acerina*	RR	BC397	72	n/a	Pure World
Cimicifuga	*simplex*	PX	BC588	64	6/2008	Showa Pharmaceutical University, Japan
Cimicifuga	*simplex*	RR	BC587	62	6/2008	Showa Pharmaceutical University, Japan
Cimicifuga	*simplex*	RR	BC393	60	n/a	Pure World

4.1.2 *Extraction and Sample Preparation*

A 10 ml aliquot of 70% aqueous MeOH was added to 1 g of dried, ground plant material and the mixture sonicated for 30 minutes. The extract was left overnight at room temperature and then filtered. The residue was similarly extracted and the two filtrates combined. The combined extracts were dried in forced air, to yield the crude extract for metabolomic analysis.

A volume of 650 μl of DMSO-d_6 (Cambridge Isotopes, lot#8L-052, 99.9% D) was added to between 11 and 27 mg of dried extract in an Eppendorf vial, followed by sonication for 5 min. After sonication, the vial was centrifuged and 600 μl of supernatant were transferred to a 5 mm NMR tube, leaving any insoluble residue in the vial. BC036 was also prepared in pyridine-d_5 in the same fashion for the purpose of identifying a reference compound.

4.1.3 *NMR Quantitative Analysis*

The quantitative ^{1}H NMR method (qHNMR) was employed to obtain the quantity of specific types of compounds in the crude extract by using the residual DMSO-d_5 resonance as a reference. To make the integrated intensity of a ^{1}H NMR signal accurately proportional to the number of observed nuclei, acquisition parameters should be chosen appropriately. Accordingly, “quantitative experimental conditions” (82), including appropriate parameter selection such as relaxation delay and digitization, were carefully chosen for *Cimicifuga* extract analysis, as shown in the Table XXII. The calibration curve was generated by Dr. Gödecke from the UIC/NIH botanical center (83), using dimethylsulfone ($DMSO_2$) as external standard, and the residual DMSO-d_5 signal was used

as internal calibrant for both the $DMSO_2$ calibrant samples as well as the extracts. To verify the calibration curve, a mixed sample of $DMSO_2$ and caffeine was used.

$$y = 0.0127x \qquad \textbf{Equation 4}$$

$$R^2 = 0.9975 \qquad \textbf{Equation 5}$$

Where y is mM concentration, x is relative integral value of ^1H (integral value ^1H integral residual DMSO-d_5).

TABLE XXII. ACQUISITION PARAMETERS USED FOR QHNMR

parameter	value used
acquisition time (aq)	4 s
relaxation delay (d1)	60 s
pulse width (pw)	30
time domain (TD)	144k
number of scan (NS)	64

4.1.4 *Chemometric Analysis*

Multivariate data analysis of ^1H spectra was carried out to recognize patterns and find discriminating signals that could be used to distinguish between species. Among multivariate data analyses, the most common unsupervised method is principal component analysis (PCA). PCA is designed to extract and display the systematic variation in a complex data matrix. In brief, PCA is a projection method which reduces the original data to selected principal components in order to describe variation within the data. All raw data (e.g., the integral values as a function of chemical shifts in a ^1H NMR spectrum) of samples are plotted in a K-dimensional space (K = number of variables, e.g., chemical shift bins in ^1H NMR spectra). The analyzed spectra are projected onto the line generated

by least square analysis (principal component [PC] line) as dots. The score of each sample is obtained along the first PC line. The next principal component can also be calculated by projection onto the line which is orthogonal to the previous principal component line or space (84,85).

In preparation for PCA, all the ^{1}H spectra of American and Asian species were individually processed with the following parameters: EM (LB 0.3 Hz), zero filling to SI = 512k while TD is 65536, automatic phasing, and automatic baseline correction, using Bruker Topspin version 3.0. The spectra were then referenced to the residual proton signal in DMSO-d_6 at 2.500 ppm. Next, a bucket table was created in Bruker AMIX statistics, version 3.9.7, using the pointwise bucketing method between 0.00 ppm and 1.80 ppm. The rows in the bucket table were scaled to the biggest bucket, and the columns were not scaled. The bucket table was then analyzed by PCA.

4.2. *Results and Discussion*

4.2.1 *General observation*

^{1}H NMR spectral profiles

As expected, the ^{1}H NMR spectra of *Cimicifuga* extracts exhibited constituents, such as cycloartane triterpenes, carbohydrates, phenolic compounds etc., which are described in section 2.4. These three major constituents are best characterized in the following three regions of ^{1}H NMR spectra:

A. triterpene aglycone region between 0.0 to 2.2 ppm
B. carbohydrate region between 3.0 to 4.0 ppm
C. phenolic region between 6.0 to 8.0 ppm

The regions A, B, and C, were shown along with a typical ^{1}H NMR spectrum of *Cimicifuga* extracts (BC036) in Figure 71. Other samples showed a similar profile. In addition to these three regions, a broad hump in the spectral region between 4.0 to 5.0 ppm was observed in all of the spectra. This is likely to be an overlap of numerous hydroxyl groups, considering the chemical shift and the *Cimicifuga* compounds are highly oxygenated. Even though the extracts were carefully dried, H_2O/HDO was observed as a broad peak overlapped with carbohydrate signals between 3.3 to 3.6 ppm to different degrees across the samples. The residual DMSO-d_5 peak was observed as a 1:2:2:2:1 quintet and the spectra were calibrated to this peak at 2.500 ppm. Regardless of the species/plant parts, the most crowded region is B, followed by A region. C is the least crowded. Approximate amounts of each of the major classes of compound can be calculated as a representative compound by the qHNMR method. For example, triterpene content in an extract can be calculated as 23-*epi*-26-deoxyactein, of which, the molecular formula is $C_{37}H_{56}O_{10}$ and the molecular weight is 660.83 g/mol. Since 15 protons, including H-24, H-26α&β, H-16, H-3, H-12 and nine sugar protons, are deshielded due to the neighboring oxygen, only 41 protons are expected to be in A region (0.0-2.2 ppm). An integral value of one proton is obtained by dividing the total integral value in A region by a number of expected protons. Theoretically, the molar concentration of triterpenes can be calculated by using the residual DMSO-d_5 signal as an internal standard, however, appropriate reference compound determination and parameter selection for data processing, such as base line correction and window function, are necessary to carry out accurate quantitation of chemical groups in an extract.

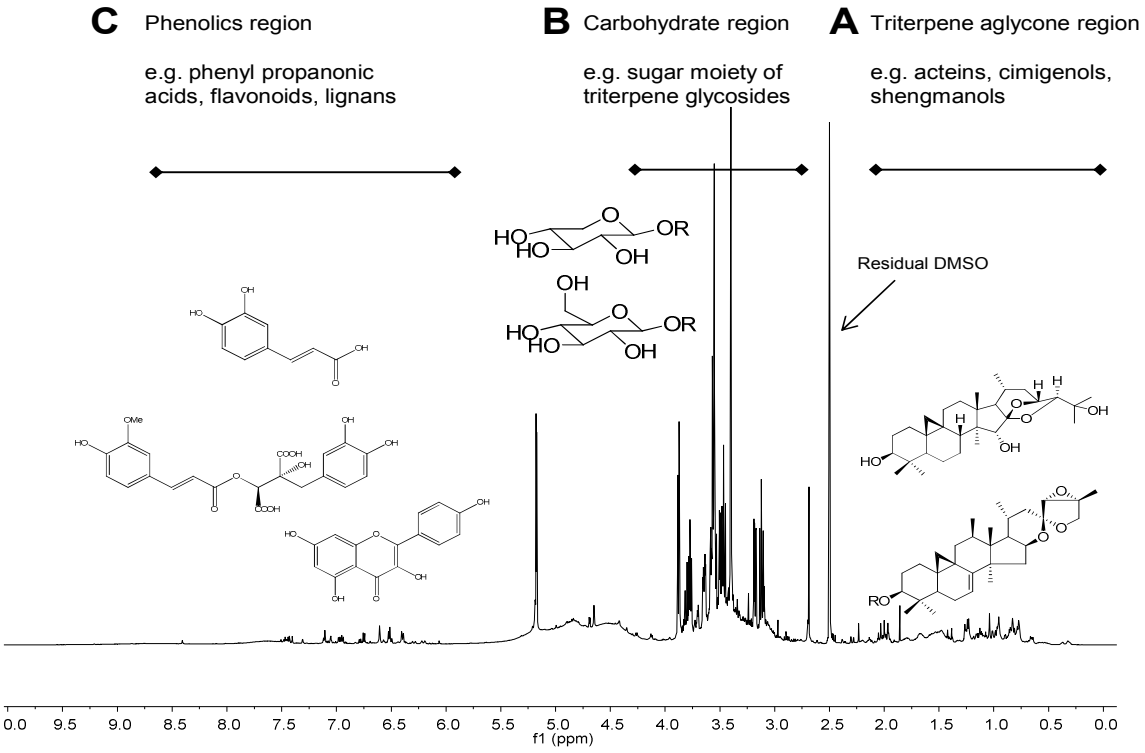

Figure 71. A typical 600 MHz ^{1}H spectrum of a 70% aqueous MeOH extracts of CRRR

12.60 mg of extract (BC036) in 600 μl of DMSO-d_6, Chemical shifts were calibrated to 2.500 ppm for the residual DMSO-d_5.

Sample Preparation and Solubility

After sample preparation, the residual extract in the Eppendorf vial was dried under the air and weighed to calculate sample concentration in the NMR tube. Dry powder samples were easy to dissolve; however, hardened solid extracts were difficult to dissolve. Although solubility of some samples was lower than the other, ^{1}H NMR spectra did not look atypical when BC582 and BC028 were compared to other samples in the same group. Exact sample concentration is required for quantitative ^{1}H NMR analysis.

TABLE XXIII. EXTRACT AMOUNT DISSOLVED IN THE NMR TUBE

Plant Code	BC number	Original amount (mg)	Insoluble (mg)	Soluble (mg)	Solubility (mg/mL)
CRPX	BC624	27.65	1.91	25.74	15.44
CRPX	BC582	25.27	16.79	8.48	5.09
CRPX	BC404	21.73	3.99	17.74	10.64
CRPX	BC027	22.51	4.15	18.36	11.02
CRPX	BC026	20.51	2.85	17.66	10.60
CRPX	BC025	19.87	1.20	18.67	11.20
CRRR	BC629	20.19	3.88	16.31	9.79
CRRR	BC627	23.73	2.52	21.21	12.73
CRRR	BC626	21.70	3.24	18.46	11.08
CRRR	BC581	20.02	5.17	14.85	8.91
CRRR	BC094	15.87	4.86	11.01	6.61
CRRR	BC036	22.13	9.53	12.60	7.56
CRRR	BC007	22.84	6.80	16.04	9.62
CAPX	BC029	22.25	7.53	14.72	8.83
CAPX	BC028	24.07	13.86	10.21	6.13
CAPX	BC020	22.84	8.74	14.10	8.46
CARR	BC011	22.84	3.87	18.97	11.38
CARR	BC008	21.12	1.34	19.78	11.87
CARR	BC006	24.25	3.81	20.44	12.26
CUPX	BC023	21.18	5.81	15.37	9.22
CUPX	BC022	20.67	7.68	12.99	7.79
CURR	BC016	21.89	3.61	18.28	10.97
CURR	BC015	23.40	6.62	16.78	10.07
CURR	BC003	22.14	2.70	19.44	11.66
CHRR	BC396	23.22	3.98	19.24	11.54
CJPX	BC586	21.62	2.09	19.53	11.72
CJRR	BC395	12.17	0.15	12.02	7.21
CJRR	BC585	20.15	3.68	16.47	9.88
CSPX	BC588	24.99	12.91	12.08	7.25
CSRR	BC393	22.50	6.54	15.96	9.58
CSRR	BC587	24.00	3.93	20.07	12.04
CEPX	BC584	19.35	7.24	12.11	7.27
CERR	BC397	11.98	2.67	9.31	5.59
CERR	BC583	23.98	4.25	19.73	11.84

4.2.2 **Quantitative Analysis of Cycloartane Triterpenes**

The quantity of cycloartane triterpenes can be calculated from an integral value of one of the cyclopropane proton signals by using a qHNMR method. An accumulation of H-19 exo signals of various cycloartane triterpenes is observed in the spectral region between 0.20 to 0.45 ppm. The COSY cross peaks of all of signals between 0.20 to 0.45 ppm are coupled to signals between 0.46 to 0.62 ppm, which confirms that resonances between 0.20 and 0.45 ppm are derived only from H-19 exo, and resonances between 0.46 to 0.62 ppm are only from H-19 endo protons. Since no other correlations were observed in COSY spectrum for signals < 0.62 ppm, it is reasonable to deduce that the total integral value represents only triterpene protons. The quantity of cycloartane triterpenes was calculated using the integral value between 0.20 - 0.45 ppm as one proton of a representative cycloartane, for example 23-*epi*-26-deoxyactein ($C_{37}H_{56}O_{10}$ 660.83 g/mol). By using the residual DMSO-d_5 peak as an internal standard, the amount of cycloartane triterpene aglycones was calculated as 23-*epi*-26-deoxyactein. There are two advantages in this method over integrating a broader ppm range of the spectrum: First, since this spectral region (0.20 – 0.45 ppm) is very specific for cycloartane, the chance of including unrelated signals is low. Secondly, this region is surrounded with baseline regions, which makes baseline correction easy and hence less chance of a baseline correction error.

The triterpene content in the metabolomic study samples was calculated by this method. On average, CRRR contains 23.5% of cycloartane triterpenes, which is the highest content of all other species/plant parts. Next is CURR of which the cycloartane triterpene content is 20.5%. Both the CRPX and CUPX contain significantly lower quantities, at 10.5% and 8.0% respectively, compared to the RR of the same species.

However, it has to be noted that the six of CRPX samples had a large variation; from 3.8 to 21.7%. Two of the CRPX samples contained over 20% of cycloartane triterpenes. Further experiments are required to confirm the particularly high numbers. On the other hand, the rest only contains between 3.8 and 5.9% cycloartane triterpenes. The two samples with the highest content do not have a significant common point, such as collection season or collection site. Although there are variations, cycloartane triterpene content in PX is generally lower than in RR in all of the species.

CA contains significantly a lower amount of cycloartane triterpenes compared to CR and CU. The average amount for CAPX and CARR were 2.5 and 3.0%, respectively. This is obvious when you observe ^{1}H NMR spectra, which is discussed in the CA section (4.2.4).

TABLE XXIV. CALCULATED TRITERPENE CONTENTS IN 70% METHANOLIC EXTRACT OF *CIMICIFUGA* SPECIES

Integral value was obtained relative to that of DMSO-d_5

Plant code	BC Number	Sample weight	Integral Value	Triterpene Weight	Triterpene Percentage	Average
CRPX	BC026	17.66	3.34%	1.043	**5.9%**	10.5%
CRPX	BC027	18.36	3.32%	1.037	**5.6%**	
CRPX	BC624	25.74	3.15%	0.983	**3.8%**	
CRPX	BC404	17.74	2.86%	0.893	**5.0%**	
CRPX	BC582	8.48	5.74%	1.792	**21.1%**	
CRPX	BC025	18.67	12.97%	4.049	**21.7%**	
CRRR	BC626	18.46	16.10%	5.026	**27.2%**	23.5%
CRRR	BC036	12.60	10.26%	3.203	**25.4%**	
CRRR	BC007	16.04	9.40%	2.935	**18.3%**	
CRRR	BC094	11.01	9.09%	2.838	**25.8%**	
CRRR	BC629	16.31	6.61%	2.064	**12.7%**	
CRRR	BC581	14.85	14.93%	4.661	**31.4%**	
CAPX	BC029	14.72	1.50%	0.468	**3.2%**	2.5%
CAPX	BC020	14.10	0.84%	0.262	**1.9%**	
CAPX	BC028	10.21	0.79%	0.247	**2.4%**	
CARR	BC006	20.44	0.80%	0.250	**1.2%**	3.0%
CARR	BC008	19.78	3.07%	0.958	**4.8%**	
CARR	BC011	18.97	1.81%	0.565	**3.0%**	
CUPX	BC022	12.99	3.61%	1.127	**8.7%**	8.0%
CUPX	BC023	15.37	3.64%	1.136	**7.4%**	
CURR	BC015	16.78	13.78%	4.302	**25.6%**	20.5%
CURR	BC003	19.44	8.83%	2.757	**14.2%**	
CURR	BC016	18.28	12.69%	3.962	**21.7%**	

4.2.3 *Cimicifuga racemosa Fingerprinting*

The following observations are based on a ^{1}H NMR PCA analysis of twelve CR samples, six RR and six PX, as shown in Figure 72.

For most of the samples, the B region (carbohydrates) is the most complex region of the spectra, followed by relatively fewer signals in the A region (triterpenes) and even

smaller signals in the C region (phenolics). Exceptions were BC007 CRRR (6/30/1999, Sevier County, TN.) and BC025 CRPX (6/29/1999, Rockbridge County, VA.), where the carbohydrate content was rather small and reduced to nearly the same content level as the triterpenes. Other samples of both PX and RR that were also collected in June (CRPX; BC026, 027, 624, CRRR; BC 626, 036, 629) displayed large carbohydrate signals. Hence, it is unlikely that the lower carbohydrate content is related to either seasonal differences or plant part differences (PX vs RR). Additional samples need to be analyzed to explore this phenomenon.

Although it was observed that the composition of the three major compound classes (A, B and C regions) of functional groups exhibited variation, the spectral pattern of each plant part was rather consistent within the spectral region and scaled accordingly and discussed in later section. (Figures 75 and 76).

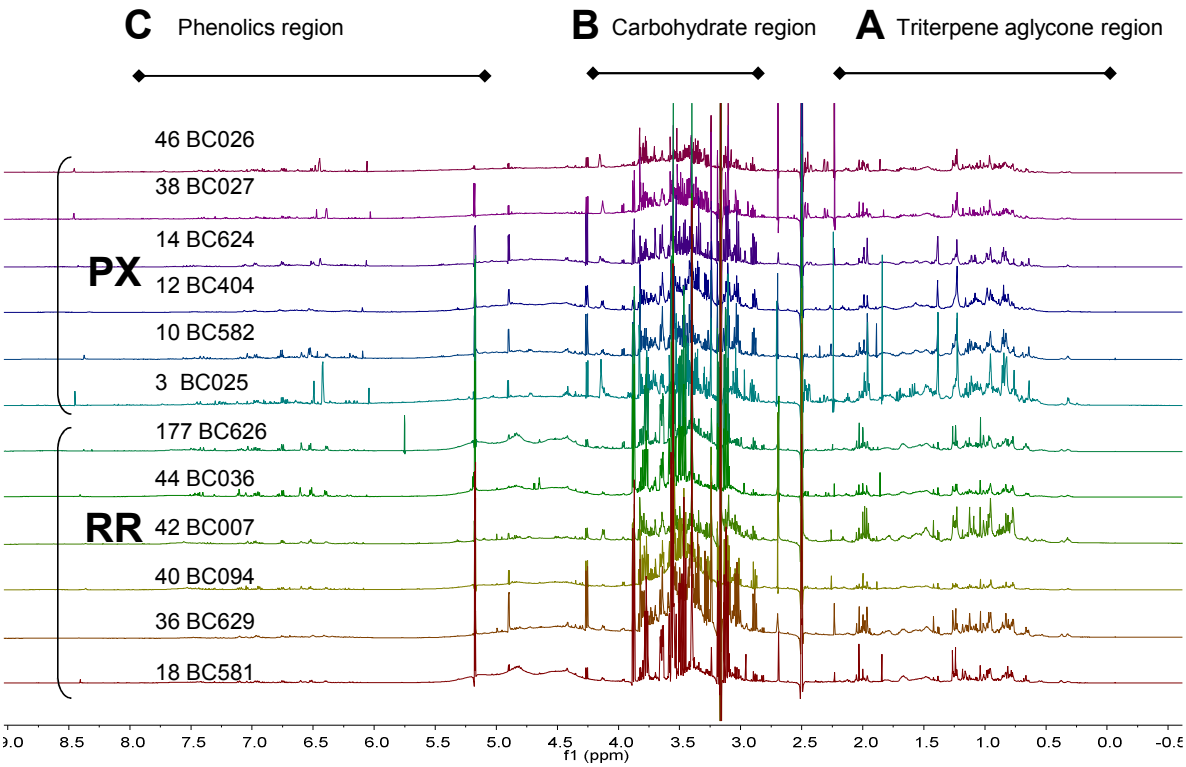

Figure 72. **The ^{1}H spectra of 70% aqueous MeOH extracts of *C. racemosa* (600 MHz)**
All spectra was scaled to residual DMSO-d_5 peak

Reference Compound Identification

Two of the reference compounds, 23-*epi*-26 deoxyactein (**16**) and actein (**17**), were identified in the ^{1}H NMR spectrum of the extracts by comparison with the data of reference material. These reference compounds were obtained from USP and their spectra in DMSO-d_6 were obtained by Dr. Tanja Gödecke on the same instrument (600 MHz). Even though the NMR data of these compounds in DMSO-d_6 was not available in the literature, the signal assignments were done using COSY, HMBC and HSQC correlations as well as reported data for these compounds in pyridine-d_5 as a guide (86,87). When the ^{1}H NMR spectra of the two reference compounds were compared to a resolution enhanced spectrum of the extract (BC036), all of the seven methyl group signals were identified as

shown in Figure 73. As described in 3.2.3, the chemical shifts of the protons of methyl groups of triterpenes are sensitively influenced by the environment of these groups, hence these work as “reporter” signals for a particular compound. The presence and positions of these methyl signals is a strong indication of the existence of particular compounds. In addition to the ^{1}H spectral evidence, the COSY spectra were examined for compounds **16** and **17**. The spectra of reference compounds were superimposed on the spectrum of BC036. As a result, all of the key cross peaks of compound **16** and **17** were observed in the BC036 COSY spectrum. Specifically, correlations H-16/H-15a, H-16/H-15b, and H-16/H-17 were clearly observed in both cases. These are characteristic for actein types of side chains. Furthermore, the following correlations were observed, H-12/H-11α&β confirms an OAc moiety at C-12, H-3/H2 α&β confirms the sugar position, and 19 exo/endo represents a cycloartane moiety. Altogether, the presence of **16** and **17** in the BC036 extract was revealed since each COSY cross peak gives information of a part of the structure. Cross peaks that did not match with the reference materials were cross peaks between hydroxyl groups and sugar protons that were shown in a solid square in the Figure 73. Since hydroxyl groups can have hydrogen bonding with other components in the mixture, and they may behave differently as pure reference compounds, it is reasonable to assume that such cross peaks may not match up. Hence, from ^{1}H and COSY evidence, 23-*epi*-26-deoxyactein and actein were identified in the CRRR extract (BC036).

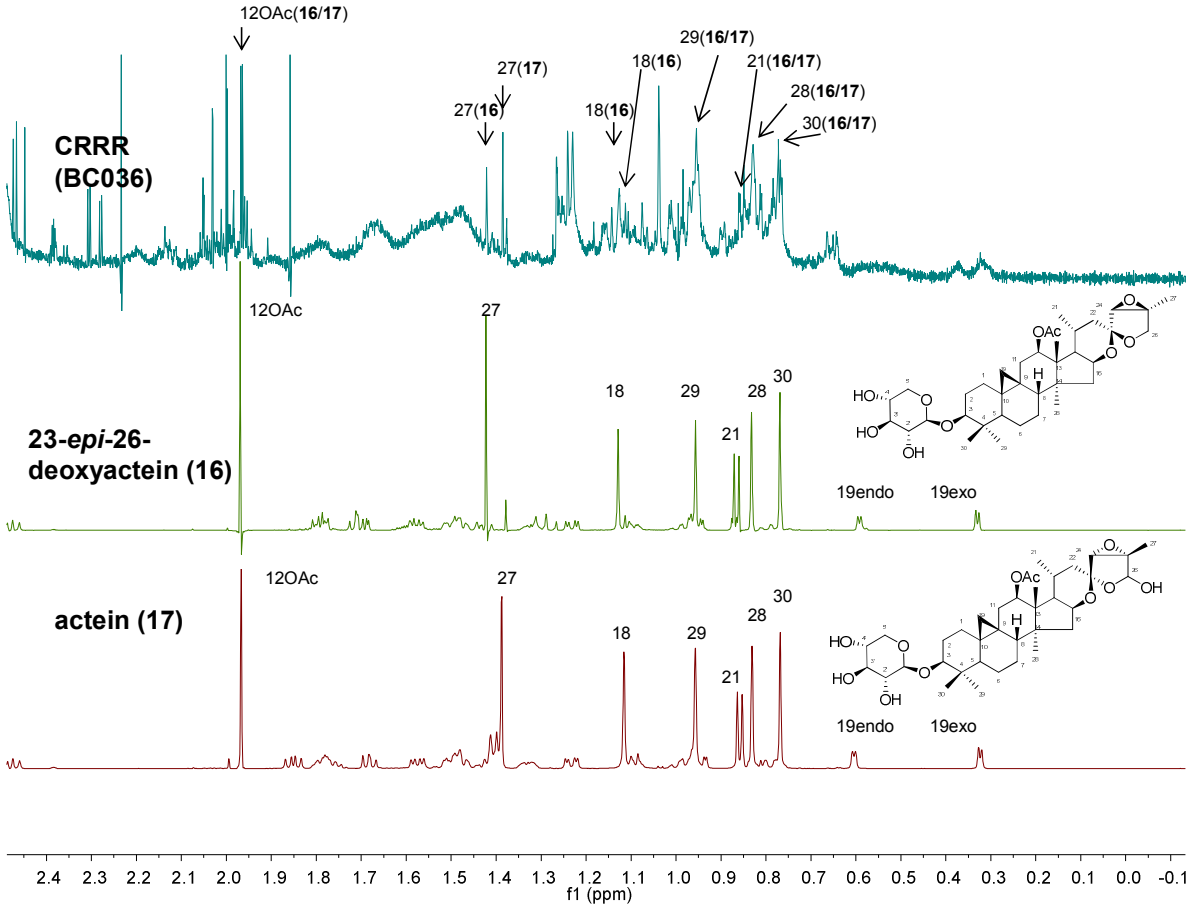

Figure 73. Identification of 23-*epi*-26 deoxyactein (16) and actein (17) by ^{1}H NMR as two of the major constituents of CRRR extract (BC036) 600 MHz

Digitization as follows: BC036 GM(LB -3.0 Hz, GB 0.1), compound (**16**,**17**) GM(LB -1.0 Hz, GB 0.1),

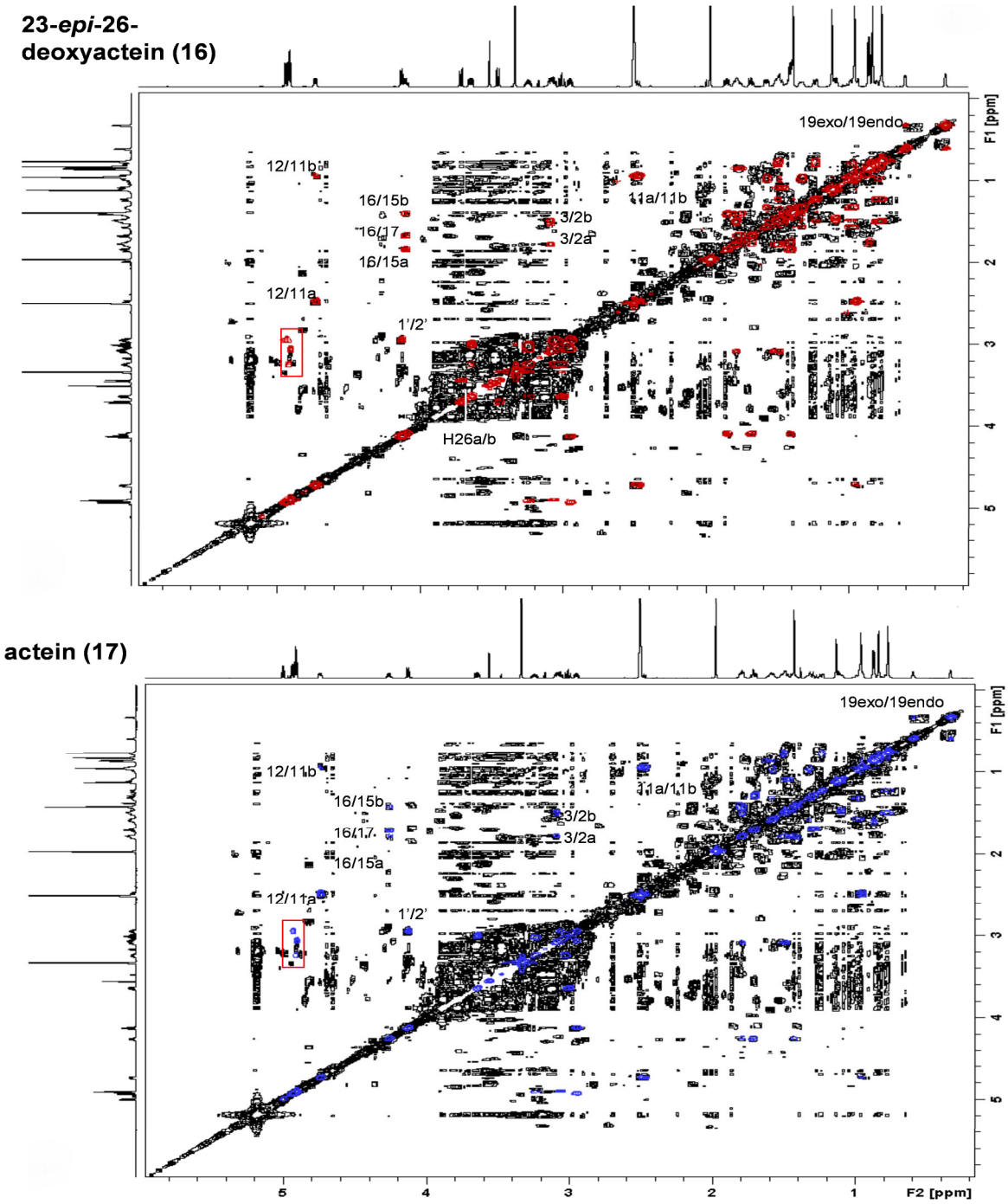

Figure 74. Identification of 23-*epi*-26 deoxyactein (16) and actein (17) by COSY as two of the major constituents of CRRR extract (BC036) 600MHz

COSY spectra of compound **16** and **17** are superimposed on a CRRR COSY spectrum, respectively. External projections are ^{1}H spectra of each reference compound. Cross peaks in the solid rectangle are OH-CH couplings.

Fingerprinting

The spectral patterns of A region were closely examined for 12 CR extracts (Figure 74). First, all of the RR samples have distinctive signals at 1.42 and 1.38 ppm, which correspond to the Me-27 singlets of compounds **16** and **17**, respectively. Due to a reasonable match of other methyl signals and COSY cross peaks, it was shown that all of the CRRR samples contained compounds **16** and **17**. In CRPX, a singlet at 1.42 ppm (Ab) was not clearly observed, which suggest that content of **16** is very low or absent. A singlet at 1.38 ppm, which is likely to be derived from Me-27 of compound **17**, was observed in four of the PX samples (BC624, 404, 582, 025). The presence of **17** in these four samples was supported also by COSY cross peaks. However, **17** was not observed in BC026 or BC027. Although the singlet at 1.38 ppm correspond to Me 27 of **17**, it should be noted that other compounds are likely to be contributing to its strong intensity, since its intensity is significantly stronger than the other methyl signals of **17**.

Despite the fact that corresponding compounds were not identified, other characteristic peak patterns in ^{1}H NMR spectra were examined. First, throughout all the samples, an acetyl singlet cluster in the sub-region 1.93-2.05 ppm, as indicated by a recutangular in Figure 75, was observed. Signals in this sub-region are more crowded in RR then in PX. For PX and RR differentiation, peaks at 1.42 (Ad) and 1.04 ppm (Ae) can be used, because they are insignificant or absent in PX extracts. On the other hand, peaks at 1.38 (Ab) and 1.23ppm (Ac) tend to be more significant in the PX extracts.

In the C region (Figure 76), three peaks were consistently observed in the RR samples: a doublet at 6.40 (Ca), a doublet at 6.52 (Cb), and a doublet at 6.75 (Cc) ppm. The doublets (Ca) and (Cb) have a roofing effect to each other suggesting that they are coupled to each other. The PX samples have more variations between them.

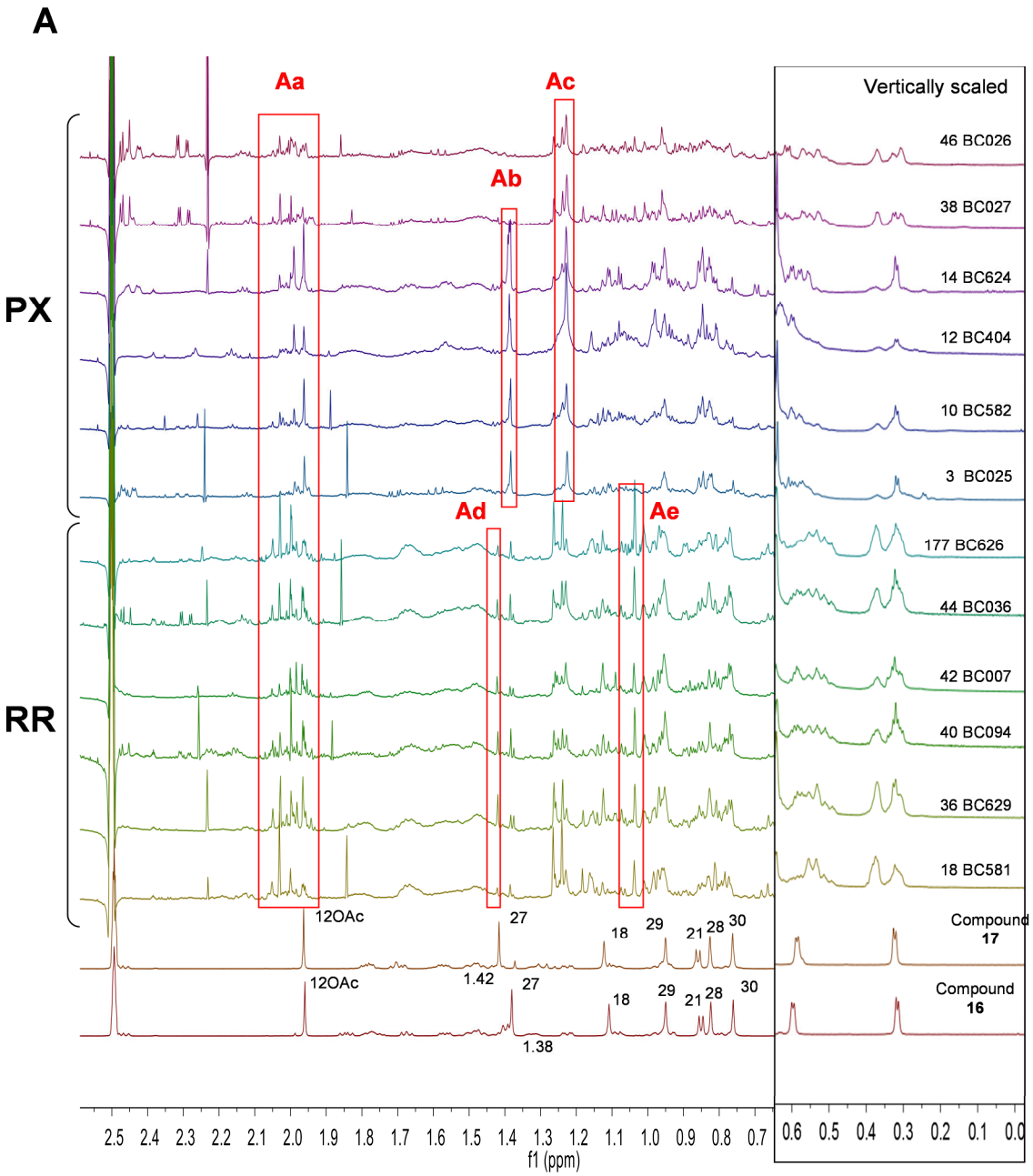

Figure 75. The expansion of A region in ^{1}H spectra of 70% aqueous MeOH extracts of *C. racemosa* 600MHz

Characteristic signal clusters Aa, Ab, Ac, Ad and Ae are marked and discussed in the main text. Expanded spectra were scaled accordingly.

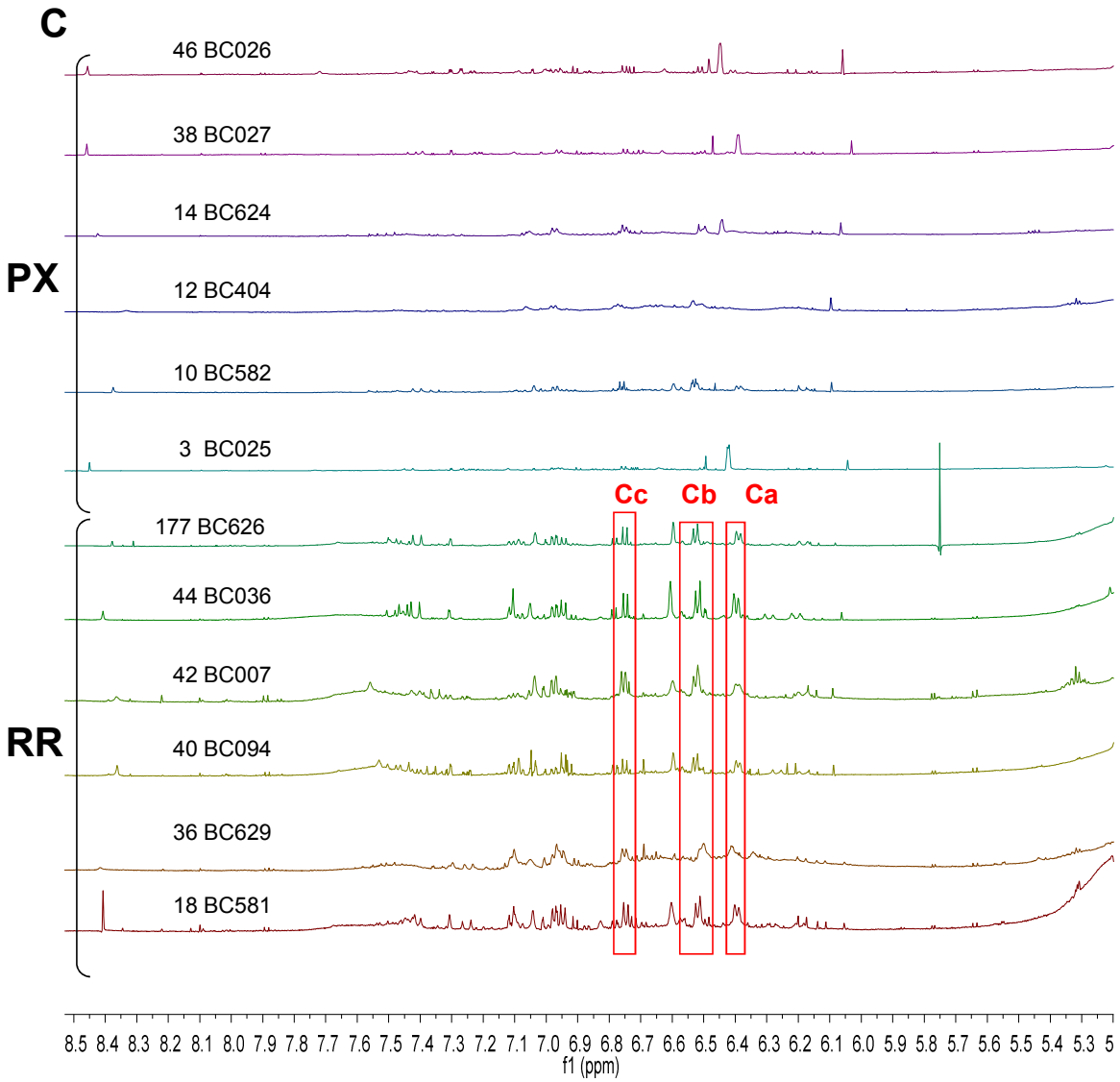

Figure 76. The expansion of the C region in the ^{1}H Spectra of 70% aqueous MeOH extracts of *C. racemosa* 600MHz

Characteristic signal clusters Ca, Cb, and Cc are marked and discussed in the main text. The spectra were scaled accordingly.

4.2.4 *Cimicifuga americana* Fingerprinting

In order to study this species, ^{1}H NMR spectra of three PX extracts and three RR extracts were obtained (Figure 77). The spectral patterns were consistent throughout all the samples within each plant part (PX vs. RR), even though the samples were obtained from different locations (Sevier County, TN., Swain County, NC. and Rockbridge County, VA.).

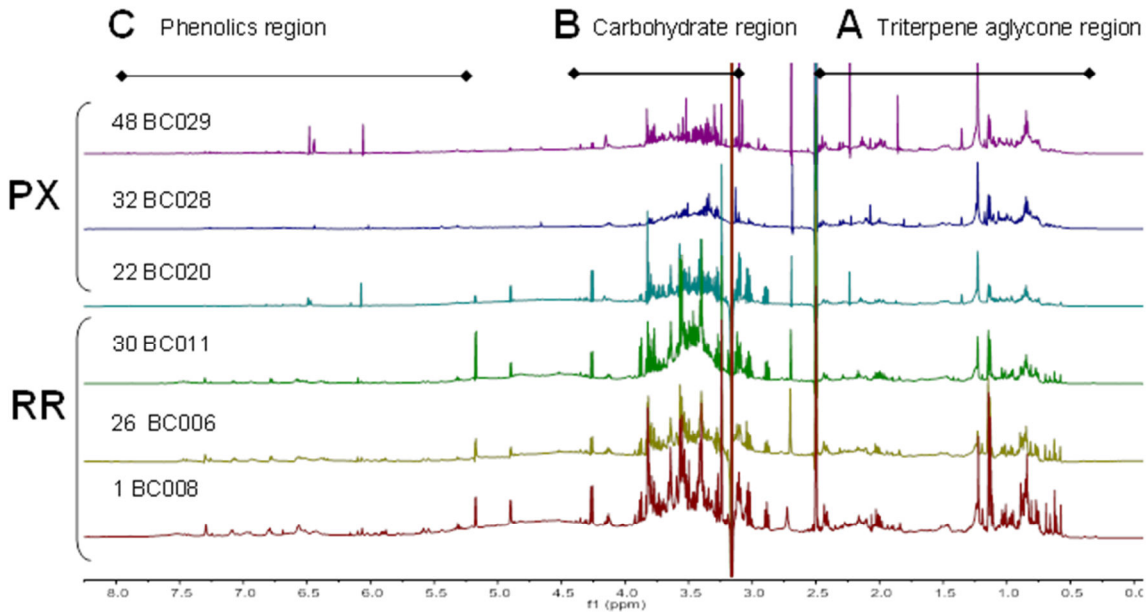

Figure 77. The ^{1}H spectra of 70% aqueous MeOH extracts of *C. americana* 600MHz
All spectra was scaled to the residual DMSO-d_5 peak.

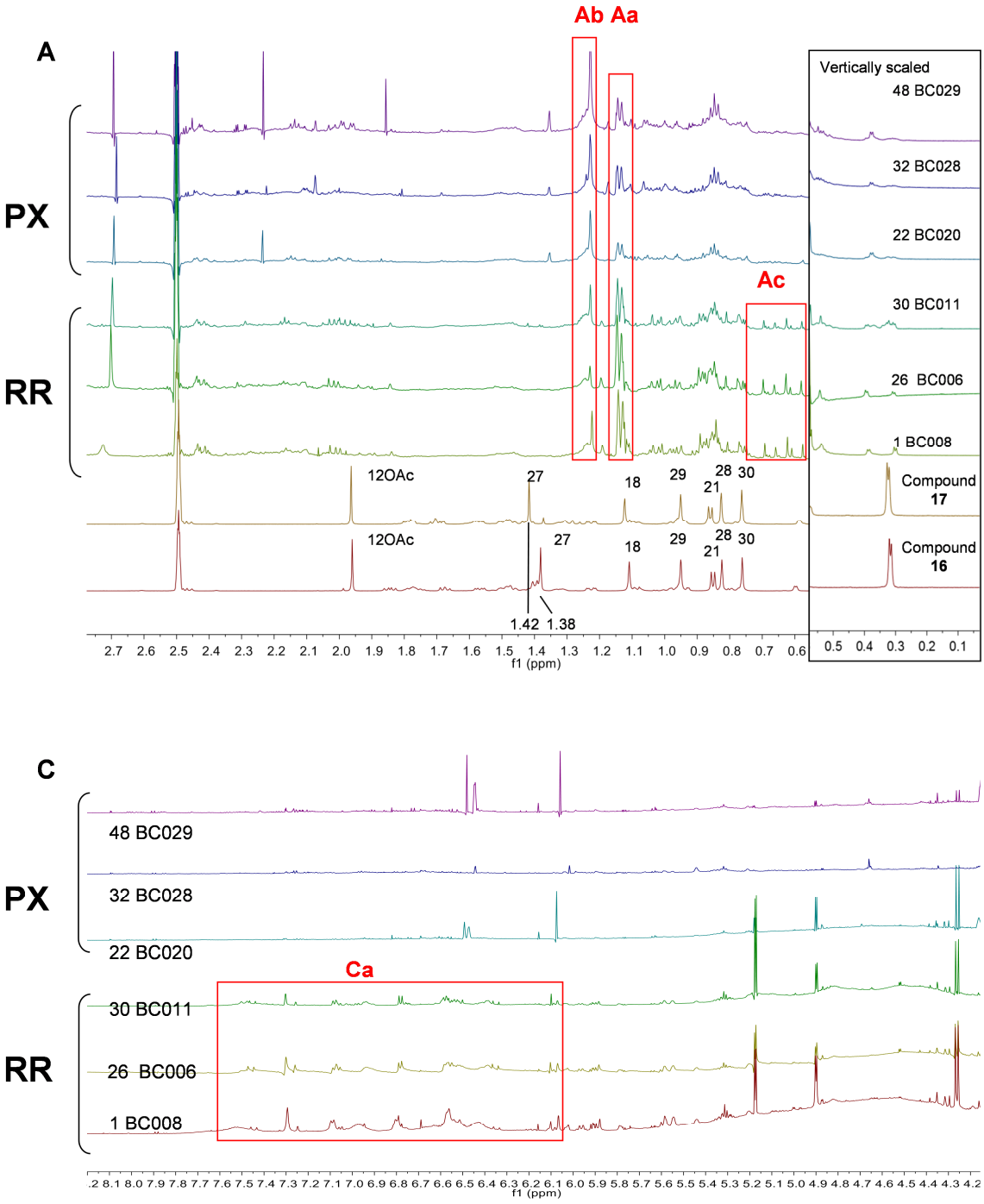

Figure 78. The expanded regions A and C of ^{1}H spectra of 70% aqueous MeOH extracts of *C. americana* 600MHz

Characteristic signal clusters Aa, Ab, Ac and Ca are marked and discussed in the main text. All spectra was scaled to the residual DMSO-d_5 peak.

The most characteristic pattern was observed in the 1.11 - 1.16 ppm sub-region (Aa) as “a pair of peaks” when resolution enhancement was done with routine parameters (EM, GB -0.3) (Figure 78). When the resolution of the spectrum was enhanced using different digitation parameters (GM, GB -3.0, GB 0.3) (Figure 79), it revealed that “a pair of peaks” was an overlap of signals, but it still needs to be examined if the line separation is associated with coupling constant or chemical shift. To examine this pattern, the ^{1}H NMR of one of the CARR samples, BC008, was measured at two different magnetic field at 400 MHz and the spectrum was compared with existing 600MHz spectrum. As a result, it was shown that distances between major peaks ($\Delta\delta$) are 5.8 Hz from the 400 Hz data and 8.8 Hz from the 600 MHz data, which is a 1.5 fold difference. Since the distance is field strength dependent, the line separation was deduced to be chemical shift. No strong couplings to these characteristic peaks were observed in a COSY experiment, which confirms that those signals are independent singlets. A large peak at 1.23 ppm (Ab) was observed in all of the CAPX and CARR extracts. In both PX and RR samples, only weak peaks were observed for the region below 0.42 ppm, suggesting that the cycloartane triterpene content of CA is relatively low. As discussed in 4.2.2, cycloartane triterpene contents were calculated as 23-*epi*-26-deoxyactein to be 2.5 % and 3.0 % in PX and RR, respectively, by the qHNMR method. Compared to CR and CU extracts, the cycloartane triterpene content of CA is significantly lower. When the PX and RR extracts were compared, the PX extracts lack some characteristic signal patterns that were present in the RR samples. Most notably, 5 sharp singlets between 0.56-0.71 ppm (Ac) and phenolic compound peaks between 5.2-7.2 ppm (Ca) were observed in all three RR samples.

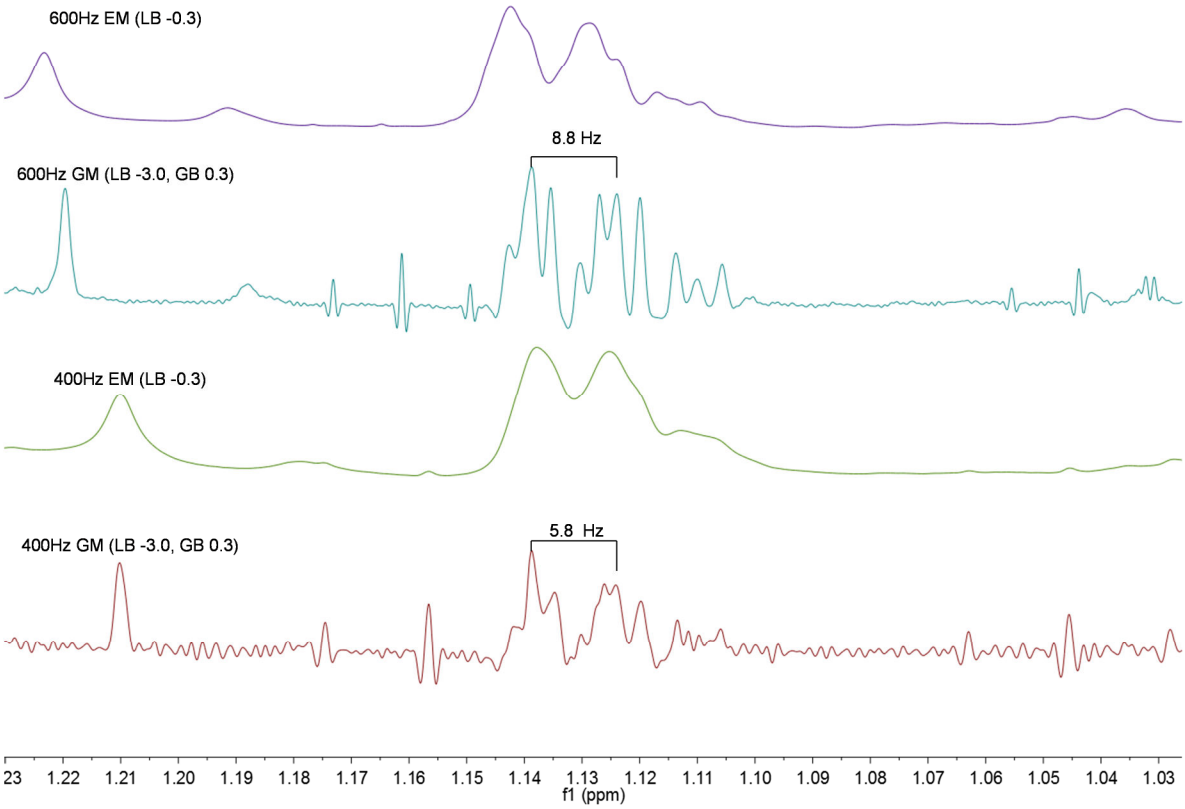

Figure 79. The detailed analysis of CARR fingerprint peaks (BC008) 600MHz

The ^{1}H NMR spectra of BC008 were obtained both at 400 Hz and 600 Hz instruments followed by two window functions (1); EM (LB 0.3), (2); GM (LB -3.0, GB 0.3).

4.2.5 *Cimicifuga rubifolia* Fingerprinting

The following data was collected by analyzing the ^{1}H NMR spectra of extracts of three RR samples and two of the PX extracts of *C. rubifolia* (CU) from plant material collected in Scott County, VA, in 1999.

The spectra were scaled to the intensity of the residual DMSO-d_5 (Figure 80). The expanded spectra are exhibited in Figure 81. As in the spectra of CR and CA, most signals were shown in B region (carbohydrate), followed by A region (triterpenes) and C region (phenolics). The relative triterpene content as measured by integration of both PX samples is lower than that of the RR samples.

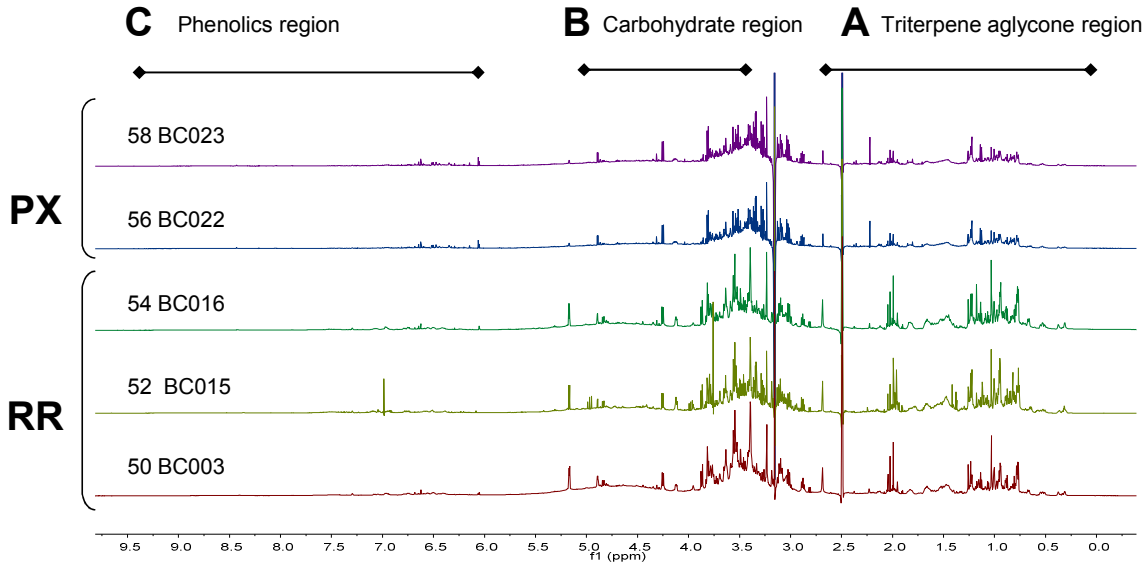

Figure 80. The ^{1}H spectra of 70% aqueous MeOH extracts of *C. rubifolia* 600MHz
All spectra was scaled to the residual DMSO-d_5 peak.

Some characteristic sub-regions were identified in the ^{1}H NMR spectra. In all of the spectra including PX and RR, several sharp signals are observed in the sub-region 1.93-2.05 ppm (Aa), which is populated principally by acetyl group signals. No significant peak at 1.96 ppm was observed in most of the extracts except for BC015. Since a sharp singlet at 1.96 ppm can be a 12-OAc signal of the reference compounds **16** and **17**, BC015 was checked for compounds **16** and **17** with other methyl signals in the ^{1}H spectrum as well as pertinent cross peaks in the COSY spectrum. Compounds **16** and **17** specific signals of 1.41 and 1.38 ppm were clearly observed along with another five methyl groups in a crowded region. The COSY spectrum of BC015 showed key cross peaks from both **16** and **17**, such as H-16/H-15a, H-16/H-15b, and H-16/H-17 as shown Figure 81. In contrast, the COSY spectrum of BC016 is missing cross peaks from H-12/H-11ab and H-16/H15ab, and **17**. Cross peaks from H-1'/H-2' and H-3/2a&b were also observed in BC016, which is consistent, because a 3-*O*-xylopyranoside moiety is not unique to compounds **16** and **17**. From both ^{1}H NMR and COSY examination, BC015 most likely contains the compounds **16** and **17**. However, other CU samples clearly did not show the existence of **16** and **17**. According to a NAPRALERT database search, there are only two reports on CU compounds and compounds **16** nor **17** have not been previously reported (46,88). Further research is necessary to determine the presence of **16** and **17** in CU.

In terms of differentiation between RR and PX, diagnostic peaks were suggested for each group. A sharp singlet at 1.03 ppm (Ac) is distinct in all of the RR extracts. The same pattern was observed in CRRR as well, but not in CRPX. The PX samples have two sharp peaks at 1.13 and 1.14 ppm (Ab). The most prominent difference between RX and RR in the C region is the cluster of signals between 6.3-6.7 ppm (Ca).

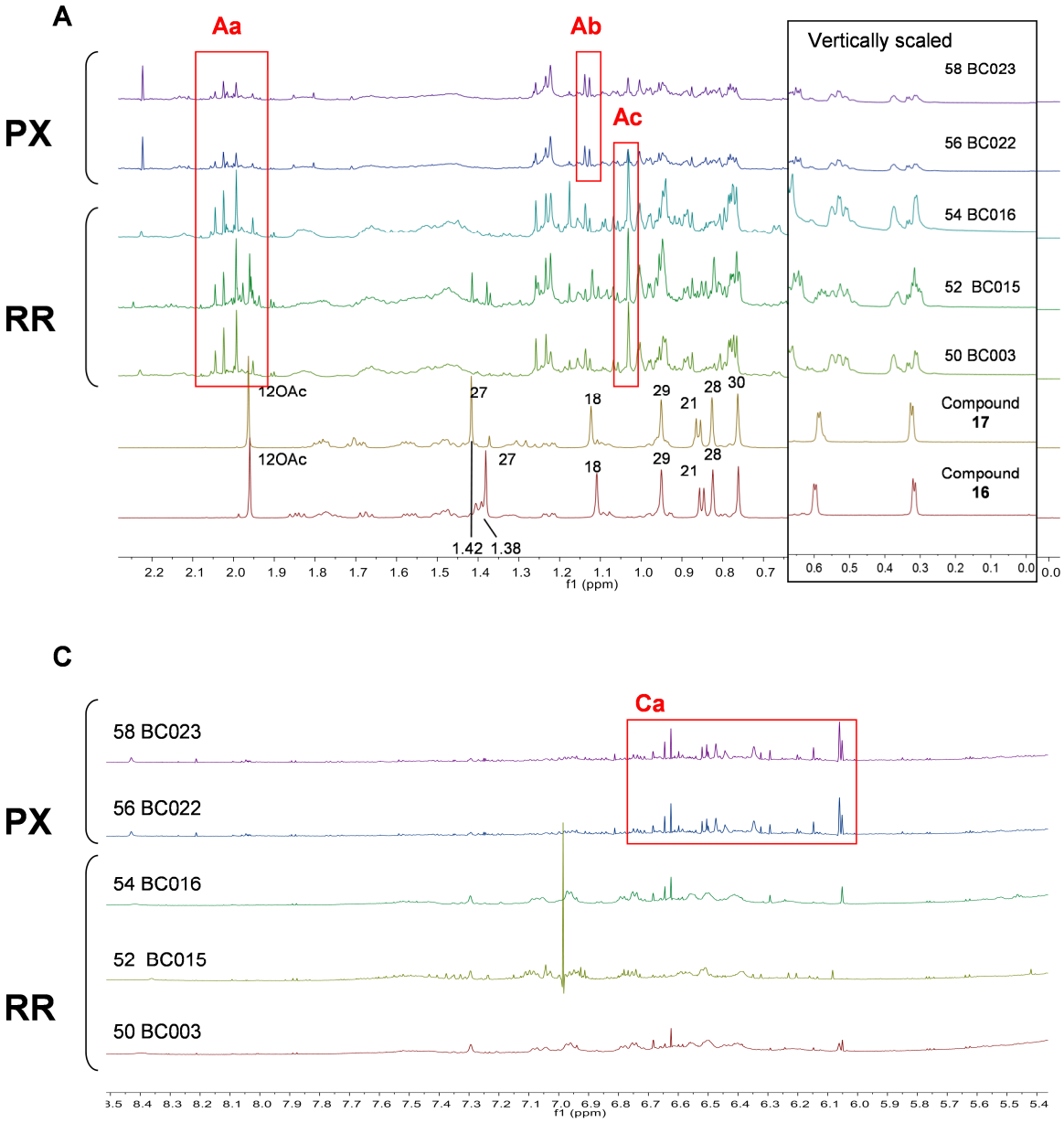

Figure 81. The expanded regions A and C of 70% aqueous MeOH extracts of *C. rubifolia* 600MHz

Characteristic signal clusters Aa, Ab, Ac and Ca are marked and discussed in the main text. All spectra were scaled to DMSO-d_5 peaks.

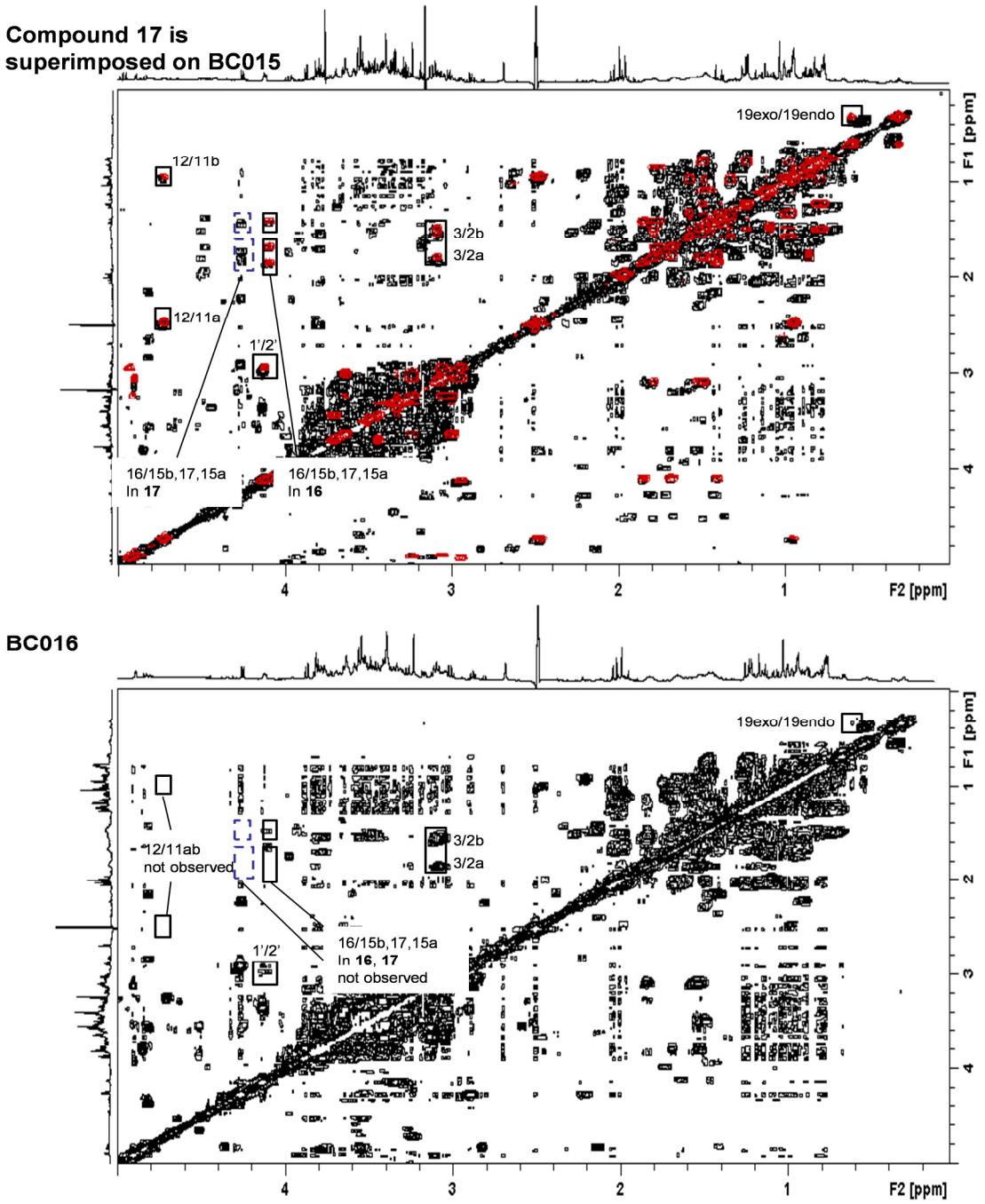

Figure 82. Identification of 23-*epi*-26 deoxyactein (16) and actein (17) in CURR extracts (BC015 and BC016) 600MHz

Characteristic cross peaks of **16** were identified in BC015. Compound **17** and **16** share cross peaks except H-16/H-15a, H-16/H-15b, and H-16/H-17 . Compound **17** specific cross peaks were also identified. In BC016, characteristic peaks were missing in the expected region represented in the rectangles.

4.2.6 *Summary of NMR fingerprinting of American Cimicifuga Species*

For three American species, spectra for a total of 23 samples were obtained and their characteristic peaks were discussed in the previous section. To simplify the comparisons between the six groups of *Cimicifuga* species, a sum of ^{1}H spectra within each group was assembled using Bruker Topspin software (Figure 83). In this section, the key spectral patterns for the identification of species/parts are summarized.

- CA samples may be distinguished from both CR and CU by strong indicator peaks at 1.11 - 1.16 ppm (Aa). A lack of acetyl groups can also be an indicator for CA.
- Triterpene patterns of CU and CR are particularly similar. The reference compounds **16** and **17** were identified in all of the CRRR extracts, but only in one of the CU extracts. This observation needs separate follow-up for further investigation.
- A possible indicator peak at 1.03 ppm (Ad) to distinguish between RR and PX in CR and CU was identified.
- Across all of the species, RR has more carbohydrate content than PX. Especially peaks at 3.24, 3.40 3.55, and 3.57 are prominent in the B region of the spectra of RR extracts.

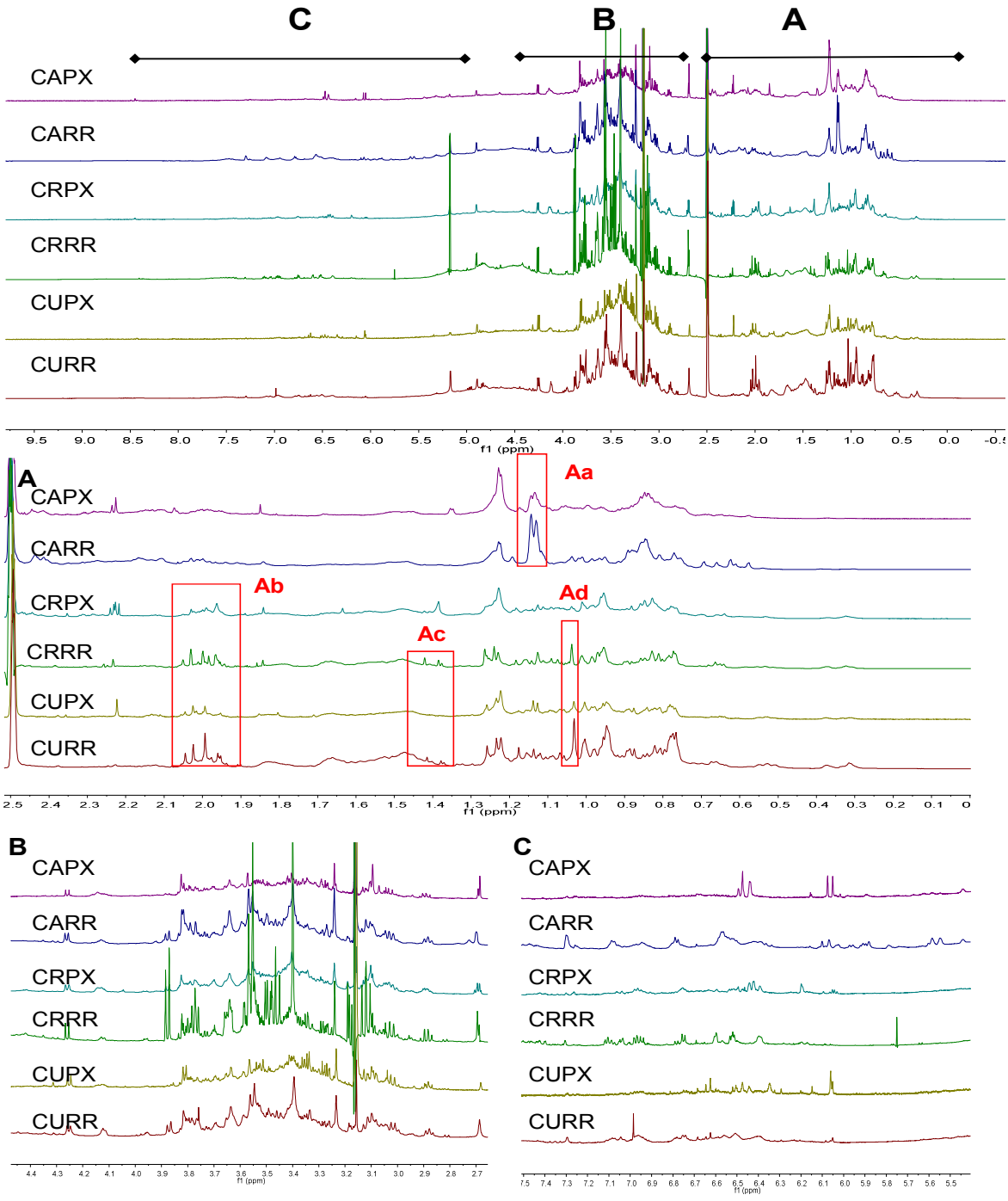

Figure 83. The sum of ^{1}H spectra of *Cimicifuga* species extracts 600MHz

Expanded triterpene region (A), carbohydrate region (B) and phenolic region (C) are shown along with the stacked whole spectra. Characteristic signal clusters Aa, Ab, Ac, and Ad are marked and discussed in the text. All spectra were scaled to the residual DMSO-d_5 peaks

4.2.7 *Asian Species*

In addition to three American species, NMR profiles were obtained for four Asian *Cimicifuga* species, namely: *C. heracleifolia* (CH), *C. japonica* (CJ), *C. acerina* (CE), *C. simplex* (CS). All of the samples predominantly contained carbohydrate signals, but also corresponding signals for triterpenes and phenolic compounds. The spectra of Asian species are shown in Figures 84 and 85, along with sum of the spectra from the American species. It is noteworthy that prominent cycloartane methylene signals were observed in all of the Asian samples in the 0-0.62 ppm interval. Fingerprint characteristics of each species are not described here, mainly because there was an insufficient number of samples for each species. However, the spectra of Asian species were examined in order to differentiate them from the American species, especially *C. racemosa*. Most of the samples exhibited a cluster of acetyl methyl signals. Indicator signals for compounds **16** and **17** (1.38 and 1.42 ppm, Aa in Figure 85) were not distinctively observed in most of the Asian *Cimicifuga* extracts, except in one sample of CSRR (BC587). The COSY spectrum of BC587 did not show distinguishable cross peaks for actein type compounds and the other CSRR (BC393) did not exhibit these indicator signals in their ^{1}H spectra. Although comprehensive NMR data analysis (^{1}H/COSY of BC587 and BC393) failed to detect the existence of **16** and **17** in this study, it is possible for CSRR to contain **16** and **17**, since they have been isolated from CS before by Koeda *et al.* (89). The reported yields of **16** and **17** from CSRR were 0.08 and 0.01%, respectively. More investigation is necessary to determine the existence of **16** and **17** in CSRR. Extracts with a strong signal at 1.03 ppm (Ab) tend to be from RR. The compound, which gives rise to this characteristic signal has not been identified. This would be a worthwhile aim of a future project.

,

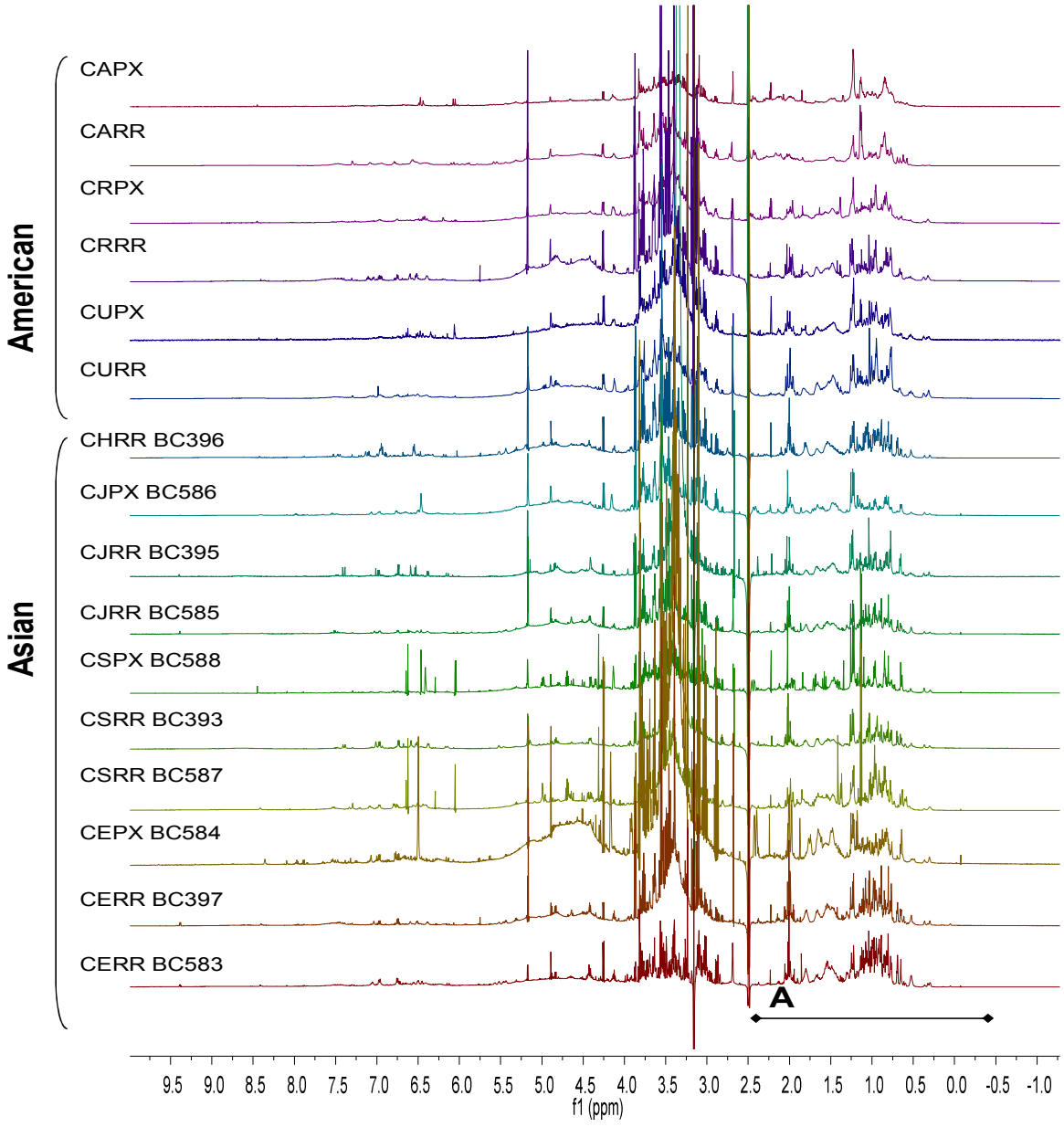

Figure 84. Full ^{1}H NMR spectra of Asian species along with sum of American species 600MHz

All spectra were scaled to residual DMSO-d_5 peak.

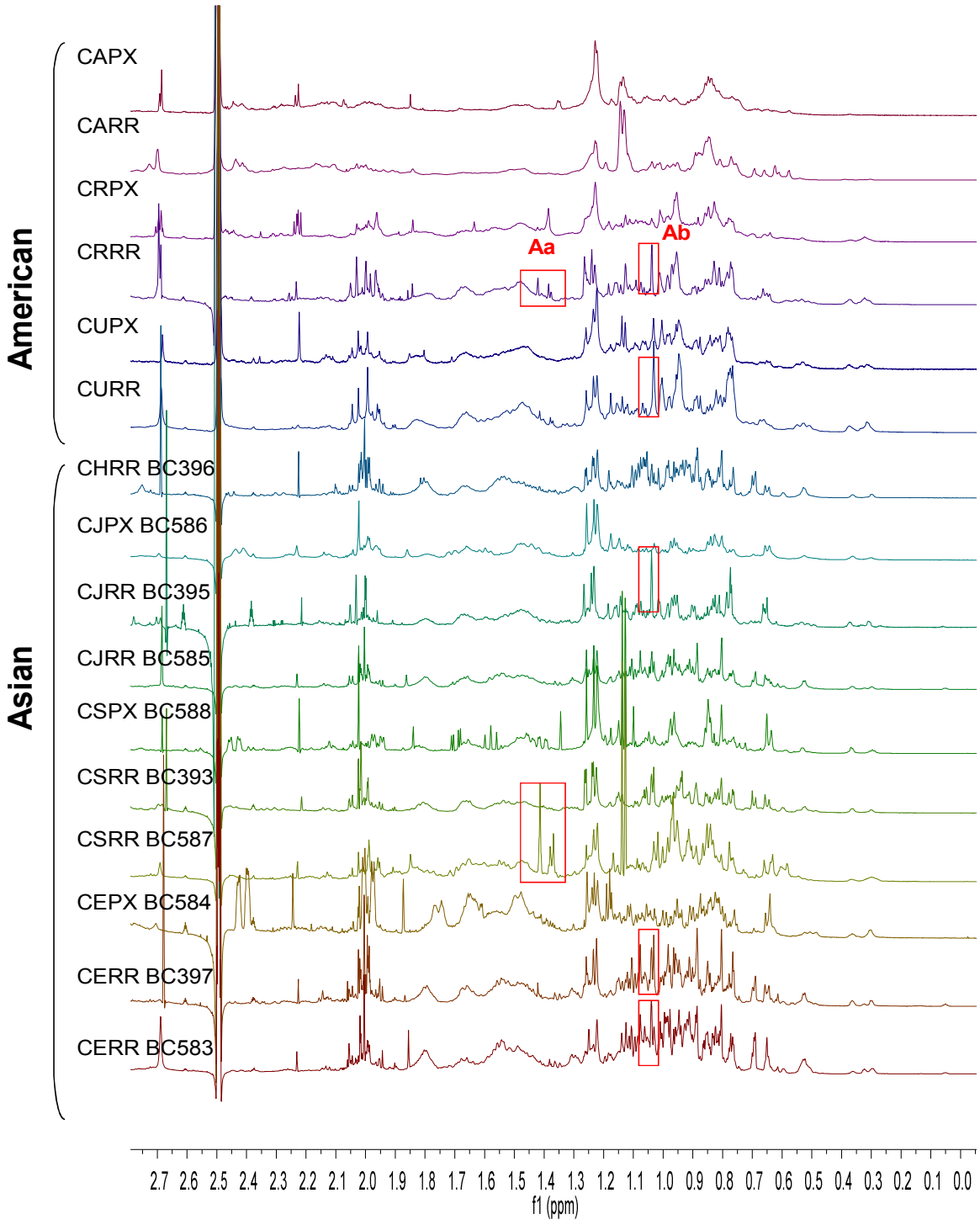

Figure 85. A region of Asian species along with sum of American species 600MHz

All spectra were scaled to the residual DMSO-d_5 peak. Regions/ peaks marked with Aa and Ab are discussed in the main text.

4.2.8 *Solvent Effects*

An extract, BC036, that showed a typical CRRR ^{1}H NMR pattern in DMSO-d_6 was dissolved in pyridine-d_5 and the 1D ^{1}H and 2D COSY NMR spectra were acquired at 600 MHz (Figure 86). The pyridine-d_5 extract was prepared in the same manner as was described for the DMSO-d_6 sample.

As previously mentioned, the ^{1}H spectrum of the DMSO-d_6 sample exhibits A, B and C regions covering the three major classes of compounds, such as triterpenes, carbohydrates, and phenolics. However, the pyridine-d_5 spectrum of the same sample has triterpene and carbohydrate signals but only a trace of signals associated with the phenolic compounds. Moreover, the residual solvent peaks in pyridine-d_5 and their respective ^{13}C satellites appear in the same region as the phenolic peaks and partially overlap with them. DMSO-d_6 solvent peak appears at 2.500 ppm in a less crowded spectral region. The DMSO-d_6 is shown to be a more efficient solvent for the *Cimicifuga* metabolomic studies of species for three reasons, 1) it dissolves the three known major classes of *Cimicifuga* compounds, 2) the residual solvent peak does not overlap significantly with peaks of interest in the spectrum; and 3) DMSO-d_6 is a near-universal solvent and possibly dissolves additional compounds.

Although triterpene skeletal signals appear in the same range (0.5 ppm – 2.5 ppm) of both DMSO-d_6 and pyridine-d_5 spectra, the carbohydrate signals are clearly affected by the solvent. The carbohydrate signals in pyridine-d_5 are shifted about 1.2 ppm downfield compared to their position in DMSO-d_6. The ^{1}H resonances of the carbohydrate fall in the range of 3.0 - 4.0 ppm in DMSO-d_6 vs 4.2 - 5.2 ppm in pyridine-d_5.

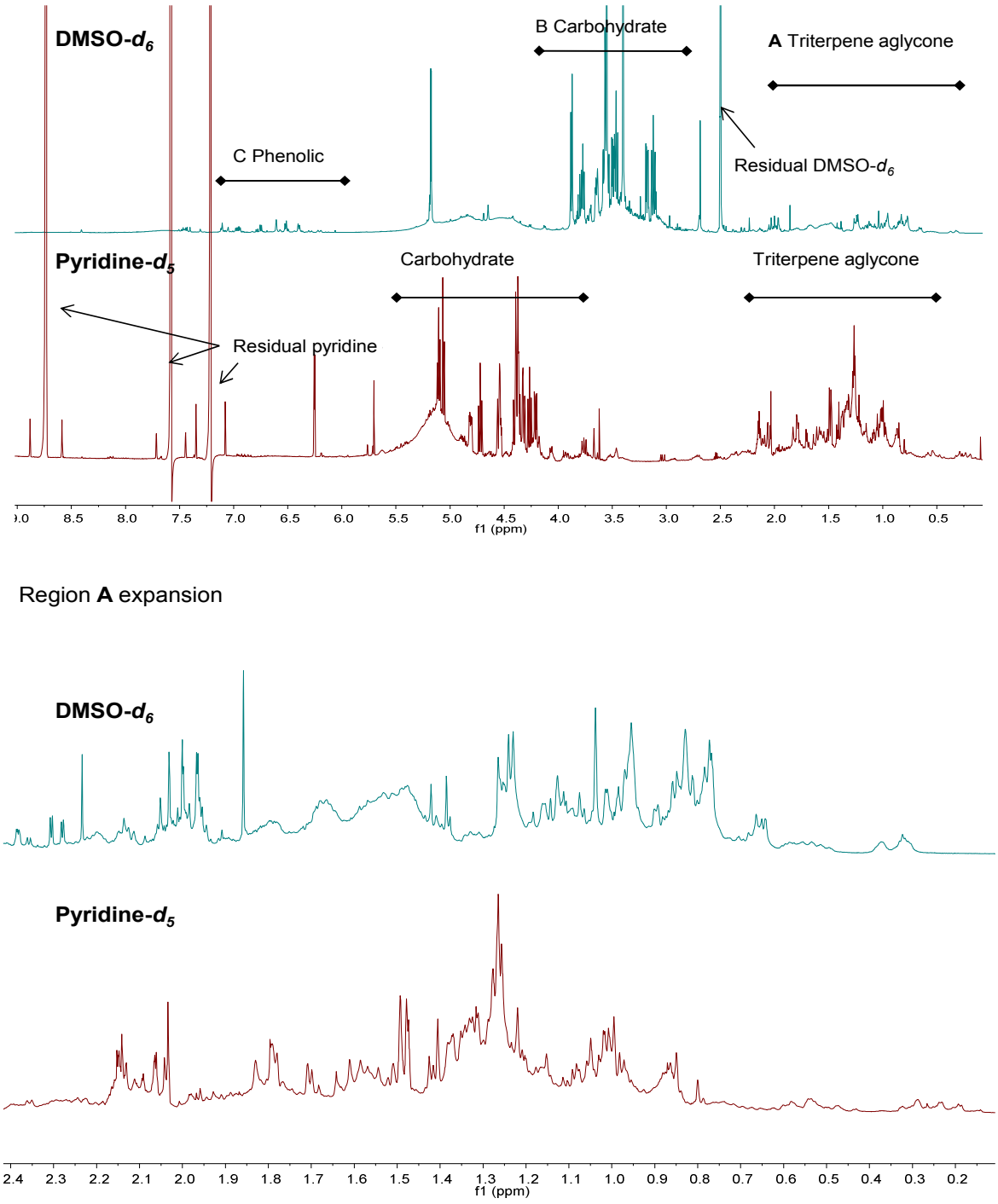

Figure 86. Comparison of CRRR BC036 spectra in DMSO-d_6 and pyridine-d_5 600MHz

Top spectra are in DMSO-d_6, Bottom spectra are in pyridine-d_5 in both whole spectral view and expanded view. Digitization was as follows: GM (LB -1.0 Hz, GB 0.1).

Although two of the major cycloartane triterpenes (**16** and **17**) were successfully identified in DMSO-d_6 by comparison of ^{1}H and COSY spectra, pyridine-d_5 is more practical since the vast majority of NMR data for these compounds has been reported in this solvent. Here, the ^{1}H NMR spectra of twelve isolates from the CRPX (Chapter 3) were used as reference to identify compounds in the extract (Figure 87). An equimolar sum of twelve isolates was exhibited as well. Two predominant signals around 1.45-1.55 in the extract share the same chemical shift with Me-26, 27 signals of compound **3** and **4**, which are 1α-hydroxycimigenol 3-*O*-α-L-arabinopyranoside and 1α-hydroxycimigenol 3-*O*-β-D-xylopyranoside. Even though other methyl signals could not be clearly identified in the extract, this characteristic pattern is possibly attributed to Me-26 and Me-27 of 1α-hydroxycimigenol type of compounds (Aa sub-region in Figure 87). A cluster in Ab sub-region of the CRRR is observed similar to the same region of the equimolar mix of the isolates, which are an accumulation of Me-21 signals of cycloartane triterpenes.

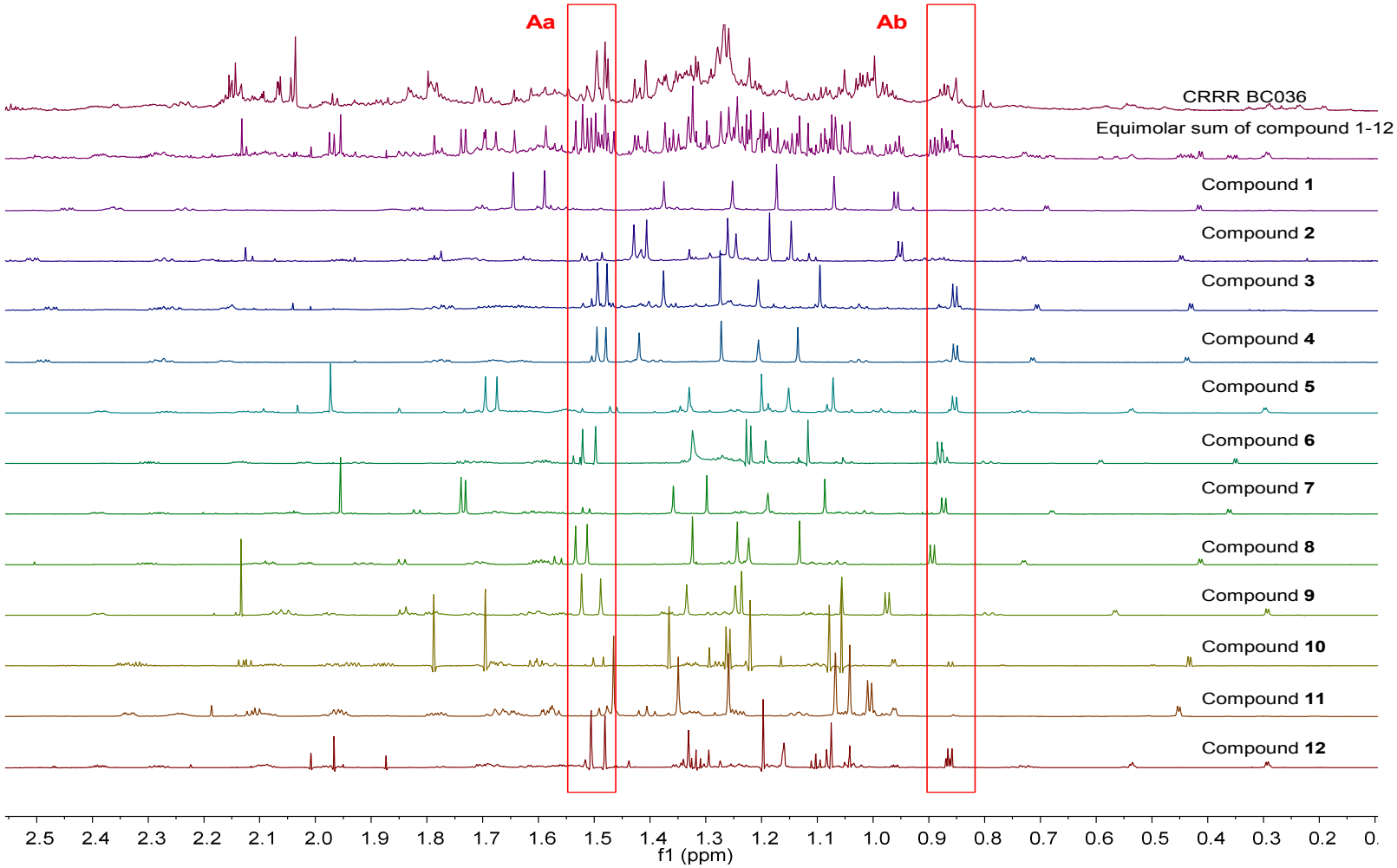

Figure 87. CRRR (BC036) extract spectra along with spectra of reference compounds 900 MHz

Chemical shifts were calibrated to 7.217 ppm for the residual protonated species of pyridine-d4. Digitization was as follows: GM (LB -1.0Hz, GB 0.1). Aa sub-regions contain Me-27 and Me-27 of 1α-hydroxycimigenol type compounds. Ab sub-region contain Me-21 peaks

4.2.9 *Chemometric Analysis of the ^{1}H NMR Metabolomic Fingerprints of Cimicifuga species*

The ^{1}H NMR fingerprint patterns of several American *Cimicifuga* species were observed and discussed in the previous sections. In the case of CR vs CA, using both the qualitative + semi-quantitative visual interpretation, such as identification of compound **16** and **17** and analysis of triterpene content, it is already possible to differentiate samples of species + plant parts. However, it is still likely that subtle lines of demarcation are overlooked by this method. The more complex case is CR vs CU. Due to the apparent similarity of their spectra, it is difficult to identify marker peaks or pattern through visual examination. Therefore, a statistic method, Principal Component Analysis (PCA), was chosen as a next logical step to allow differentiation between the more similar spectra.

As considered in sections 4.2.3 to 4.2.5, the composition of the triterpene fingerprint region was relatively consistent within a specific plant + plant parts group. This suggested that the spectral region between 0.0 and 1.8 ppm is a good candidate data for targeted metabolic fingerprinting by PCA analysis.

The ^{1}H NMR spectra of PX and RR extracts of three American *Cimicifuga* species were examined using AMIX NMR Statistics software, with a total of 23 spectra in a bucket table. Pointwise bucketing led to the definition of 7872 buckets for each spectrum between 0-1.8 ppm. This is equivalent to 43 or 44 buckets for every 0.01 ppm-interval of the ^{1}H NMR spectra. PCA of this extensive bucket table revealed that 95.9 % of the total variance could be explained by eight principal components/ explained variance. As shown in the influence plot (Figure 88), all of the 23 spectra were within the model space.

Plotting PC1 vs PC 2 explained 76.0 % of the total variance (Figure 89). By looking into 2-dimensional sub-spaces in Figure 89 (PC1 vs. PC2), it becomes evident that the spectra of the same species occupy similar positions (scores) with respect to the corresponding part of the variance. The corresponding variance can be seen in the 2D loadings plot: Both RR and PX of CA spectra are found on the left side of the scores plot. On the 2D loadings plot, it is shown that the buckets that are contributing to the CA cluster were buckets at 1.14, 1.13, and 1.15 ppm, which match with the CA-characteristic fingerprint signals discussed in section 4.2.4 (Aa sub-region in Figure 78). CU spectra are clustered at the top of the scores plot. While distribution of CRRR overlaps with CUPX 58 and 56, there is still a trend for the CURR samples above the CUPX samples. Specific buckets that allow direct differentiation between CU and CR were not identified, but it is reasonable to conclude that PC2 contributes to their differentiation. PC3 explains 7.64 % of the total variance. In general the PC1 vs. PC2 plot (Figure 89) shows better separation between species or plant parts than the PC2 vs. PC3 plot (Figure 90), except for CA species. Although CARR and CAPX are plotted in a similar area in the PC1 vs. PC2 plot, the separation between the two groups is clearer in the PC2 vs. PC3 plot. On the PC3 axis, the most predominant buckets are CA characteristic buckets of 1.13, 1.14 and 1.15 ppm.

In the previous sections, visible fingerprinting peaks or signal patterns were identified. After PCA, the buckets that include the fingerprinting peaks were conspicuously plotted in the edge of the 2D loadings separated from the crowd of buckets, such as 1.13-1.16 ppm for CA and 1.04 ppm for CRRR and CURR. Upon visual examination, it is difficult to account for the numerous but relatively small peaks. However, the PCA method includes all of the buckets of the entire spectra, including prominent fingerprinting peaks.

Buckets, which only a statistical method can take into account, are shown as a cluster in the 2D loadings plot (marked as PCA-only region in Figure 89). In other words, the outer area of the 2D loadings is a fingerprinting region and the center of the 2D loadings is the PCA-only region.

When plotting the same datasets with different groupings of PCs (Figure 90, PX samples with dotted and RR with solid lines), there is differentiation in the PX and RR with minimal overlap regardless of the species. PC2 remains a main contributing variant for this differentiation.

As shown by this data, PCA of ^{1}H NMR spectra of crude extracts is a useful method for a metabolomic approach to the botanical distinction of *Cimicifuga* species and/or plant parts. Though this approach does not require identification of phytoconstituents of the observed signals, it can be very useful to suggest the key peaks, with a potential to identify target specific compounds and can serve as marker compounds for ^{1}H NMR PCA-based quality control of *Cimicifuga* botanical preparations as principal component contributors.

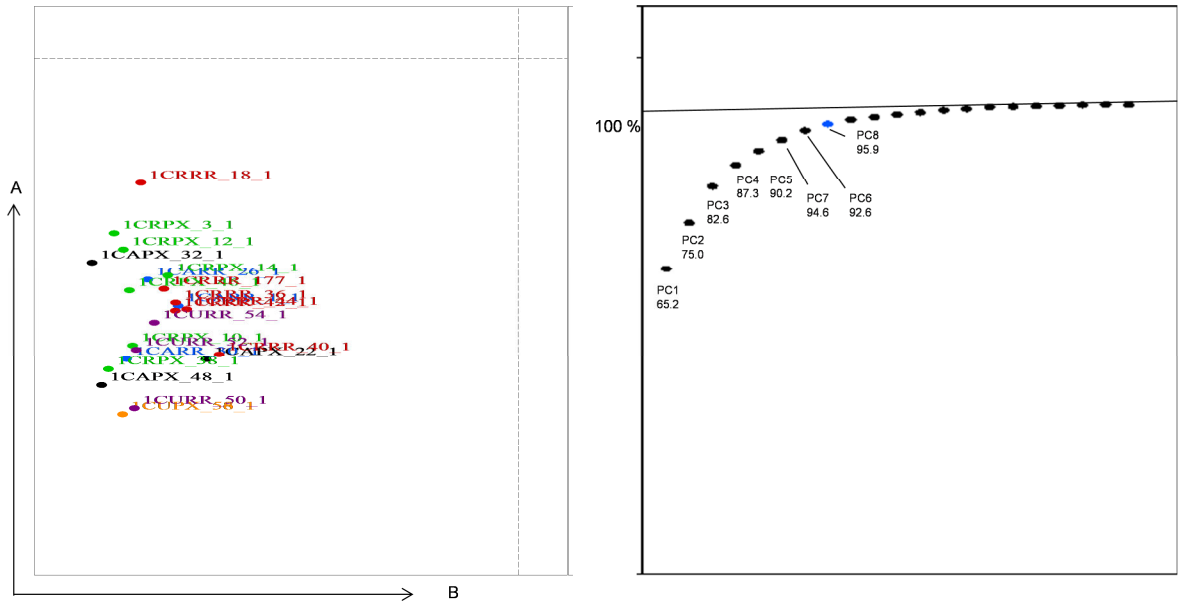

Figure 88. Influence (left) and explained variance plots (right)

Influence plot: A axis is a measure how far away a spectrum is from the model space. B axis is a measure how far away a spectrum is from the model center after being projected into the model space. The 2 dotted lines displayed inside the plot are 95 % confidence limits. Spectra inside these limit belong to the model with a probability of 95%.
Explained variance: Shows how the cumulative explained variance gets larger as the number of the PCs increases (horizontal axis).

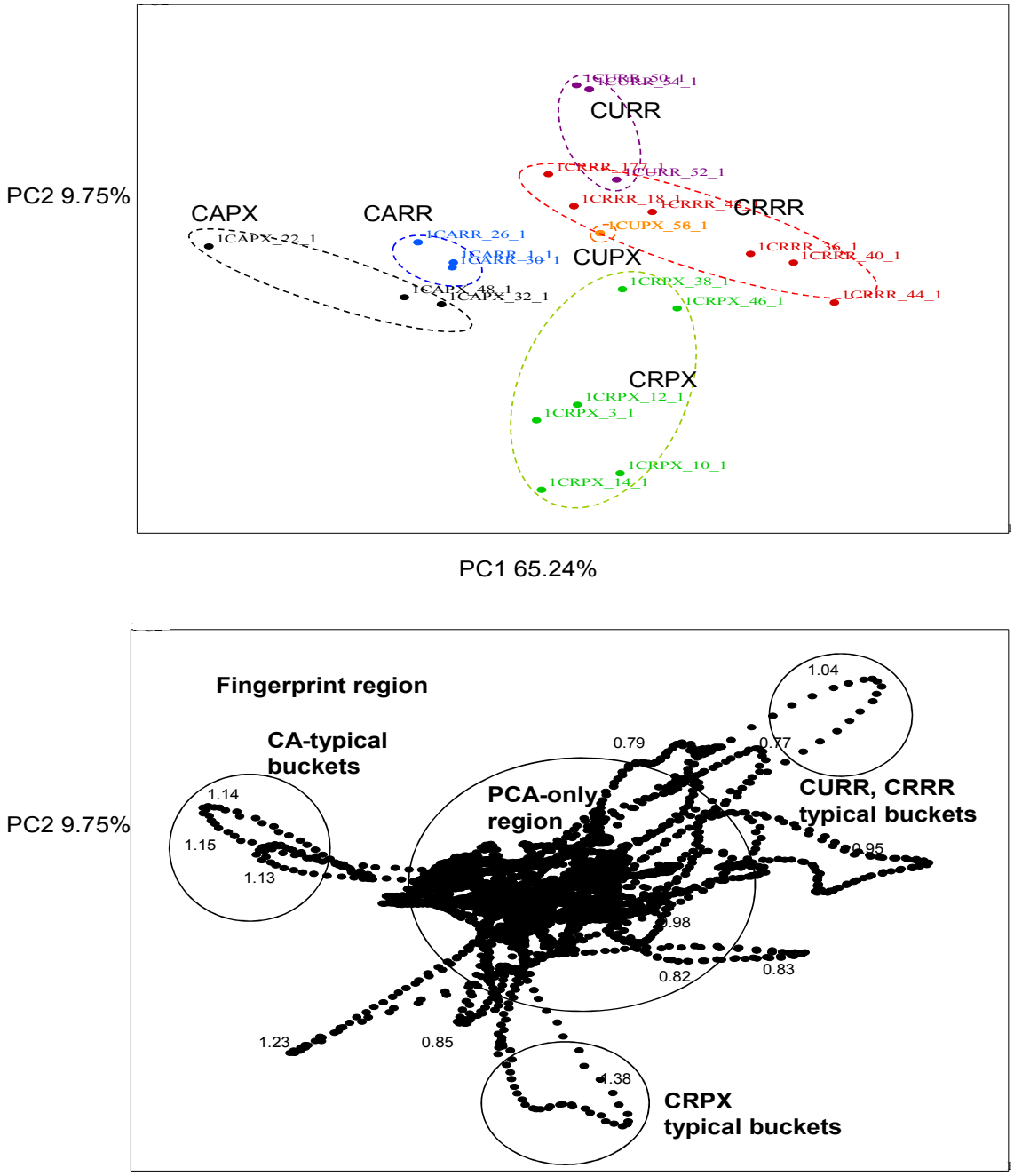

Figure 89. Scores (top) and 2D loading (bottom) plots derived from *Cimicifuga* ^{1}H NMR spectra (PC1 vs PC2)

Separation in six plant groups is observed in score plot. Loading plot shows how buckets contributed to the construction of the principal component space. Edge of the space represents fingerprint region, representing typical buckets for each group. The center of the plot is PCA-only region, which is discussed in text.

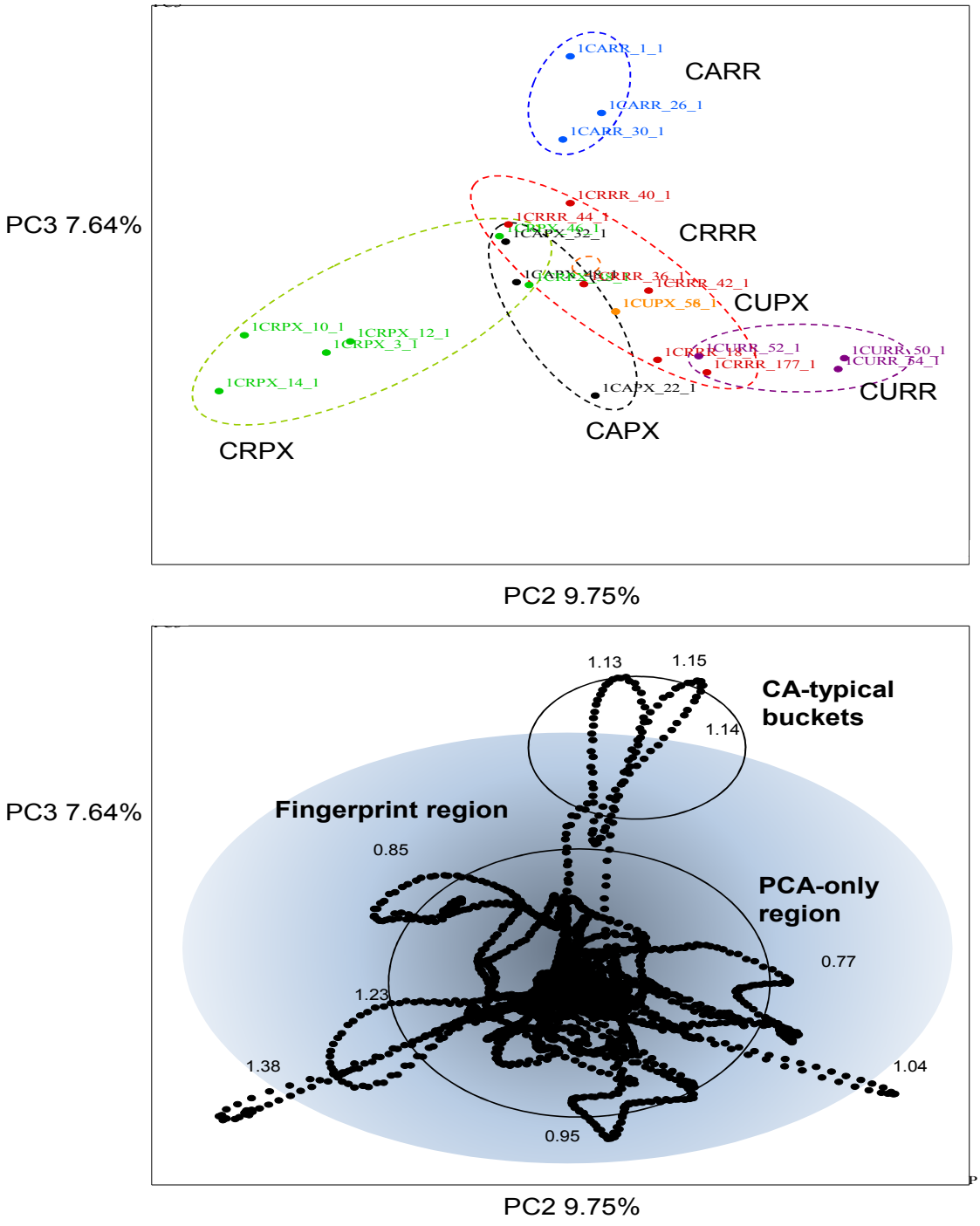

Figure 90. Scores (top) and 2D loading (bottom) plots derived from *Cimicifuga* ^{1}H NMR spectra (PC2 vs PC3)

Clear separation of CARR was observed. Loading plot shows how buckets contributed to the construction of the principal component space.

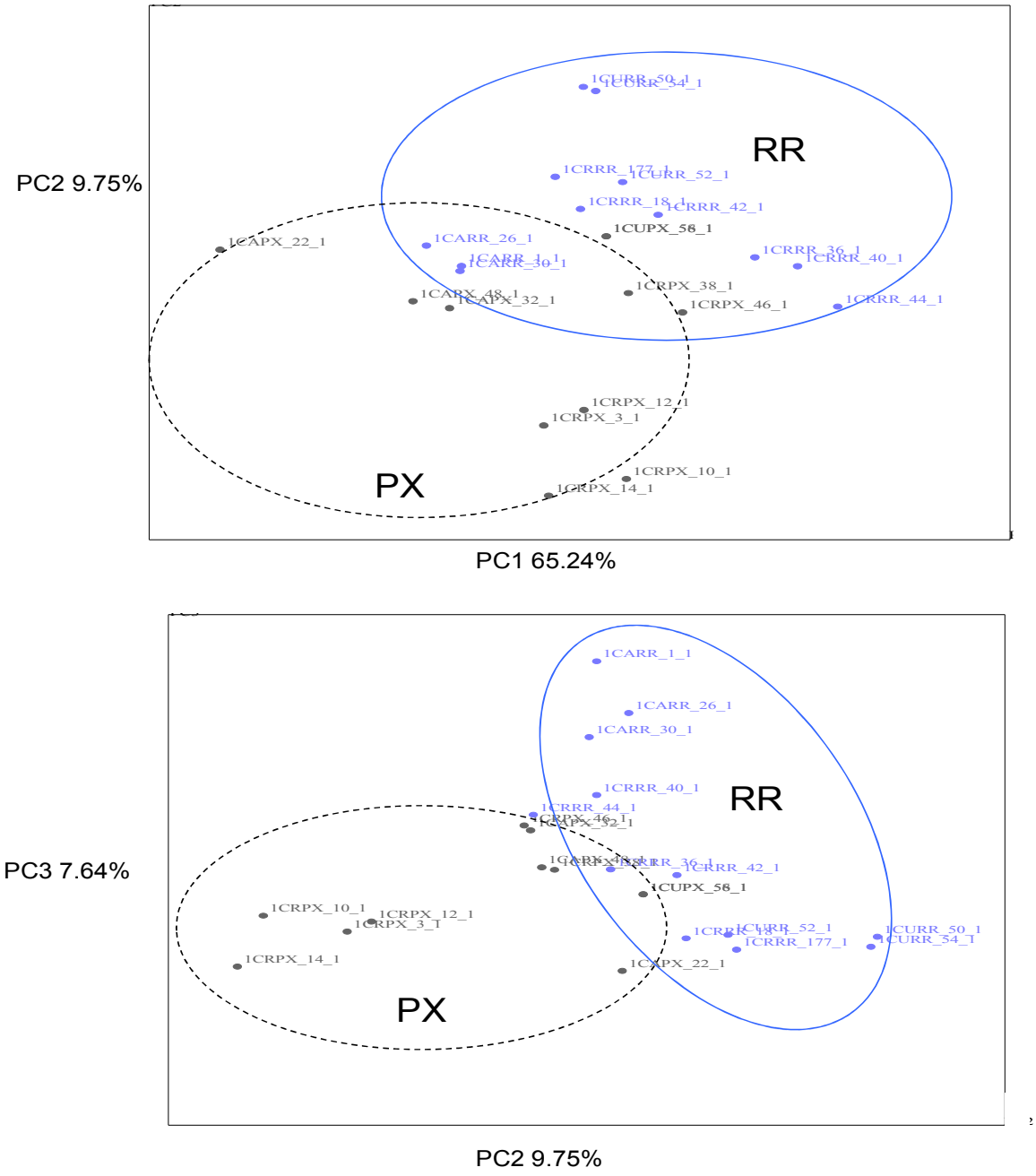

Figure 91. Scores plot of PC1 vs PC2 and PC2 and PC3 derived from *Cimicifuga* ^{1}H NMR spectra

PX (black dotted line) samples and RR (blue solid line) samples are plotted in PC1-PC2 space and PC2-PC3 spaces. In both space, it is represented that PC2 is contributing the most to the differentiation of PX and RR.

4.3. *Summary of Results from Aim 2*

^{1}H NMR spectra of crude extracts from a total of 34 *Cimicifuga* plant samples were obtained and analyzed for their species -and plant part- specific metabolomic characters by 1) quantitation of cycloartane triterpenes by qHNMR 2) Identifying fingerprint peaks by both observation and using reference compounds, 3) Metabolic fingerprinting by PCA. The main study subjects were the roots/rhizomes (RR) and aerial parts (PX) of three American species, *C. racemosa* (CR), *C. americana* (CA) and *C. rubifolia* (CU). Quantitative analysis method using ^{1}H NMR spectra was presented in this section and revealed that CA contains less cycloartane triterpenes than CR and CU. There is a tendency for RR to contain more cycloartane triterpenes than PX. Qualitative analysis was carried out and fingerprint peaks were described. CA exhibited a distinctly different chemical profile and strong indicator peaks were identified for this species. CR and CU were shown to have similar ^{1}H spectral patterns that are not easily distinguished without a statistical method. The presence of 23-*epi*-26-deoxyactein (**16**) and actein (**17**) remain unclear as a diagnostic character for CRRR. In all CRRR extracts, **16** and **17** were identified in the extract by comparison with previously isolated compounds as standards. However those reference compounds were likely to be in one other sample (CURR BC015). Several characteristic peaks and peak pattern were discussed for each group of samples.

After quantitative and qualitative analysis, a statistical method using PCA was employed to provide the metabolomic profile for visually minor but statistical significant differences. PCA scores allowed differentiation between the three American *Cimicifuga* species, as well as the ability to differentiate between PX and RR plant parts.

Overall, metabolomic fingerprinting of botanical extracts by 1D ^{1}H NMR is proven to be a useful technique to 1) identify a particular *Cimicifuga* species, 2) distinguish between

roots/rhizomes (RR) and aerial parts (PX) extracts of a given species, 3) differentiate between all major *Cimicifuga* species currently marketed or of relevance, 4) identify the presence of a particular compound in a crude extract.

5. **Aim 3 Biological Assessment of CR Aerial Parts**

CR is one of the most intensely studied botanicals for alleviation of menopause. Since menopause is a complex condition, various bioassays have been conducted for CRRR samples. However, due to a lack of historical use, there are only a few studies that evaluated activity of CRPX, such as anti-inflammatory activity (90) and estrogenicity (91).

To evaluate biological potential of CRPX as a source for botanical dietary supplements for women's health, the extracts and some of the isolates were tested in multiple bioassays that are related to women's health, such as chemoprevention, estrogenicity, serotonergic activity, and metabolic interactions with Tamoxifen. CRRR has been studied intensely in the past and already been evaluated for such activities. In this study, the activity of CRPX was evaluated and compared to that of CRRR.

5.1. *Chemopreventive Activity*

5.1.1 *Introduction*

Burdette *et al*. reported that methanol extracts of *C. racemosa* contain antioxidant compounds and concluded that methyl caffeate, ferulic acid, and caffeic acid are the primary compounds responsible for the activity (92). Phenolic compounds such as actaealactone, cimicifugic acid G, cimicifugic acid A, cimicifugic acid B, and fukinolic acid showed antioxidant activities in the 1,1-diphenyl-2-picrylhydrazyl (DPPH) assay with IC_{50} values of 26, 37, 12, 21, and 23 μM, respectively. However, it was also suggested that minor components such as cimiracemate A and B may contribute to the antioxidant activity.

In this study, the potential chemopreventive activity of CRPX was tested by measuring the relative ability to induce the detoxification enzyme, NAD(P)H:quinone oxidoreductase 1 (NQO1), compared with the activity of the extracts of CRRR. All of the chemoprevention bioassay experiments were carried out in collaboration with Project 2 in our UIC/NIH Botanical Center, using the methods employed to study other Center plants (93). The PE, DCM and 70% EtOH extracts of CRPX and CRRR were evaluated in the *in vitro* NQO1 assay and cytotoxicity assay.

5.1.2 *Methods*

Plant Material: PE, DCM and 75% EtOH extracts of CRPX (BC 582) and CRRR (BC 581) were obtained as described in 3.2.1.

***In vitro* NQO1 Assay:** Induction of NQO1 activity was assessed using Hepa-1c1c7 murine hepatoma cells as described previously (94), with minor modifications. Briefly, Hepa-lclc7 cells were seeded in 96-well plates at a density of 1.25×10^4 cells/mL in 190 μL media. After 24 h incubation, test samples were added to each well and the cells incubated for an additional 48 h. The medium was decanted and the cells incubated at 37 °C for 10 min with 50 μL of 0.8% digitonin and 2 mM EDTA solution (pH 7.8). Next, the plates were agitated on an orbital shaker (100 rpm) for 10 min at room temperature. Then 200 μL of reaction mixture (bovine serum albumin, 3-(4,5-dimethylthiazo-2-yl)-2,5-diphenyltetrazolium bromide (MTT), 0.5 M Tris-HCl, 1.5% Tween 20, 7.5 mM FAD, 150 mM glucose-6-phosphate, 50 mM NADP, glucose-6-phosphate dehydrogenase 2 units/mL, and 50 mM menadione) were added to each well. After 5 min, the plates were scanned at 595 nm. The specific activity of NQO1 was determined by measuring NADPH-dependent menadione-mediated reduction of MTT to form blue formazan. Induction of NQO1 activity

was calculated by comparing the NQO1 specific activity of sample treated cells with that of solvent-treated cells. CD (Concentration Doubling) values represent the concentration required to double NQO1 induction. The chemopreventive index was then calculated, by dividing the IC_{50} by the CD value for a particular compound or extract (IC_{50}/CD) (95).

Cytotoxicity assay: Cells were plated and treated as described for the NQO1 assay. After the cells were treated with test samples for 48 h, the medium was decanted, and 200 μL of 0.2% crystal violet solution in 2% ethanol added. After 10 min, the plates were rinsed for 2 min with water and dried. The bound dye was solubilized by incubation at 37 °C for 1 h with 200 μL of 0.5% SDS in 50% ethanol. The absorption of crystal violet was measured at 595 nm, and the IC_{50} values were determined.

5.1.3 *Results and Discussion*

Both the CRPX and CRRR of a single plant were tested against induction of NQO1. Extracts from one plant (BC 582, PX and BC 581, RR) were tested for fold induction at three different concentrations: (2.5, 5, 10, and 20 μg/ml). The concentrations of the active PE and DCM extracts required to double NQO1 activity (CD-value) are shown in the following table. While activity of the aerial parts PE extracts differ by > 3-fold, the extracts of the aerial parts of CR still have chemopreventive potential *in vitro* in a comparable concentration range.

TABLE XXV. NQO1 ACTIVITY OF *C. RACEMOSA* EXTRACTS IN CD VALUE

Parts	Extract type	CD value in μg/ml
CRPX (BC582)	PE extract	**8.6 ± 1.8**
	DCM extract	**10.0 ± 0.8**
	75%EtOH extract	> 20
CRRR (BC581).	PE extract	**< 2.5**
	DCM extract	**9.82 ± 5.0**
	75%EtOH extract	> 20

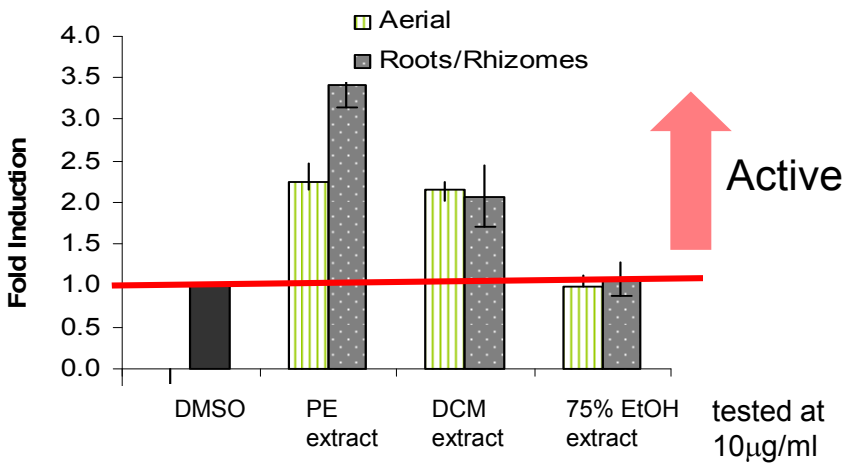

Figure 92. NQO1 fold induction of *C. racemosa* extracts tested at 10 μg/ml

5.2. *Estrogenicity of CR Aerial Parts*

5.2.1 *Introduction*

Because of its effectiveness for a variety of neuroendocrine indications, CRRR was originally considered an estrogenic agent (96). The majority of ER binding studies that have been carried out on black cohosh extract or compounds have reported no activity. Liu *et al*. from our UIC/NIH Botanical Center also reported that CRRR displayed no ER binding (< 20% at a concentration of 200 μg/mL). The ability of *C. racemosa* extracts to induce alkaline phosphatase (ALP), a stimulant of the estrogen-sensitive gene, pS2 (presenelin-2), or progestin receptors was also not detectable (97). In a few contradicting publications, estrogenic effects are claimed for black cohosh (25,26,98). Jarry *et al.* reported the presence of the isoflavone formononetin in the CRRR methanol extract. However, later studies failed to identify formononetin in CRRR extracts (27,28).

In this study, the estrogenicity of CRPX was evaluated in both estrogen receptors α & β (ERα&ERβ) competitive binding assay and induction of ALP in cultured Ishikawa cells. The two assays are targeting different points in the ER signaling pathway. The binding of a ligand to ER initiates downstream effects; therefore the competitive binding assay is often used as a primary screen. The cell-based ALP assay evaluates the estrogen activity along with their functional activity as either an agonist or an antagonist. The bioassay experiments for estrogenicity were carried out with Project 2 of our UIC/NIH Botanical Center using the method by which other Center plants were tested (91).

5.2.2 *Methods*

Plant Material: PE, DCM and 75% EtOH extracts of CRPX (BC 582) and CRRR (BC 581, BC017) were obtained as described in 3.2.1.

ERα and ERβ Competitive Binding Assays: Competitive ERα and ERβ binding assays were performed with tritiated estradiol (E_2) based on the method of Obourn *et al.* (99,100) with minor modifications. The reaction mixture consisted of a sample in DMSO (5 µL), pure human recombinant ERα and ERβ in ER binding buffer (0.5 pmol, 5 µL), "Hot Mix" [400 nM, 5 µL prepared fresh using 95 Ci/mmol [^{3}H] estradiol diluted in 1:1 ethanol :ER binding buffer obtained from NEN Life Science Products (Boston, MA)], and ER binding buffer (85 µL). The incubation was carried out at room temperature for 2 h before a hydroxyapatite slurry (50% HAPs, 100 µL) was added. The tubes were incubated on ice for 15 min with vortexing every 5 min. The appropriate ER wash buffer was added (1 mL), and the tubes were vortexed before centrifuging at 10,000 g for 1 min. The supernatant was discarded, and this wash step was repeated three times. The HAPs pellet containing the ligand-receptor complex was resuspended in ethanol (200 µL) and transferred to scintillation vials. An additional volume of ethanol (200 µL) was used to rinse the centrifuge tube. Cytoscint [4 mL/vial; ICN (Costa Mesa, CA)] was added, and the radioactivity was counted using a Beckman LS 5801 liquid scintillation counter (Schaumburg, IL). The percent inhibition of [^{3}H] estradiol binding to each ER was determined using Equation 6. The binding capability (percent) of the sample was calculated in comparison with that of estradiol (50 nM, 90%).

$$\left[1 - \frac{(dpm_{sample} - dpm_{blank})}{(dpm_{DMSO} - dpm_{blank})}\right] \times 100 = \%\ sample\ binding \qquad \textbf{Equation 6}$$

Induction of Alkaline Phosphatase in Cultured Ishikawa Cells (ALP): The procedure of Pisha *et al.* (100) with minor modifications was used. Ishikawa cells (1.5×10^4 cells/190 µL/well) were preincubated in 96-well plates overnight in an estrogen-free medium. Test samples (20 µg/mL final concentration in DMSO) were added to the cells in a total volume of 200 µL media/well were incubated at 37 °C for 4 days. For the determination of antiestrogenic activity, the media used to dilute the test samples were supplemented with estradiol (2 nM). The induction plates were processed by washing the plates with PBS and adding Triton x 100 (0.01%, 50 µL) in Tris buffer (pH 9.8, 0.1 M). Plates were subjected to a freeze thaw (-80 ºC for at least 24 h before warming to 37 ºC). An aliquot (150 µL) of *p*-nitrophenylphosphate (phosphatase substrate, 1 mg/mL) in Tris buffer (pH. 9.8, 0.1 M) was added to each well. The enzyme activity was measured by reading the release of *p*-nitrophenol at 405 nm every 15 s, with a 10 s shake between readings, for 16 readings using a Power Wave 200 microplate scanning spectrophotometer (Bio-Tek Instruments, Winooski, VT). The maximal slopes of the lines generated by the kinetic readings were calculated. Estrogenic induction was calculated using Equation 7, and for antiestrogenic determination, the percent induction as compared with the background induction control was calculated using Equation 8.

$$\left[\frac{(slope_{sample} - slope_{cells*})}{(slope_{estrogen} - slope_{cells*})}\right] \times \mathbf{100} = \%\ \boldsymbol{estrogenic\ induction} \qquad \textbf{Equation 7}$$

$$\left[\mathbf{1} - \frac{(slope_{sample} - slope_{cells*})}{(slope_{estrogen} - slope_{cells*})}\right] \times \mathbf{100} = \%\ \boldsymbol{antiestrogenic\ induction} \qquad \textbf{Equation 8}$$

*Cells means control cells, which are not treated with estrogen containing media or DMSO.

Cytotoxicity Assay: Cytotoxicity was determined for the Ishikawa alkaline phosphatase induction assays using ~1,000 cells per well in a 96-well plate (5 x 10^6 cells/mL). Cells were treated with the same samples used in the induction assays for the respective cell lines. The plates were harvested after 96 h. A "day zero" plate was prepared by plating at least half of a 96-well plate and allowing the cells to settle overnight. To process the plates, 50 µL of cold 50% trichloroacetic acid (TCA) was added to the media (final concentration 20%) and chilled at 4 ºC for 30 min. The plates were then washed with tap water and dried overnight. On the following day, the plates were stained with 100 µL of sulphorhodamine B (SRB) at room temperature, washed with 1% acetic acid and dried in the dark overnight. The dye was suspended in 200 µL Tris buffer (0.1 mM) and mixed using a plate shaker until the dye was completely solubilized. The plates were read using the endpoint mode at 515 nm. Calculation of the percent cytotoxicity was determined using Equation 9. Generally cytotoxicity greater than 20% will interfere with cell-based alkaline phosphatase assays.

$$\left[1 - \left(\frac{(OD_{sample} - OD_{day0})}{OD_{DMSO} - OD_{day0}}\right)\right] \times 100 = \%\ cytotoxic \qquad \textbf{Equation 8}$$

Estradiol (E_2 1uM stock) and 4OH-Tamoxifen (10mM) were used as controls for estrogenicity and antiestrogenicity, respectively, in abovementioned experiments.

5.2.3 *Results and Discussion*

The PE, DCM and 75% EtOH extracts of CRPX (BC017) were tested in the ERα and ERβ competitive binding assays at 200 µg/mL (n=5, two independent measurements) as well as the ALP assay. The results were reported in 2008 as part of a high throughput screening study, along with other plant extracts (91). As shown in Table XXVI, the PE

extract showed 55 ± 8% binding in the ERα assay and 64 ± 8 % in ERβ assay; however it is likely a "false positive" activity from fatty acids contained in PE extract. Liu *et al.* reported the identification of linoleic acid as an estrogen receptor ligand capable of displacing estradiol from the ER and binding to the ligand binding domain of the protein (101). Other fatty acids were also shown to bind to ER, while they did not stimulate the ALP activity, hence they are not considered estrogenic. This example displays the downside of bioassay guided fractionation for the purpose of identification of active compounds. Non specific binding can potentially lead the fractionation scheme to the identification of a "false" activity. In the previous study at the UIC/NIH Botanical Center, CRRR methanolic extract displayed no binding to ERα nor ERβ (< 20% at a concentration of 200 μg/mL) (97).

Interestingly, the 75% EtOH extract appeared to have a greater estrogenic response when combined with estradiol than the extract alone: the 75% ethanol extract of CRPX had a -48% antiestrogenic response indicating that more alkaline phosphatase enzyme was induced when compared to the extract without 17β estradiol (4%).

In a separate study, one whole plant of CR that was collected from the UIC Atkins Garden and carefully separated into CRRR (BC 581) and CRPX (BC 582). PE, DCM and 75% EtOH extracts were obtained in the same manner for both BC581 and BC582 and were tested twice and independently in the for ALP assay. At 5 μg/mL, none of the extracts exhibited estrogenicity, antiestrogenicity or cytotoxicity.

Since the ALP assay did not show clear estrogenic response, CRPX is not judged to be estrogenic.

TABLE XXVI. RESULTS OF ER BINDING AND ALKALINE PHOSPHATASE ALP BIOASSAYS OF PE, DCM AND 75% ETHANOLIC EXTRACT OF *C. RACEMOSA*

Sample name	Extract type	Conc.	Binding ERα %	±	std	Binding ERβ %	±	std	ALP Estrogenic %	±	std	ALP Antiestrogenic %	±	std	SRB Cytotoxicity %	±	std
DMSO		Control	0			0			1	±	2	0	±	5	1	±	2
E_2 (1uM stock)		Control	**95**	**±**	**1**	**90**	**±**	**1**	**100**	**±**	**10**	-10	±	8	4	±	2
4OH-Tamoxifen (10mM)		Control	**96**	**±**	**1**	**94**	**±**	1	0	±	5	**94**	**±**	**1**	2	±	1
	PE extract	200μg/ml	**55**	**±**	**8**	**64**	**±**	**8**	-5	±	5	21.3	±	7.2	4.8	±	10.9
CRPX(BC017)	DCM extract	200μg/ml	34	±	7	45	±	3	-3	±	1	3.5	±	8.7	8.3	±	5.2
	75% EtOH extract	200μg/ml	21	±	5	23	±	3	4	±	5	**-48.4**	**±**	**4.9**	0.1	±	5.7
Blank				-					2	±	7	0	±	0	1	±	3
DMSO									2	±	5	0	±	2	1	±	1
E_2 (1uM stock)[3]									**100**	±	7	6	±	6	-8	±	**19**
4OH-Tamoxifen (10mM)									-29	±	6	**95**	±	3	11	±	**12**
TP1-45-27 (4mg/ml)									**56**	±	8	12	±	5	-19	±	7
	PE extract	5μg/ml							-38	±	7	27	±	5	-75	±	36
CRPX (BC582)[1]	DCM extract	5μg/ml							-33	±	4	9	±	1	-11	±	4
	75% EtOH extract	5μg/ml							-20	±	3	16	±	4	23	±	5
	PE extract	5μg/ml							-37	±	5	14	±	7	72	±	21
CRRR (BC581)[1]	DCM extract	5μg/ml							-25	±	3	19	±	0	4	±	6
	75% EtOH extract	5μg/ml							-70	±	12	17	±	12	-7	±	5
	PE extract	5μg/ml							-7	±	6	19	±	8	-18	±	4
CRPX (BC582)[2]	DCM extract	5μg/ml							-13	±	6	7	±	7	-31	±	6
	75% EtOH extract	5μg/ml							-7	±	0	-17	±	3	-19	±	1
	PE extract	5μg/ml							-8	±	3	1	±	9	-21	±	1
CRRR (BC581)[2]	DCM extract	5μg/ml							-3	±	1	31	±	23	-28	±	4
	75% EtOH extract	5μg/ml							-40	±	4	-22	±	26	32	±	6

[1]1st experiment, [2]2nd experiment. [3]E_2, estradiol,

5.3. *Serotonergic Activity of CR Aerial Parts*

5.3.1 *Introduction*

Although CRRR was originally considered an estrogenic agent, the majority of later studies showed a lack of estrogenic activity (102,103). Instead, a non-hormonal mechanism of action has been investigated for CRRR. Serotonergic activity has been intensely studied at our UIC/NIH Botanical Center, and these studies revealed CRRR to be active and an active principle (N_{ω}-methylserotonin) was identified (22,23,104).

The relationship between serotonergic activity and the alleviation of menopausal symptom has been studied. Selective serotonin re-uptake inhibitors (SSRIs), which operate through the serotonin transporter, have been shown to alleviate hot flashes (19). Especially 5-HT_7 and 5-HT_{1A} serotonin receptors are involved in thermoregulation, which suggests that agonists for these receptors might be beneficial for the alleviation of hot flashes (21). Accordingly, the serotonergic system was examined as an alternative pathway through which black cohosh may reduce menopausal hot flashes.

In this section, CRPX extracts and fractions were evaluated for serotonergic activity by $5HT_7$ binding assay as well as cell-based cAMP assay. The known active compound, N_{ω}-methylserotonin, in the extracts of CRRR and CRPX was analyzed as well as in extracts of *Cimicifuga* species. The bioassay experiments for serotonergic activity were carried out in collaboration with Project 2 and 3 in our UIC/NIH Botanical Center.

5.3.2 *Methods*

Plant Material: Extracts and fractions of CRPX (BC401, BC032, BC043, BC018) were obtained as described in 3.2.2. For the quantitation of N_{ω}-methylserotonin, the following samples were extracted in MeOH: PX and RR of *C. americana* (BC008, 029), RR of *C. simplex* (BC393, 394), PX and RR of *C. rubifolia* (BC016, 023), PX and RR of *C. racemosa* (BC036, 025), RR of *C. dahurica* (BC392), RR of *C. japonica* (BC395), RR of *C. heracleifolia* (BC396), and RR of *C. acerina* (BC397). Most of the samples were the same as used in the metabolomic study and information is available in Table XXI. BC394 and BC392 were obtained from Pure World.

Serotonin Receptor Competitive Binding Assay: Human 5-HT_7 Chinese hamster ovary (CHO) cells were plated on dishes (150 mm × 10 mm) and cultured to confluence in order to collect membranes as previously described (105). Briefly, a hypotonic buffer (15 mM Tris, 1.25 mM $MgCl_2$, and 1 mM EDTA, pH 7.4) was added to the dishes which were incubated at 4 °C for 10-15 min. The cells were scraped from the dishes on ice, and the lysate was centrifuged. The hypotonic buffer was removed, and the membrane pellet was suspended in TEM buffer (75 mM Tris, 12.5 mM $MgCl_2$, 1 mM EDTA, pH 7.4). The cell membranes were homogenized and centrifuged twice at 12000 g for 20 min. The pellets were dissolved in a TEM buffer and stored at -80 °C. Protein concentrations were determined according to the protein assay method using bovine serum albumin as the standard from Bio-Rad Laboratories (Hercules, CA). The 5-HT_7 receptor binding assay was performed as described previously with minor modifications using human recombinant CHO cell membrane and [^{3}H] lysergic acid diethylamide (LSD) (5.67 nM) in an incubation buffer (50 mM Tris, 10 mM MgCl 2 , 0.5 mM EDTA, pH 7.4) (106). After a 1 h incubation at 37 °C, the mixture was filtered over a 934-AH Whatman

filter that had been presoaked in 0.5% polyethylenimine (PEI) and washed three times in ice-cold wash buffer (50 mM Tris buffer, pH 7.4) and simultaneously washed and aspirated five times using a 96-well Tomtec-Harvester (Orange, CT). Each filter was dried, suspended in Wallac microbeta plate scintillation fluid (PerkinElmer Life Sciences), and counted with a Wallac 1450 Microbeta liquid scintillation counter (PerkinElmer Life Sciences). Serotonin (1 μM) was used to define nonspecific binding, which accounted for < 10% of total binding. The percent inhibition of ^{3}H-labeled ligand bound to each 5-HT$_7$ receptor was determined using Equation 10.

$$\%\ \boldsymbol{sample\ binding} = \left[\mathbf{1} - \frac{(\boldsymbol{cpm_{sample} - cpm_{blank}})}{\boldsymbol{cpm_{DMSO} - cpm_{blank}}}\right] \boldsymbol{x}\ \mathbf{100} \qquad \textbf{Equation 10}$$

Intracellular cAMP Assay: Extracts were also tested at a concentration of 20 μg/m for modulation of intracellular levels of cyclic adenosine monophosphate (cAMP). Extracts that induced at least 5 pmol/mL of cAMP at the tested concentration were considered to be agonists. The elevation of intracellular cAMP was assayed as previously described (107,108), with minor modifications. Briefly, human 5-HT$_7$ -transfected HEK293 cells were grown for 4 days in serum-free media and then plated in poly-D-lysine-coated 12-well plates (100 × 10^4 cells/well) and left for 24 h. The following day, the cells were washed twice with 2 mL of incubation buffer (150 nM NaCl, 5 mM KCl, 1 mM $MgSO_4$, 2 mM $CaCl_2$, 10 mM glucose, 10 mM HEPES, 500 μM isobutylmethylxanthine, 1 μM ascorbic acid, 10 μM pargyline, pH 7.4) and then incubated for 20 min at 37 °C. The compounds and extracts were added and the plates were incubated at 37 °C for 10 min. Forskolin (20 nM) and serotonin (10 nM) were used as positive controls. If stimulation could be blocked by co-incubation of serotonin with the 5-HT$_7$ receptor antagonist, SB-269970, the treatment was considered to be receptor mediated. The reactions were

terminated by aspirating the buffer and adding 0.1 M HCl with 0.1% Triton-X detergent to lyse the cells. The cells were collected in microcentrifuge tubes and centrifuged for 5 min at 1000 rpm at room temperature. The cell supernatant was obtained and stored at -80 °C until the treated samples were analyzed. An aliquot of the cell supernatant (100 µL) was transferred to the Trevigen HT Direct cAMP EIA competitive immunoassay kit for the quantitative determination of cAMP in treated cells as per the manufacturer's protocol (Trevigen Inc., Gaithersburg, MD). The plate was read immediately in a Powerwave 200 microplate spectrophotometer (BioTek Instruments, Winooski, VT) at 405 nm. The concentration of cAMP was determined by measuring the optical density (OD) minus the nonspecific binding (NSB). The intensity of the yellow color was inversely proportional to the concentration of cAMP. The percentage of cAMP bound was determined using Equation 11, based on the maximum available binding (B_{max}). The amount of cAMP was calculated using a standard curve, and the data were expressed as pmol/ mL induction and compared to the basal cellular cAMP level observed.

$$\left(\frac{net\ OD}{net\ B_{max} OD}\right) x\ 100 = \%\ bound \qquad \textbf{Equation 11}$$

Quantitative Analysis of N_ω-methylserotonin: The analyses were carried out using an Agilent (Santa Clara, CA) 1200 HPLC system interfaced to an Agilent 6410 triple quadruple mass spectrometer. The analytes were separated on an Agilent Zorbax Eclipse XDB C_{18} column (4.6 x 50 mm, 1.8 µm particle size) using an isocratic mobile phase of 8.5% methanol in water containing 0.1% formic acid. The flow rate was 300 µL/min and the column temperature 25ºC. The retention time of N_ω-methylserotonin and serotonin were 4.8 min and 4.3 min, respectively.

Positive ion electrospray tandem mass spectrometry at unit resolution was used to measure N_ω-methylserotonin and serotonin with collision-induced dissociation (CID) and selected reaction monitoring (SRM). Nitrogen was used as a collision gas. During SRM, the analytes were measured by monitoring the transition of the protonated molecule of *m/z* 192 (N_ω-methylserotonin) and *m/z* 177 (serotonin) to the most abundant fragment ion of *m/z* 160. The SRM dwell time was 1 sec/ion. The ion source parameters were as follows: capillary voltage, 4000 V; nebulizer gas pressure, 25 psi; fragmentor voltage, 95 V (N_ω-methylserotonin) and 70 V (serotonin); collision gas temperature, 300°C; collision gas flow, 6 l/min; and collision energy, 3 eV (N_ω-methylserotonin) and 5 eV (serotonin). Data were acquired and analyzed using Agilent MassHunter Workstation software. Reference material was authenticated by qHNMR prior to use.

Plant Sample Analysis: Sixteen extracts from eight *Cimicifuga* species were analyzed for the quantitation of N_ω-methylserotonin. Each methanolic extract was diluted to 2.5 µg/mL using 50% methanol. Ten (10) µL aliquots of the test solutions were injected onto the LC-MS-MS to measure N_ω-methylserotonin. The quantitation of N_ω-methylserotonin was performed using the standard curve that was prepared and shown in Figure 94.

(A)

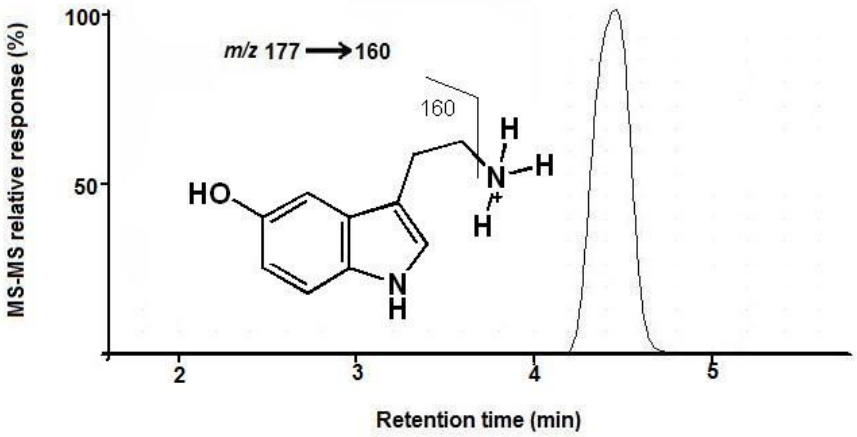

(B)

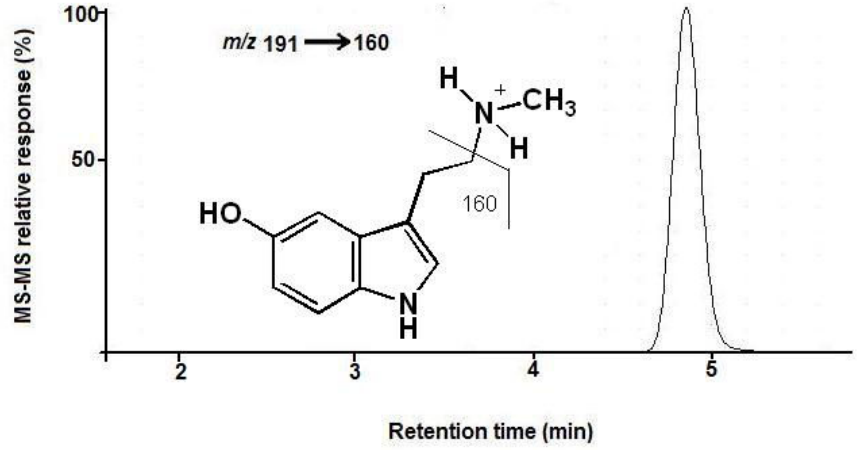

Figure 93. LC-MS-MS SRM chromatogram of serotonin (A) and N_ω-methylserotonin (B)

During collision-induced dissociation with SRM, the transition of the protonated molecules of *m/z* 177 (serotonin) and *m/z* 191 (N_ω-methylserotonin) to the most abundant fragment ion of *m/z* 160 was recorded. Serotonin was detected at a retention time of 4.3 min and N_ω-methylserotonin eluted at 4.8 min. The analyses were carried out in duplicate.

5.3.3 *Results and Discussion*

Parallel with the fractionation process of CR aerial parts extracts, serotonergic activities of obtained fractions were analyzed for both binding activity and the functional activity. Results are shown in Figure 95 along with the fractionation scheme. First, three crude extracts (PE, DCM and 75% EtOH) were tested in the 5-HT_7 binding assay. The three extracts showed 5-HT_7 binding activity at 66 ± 4 %, 66 ± 1 %, and 72 ± 1 % respectively. They were also tested in the cAMP assay and only the 75% EtOH extract demonstrated activity (3.4 ± 0.1). The PE and DCM extracts displayed 1.1 ± 0.1, 1.2 ± 0.1 inductions respectively.

The fractions of the 75% EtOH extract were further tested for serotonergic activity because it showed the strongest activity in the binding assay as well as the cAMP assay. The extract was separated into four fractions (CR10-80-01, CR10-80-05, CR10-80-09, CR10-80-11) by liquid-liquid partition and XAD column fractionation (details of the fractionation method are described in 3.2.2). The XAD MeOH fraction was only active in cAMP at 3.8 ± 0.2 induction. The results match with previous results obtained by Powell, Gödecke *et al*. of our UIC/NIH Botanical Center' on the roots/rhizomes of *C. racemosa.* The active fraction 10-80-11 was further fractionated by a reverse phase VLC to yield thirteen subfractions (23,104). The activity was concentrated in the polar fractions, CR10-88-01 to CR10-88-05. Of these fractions, CR10-88-03 showed the strongest activity of 29.0 ± 17.3 % at 20 μg/ml in 5-HT_7 binding assay.

Since it has shown that the distribution of activity is similar to that of CRRR, the quantity of the known active compound N_ω-methylserotonin was obtained by LC-MS-MS SRM. The N_ω-methylserotonin quantity of each fraction was shown in Table XXVII along

with the cAMP fold induction value. Figure 96 shows biochromatogram of the cAMP induction activity and N_{ω}-methylserotonin, which demonstrates the correlation between biological activity and the potentially active compound (109). The most active fraction, CR10-80-3, in cAMP induction contained the highest amount of N_{ω}-methylserotonin at 4.86 µg/mg. Moreover, the biological activities of other fractions follow the amount of N_{ω}-methylserotonin, which clearly showed a positive correlation between the two. Hence it is concluded that the observed cAMP induction was caused by N_{ω}-methylserotonin as the single active serotonergic principle in CRPX, just as has been reported for CRRR.

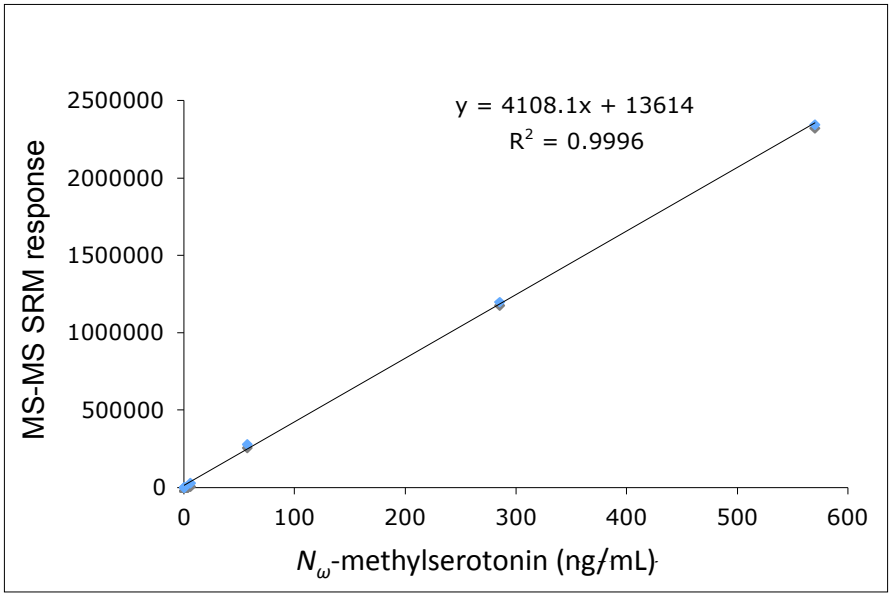

Figure 94. LC-MS-MS standard curve of N_{ω}-methylserotonin

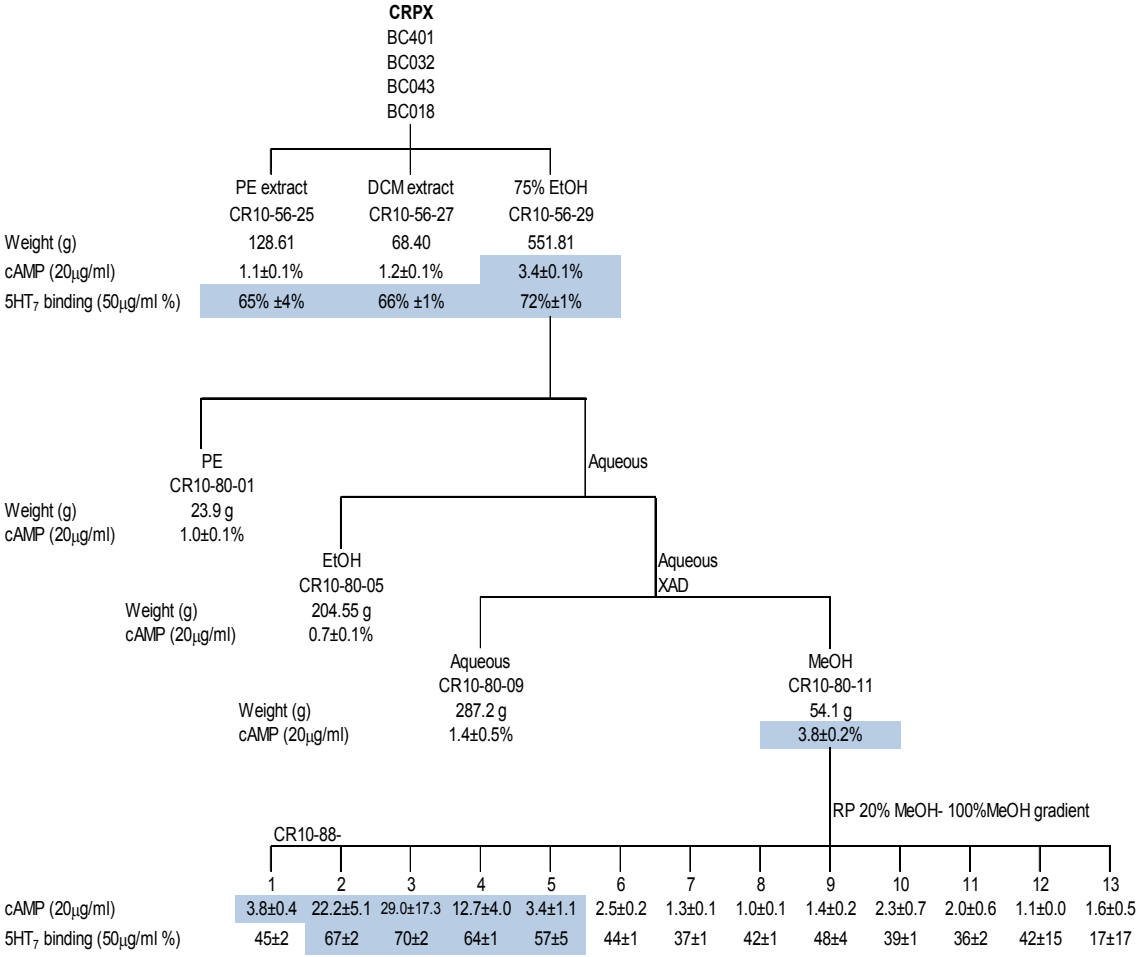

Figure 95. Bioassay-focused fractionation scheme showing the distribution of the 5-HT_7 binding and cAMP induction activity

TABLE XXVII. N_ω-METHYLSEROTONIN CONTENT AND CAMP FOLD INDUCTION OF FRACTIONS IN THE CR10-88 SERIES

The content of N_ω-methylserotonin was expressed by µg in 1 mg of extract. The LOQ was 0.057 ng/mL (on column).

Sample No.	N_ω-methylserotonin*	cAMP folding		SD
CR10-88-01	0.34	3.8	±	0.4
CR10-88-02	1.63	22.2	±	5.1
CR10-88-03	4.86	29.0	±	17.3
CR10-88-04	0.86	12.7	±	4.0
CR10-88-05	1.02	3.4	±	1.1
CR10-88-06	0.32	2.5	±	0.2
CR10-88-07	< LOQ	1.3	±	0.1
CR10-88-08	< LOQ	1.0	±	0.1
CR10-88-09	< LOQ	1.4	±	0.2
CR10-88-10	0.16	2.3	±	0.7
CR10-88-11	0.062	2.0	±	0.6
CR10-88-12	< LOQ	1.1	±	0.0
CR10-88-13	< LOQ	1.6	±	0.5

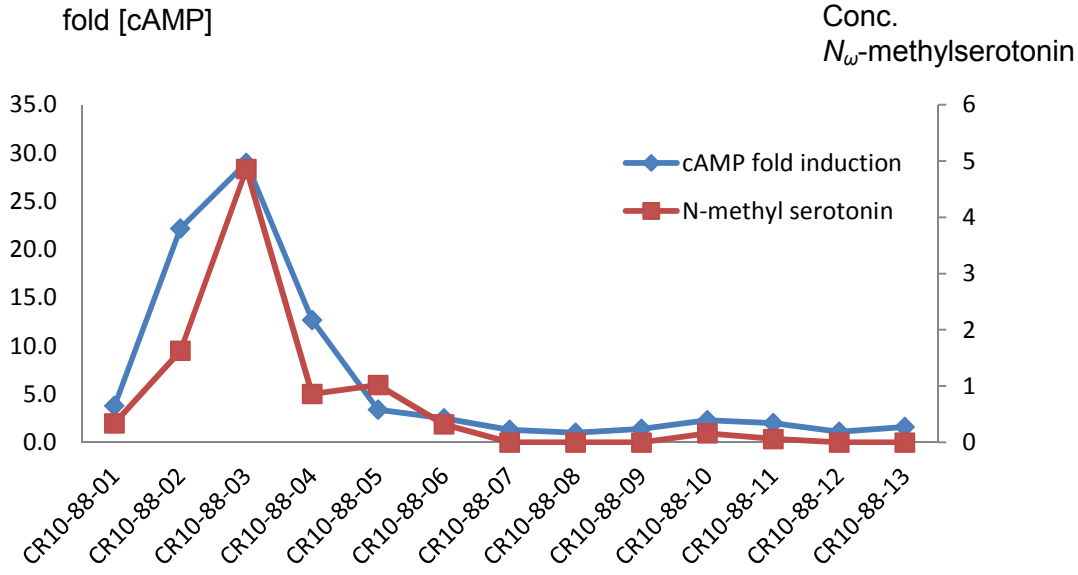

Figure 96. N_ω-Methylserotonin content and cAMP fold induction of subfractions CR10-88 series

The content of N_ω-methylserotonin was expressed as µg in 1 mg of extract.

The activity in CRPX and the active compound for the serotonergic activity was confirmed in the previous section. To explore the possibility of this active compound as a marker compound for authentication of the CR dietary supplements, the extracts of other *Cimicifuga* species were analyzed for N_{ω}-methylserotonin content. The results show that all of the samples contain N_{ω}-methylserotonin. CRRR contained the highest amount of N_{ω}-methylserotonin at 0.091 % (910 ppm), and CDRR (*C. dahurica*) extract contained the lowest amount at 0.061 % (610 ppm). The level of N_{ω}-methylserotonin content found in this study is higher than the previously reported value in CRRR extract of about 30 ppm (23). The extracts tested in this study are MeOH extracts, while the previously tested sample was a 75% EtOH extract. N_{ω}-methylserotonin was first identified in *Cimicifuga* species by Powell *et al.* (23), however the compound had been isolated from natural resourse in 1974 by pH-gradient and column chromatography (110): in which the plant material was processed by a weak acidic solution (aqueous 4 % acetic acid) first. Then a base (ammonia) was added to achieve three pH levels (4, 7 and 9) and each fraction was extracted with $CHCl_3$. Nω-methylserotonin was extracted at pH 9. CRPX contained 0.075 % of N_{ω}-methylserotonin. Since it is observed in all of the species, N_{ω}-methylserotonin cannot be a marker compound for any particular species. It is reasonable that medicinally used species contain this serotonergic active compound, however non-medicinal species, such as CA and PX, and their parts also contained similar level of N_{ω}-methylserotonin to those of the therapeutically used species.

TABLE XXVIII. N_ω-METHYLSEROTONIN CONTENT IN METHANOLIC EXTRACTS OF *CIMICIFUGA* SPECIES

Sample No.	Species	Part	N_ω-methylserotonin content(%)
BC008	*C. americana*	root	0.081
BC029	*C. americana*	aerial	0.082
BC393	*C. simplex*	root	0.075
BC394	*C. simplex*	root	0.076
BC016	*C. rubifolia*	root	0.078
BC023	*C. rubifolia*	aerial	0.077
BC036	*C. racemosa*	root	0.091
BC025	*C. racemosa*	aerial	0.075
BC392	*C. dahurica*	root	0.061
BC395	*C. japonica*	root	0.071
BC396	*C. heracleifolia*	root	0.070
BC397	*C. acerina*	root	0.075

5.4. *Potential In vitro Metabolic Interaction of CR with Tamoxifen Metabolism*

5.4.1 *Introduction*

Tamoxifen (TAM) is the drug of choice for the treatment or prevention of estrogen receptor-positive breast cancer. It reduces the risk of breast cancer in women at high risk by almost 50% and the rate of mortality of patients by approximately 25% (111,112). Pharmacological efficacy of TAM depends on the metabolic conversion into two active metabolites, 4-hydroxytamoxifen (4-OH TAM) and *N*-desmethyl-4-hydroxytamoxifen (endoxifen), with endoxifen being more abundant *in vivo* (113,114). Extensive *in vitro* studies have identified cytochromes P450 3A4 (CYP3A4) as the dominant, although not exclusive, isoforms responsible for the production of the active metabolites (115), TAM is also converted into a number of therapeutically inactive metabolites, most notably α-hydroxytamoxifen (α-OH TAM), which has been implicated as a genotoxic metabolite of TAM (116).

Previously, a 75% ethanolic extract of CRRR has been found to interfere with TAM metabolism by the inhibition of cytochrome P450 2D6 (CYP2D6) and CYP3A4 (116,117). Triterpene glycosides were found to be responsible for CYP3A4 inhibition, while two alkaloids, protopine and allocryptopine, were identified as potent inhibitors of CYP2D6.

The current study focused on the potential of CRPX, to provide the same activity. The CRPX extracts/fractions were evaluated for both CYP3A4 and CYP2D6 inhibitory activity along with the fractionation scheme. Isolates of the aerial parts were also tested.

The LC-MS experiments were carried out in collaboration with Project 3 of our UIC/NIH Botanical Center.

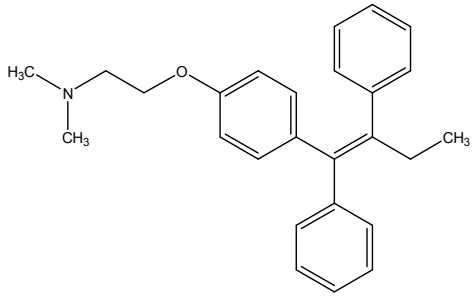

Figure 97. Structure of tamoxifen

5.4.2 *Methods*

Plant Material: Extracts and fractions of CRPX (BC401, BC032, BC043, BC018) were obtained as described in 3.2.2. Pure compounds were also obtained and characterized as described in Chapter 3.

CYP2D6 and CYP3A4 Probe Metabolism Inhibition Assay:

Microsomal dextromethorphan N-demethylation and midazolam 1'-hydroxylation activities were used as markers for CYP2D6 and CYP3A4 activity, respectively. All assays were carried out as previously described with minor modifications (118). Incubation mixtures (100 µL total volume) containing human liver microsomes (0.03 mg/mL), dextromethorphan (5 µM) or midazolam (2 µM), and black cohosh fractions (various concentrations) or isolated compounds (10 µM) were pre-incubated for 10 min at 37°C before addition of NADPH (1 mM). Incubations were carried out for 10 or 4 min for CYP2D6 and CYP3A4 activity, respectively. Reactions were terminated by adding ice-cold stop solution (CH_3CN/H_2O/HCOOH; 90:10:4) containing internal standard (dextrorphan-d_3 or flurazepam). Dextromethorphan metabolites were separated using a Zorbax Eclipse

XDB (2.1 x 50 mm 1.8 μm) C_{18} column (Agilent, Santa Clara, CA) and a mobile phase consisting of 0.1 % formic acid in water (mobile phase A) and methanol (mobile phase B). The following gradient program was used: 19 % B for 2 min, 19 to 80 % B in 0.1 min, 80% B for 9 min, and finally returning to 19% B. Midazolam metabolites were separated using the same column and the mobile phase except that the gradient program consisted of 40% B for 2 min, 40 to 80% in 1 min, 80% B for 4 min, and finally returning to 40% B. The flow rate was 0.2 mL/min and the column temperature was 33° C for all analyses. Positive ion electrospray ionization was used with SIM detection to measure protonated molecules of dextrorphan at *m/z* 258.1 and internal standard dextrorphan-d_3 at *m/z* 261.1, protonated molecule of 1'-hydroxy-midazolam at *m/z* 342.2, and flurazepam at *m/z* 388.2.

5.4.3 ***Results and Discussion***

The DCM extracts of *C. racemosa* aerial parts exhibited 82% and 74% CYP3A4 and CYP2D6 inhibition, respectively, at 25 μg/ml. The 75% EtOH extract did not show CYP3A4 and CYP2D6 inhibitory activity. After the extract was defatted with PE to remove the majority of the fatty acids, it was further fractionated as described in 3.2.2. The second level fractions were tested for CYP3A4 inhibition at 25 μg/ml, revealing that fractions 4, 6, 7, 8 and 9 (CR10-90-04 and CR10-90-06-09) were potent inhibitors. It was noted that the non-polar fractions showed a green color and obviously contained large amounts of chlorophylls. Since 25 μg/ml exceeded the dynamic range of the bioassay response, CYP2D6 was re-tested at a reduced concentration of 12.5 μg/ml. CR10-90-04 had the highest potency with 64.3 ± 0.2 % for CYP2D6 inhibition. Since CR10-90-04 had inhibition activities in both CYP3A4 and CYP2D6, and also because the fraction contained the least amount of chlorophyll compared to the more lipophilic fractions, it was further fractionated.

Of the resulting subfractions CR10-91-02-03, and -06 showed further enhanced activity of 61.5 % and 67.5% inhibition for CYP3A4, respectively, at further reduced concentrations of 2 μg/ml. No significant inhibition was observed for CYP2D6 at 2 μg/ml.

Fractions CR10-91-02 and -03 were not directly tested because they separated into two distinct entities in the storage vials; white needle like powders, and greenish yellow residue. The white powders from each fraction (CR10-94-03, -09) were separated from the rest by washing with MeOH and tested for activity for CYP3A4 at 2 μg/ml. While that of CR10-94-03 showed 32.6 ± 2.9 %, CR10-94-09 showed 19.7 ± 0.8 % activity. After NMR analysis, it was shown that CR10-94-09 contained mainly cimiracemoside I and CR10-94-03 was shown to be a mixture of cycloartane triterpenes, which were not individually identified. The tested concentration for cimiracemoside I was calculated according to its exact mass of 600.37 to 3.3μM. Considering that the several other sub-fractions exhibit over 60% inhibitory activity for CYP3A4 at 2 μl/m (CR10-91-02, -03, and -06), it is reasonable to expect that several more compounds contribute to the activity. According to TLC profile, CR10-91 series were triterpene rich sub-fractions. Some of the isolates of CRPX were evaluated for their activity and the results are shown in Table XXIX. Interestingly, all three of the active compounds of CRPX have different side chains. Moreover, both aglycones and glycosides were found to be active. Although six other cycloartane triterpenes from CRRR were reported for CYP3A4 inhibition activity (116) structural similarity was not distinguished other than they are all cycloartane triterpenes.

In summary, CRPX was found to interfere with TAM metabolism by inhibition of CYP2D6 and CYP3A4. This is analogous to previous observations with extracts from CRRR. Cimiracemoside I, 7β-hydroxycimigenol aglycone, and 25-*O*-acetyl-7β-

hydroxycimigenol-3-*O*-β-D-xylopyranoside were identified as key active principles for the inhibitory activity for CYP3A4.

TABLE XXIX. CYP3A4 INHIBITION BY AERIAL *C. RACEMOSA* TRITERPENES

No.	Compound	% inhibition[1]	IC50(μM)
3	1α-hydroxycimigenol-3-*O*-L-arabinopyranoside	NA	
4	1α–hydroxycimigenol-3-*O*-D-xylopyranoside	NA	
5	7β-hydroxycimigenol aglycone	64.9±1.1	N/D
6	25-*O*-acetyl-7β-hydroxycimigenol-3-*O*-D-xylopyranoside	61.8±0.2	N/D
11	Cimiracemoside I	19.7±0.8	N/D

[1]% inhibition was tested at 10 μM except for **11**.
[2]**11** was tested at 3.3 μg/ml

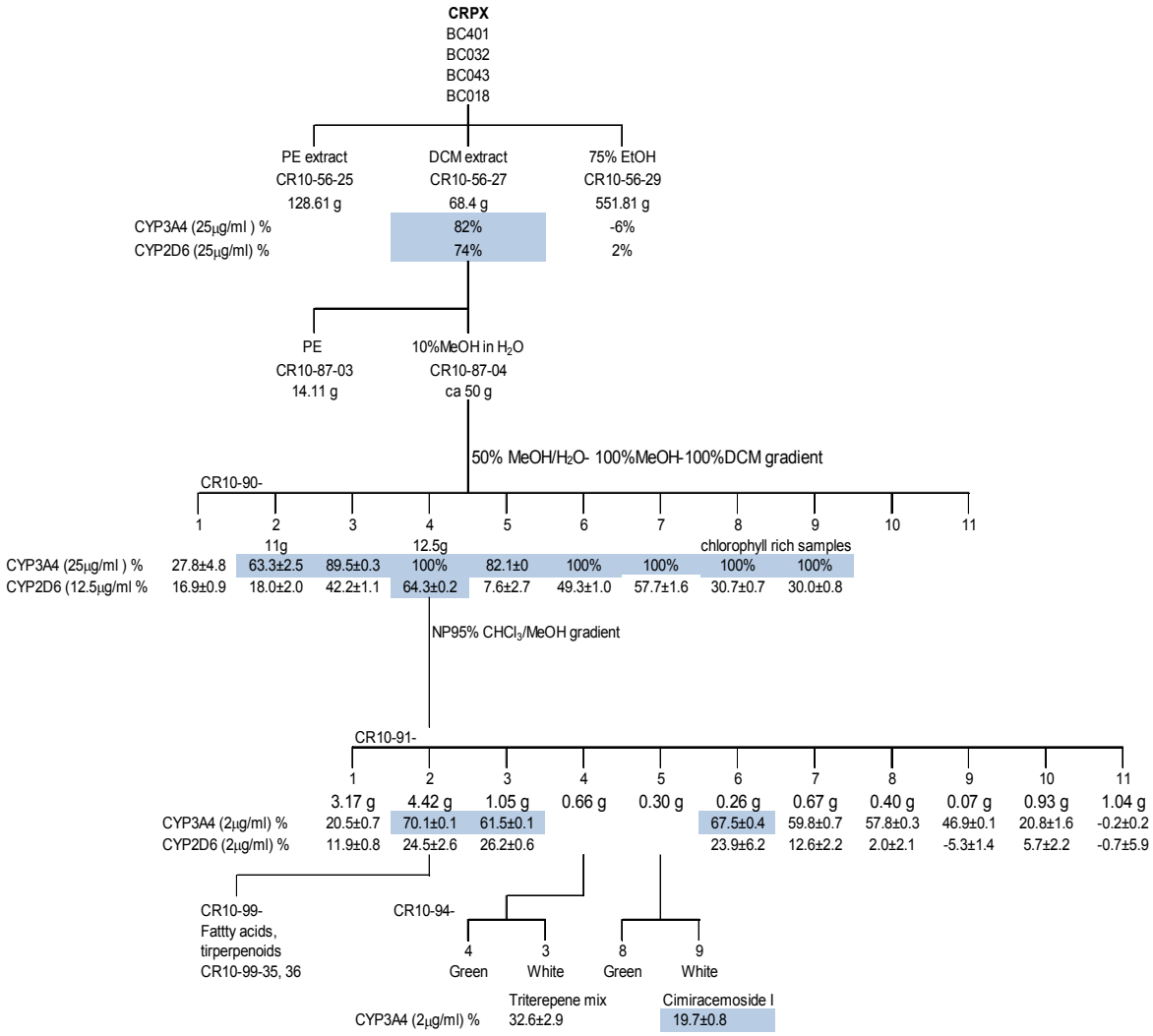

Figure 98. Bioassay-focused fractionation scheme showing the distribution of the CYP3A4 and CYP2D6 activity

5.5. *Summary of Aim 3*

Chemoprevention

Both the aerial parts and the roots extracts of a single plant were tested against induction of NQO1. PE and DCM extracts of the aerial parts showed CD values of 8.6 ± 1.8 and 10.0 ± 0.8 μg/ml, respectively. While the activity of both PE extract and DCM extract is weaker than the CRRR extracts, CRPX shows chemopreventive potential *in vitro.*

Estrogenicity

The PE extract of CRPX showed 55 ± 8% binding activity in the ERα assay and 64 ± 8 % in ERβ assay at 200 μg/mL, most likely false activity of fatty acids. In ALP assay at the same concentration, none showed simple estrogenicity. The 75% ethanol extract of CRPX had a negative antiestrogenic response (-48 %). This indicated that more ALP was induced when compared to the extract without 17β estradiol (4%). Both CRPX and CRRR extracts were simultaneously tested in an ALP assay, in two independent experiments at different times. A 60-fold lower concentration of 5 μg/mL concentration, none of the CRRR and CRPX extracts showed estrogenicity, antiestrogenicity or cytotoxicity.

Serotonin

Along with the fractionation process of CR aerial parts extracts, serotonergic activities of obtained fractions were analyzed for both binding activity and functional activity. The results matched closely with previous findings in our UIC/NIH Botanical Center's (23,104) study of the roots/rhizomes of *C. racemosa.* It was shown that the most active fraction of the aerial parts contains the highest amount of N_{ω}-methylserotonin and that its concentration in the fractions correlated with the activity.

The quantity of the active compound N_{ω}-methylserotonin was analyzed in the methanolic extract of both aerial CR and roots/rhizomes of CR along with other species by LC-MS-MS SRM. The N_{ω}-methylserotonin content of the aerial CR is 0.075% while the roots/rhizome CR is 0.091%.

***In vitro* Metabolic Interactions with Tamoxifen**

The DCM extract exhibited inhibitory activity for both CYP3A4 and CYP2D6 at 82% and 74%, respectively. After several fractionations, the activity was concentrated and three fractions showed more than 61% of inhibitory activity at 2 μg/ml. Cimiracemoside I was isolated from this fraction showed weak inhibitory activity to CUP3A4. 7β-Hydroxycimigenol aglycone and 25-*O*-acetyl-7β-hydroxycimigenol-3-*O*-β-D-xylopyranoside were also identified as active principles.

Overall Summary

In Aim 3, the biological potential of CRPX was presented for four different aspects. Serotonergic activity was straight-forward. The active compound, which was identified from CRRR, was also identified in CRPX in slightly different level. For chemoprevention and CYP inhibition, activity was exhibited from both CRPX and CRRR. The active component for chemoprevention was not investigated. For CYP3A4 inhibition, three compounds showed activity, of which, two have not been identified in CRRR before. It suggests that the responsible active constituents are different in CRPX and CRRR, although they are all in the same class of compounds. It appears that multiple compounds are contributing to CYP3A4 inhibition rather than a single entity. Estrogenicity was rather complicated. ALP assay did not show positive estrogenicity, so it was not considered estrogenic. However the PE extract showed binding activity to ERα and ERβ, which agrees with the previously reported false activity of fatty acids.

TABLE XXX. SUMMARY OF AIM 2: COMPARISON OF BIOLOGICAL ACTIVITY BETWEEN CRPX AND CRRR

	PX		RR	
Chemoprevention	+	NQO1 activity exhibited PE extract 8.6% ± 1.8 DCM extract 10.0 ± 0.8 (CD value)	+	NQO1 activity exhibited PE extract < 2.5 DCM extract 9.82 ± 5.0 (CD value)
Estrogenic activity	-	ALP assay result did not show estrogenicity	-	ALP assay result did not show estrogenicity
Serotonergic activity	+	The active compound Nω-methylserotonin identified 0.075 %	+	The active compound Nω-methylserotonin identified 0.091 %
CYP inhibition	+	CYP3A4, 2D6 inhibition exhibited Three isolates showed activity for CYP3A4 inhibition	+	CYP3A4, 2D6 inhibitory activity (116)

6. **Conclusions of Study**

6.1. *Aim 1 Phytochemical Investigation*

To isolate and identify as many secondary metabolites as possible from the aerial parts of *C. racemosa* and to compare these metabolites with those known from the roots and believed to have therapeutic effects.

The composition of extracts of the aerial parts of *Cimicifuga racemosa* was shown to be different than that of the extracts of the roots/rhizomes. More lipophilic extracts were obtained from the former than from the latter. Differences were observed, not only in the composition but also in the amount of extract obtained. The combined lipophilic extracts (petroleum ether and dichloromethane) comprised more than 3 % of the weight of the dried aerial parts, whereas, the same extracts of the dried roots/rhizomes produced only 0.8 % of the dried plant material.

Two new cycloartane triterpene glycosides, 24-*epi*-1α-hydroxycimigenol-3-*O*-β-D-xylopyranoside and 1α-hydroxydahurinol-3-*O*-α-L-arabinopyranoside were isolated and their structures elucidated. To analyze the stereochemistry of the compound, full spin simulation was successfully carried out using the PERCH program. This revealed key long range couplings that otherwise would not have been overlooked such as several couplings to each of the C-19 methylene protons and a coupling between Me-18 and H-12β. The comparison of ROESY spectra of an epimeric pair (23*R*,24*R* and 23*R*,24*S*) was carried out for the cimigenol side chain system, which also confirmed the stereochemistry of C-24. The configurations of methylenes (H-19 endo,exo, H-2α,β, H-6α,β, H7α,β, H-11α,β, and H-12α,β) were assigned unambiguously based on ROE information. The structure of 1α-

hydroxydahurinol-3-*O*-α-L-arabinopyranoside was determined by a combination of ^{1}H NMR and COSY. Additionally, typical ketone signals were observed in the HMBC. Along with the two new compounds, five triterpenes were isolated for the first time from *C. racemosa*. In particular, 7β-hydroxycimigenol aglycone has only been obtained by enzymatic hydrolysis and has not been isolated as an aglycone. 1α/7β-OH derivatives of cycloartane triterpenes were isolated in the aerial parts, while they have not been isolated from the roots. In this study, cimigenol, dahurinol, and shengmanol types of triterpenes were isolated from aerial *C. racemosa*. However other major types of triterpenes in the roots/rhizomes were not isolated from the aerial parts. Given that this is the first study on aerial *C. racemosa,* it is reasonable to expect that the aerial parts and the roots/rhizomes contain some of the same compounds.

Two flavonol diglycosides, quercetin 3-*O*-β-arabinopyranosyl-(1→6)-β-galactopyranoside and kaempferol 3-*O*-β-arabinopyranosyl-(1→6)-β-galactopyranoside, were isolated but not separated. However their structures were unambiguously elucidated from spectra of the mixture. The serotonergic active principle N_{ω}–methylserotonin was identified by the LC-MS method in a collaborative work in our UIC/NIH Botanical Center. Other alkaloids were not isolated.

In this aim, the first chemical investigation of the aerial parts of *C. racemosa* was carried out and revealed the presence of a total of 15 compounds.

6.2. *Aim 2 Metabolic Fingerprinting and Standardization*

To establish a method for differentiation and identification of *Cimicifuga* species and plant parts in black cohosh dietary supplements

^{1}H NMR spectra of a total of 34 *Cimicifuga* crude extracts were obtained and analyzed for their fingerprint peaks by visual observation. The roots/rhizomes and aerial parts of three American species (*C. racemosa*, *C. americana*, and *C. rubifolia*) were studied, as the last two are the most likely contaminants in commercial preparation of the first. The ^{1}H NMR spectra of the *C. americana* extracts was substantially different from those of the other two species. Strong indicator peaks (1.11 - 1.16 ppm) for this species were identified. The extracts of *C. racemosa* and *C. rubifolia* gave very similar ^{1}H NMR spectral patterns in A region. In the crude extract of the roots/rhizomes of *C. racemosa*, 23-*epi*-26-deoxyactein and actein were identified by comparison with a previously isolated compound as a reference. The six quaternary methyls, one secondary methyl and one acetyl methyl peak were all identified in a spectrum of the extract, and structure identification was supported by distinctive COSY cross peaks.

Not only was qualitative analysis of the spectra possible, quantitative aspects were employed to differentiate plant groups. The quantitative ^{1}H NMR method was developed using the characteristic C-19 cyclopropane signals in a unique spectral region, which revealed that *C. americana* extract can also be differentiated from a *C. racemosa* sample by a small amount of cycloartane.

A statistical method using Principal Component Analysis (PCA) was employed to take into account small peaks in the spectra for the identification of extractives of these species. PCA scores enabled the identification of both the aerial parts and the roots/rhizomes of each of the three of American *Cimicifuga* species in crude extracts.

This metabolomic Aim 2 complements Aim1 for the purpose of profiling the secondary metabolites of the roots/rhizomes by taking unknown/unidentified compounds into account.

6.3. *Aim 3 Biological Assessment*

To evaluate biological potential, in terms of safety and efficacy, of *Cimicifuga racemosa* aerial parts extract and compounds in terms of chemoprevention, estrogenicity, serotonergic activity, and drug interactions.

Chemopreventive, estrogenic, and serotonergic activity and inhibition of CYP3A4 and CYP2D6 activity were demonstrated for the extracts of the aerial parts of *C. racemosa*. For chemoprevention, the level of activity was less than that exhibited by extracts of the roots/rhizomes of this species. This was true for both the petroleum ether and dichloromethane extracts. Serotonergic activity was monitored by a combination of 5-HT_7 binding and cAMP induction assays. These, along with the purity/activity relationships followed through fractionation confirm that the compound N_ω-methylserotonin is an active principle mediating serotonergic effects, as previously reported by Powell, Gödecke *et al*. (23,104). The N_ω-methylserotonin content of the dried aerial parts of *C. racemosa* was found to be 0.075%. This compared closely with the content found in the dried roots/rhizome at 0.091%. For estrogenicity, when PE, DCM and 75% EtOH extracts were tested at 200 μg/mL. The PE extract exhibited 55 ± 8% binding activity in the ERα assay and 64 ± 8% in the ERβ assay, which is most likely a false activity from fatty acids. However, in the ALP assay, estrogenicity was not exhibited for the same extracts when the extracts were tested at 20 μg/mL. Potential for drug interaction was evaluated by inhibition of cytochromes P450 3A4 (CYP3A4) and CYP2D6. Bioassay guided fractionation by a CYP3A4 inhibitory assay led to a weakly active compound cimiracemoside I (19.7 ± 0.8 % inhibition at a concentration of 2 μg/mL). Previously isolated compounds 7β-hydroxycimigenol aglycone and 25-*O*-acetyl-7β-hydroxycimigenol-3-*O*-β–D-xylopyranoside

also exhibited CYP3A4 inhibitory activity (64.9 ± 1.1, 61.8±0.2 % inhibition at a concentration of 10 μg/mL, respectively)

6.4. *Answer to Initial Hypothesis*

Aerial *C. racemosa* can be developed into a botanical dietary supplement that can substitute products currently produced from below ground parts.

In this study, extracts of the aerial parts of *C. racemosa* demonstrated similar biological activities to that seen in extracts of the roots/rhizomes. Similarities include beneficial biological activities such as serotonergic and chemopreventive activities as well as potentially negative metabolic interactions with tamoxifen. Estrogenicity was also tested, but an *in vitro* cell-based assay did not detect activity from either extracted. However, it has been shown that the levels of activity can vary between the roots/rhizomes and the aerial parts: Examples include CD values for chemopreventive activity and N_{ω}-methylserotonin content for serotonergic activity. Furthermore, not only the levels of activity vary, but the active compounds can be different. An aerial parts isolate, 7β-hydroxycimigenol aglycone, was shown as one of the active triterpenes for inhibition of CYP3A4. However, it has not been identified in the roots/rhizomes. Instead, the roots/rhizomes contain other active triterpenes that have not been reported from the aerial parts.

Phytochemically, even though structurally-related cycloartane triterpenes were isolated, there are similarities between the constituents of the roots/rhizomes and those of the aerial parts of *C .racemosa.* Some differences were suggested in this study, such as the presence of more oxygenated triterpenes in the aerial parts and different phenolic compound composition, such as flavonoids isolated in the aerial parts. In this study, 9 out

of 15 compounds were identified for the first time from *C. racemosa*, but they are all analogs of previously isolated compounds. A metabolomic study also revealed differences in the extracts of the aerial parts and the roots/rhizomes. Considering a lack of safety information for the aerial parts of *C. racemosa*, more comprehensive research is required before the use of the aerial parts as a dietary supplement is fully accepted. However, the benefits of pursuing that goal have been clearly outlined in this study.

.

APPENDICES

APPENDIX A
TRITERPENES

1 ACTAEAEPOXSIDE-3-O-BETA-D-XYLOPYRANOSIDE
2 ACTEIN
3 ACTEIN,23-EPI: 26-DEOXY:
4 ACTEIN,26(S):
5 ACTEIN,26-DEOXY:
6 ACTEIN,2'-O-ACETYL:
7 ACTEIN,BETA-D-XYLOPYRANOSIDE
8 ACTEIN,DEACETYL:
9 ACTEOL,27-DEOXY: ACETYL:
10 CIMIACEROSIDE A
11 CIMICIFUGOSIDE
12 CIMICIFUGOSIDE H-1
13 CIMICIFUGOSIDE H-2
14 CIMICIFUGOSIDE M
15 CIMICIFUGOSIDE,26-DEOXY:
16 CIMICIGENOSIDE A,NEO:
17 CIMICIGENOSIDE B,NEO:
18 CIMIGENOL ARABINOSIDE
19 CIMIGENOL,12-BETA-21-DIHYDROXY: 3-O-ALPHA-L-ARABINOPYRANOSIDE
20 CIMIGENOL,12-BETA-HYDROXY: 3-O-ALPHA-L-ARABINOPYRANOSIDE
21 CIMIGENOL,12-BETA-HYDROXY: 3-O-BETA-D-XYLOPYRANOSIDE
22 CIMIGENOL,21-HYDROXY: 3-O-BETA-D-XYLOPYRANOSIDE
23 CIMIGENOL,24(S): 3-O-ALPHA-L-ARABINOSIDE
24 CIMIGENOL,24(S): 3-O-BETA-D-XYLOSIDE
25 CIMIGENOL,24-EPI: 7-8-DIDEHYDRO: 3-O-BETA-XYLOSIDE
26 CIMIGENOL,25-ACETYL: XYLOSIDE
27 CIMIGENOL,25-ANHYDRO: 3-0-BETA-D-XYLOPYRANOSIDE
28 CIMIGENOL,25-ANHYDRO: 3-O-ALPHA-L-ARABINOSIDE
29 CIMIGENOL,25-O-ACETYL: 3-O-ALPHA-L-ARABINOSIDE
30 CIMIGENOL,25-O-ACETYL: 3-O-BETA-D-XYLOSIDE
31 CIMIGENOL,25-O-ACETYL: ARABINOSIDE
32 CIMIGENOL,25-O-ACETYL: XYLOSIDE
33 CIMIGENOL,25-O-ACETYL-12-BETA-HYDROXY: 3-O-ALPHA-L-ARABINOPYRANOSIDE
34 CIMIGENOL,25-O-METHYL: 3-O-ALPHA-L-ARABINOPYRANOSIDE
35 CIMIGENOL,25-O-METHYL: 3-O-BETA-D-XYLOPYRANOSIDE
36 CIMIGENOL,25-O-METHYL: XYLOSIDE
37 CIMIGENOL,DEOXY: 25-CHLORO: 3-O-BETA-D-XYLOSIDE
38 CIMIGENOL-3-O-ALPHA-L-ARABINOPYRANOSIDE
39 CIMIGENOL-3-O-BETA-D-XYLOPYRANOSIDE
40 CIMIGENOSIDE
41 CIMIRACEMOSIDE
42 CIMIRACEMOSIDE A
43 CIMIRACEMOSIDE B
44 CIMIRACEMOSIDE C
45 CIMIRACEMOSIDE D

APPENDIX A (continued)

46 CIMIRACEMOSIDE E
47 CIMIRACEMOSIDE F
48 CIMIRACEMOSIDE G
49 CIMIRACEMOSIDE H
50 CIMIRACEMOSIDE I
51 CIMIRACEMOSIDE J
52 CIMIRACEMOSIDE K
53 CIMIRACEMOSIDE L
54 CIMIRACEMOSIDE M
55 CIMIRACEMOSIDE N
56 CIMIRACEMOSIDE O
57 CIMIRACEMOSIDE P
58 CIMIRACEMOSIDE Q
59 FOETIDINOL-3-O-BETA-XYLOSIDE
60 SHENGMANOL,23-ACETOXY: 3-O-BETA-D-XYLOSIDE
61 SHENGMANOL,23-O-ACETYL: 3-ALPHA-L-ARABINOSIDE
62 SHENGMANOL,24-O-ACETYL:
63 SHENGMANOL-3-O-ALPHA-L-ARABINOPYRANOSIDE

PHENYLPROPANOIDS
64 CAFFEIC ACID
65 CAFFEIC ACID METHYL ESTER
66 CAFFEOYL-GLYCOLIC ACID
67 CIMICIFUGIC ACID G
68 CIMICIPHENOL
69 CIMICIPHENONE
70 CIMIRACEMATE A
71 CIMIRACEMATE B
72 CIMIRACEMATE C
73 CIMIRACEMATE D
74 COUMARIC ACID,PARA:
75 FERULIC ACID
76 FERULIC ACID METHYL ESTER
77 FERULIC ACID,ISO:
78 FERULIC ACID,ISO: 1-O-BETA-D-GLUCOSIDE
79 PETASIPHENONE

LIGNANS
80 ACTAEALACTONE
81 CIMICIFUGIC ACID A
82 CIMICIFUGIC ACID A,DEHYDRO:
83 CIMICIFUGIC ACID B,DEHYDRO:
84 CIMICIFUGIC ACID D
85 CIMICIFUGIC ACID E
86 CIMICIFUGIC ACID F
87 FUKIIC ACID

APPENDIX A (continued)

88 FUKINOLIC ACID
89 PISCIDIC ACID,2-FERULOYL:
90 PISCIDIC ACID,2-ISO-FERULOYL:

ALKALOIDS
91 CIMIPRONIDINE
92 CIMIPRONIDINE METHYL ESTER
93 CYCLO-CIMIPRONIDINE
94 DOPARGINE
95 TRYPTAMINE,N(B)-METHYL 5-HYDROXY::
96 CYTISINE,N-METHYL:
97 SEROTONIN,N-OMEGA METHYL
98 TYROSOL,3-HYDROXY: 3-0-BETA-D-GLUCOSIDE

FLAVONOIDS
97 CINNERACEMATE A
98 SHENGMANOL,HYDRO: 24-D-ACETYL: 3-O-BETA-D-XYLOSIDE
99 KAEMPFEROL
100 DAIDZEIN
101 FORMONONETIN
102 GENISTEIN

STEROIDS
103 DAUCOSTEROL-6'-LINOLEATE

BENZENOIDS
104 CIMIDAHURINE
105 CIMIDAHURININE
106 PROTOCATECHUALDEHYDE
107 PROTOCATECHUIC ACID
108 TYROSOL,3-HYDROXY: 3-0-BETA-D-GLUCOSIDE

CHROMONES
109 CIMIFUGIN

LIPIDS
110 FATTY ACID PATTERN
111 FATTY ACIDS(CIS)
112 GLYCEROL-1-PALMITATE

CITED LITERATURE

1. Sakurai, N., Koeda, M., Inoue, T. & Nagai, M. (1994) Studies on the Chinese crude drug "Shoma." VIII. Two new triterpenol bisdesmosides, 3-arabinosyl-24-O-acetylhydroshengmanol 15-glucoside and 3-xylosyl-24-O-acetylhydroshengmanol 15-glucoside, from Cimicifuga dahurica. Chemical & Pharmaceutical Bulletin 42: 48-51.

2. Compton, J. A., Culham, A. & jury, S. L. (1998) Reclassification of *Actaea* to Include *Cimicifuga* and *Souliea (Ranunculaceae):* Phylogeny Inferred from Morphology, nrDNA ITS, and cpDNA trnL-F Sequence Variation. Taxon 47: 593-634.

3. Foster, S. (1999) Black cohosh: *Cimicifuga racemosa* a literature review. HerbalGram 45: 35-41.

4. Wende, K., Mugge, C., Thurow, K., Schopke, T. & Lindequist, U. (2001) Actaeaepoxide 3-O-beta-D-xylopyranoside, a new cycloartane glycoside from the rhizomes of Actaea racemosa (Cimicifuga racemosa). J Nat Prod 64: 986-989.

5. Cavaliere, C. R., Patrick Lynch, Mary, Ellen Blumenthal, Mark (2009) Herbal supplement sales experience slight increase in 2008. HerbalGram 82: 58-61.

6. McCoy, J. A., Davis, J., Camper, N., Kahn, I. & Bharathi, A. (2006) Influence of rhizome propagule size on yields and triterpene glycoside concentrations of black cohosh (*Actaea racemosa* L.) HortScience.2007; 42: 61-64

7. MacLennan, A. H., Henderson, V. W., Paine, B. J., Mathias, J., Ramsay, E. N., Ryan, P., Stocks, N. P. & Taylor, A. W. (2006) Hormone therapy, timing of initiation, and cognition in women aged older than 60 years: the REMEMBER pilot study. Menopause 13: 28-36.

8. Haas, J. S., Kaplan, C. P., Gerstenberger, E. P. & Kerlikowske, K. (2004) Changes in the use of postmenopausal hormone therapy after the publication of clinical trial results. Annals of Internal Medicine 140: 184-188.

9. Borrelli, F., Izzo, A. A. & Ernst, E. (2003) Pharmacological effects of *Cimicifuga racemosa*. Life Sciences 73: 1215-1229.

10. Osmers, R., Friede, M., Liske, E., Schnitker, J., Freudenstein, J. & Henneicke-von Zepelin, H.-H. (2005) Efficacy and safety of isopropanolic black cohosh extract for climacteric symptoms. Obstetrics & Gynecology 105: 1074-1083.

11. Wuttke, W., Seidlova-Wuttke, D. & Gorkow, C. (2003) The *Cimicifuga* preparation BNO 1055 vs. conjugated estrogens in a double-blind placebo-controlled study: effects on menopause symptoms and bone markers. Maturitas 44 Suppl 1: S67-77.

12. Frei-Kleiner, S., Schaffner, W., Rahlfs, V. W., Bodmer, C. & Birkhauser, M. (2005) *Cimicifuga racemosa* dried ethanolic extract in menopausal disorders: a double-blind placebo-controlled clinical trial. Maturitas 51: 397-404.

13. Liske, E., Hanggi, W., Henneicke-von Zepelin, H. H., Boblitz, N., Wustenberg, P. & Rahlfs, V. W. (2002) Physiological investigation of a unique extract of black cohosh (*Cimicifugae racemosae* rhizoma): a 6-month clinical study demonstrates no systemic estrogenic effect. Journal of Women's Health & Gender-Based Medicine 11: 163-174.

14. Newton, K. M., Reed, S. D., Grothaus, L., Ehrlich, K., Guiltinan, J., Ludman, E. & LaCroix, A. Z. (2005) The Herbal Alternatives for Menopause (HALT) Study: background and study design. Maturitas 52: 134-146.

15. Borrelli, F. & Ernst, E. (2008) Black cohosh (*Cimicifuga racemosa*) for menopausal symptoms: a systematic review of its efficacy. Pharmacological Research 58: 8-14.

16. Geller, S. E., Shulman, L. P., van Breemen, R. B., Banuvar, S., Zhou, Y., Epstein, G., Hedayat, S., Nikolic, D., Krause, E. C., Piersen, C. E., Bolton, J. L., Pauli, G.

F. & Farnsworth, N. R. (2009) Safety and efficacy of black cohosh and red clover for the management of vasomotor symptoms: a randomized controlled trial. Menopause 16: 1156-1166.

17. Shulman, L. P., Banuvar, S., Fong, H. H. & Farnsworth, N. R. (2011) Discussion of a well-designed clinical trial which did not demonstrate effectiveness: UIC center for botanical dietary supplements research study of black cohosh and red clover. Fitoterapia 82: 88-91.

18. Viereck, V., Emons, G. & Wuttke, W. (2005) Black cohosh: just another phytoestrogen? Trends in Endocrinology and Metabolism 16: 214-221.

19. Carpenter, J. S. (2005) State of the science: hot flashes and cancer. Part 2: management and future directions. Oncology Nursing Forum 32: 969-978.

20. Rossouw, J. E., Anderson, G. L., Prentice, R. L., LaCroix, A. Z., Kooperberg, C., Stefanick, M. L., Jackson, R. D., Beresford, S. A., Howard, B. V., Johnson, K. C., Kotchen, J. M., Ockene, J. & Writing Group for the Women's Health Initiative, I. (2002) Risks and benefits of estrogen plus progestin in ealthy postmenopausal women: principal results from the women's health Initiative randomized controlled trial. Jama 288: 321-333.

21. Hedlund, P. B. & Sutcliffe, J. G. (2004) Functional, molecular and pharmacological advances in 5-HT_7 receptor research. Trends in Pharmacological Sciences 25: 481-486.

22. Burdette, J. E., Liu, J., Chen, S. N., Fabricant, D. S., Piersen, C. E., Barker, E. L., Pezzuto, J. M., Mesecar, A., Van Breemen, R. B., Farnsworth, N. R. & Bolton, J. L. (2003) Black cohosh acts as a mixed competitive ligand and partial agonist of the serotonin receptor. Journal of Agricultural and Food Chemistry 51: 5661-5670.

23. Powell, S. L., Gödecke, T., Nikolic, D., Chen, S. N., Ahn, S., Dietz, B., Farnsworth, N. R., van Breemen, R. B., Lankin, D. C., Pauli, G. F. & Bolton, J. L. (2008) In vitro serotonergic activity of black cohosh and identification of N(omega)-methylserotonin as a potential active constituent. J Agric Food Chem 56: 11718-11726.

24. Fabricant, D. S., Nikolic, D., Lankin, D. C., Chen, S. N., Jaki, B. U., Krunic, A., van Breemen, R. B., Fong, H. H., Farnsworth, N. R. & Pauli, G. F. (2005) Cimipronidine, a cyclic guanidine alkaloid from *Cimicifuga racemosa*. Journal of Natural Products 68: 1266-1270.

25. Jarry, H. & Harnischfeger, G. (1985) Studies on the endocrine effects of the contents of *Cimicifuga racemosa*. Planta Medica 51: 46-49.

26. Jarry, H., Harnischfeger, G. & Duker, E. (1985) Studies on the endocrine effects of the contents of *Cimicifuga racemosa* 2. in vitro binding of compounds to estrogen receptors. Planta Medica 51: 316-319.

27. Kennelly, E. J., Baggett, S., Nuntanakorn, P., Ososki, A. L., Mori, S. A., Duke, J., Coleton, M. & Kronenberg, F. (2002) Analysis of thirteen populations of black cohosh for formononetin. Phytomedicine 9: 461-467.

28. Struck, D., Tegtmeier, M. & Harnischfeger, G. (1997) Flavones in extracts of *Cimicifuga racemosa*. Planta Medica 63: 289.

29. Gödecke, T., Lankin, D. C., Nikolic, D., Chen, S. N., van Breemen, R. B., Farnsworth, N. R. & Pauli, G. F. (2009) Guanidine alkaloids and Pictet-Spengler adducts from black cohosh (*Cimicifuga racemosa*) Journal of Natural Products 72: 433-437.

30. Crum, J. D., Cassady, J. M., Olmstead, P. M. & Picha, N. J. (1965) Chemistry of alkaloids. I. The screening of some native ohio plants. West Virginia Academy of Science 37: 143-147.

31. Kusano, G., Shibano, M., Idoji, M. & Minoura, K. (1993) A new alkaloid, 2-hydroxy-7-methyl-9H-carbazole from *Cimicifuga Simplex*. Heterocycles 36: 2367-2371.

32. Kusano, A., Shibano, M., KItagawa, S., Kusano, G., Nozoe, S. & Fushiya, S. (1994) Studies on the constituents of *Cimicifuga* species. XV. Two new diglycosides from the aerial parts of *Cimicifuga simplex*. Chemical & Pharmaceutical Bulletin 42: 1940-1943.

33. Liu, Y., Chen, D. H., Si, J. Y., Pan, R. L., Tu, G. Z. & An, D. G. (2003) Studies on the chemical constituents from the aerial parts of Cimicifuga dahurica (Chinese). Yao Xue Xue Bao 38: 763-766.

34. Kusano, A., Takahira, M., Shibano, M., Miyase, T. & Kusano, G. (1999) Studies on the constituents of *Cimicifuga* species. XXVI. Twelve new cyclolanostanol glycosided from the underground parts of *Cimicifuga simplex* Wormsk. Chemical & Pharmaceutical Bulletin 47: 511-516.

35. Kusano, G. (2001) Studies on the constituents of *Cimicifuga* species (Japanese). Yakugaku Zasshi 121: 497-521.

36. Ankli, A., Reich, E. & Steiner, M. (2008) Rapid high-performance thin-layer chromatographic method for detection of 5% adulteration of black cohosh with *Cimicifuga foetida*, *C. heracleifolia*, *C. dahurica*, or *C. americana*. Journal of AOAC International 91: 1257-1264.

37. Mahady, G. B., Low Dog, T., Barrett, M. L., Chavez, M. L., Gardiner, P., Ko, R., Marles, R. J., Pellicore, L. S., Giancaspro, G. I. & Sarma, D. N. (2008) United States Pharmacopeia review of the black cohosh case reports of hepatotoxicity. Menopause 15: 628-638.

38. van Breemen, R. B., Fong, H. H. & Farnsworth, N. R. (2008) Ensuring the safety of botanical dietary supplements. American Journal of Clinical Nutrition 87: 509S-513S.

39. Verbitski, S. M., Gourdin, G. T., Ikenouye, L. M., McChesney, J. D. & Hildreth, J. (2008) Detection of *Actaea racemosa* adulteration by thin-layer chromatography and combined thin-layer chromatography-bioluminescence. The Journal of AOAC International 91: 268-275.

40. Stephens, H. A. (1980) Poisonous plants of the central United States,. The Regents Press of Kansas.

41. Barceloux, D. G. (2008) Medical toxicology of natural substances : foods, fungi, medicinal herbs, plants, and venomous animals, p. 745. John Wiley & Sons.

42. Gafner, S., Sudberg, S., Sudberg, E., Villinski, J., Gauthier, R. & Bergeron, C. (2006) Chromatographic fingerprinting as a means of quality control: distinction between *Actaea racemosa* and four different *Actaea* species. Acta Horticulturae: 83-94.

43. Avula, B., Ali, Z. & Khan, I. A. (2007) Chemical fingerprinting of *Actaea racemosa* (Black Cohosh) and its comparison study with closely related *Actaea* species (*A. pachypoda*, *A. podocarpa*, *A. rubra*) by HPLC. Chromatographia 66: 757-762.

44. He, K., Zheng, B., Kim, C. H., Rogers, L. & Zheng, Q. (2000) Direct analysis and identification of triterpene glycosides by LC/MS in black cohosh, *Cimicifuga racemosa*, and in several commercially available black cohosh products. Planta Medica 66: 635-640.

45. Jiang, B., Ma, C., Motley, T., Kronenberg, F. & Kennelly, E. J. (2011) Phytochemical fingerprinting to thwart black cohosh adulteration: a 15 *Actaea* species analysis. Phytochemical Analysis 22: 339-351.

46. He, K., Pauli, G. F., Zheng, B., Wang, H., Bai, N., Peng, T., Roller, M. & Zheng, Q. (2006) *Cimicifuga* species identification by high performance liquid chromatography-photodiode array/mass spectrometric/evaporative light scattering detection for quality control of black cohosh products. Journal of Chromatography A 1112: 241-254.

47. Ali, Z., Khan, S. I., Fronczek, F. R. & Khan, I. A. (2007) 9,10-seco-9,19-Cyclolanostane arabinosides from the roots of *Actaea podocarpa*. Phytochemistry 68: 373-382.

48. Fabricant, D. (2005) Pharmacognostic Investigation of Black Cohosh (*Cimicifuga racemosa* (L.) Nutt.) (Ph.D Dissertation).

49. Friesen, J. B. & Pauli, G. F. (2005) G.U.E.S.S. - a generally useful estimate of solvent systems for CCC. Journal of Liquid Chromatography & Related Technologies 28: 2777-2806.

50. Pearson, A. G. (1987) Optimization of Gaussian resolution enhancement. Journal of Magnetic Resonance 74: 541-545.

51. Takemoto, T., Kusano, G. & Yamamoto, N. (1970) Studies on the constituents of *Cimicifuga* spp. VII. Structure of cimicifugenol (Japanese). Yakugaku Zasshi 90: 68-72.

52. Li, J. X. & Yu, Z. Y. (2006) *Cimicifugae* rhizoma: from origins, bioactive constituents to clinical outcomes. Current Medicinal Chemistry 13: 2927-2951.

53. Zhang, Q. W., Ye, W. C., Hsiao, W. W., Zhao, S. X. & Che, C. T. (2001) Cycloartane glycosides from *Cimicifuga dahurica*. Chemical & Pharmaceutical Bulletin 49: 1468-1470.

54. Kusano, A., Shimizu, K., Idoji, M., Shibano, M., Minoura, K. & Kusano, G. (1995) Studies on the constituents of *Cimicifuga* species. XVI. Three new cycloartane xylosides from the aerial parts of *Cimicifuga simplex* Wormskjord. Chemical & Pharmaceutical Bulletin 43: 279-283.

55. Karplus, M. (1959) Contact electron-spin coupling of nuclear magnetic moments. The Journal of Chemical Physics 30: 11-15.

56. Karplus, M. (1961) The analysis of molecular wave functions by nuclear magnetic resonance spectroscopy. The Journal of Physical Chemistry 64: 1793-1798.

57. Karplus, M. (1963) Vicinal Proton Coupling in Nuclear Magnetic Resonance. Journal of American Chemical Society 85: 2870-2871.

58. Bax, A. & Davis, D. G. (1985) Practical aspects of two-dimensional transverse NOE spectroscopy. Journal of Magnetic Resonance 63: 207-213.

59. Akihisa, T., Watanabe, K., Yoneima, R., Suzuki, T. & Kimura, Y. (2006) Biotransformation of cycloartane-type triterpenes by the fungus *Glomerella fusarioides*. Journal of Natural Products 69: 604-607.

60. Pan, R. L., Chen, D. H., Si, J. Y., Zhao, X. H., Li, Z. & Cao, L. (2009) Immunosuppressive effects of new cyclolanostane triterpene diglycosides from the aerial part of Cimicifuga foetida. Arch Pharm Res 32: 185-190.

61. Kusano, G., Idoji, M., Sogoh, Y., Shibano, M., Kusano, A. & Iwashita, T. (1994) Studies on the constituents of *Cimicifuga* Species. XIV. A new xyloside from the

aerial parts of *Cimicifuga simplex* WORMSK. Chemical & Pharmaceutical Bulletin 42: 1106-1110.

62. Kusano, A., Shibano, M. & Kusano, G. (1995) Studies on the constituents of *Cimicifuga* species. XVII. Four glycosides from the aerial parts of *Cimicifuga simplex* Wormsk. Chemical & Pharmaceutical Bulletin 43: 1167-1170.

63. Ye, W., Zhang, J., Che, C. T., Ye, T. & Zhao, S. (1999) New cycloartane glycosides from *Cimicifuga dahurica*. Planta Medica 65: 770-772.

64. Chen, S. N., Fabricant, D. S., Lu, Z. Z., Fong, H. H. & Farnsworth, N. R. (2002) Cimiracemosides I-P, new 9,19-cyclolanostane triterpene glycosides from *Cimicifuga racemosa*. Journal of Natural Products 65: 1391-1397.

65. Takemoto, T., Kusano, G. & Kawahara, M. (1970) Studies on the constituents of Cimicifuga spp. VI. Structures of 25-O-acetylcimigenoside and 25-O-methylcimigenoside (Japanese). Yakugaku Zasshi 90: 64-67.

66. Kusano, G., Hojo, S., Kondo, Y. & Takemoto, T. (1977) Studies on the constituents of *Cimicifuga* species. XIII. Structure of cimicifugoside. Chemical & Pharmaceutical Bulletin 25: 3182-3189.

67. Liu, Y., Chen, D., Si, J., Tu, G. & An, D. (2002) Two new cyclolanostanol xylosides from the aerial parts of *Cimicifuga dahurica*. Journal of Natural Products 65: 1486-1488.

68. Sakurai, N., Kimura, O., Inoue, T. & Nagai, M. (1981) Studies on the chinese crude drug "Shoma." V. structures of 24-O-acetylhydroshengmanol xyloside and 22-hydroxycimigenol xyloside. Chemical & Pharmaceutical Bulletin 24: 955-960.

69. Ali, Z., Khan, S. I. & Khan, I. A. (2006) Phytochemical study of *Actaea rubra* and biological screenings of isolates. Planta Medica 72: 1350-1352.

70. Kimura, O., Sakurai, N. & Inoue, T. (1983) Studies on the Chinese crude drug "Shoma." VII. Isolation and determination of genuine natural products, acetyl shengmanol xyloside, 24-O-acetylhydroshengmanol xyloside, and shengmanol xyloside, in *Cimicifuga dahurica* and the other *Cimicifuga* plants (Japanese). Yakugaku Zasshi 103: 293-299.

71. Sakurai, N., Inoue, T. & Nagai, M. (1972) Studies on the Chinese crude drug "Shoma." II. Triterpenes of *Cimicifuga dahurica* Maxim (Japanese). Yakugaku Zasshi 92: 724-728.

72. Kusano, A., Takahira, M., Shibano, M., Miyase, T., Okuyama, T. & kusano, G. (1998) Structures of two new cyclolanostanol xylosides, cimiacerosides A and B. Heterocycles 48: 1003-1013.

73. Jiang, B., Kronenberg, F., Nuntanakorn, P., Qiu, M. H. & Kennelly, E. J. (2006) Evaluation of the botanical authenticity and phytochemical profile of black cohosh products by high-performance liquid chromatography with selected ion monitoring liquid chromatography-mass spectrometry. Journal of Agricultural and Food Chemistry 54: 3242-3253.

74. Shao, Y., Harris, A., Wang, M., Zhang, H., Cordell, G. A., Bowman, M. & Lemmo, E. (2000) Triterpene glycosides from *Cimicifuga racemosa*. Journal of Natural Products 63: 905-910.

75. Calderon-Montano, J. M., Burgos-Moron, E., Perez-Guerrero, C. & Lopez-Lazaro, M. (2011) A review on the dietary flavonoid kaempferol. Mini-Reviews in Medicinal Chemistry 11: 298-344.

76. Choi, Y. H., Sertic, S., Kim, H. K., Wilson, E. G., Michopoulos, F., Lefeber, A. W., Erkelens, C., Prat Kricun, S. D. & Verpoorte, R. (2005) Classification of *Ilex* species based on metabolomic fingerprinting using nuclear magnetic resonance and multivariate data analysis. Journal of Agricultural and Food Chemistry 53: 1237-1245.

77. Kim, H. K., Choi, Y. H., Erkelens, C., Lefeber, A. W. & Verpoorte, R. (2005) Metabolic Fingerprinting of *Ephedra* Species Using ^{1}H-NMR Spectroscopy and Principal Component Analysis. Chemical & Pharmaceutical Bulletin 53: 105-109.

78. Lee, J. E., Lee, B. J., Chung, J. O., Hwang, J. A., Lee, S. J., Lee, C. H. & Hong, Y. S. Geographical and climatic dependencies of green tea (*Camellia sinensi*s) metabolites: a^{1}H NMR-based metabolomics study. Journal of Agricultural and Food Chemistry 58: 10582-10589.

79. Choi, Y. H., Tapias, E. C., Kim, H. K., Lefeber, A. W., Erkelens, C., Verhoeven, J. T., Brzin, J., Zel, J. & Verpoorte, R. (2004) Metabolic discrimination of *Catharanthus roseus* leaves rnfected by phytoplasma using ^{1}H-NMR spectroscopy and multivariate data analysis. Plant Physiology 135: 2398-2410.

80. van der Kooy, F., Maltese, F., Hae Choi, Y., Kyong Kim, H. & Verpoorte, R. (2009) Quality control of herbal material and phytopharmaceuticals with MS and NMR based metabolic fingerprinting. Planta Medica 75: 763-775.

81. Villas-Boas, S. G., Rasmussen, S. & Lane, G. A. (2005) Metabolomics or Metabolite Profiles? Trends in Biotechnology 23: 385-386.

82. Pauli, G. F., Jaki, B. U. & Lankin, D. C. (2005) Quantitative 1H NMR: development and potential of a method for natural products analysis. Journal of Natural Products 68: 133-149.

83. Godecke, T., Napolitano, J. G., Yao, P., Nikolic, D., Dietz, B., Bolton, J. L., van Breemen, R. B., Farnsworth, N. R., Chen, S. N., Lankin, D. C. & Pauli, G. F. (In preparation) Integrated standardization concept for Angelica botanicals using quantitative NMR.

84. Prochaska, H. J. & Santamaria, A. B. (1988) Direct measurement of NAD(P)H:quinone reductase from cells cultured in microtiter wells: a screening assay for anticarcinogenic enzyme inducers. Analytical Biochemistry 169: 328-336.

85. Fahey, J. W., Dinkova-Kostova, A. T., Stephenson, K. K. & Talalay, P. (2004) The "Prochaska" Microtiter Plate Bioassay for Inducers of NQO1. Methods in Enzymology 382: 243-258.

86. Chen, S. N., Li, W., Fabricant, D. S., Santarsiero, B. D., Mesecar, A., Fitzloff, J. F., Fong, H. H. & Farnsworth, N. R. (2002) Isolation, structure elucidation, and absolute configuration of 26-deoxyactein from *Cimicifuga racemosa* and clarification of nomenclature associated with 27-deoxyactein. Journal of Natural Products 65: 601-605.

87. Kusano, A., Takahira, M., Shibano, M., In, Y., Ishida, T., Miyase, T. & Kusano, G. (1998) Studies on the constituents of *Cimicifuga* Species. XX. Absolute stereostructures of cimicifugoside and actein from C*imicifuga simplex* WORMSK. Chemical & Pharmaceutical Bulletin 46: 467-472.

88. Groth, I., Bergstrom, G. & Pellmyr, O. (1987) Floral fragrances in *Cimicifuga*: chemical polymorphism and incipient speciation in *Cimicifuga simplex*. Biochemical Systematics and Ecology 15: 441-444.

89. Koeda, M., Aoki, Y., Sakurai, N. & Nagai, M. (1995) Studies on the Chinese crude drug "shoma." IX. Three novel cyclolanostanol xylosides, cimicifugosides H-1, H-2 and H-5, from cimicifuga rhizome. Chemical & Pharmaceutical Bulletin 43: 771-776.

90. Benoit, P. S., Fong, H. H., Svoboda, G. H. & Farmsworth, N. R. (1976) Biological and phytochemical evaluation of plants. XIV. Antiinflammatory evaluation of 163 species of plants. LLOYDIA 39: 160-171.

91. Overk, C. R., Yao, P., Chen, S., Deng, S., Imai, A., Main, M., Schinkovitz, A., Farnsworth, N. R., Pauli, G. F. & Bolton, J. L. (2008) High-content screening and mechanism-based evaluation of estrogenic botanical extracts. Combinatorial Chemistry & High Throughput Screen 11: 283-293.

92. Burdette, J. E., Chen, S. N., Lu, Z. Z., Xu, H., White, B. E., Fabricant, D. S., Liu, J., Fong, H. H., Farnsworth, N. R., Constantinou, A. I., Van Breemen, R. B., Pezzuto, J. M. & Bolton, J. L. (2002) Black cohosh (*Cimicifuga racemosa* L.) protects against menadione-induced DNA damage through scavenging of reactive oxygen species: bioassay-directed isolation and characterization of active principles. Journal of Agricultural and Food Chemistry 50: 7022-7028.

93. Dietz, B. M., Liu, D., Hagos, G. K., Yao, P., Schinkovitz, A., Pro, S. M., Deng, S., Farnsworth, N. R., Pauli, G. F., van Breemen, R. B. & Bolton, J. L. (2008) *Angelica sinensis* and its alkylphthalides induce the detoxification enzyme NAD(P)H: quinone oxidoreductase 1 by alkylating Keap1. Chemical Research in Toxicology 21: 1939-1948.

94. Song, L. L., Kosmeder, J. W., 2nd, Lee, S. K., Gerhauser, C., Lantvit, D., Moon, R. C., Moriarty, R. M. & Pezzuto, J. M. (1999) Cancer chemopreventive activity mediated by 4'-bromoflavone, a potent inducer of phase II detoxification enzymes. Cancer Research 59: 578-585.

95. Obourn, J. D., Koszewski, N. J. & Notides, A. C. (1993) Hormone- and DNA-binding mechanisms of the recombinant human estrogen receptor. Biochemistry 32: 6229-6236.

96. Piersen, C. E. (2003) Phytoestrogens in botanical dietary supplements: implications for cancer. Integrative Cancer Therapies 2: 120-138.

97. Liu, J., Burdette, J. E., Xu, H., Gu, C., van Breemen, R. B., Bhat, K. P., Booth, N., Constantinou, A. I., Pezzuto, J. M., Fong, H. H., Farnsworth, N. R. & Bolton, J. L. (2001) Evaluation of estrogenic activity of plant extracts for the potential treatment of menopausal symptoms. Journal of Agricultural and Food Chemistry 49: 2472-2479.

98. Duker, E. M., Kopanski, L., Jarry, H. & Wuttke, W. (1991) Effects of extracts from *Cimicifuga racemosa* on gonadotropin release in menopausal women and ovariectomized rats. Planta Medica 57: 420-424.

99. Overk, C. R., Yao, P., Chadwick, L. R., Nikolic, D., Sun, Y., Cuendet, M. A., Deng, Y., Hedayat, A. S., Pauli, G. F., Farnsworth, N. R., van Breemen, R. B. & Bolton, J. L. (2005) Comparison of the in vitro estrogenic activities of compounds from hops (*Humulus lupulus*) and red clover (*Trifolium pratense*). Journal of Agricultural and Food Chemistry 53: 6246-6253.

100. Pisha, E. & Pezzuto, J. M. (1997) Cell-based assay for the determination of estrogenic and anti-estrogenic activities. Methods in Cell Science 19: 37-43.

101. Liu, J., Burdette, J. E., Sun, Y., Deng, S., Schlecht, S. M., Zheng, W., Nikolic, D., Mahady, G., van Breemen, R. B., Fong, H. H., Pezzuto, J. M., Bolton, J. L. & Farnsworth, N. R. (2004) Isolation of linoleic acid as an estrogenic compound from the fruits of *Vitex agnus-castus* L. (chaste-berry). Phytomedicine 11: 18-23.

102. Betz, J. M., Anderson, L., Avigan, M. I., Barnes, J., Farnsworth, N. R., Gerden, B., Henderson, L., Kennelly, E. J., Koetter, U., Lessard, S., Dog, T. L.,

McLaughlin, M., Naser, B., R, O., Pellicore, L. S., Senior, J. R., van Breemen, R. B., Wuttke, W. & L, C. (2009) Black cohosh considerations of safety and benefit. Nutrition Today 44: 155.

103. Mahady, G. B., Fabricant, D., Chadwick, L. R. & Dietz, B. (2002) Black cohosh: an alternative therapy for menopause? Nutrition in Clinical Care 5: 283-289.

104. Gödecke, T., Nikolic, D., Lankin, D. C., Chen, S. N., Powell, S. L., Dietz, B., Bolton, J. L., van Breemen, R. B., Farnsworth, N. R. & Pauli, G. F. (2009) Phytochemistry of cimicifugic acids and associated bases in *Cimicifuga racemosa* root extracts. Phytochemical Analysis 20: 120-133.

105. Albert, P. R., Zhou, Q. Y., Van Tol, H. H., Bunzow, J. R. & Civelli, O. (1990) Cloning, functional expression, and mRNA tissue distribution of the rat 5-hydroxytryptamine1A receptor gene. Journal of Biological Chemistry 265: 5825-5832.

106. Roth, B. L., Craigo, S. C., Choudhary, M. S., Uluer, A., Monsma, F. J., Jr., Shen, Y., Meltzer, H. Y. & Sibley, D. R. (1994) Binding of typical and atypical antipsychotic agents to 5-hydroxytryptamine-6 and 5-hydroxytryptamine-7 receptors. Journal of Pharmacology and Experimental Therapeutics 268: 1403-1410.

107. Fisher, B., Costantino, J. P., Wickerham, D. L., Cecchini, R. S., Cronin, W. M., Robidoux, A., Bevers, T. B., Kavanah, M. T., Atkins, J. N., Margolese, R. G., Runowicz, C. D., James, J. M., Ford, L. G. & Wolmark, N. (2005) Tamoxifen for the prevention of breast cancer: current status of the National Surgical Adjuvant Breast and Bowel Project P-1 study. Journal of National Cancer Institute 97: 1652-1662.

108. Group, E. B. C. T. C. (2005) Effects of chemotherapy and hormonal therapy for early breast cancer on recurrence and 15-year survival: an overview of the randomised trials. Lancet 365: 1687-1717.

109. Inui, T. (2008) Phytochemical and Biochemometric Evaluation of the Alaskan Anti-TB Ethnobotanical: *Oplopanax horridus* (Ph.D dissertation).

110. Ghosal, S., Banerjee, S. K., Bhattacharya, S. K. & Sanyal, A. K. (1972) Chemical and pharmacological evaluation of *Desmodium pulchellum*. Planta Medica 21: 398-409.

111. Lien, E. A., Solheim, E., Lea, O. A., Lundgren, S., Kvinnsland, S. & Ueland, P. M. (1989) Distribution of 4-hydroxy-N-desmethyltamoxifen and other tamoxifen metabolites in human biological fluids during tamoxifen treatment. Cancer Research 49: 2175-2183.

112. Stearns, V., Johnson, M. D., Rae, J. M., Morocho, A., Novielli, A., Bhargava, P., Hayes, D. F., Desta, Z. & Flockhart, D. A. (2003) Active tamoxifen metabolite plasma concentrations after coadministration of tamoxifen and the selective serotonin reuptake inhibitor paroxetine. Journal of National Cancer Institute 95: 1758-1764.

113. Crewe, H. K., Ellis, S. W., Lennard, M. S. & Tucker, G. T. (1997) Variable Contribution of Cytochromes P450 2D6, 2C9 and 3A4 to the 4-Hydroxylation of Tamoxifen by Human Liver Microsomes. Biochemical Pharmacology 53: 171-178.

114. Desta, Z., Ward, B. A., Soukhova, N. V. & Flockhart, D. A. (2004) Comprehensive evaluation of tamoxifen sequential biotransformation by the human cytochrome P450 system in vitro: prominent roles for CYP3A and CYP2D6. Journal of Pharmacology and Experimental Therapeutics 310: 1062-1075.

115. Phillips, D. H. (2001) Understanding the genotoxicity of tamoxifen? Carcinogenesis 22: 839-849.

116. Li, J., Gödecke, T., Chen, S. N., Imai, A., Lankin, D. C., Farnsworth, N. R., Pauli, G. F., van Breemen, R. B. & Nikolic, D. (2011) In vitro metabolic interactions between black cohosh (*Cimicifuga racemosa*) and tamoxifen via inhibition of cytochromes P450 2D6 and 3A4. Xenobiotica 41: 1021-1030.

117. Chauret, N., Gauthier, A. & Nicoll-Griffith, D. A. (1998) Effect of common organic solvents on in vitro cytochrome P450-mediated metabolic activities in human liver microsomes. Drug Metabolism and Disposition 26: 1-4.

118. Walsky, R. L. & Obach, R. S. (2004) Validated assays for human cytochrome P450 activities. Drug Metabolism and Disposition 32: 647-660.

VITA

NAME: Ayano Imai

EDUCATION: B.S., Human Life and Environmental Science, Ochanomizu University, Tokyo, Japan, 2001

M.S., Human Life and Environmental Science, Ochanomizu University, Tokyo, Japan, 2004

RESEARCH EXPERIENCE:

Research Assistant, UIC/NIH Center for Botanical Dietary Supplements Research Project 1, University of Illinois at Chicago, 2005-2011

Human Life and Environmental Science, Ochanomizu University, Tokyo, Japan, 2002-2004

HONORS: Lynn Brady Student Travel Award, 7th Annual Oxford International Conference on the Science of Botanicals & American Society of Pharmacognosy 4th Interim Meeting, 2008

University of Illinois at Chicago Fellowship, 2005-2006

Rotary Foundation Ambassadorial Scholarship, Rotary Foundation, 2004

PROFESSIONAL MEMBERSHIP:

American Society of Pharmacognosy

MANUSCRIPTS IN PREPARATION

Imai A, Chen SN, Lankin DC, Farnsworth NR, Pauli GF, New triterpenes from Aerial *Cimicifuga racemosa*

Imai A, Gödecke T, Lankin DC, Farnsworth NR, Pauli GF, Differentiation of *Cimicifuga* species by NMR Metabolomics

PEER-REVIEWED PUBLICATIONS:

Overk, C. R., Yao, P., Chen, S., Deng, S., Imai, A., Main, M., Schinkovitz, A., Farnsworth, N. R., Pauli, G. F. & Bolton, J. L. (2008) High-content screening and mechanism-based evaluation of estrogenic botanical extracts. Combinatorial Chemistry & High Throughput Screen 11: 283-293.

Li, J., Gödecke, T., Chen, S. N., Imai, A., Lankin, D. C., Farnsworth, N. R., Pauli, G. F., van Breemen, R. B. & Nikolic, D. (2011) In vitro metabolic interactions between black cohosh (*Cimicifuga racemosa*) and tamoxifen via inhibition of cytochromes P450 2D6 and 3A4. Xenobiotica 41: 1021-1030.

Qiu, F., Imai, A., McAlpine, J. B., Lankin, D. C., Burton, I., Karakach, T., Farnsworth, N. R., Chen, S. N. & Pauli, G. F. (2012) Dereplication, residual complexity, and rational naming: the case of the Actaea triterpenes. Journal of Natural Products 75: 432-443.

PRESENTATIONS:

Overk CR, Chen SN, Imai A, Main M, Schinkovitz A, Yao P, Farnsworth NR, Pauli GF, and Bolton JL. Systematic estrogenic evaluation of dietary herbal extracts for the potential treatment of menopausal symptoms. American Society of Pharmacognosy 47th annual meeting 2006

Imai A, Lankin DC, Hagos G, Bolton JL, Nikolic D, van Breemen RB, Farnsworth NR, Pauli GF, Aerial Parts of *Cimicifuga racemosa* as Potential Chemopreventive Botanical Dietary Supplement. American Society of Pharmacognosy 51st annual meeting 2010

Imai A, Yao P, Overk CR, Bolton JL, Nikolic D, van Breemen RB, Pauli GF, Phytochemical Investigation of the Estrogenic Aerial Parts of *Cimicifuga racemosa* (L.) Nutt (Ranunculaceae). 7th Annual Oxford International Conference on the Science of Botanicals & American Society of Pharmacognosy 4th Interim Meeting, 2008